UNIVERSITY OF CALIFORNIA, SAN DIEGO
SAN DIEGO STATE UNIVERSITY

Metal Complexes with Bifunctional Imidazolyl Phosphines for Catalytic Organic Transformations: Applications in Homogeneous and Polymer Supported Alkene Isomerization , and Hydrogen Deuterium Exchange

A dissertation submitted in partial satisfaction of the

requirements for the degree Doctor of Philosophy in

Chemistry

by

Gulin Erdogan

Committee in charge:

University of California, San Diego

Professor Joshua S. Figueroa
Professor William H. Gerwick
Professor Charles L. Perrin

San Diego State University

Professor Douglas B. Grotjahn, Chair
Professor B. Mikael Bergdahl
Professor Terrence G. Frey

2012

Copyright

Gulin Erdogan, 2012

All rights reserved.

The dissertation of Gulin Erdogan is approved, and it is acceptable in quality and form for publication on microfilm:

_____

_____

_____

_____

_____

_____

Chair

University of California, San Diego

San Diego State University

2012

DEDICATION

To cheese, wine, and beer.

TABLE OF CONTENTS

Signature Page iii

Dedication iv

Table of Contents v

List of Tables vi

List of Figures.....x

Acknowledgements xv

Vita, Publications and Fields of Study xx

Abstract xxiv

Chapter 1 Introduction – Bifunctional Catalysis 1

Chapter 2 Development of New Bifunctional Cyclopentadienyl Ruthenium Imidazolyl Phosphine Complexes for Controlled Alkene Isomerization 19

Chapter 3 Polymer Supported Alkene Isomerization.....120

Chapter 4 Mild and Selective Hydrogen / Deuterium Exchange at Allylic Positions of Olefins 191

Chapter 5 Conclusions and Future Directions.....232

LIST OF TABLES

PAGE

Table 2.1. Isomerization of allylic alcohols by **2.4** and **2.5** at 100 ^{o}C in 1,4-dioxane with 10 mol% Et_3NHPF_6 25

Table 2.2. Isomerization of allylic alcohols by **2.4** and **2.5** at 57 ^{o}C in chloroform-*d* 26

Table 2.3. Scope of alkene isomerization catalyst **2.10**[a] 30

Table 2.4. Important bond lengths and angles for **2.10**, **2.26**, and **2.27** 38

Table 2.5. Calculated product distribution of heptenes 41

Table 2.6. Collective isomerization data of 1-heptene, and equilibrium composition predicted from Table 2.5 44

Table 2.7. Crystal data and structure refinement for **2.26** 52

Table 2.8. Atomic coordinates (x 10^4) and equivalent isotropic displacement parameters (Å^{2}x 10^3) for **2.26**. U(eq) is defined as one third of the trace of the orthogonalized U^{ij} tensor. 53

Table 2.9. Anisotropic displacement parameters (Å^{2}x 10^3) for **2.26.** The anisotropic displacement factor exponent takes the form: $-2p^2[h^2 a^{*2}U^{11} + ... + 2 h k a^* b^* U^{12}]$ 57

Table 2.10. Bond lengths and angles for **2.26** 61

Table 2.11. Crystal data and structure refinement for **2.27** 71

Table 2.12. Atomic coordinates (x 10^4) and equivalent isotropic displacement parameters (Å^{2}x 10^3) for **2.27**. U(eq) is defined as one third of the trace of the orthogonalized U^{ij} tensor 72

Table 2.13. Anisotropic displacement parameters (Å^{2}x 10^3) for **2.27**. The anisotropic displacement factor exponent takes the form: $-2\pi^2[h^2 a^{*2}U^{11} + ... + 2 h k a^* b^* U^{12}]$ 78

Table 2.14. Bond lengths and angles for **2.27** 83

Table 2.15. 1-heptene Isomerization with 2 mol % **2.10** in NMR probe 105

Table 2.16. 1-heptene Isomerization with 2 mol % **2.19** at RT 105

Table 2.17. 1-heptene Isomerization with 2 mol % **2.19** in NMR probe 106

Table 2.18. 1-heptene Isomerization with 2 mol % **2.20** at RT 106
Table 2.19. 1-heptene isomerization with 2 mol % **2.20** at 70 ^{o}C 107
Table 2.20. 1-heptene isomerization with 2 mol % **2.21** at 70 ^{o}C 107
Table 2.21. 1-heptene isomerization with 2 mol % **2.22** at RT 108
Table 2.22. 1-heptene isomerization with 2 mol % **2.23** at RT ge715 108
Table 2.23. 1-heptene isomerization with 2 mol % **2.23** at 70 ^{o}C 109
Table 2.24. 1-heptene isomerization with 2 mol % **2.23** at 70 ^{o}C 109
Table 2.25. 1-hexene isomerization with 2 mol % **2.20** at RT and 70 ^{o}C.....110
Table 2.26. 1-decene isomerization with 2 mol % **2.20** at 70 ^{o}C.....110
Table 2.27. 1-hexene isomerization with 2 mol % **2.23** at RT 111
Table 3.1. Supports for immobilization 122
Table 3.2. Scope of polymer-supported Felkin's iridium catalyst.....129
Table 3.3. Substrate scope of **PS-1** and **PSL-1**.....134
Table 3.4. Recycling experiments performed with **PS-1** and amount of metal leaching 138
Table 3.5. Reaction conditions for optimal 1-(4-bromobenzyl)-4-(*t*Bu)-imidazole synthesis 143
Table 3.6. Isomerization of 4-allylanisole with **PS-1** 158
Table 3.7. Isomerization of 4-allylanisole with **PSL-1**.....159
Table 3.8. Isomerization of 4-allylanisole with **2.10** 159
Table 3.9. Isomerization of allyloxy(tert-butyl)dimethylsilane with **PS-1**.....160
Table 3.10. Isomerization of allyloxyallyloxy(tert-butyl)dimethylsilane with **PSL-1**.....161
Table 3.11. Isomerization of allyloxy(tert-butyl)dimethylsilane with **2.10**.....161
Table 3.12. Isomerization of *tert*-butyldimethyl(pent-4-enyloxy)silane with 5 mol% **PS-1** 162
Table 3.13. Isomerization of *tert*-butyldimethyl(pent-4-enyloxy)silane with 5 mol% **PSL-1** 163
Table 3.14. Isomerization of *tert*-butyldimethyl(pent-4-enyloxy)silane with 2 mol% **PS-1** 163
Table 3.15. Isomerization of *tert*-butyldimethyl(pent-4-enyloxy)silane with 2 mol% **PSL-1** 164
Table 3.16. Isomerization of methylenecyclohexane with **PS-1** 165
Table 3.17. Isomerization of methylenecyclohexane with **PSL-1**.....165

Table 3.18. Isomerization of methylenecyclohexane with **2.10** 166
Table 3.19. Isomerization of allyl ether with **PS-1** 167
Table 3.20. Isomerization of allyl ether with **PSL-1** 167
Table 3.21. Isomerization of 4-penten-2-ol with **PS-1** 168
Table 3.22. Isomerization of 4-penten-2-ol with **PSL-1** 168
Table 3.23. Isomerization of 2-allylcyclohexanone with **PS-1** 169
Table 3.24. Isomerization of 2-allylcyclohexanone with **PSL-1** 170
Table 3.25. Isomerization of 2-allylcyclohexanone with **2.10** 170
Table 3.26. Isomerization of eugenol with **PS-1** 171
Table 3.27. Isomerization of eugenol with **PSL-1** 172
Table 3.28. Isomerization of eugenol with **2.10** 172
Table 3.29. Neat isomerization of 4-penten-2-ol with **PS-1** 173
Table 3.30. Neat isomerization of 4-penten-2-ol with **PSL-1** 174
Table 3.31. Neat isomerization of eugenol with **PS-1** 174
Table 3.32. Neat isomerization of eugenol with **PSL-1** 175
Table 3.33. Neat isomerization of 2-allylcyclohexanone with **PS-1** 176
Table 3.34. Neat isomerization of 2-allylcyclohexanone with **PSL-1** 176
Table 3.35. Amount of starting material and internal standard used for recycling experiments 184
Table 3.36. Isomerization activity from recycling experiments with **PS-1** and **PSL-1** 185
Table 3.37. Ruthenium leaching from recycling experiments performed with **PS-1** and **PSL-1** 186
Table 3.38. Leaching in mass ruthenium per cycle with **PS-1** 186
Table 4.1. % Hydrogen left at indicated positions of propene after specified time 209
Table 4.2. % Hydrogen atoms present at specified positions in reaction of (*Z*)-2-butene in presence of water 211
Table 4.3. % Hydrogen atoms present at specified positions in reaction of (*Z*)-2-butene in presence of deuterium oxide 213
Table 4.4. % Hydrogen atoms present at specified positions in reaction of (*E*)-2-butene in presence of water 214
Table 4.5. % Hydrogen atoms present at specified positions in reaction of (*E*)-2-butene in presence of deuterium oxide 216

Table 4.6. % Hydrogen atoms present in 2-pentene with deuterium oxide at room temperature 217

Table 4.7. % Hydrogen atoms present in 2-pentene with deuterium oxide at 70 ^{o}C 218

Table 4.8. % Hydrogen left at indicated positions of (*E*)-anethole after specified time at room temperature 219

Table 4.9. % Hydrogen left at indicated positions of (*E*)-anethole after specified time at 70 ^{o}C.....219

Table 4.10. % Hydrogen left at indicated positions of (*E*)-anethole after specified time at room temperature under biphasic setting.....221

Table 4.11. % Hydrogen left at indicated positions of (*E*)-anethole after specified time at 70 ^{o}C under biphasic setting 222

Table 4.12. % Hydrogen left at the specified positions of (*E*)-propenyl ether with deuterium oxide at room temperature 223

Table 4.13. % Hydrogen left at the specified positions of 4-methyl-2-pentene with deuterium oxide at room temperature 224

Table 4.14. % Hydrogen left at the specified positions of (+)-limonene with deuterium oxide at 70 ^{o}C.....225

Table 4.15. % Hydrogen left at the specified positions of (+)-valencene with deuterium oxide at 70 ^{o}C.....227

Table 5.1. Results of initial arylamination screening with pre-formed complexes 237

LIST OF FIGURES

PAGE

Figure 1.1 Reaction catalyzed by LADH, oxidation of ethanol 3
Figure 1.2. Alcohol dehydrogenase mechanism of action in active site.....4
Figure 1.3. Oxidation of D-galactose to D-galacto-hexodialdose 5
Figure 1.4. Organization of the galactose oxidase active site.....5
Figure 1.5. Reaction mechanism proposed for galactose oxidase 6
Figure 1.6. Shvo's catalyst and proposed bifunctional mechanism.....7
Figure 1.7. Noyori's catalyst and proposed bifunctional mechanism.....8
Figure 1.8. Dearomatization and aromatization of Milstein's complexes 9
Figure 1.9. Representative bifunctional complexes developed in the Grotjahn lab 10
Figure 1.10. *Anti*-Markovnikov alkyne hydration 11
Figure 1.11. Alkyne hydrogen bonding in intermediates related to *anti*-Markovnikov hydration 12
Figure 1.12. Importance of pendant base substituents on structure and reactivity 13
Figure 1.13. Hydration equilibrium of CpRu imidazolyl comlexes **1.12** and **1.13**.....13
Figure 1.14. Comparison of pyridine and imidazole pendant base effect on chelate opening.....14
Figure 1.15. Homogenous phase and polymer-supported alkene isomerization catalyst 15
Figure 2.1. Selected alkene isomerizations involved in industrial processes 21
Figure 2.2. Isomerization by Wilkinson's catalyst 22
Figure 2.3. Isomerization of allyl groups by metathesis catalyst **2.2**.....23
Figure 2.3. Trost's ruthenium complexes for allylic alcohol isomerization 24
Figure 2.4. Improved cyclopentadienyl ruthenium complexes for allylic alcohol isomerization by Slugovc.....26
Figure 2.5. CpRu precursor, pyridylphosphines and imidazolylphosphines used for catalytic alkene isomerization screening.....28
Figure 2.6. Organic substrates used in catalytic alkene isomerization screening.....29
Figure 2.7. Alkene isomerization catalyst developed in Grotjahn research group 29

Figure 2.8. Catalytic cycle for alkene insertion mechanism of isomerization.....31
Figure 2.9. Catalytic cycle for allyl mechanism of alkene isomerization.....32
Figure 2.10 Proposed mechanism of alkene isomerization with **2.10** 33
Figure 2.11. Proposed mechanism by Tao et al. 34
Figure 2.12. Computational model of propene (shown with yellow colored carbons) formed after loss of CH_3CN from alkene isomerization catalyst **2.10**.....35
Figure 2.13. Sites for tuning of imidazolylphosphine ligands and catalysts 36
Figure 2.14. Alkene isomerization catalyst and its more sterically hindered analogues.....37
Figure 2.15. X-ray crystal structure of **2.26**, hydrogens and counter anion hidden for clarity.....39
Figure 2.16. X-ray crystal structure of **2.27**, hydrogens and counter anion hidden for clarity.....40
Figure 2.17. Heptene isomers with CH_3 or CH_2 groups used for NMR integrations highlighted 43
Figure 2.18. Synthesis of 4-(*tert*-Butyl)-2-(di-*iso*-propylphosphino)-1-methyl-1*H*-imidazole.....48
Figure 2.19. Synthesis of 4-(*tert*-Butyl)-2-(di-cyclohexylphosphino)-1-methyl-1*H*-imidazole.....49
Figure 2.20. Complexation of **2.25** to give **2.19** 50
Figure 2.21. Anion exchange of **2.19**.....51
Figure 2.22. Synthesis of **2.20** 69
Figure 2.23. Anion exchange of **2.20**.....70
Figure 2.24. Synthesis of di-1-adamantylphosphinic chloride 96
Figure 2.25. Synthesis of di-1-adamantylphosphine.....97
Figure 2.26. Synthesis of di-1-adamantylchlorophosphine 97
Figure 2.27. Synthesis of 4-(*tert*-butyl)-2-(di-1-adamatylphosphino)-1-methyl-1*H*-imidazole.....98
Figure 2.28. Synthesis of **2.21** 99
Figure 2.29. Synthesis of 4-(1-adamantyl)-2-(di-*iso*-propylphosphino)-1-methyl-1*H*-imidazole.....100
Figure 2.30. Complexation of **2.32** to give **2.22** 101
Figure 2.31. Synthesis of 4-(1-adamantyl)-2-(di-*tert*-butylphosphino)-1-methyl-1*H*-imidazole.....102

Figure 2.32. Complexation of **2.33** to give **2.23** 103

Figure 3.1. Immobilization of (*E*)-4-hydroxyproline.....124

Figure 3.2. Reactions catalyzed by polystyrene immobilized (*E*)-4-hydroxyprline. (a) Diasteroselective direct aldol reactions, (b) Enantioselective alpha-aminoxylation of ketones, (c) Enantioselective Mannich reactions 125

Figure 3.3. **PS-DES** synthesis from Merrifield resin.....125

Figure 3.4. Polymer-supported 2nd generation Hoveyda-Grubbs metathesis catalyst 126

Figure 3.5. Polymer-supported Felkin's iridium catalyst 128

Figure 3.6. Synthesis of polymer-supported alkene isomerization catalyst **PS-1**.....131

Figure 3.7. Synthesis of polymer-supported alkene isomerization catalyst **PSL-1**.....132

Figure 3.8. Isomerizations with **PS-1** and **PSL-1** under neat conditions.....136

Figure 3.9. Sequential polymer-supported alkene isomerization and silica-supported metathesis.....137

Figure 3.10. Examples of soluble polymers.....140

Figure 3.11. Borylation of **sPS** with Ir-catalyzed C-H activation.....141

Figure 3.12. Facile functionalization of **sPS-B(pin)** 142

Figure 3.13. Benzyl spacer installment on 4-(*t*Bu)-imidazole.....143

Figure 3.14. Synthesis of **sPS-B(pin)** and ^{1}H NMR signals used to calculate % incorporation.....144

Figure 3.15. Functionalization of **sPS-B(pin)** 145

Figure 3.16. Synthesis of **sPS-1**.....146

Figure 3.17. Synthesis of polystyrene-supported 4-*tert*-butyl-1-1*H*-imidazole.....147

Figure 3.18. Synthesis of 4-*tert*-butyl-2-(diisopropylphosphino)-1*H*-imidazole 148

Figure 3.19. Synthesis of **PS-1** 149

Figure 3.20. ^{31}P NMR spectrum of **PS-2** (left) and **PS-1** (right) 150

Figure 3.21. Synthesis of 2-(3-bromopropoxy)tetrahydro-2*H*-pyran 151

Figure 3.22. Synthesis of 4-*tert*-butyl-1-(3-(tetrahydro-2*H-pyran*-2-yloxy)propyl)-1*H*-imidazole.....152

Figure 3.23. 3-(4-*tert*-butyl-1*H*-imidazol-1-yl)propan-1-ol 153

Figure 3.24. Polystyrene-supprted 4-*tert*-butyl-1*H*-imidazol-1-yl group with linker.....154

Figure 3.25. Polystyrene-supported 4-*tert*-butyl-2-(diisopropylphosphino-1*H*-imidazole.....155

Figure 3.26. Synthesis of **PSL-1**.....156

Figure 3.27. Isomerization of 4-allylanisole 158
Figure 3.28. Isomerization of allyloxy(*tert*-butyl)dimethylsilane 159
Figure 3.29. Isomerization of *tert*-butyldimethyl(pent-4-enyloxy)silane 161
Figure 3.30. Isomerization of methylenecyclohexane 164
Figure 3.31. Isomerization of allyl ether 166
Figure 3.32. Isomerization of 4-penten-2-ol 167
Figure 3.33. Isomerization of 2-allylcyclohexanone 168
Figure 3.34. Isomerization of Eugenol 171
Figure 3.35. Sequential isomerization and metathesis of 4-allylanisole 177
Figure 3.36. Sequential isomerization and metathesis of eugenol 179
Figure 3.37. Sequential isomerization and metathesis of protected eugenol, (4-allyl-2-methylphenoxy)(*tert*-butyl)dimethylsilane 181
Figure 4.1. H/D exchange of aromatic and aliphatic C-H bonds reported by Bergman and coworkers 193
Figure 4.2. Deuteration of cyclooctene under hydrothermal conditions by Matsubara and coworkers 194
Figure 4.3. Deuteration of cyclohexene using microwave irradiation 195
Figure 4.4. H/D exchange reported by Brookhart and coworkers 195
Figure 4.5. Scope of H/D exchange with [(dtbpp)Ir(H)(NH_2)] 197
Figure 4.6. Proposed mechanism of isomerization and deuteration by **2.10** 201
Figure 4.7. Isomerization of linear olefins 202
Figure 4.8. (left) ^{1}H NMR spectrum of 2-butene in presence of water. Geometrical isomerization to a mixture of (*E*)- (major) and (*Z*)- (minor) 2-butenes in acetone-d_6; (right) ^{1}H NMR spectrum of 2-butene in presence of deuterium oxide. Conclusion: Deuteration is much more rapid than geometrical isomerization. 203
Figure 4.9. Isomerization and selective deuteration of branched olefins 204
Figure 4.10. Comparison progression of isomerization and H/D exchange of 4-allylanisole in homogeneous and biphasic settings over time 205
Figure 4.11. Deuteration of propene 209
Figure 4.12. ^{1}H NMR Spectrum of (*E*)-2-butene in acetone-d_6 (upper); (*E*)- (major) and (*Z*)- (minor) 2-butenes in acetone-d_6 210
Figure 4.13. Control experiment with (*Z*)-2-butene in presence of water 211
Figure 4.14. Control experiment with (*Z*)-2-butene in presence of deuterium oxide 212

Figure 4.15. Control experiment with (*E*)-2-butene in presence of water 214
Figure 4.16. Deuteration of (*E*)-2-butene 215
Figure. 4.17. Isomerization and deuteration of 1-pentene 216
Figure 4.18. Isomerization and deuteration of 4-allylanisole 218
Figure 4.19. Isomerization and deuteration of allyl ether 222
Figure 4.20. Isomerization and deuteration of 4-methyl-1-pentene 223
Figure 4.20. Selective deuteration of (+)-limonene 224
Figure 4.21. ^{1}H NMR Spectrum of (+)-limonene methyl peak 2 226
Figure 4.22. Selective deuteration of (+)-valencene 226
Figure 5.1. Pharmaceutical applications of cross-coupling reactions. 234
Figure 5.2. Representative ligands used for cross-coupling reactions 235
Figure 5.3. (η^3-Allyl)palladium chloride complexes prepared by Reji Nair 236
Figure 5. 4. Screening reaction and conditions for arylamination 237
Figure 5.5. *In situ* arylamination screening ligands and palladium precursors 238

ACKNOWLEDGEMENTS

I have to admit my years in graduate school have been better than I hoped for. First and foremost I'd like to thank Dr. Grotjahn for his endless patience, his support and his passion for sharing chemistry. He has been more than an advisor and he is a life-long mentor. Joining his group has been the decision that has definitely moved my life in the direction for the better and I am truly grateful for his guidance.

More than anything, my group have been the source of fun through endless days and nights of chemistry. I confess, I think sometimes we had more fun in the lab than anywhere else we could have been. We even wondered what's wrong with us, 10:30 pm –still working in lab- on a St. Patrick's night. I had the pleasure to work with many great chemists. Dr. Valentin Miranda, I've been secretly envious of the number of experiments you can get done. Dr. Sara Cortes-Llamas, the time you spent in Grotjahn lab during your Fulbright Scholarship will always be remembered by the one liner "I love beer", while caressing a bottle of Sam Adams. Jeff Gustafson, you are brilliant, wish had more time working with you. Jessica Lamonte is the person who cracked my shell to expose everybody to my goofiness; she is the one to blame. Now she is known as Jessica Martin, happily married to Kenny Martin; the man who gives the best hugs ever. It has pained me that you guys moved to Tennessee. But no matter what the geographical constraints are, I am grateful to be in your lives, I pray your friendship will always be by my side. Derek Brown, you are the one person I can count on for anything and not think twice. Thank you for being my rock and my sounding board. Hi, Hai! I know you hate it but I can't

help it. My source of local dining tips, thank you for making me look cool when I had a date. Derek and Hai, can't express how much I admire your work ethic, dedication and sense of responsibility. For all of us that worked with you during your years in lab, thank you for keeping the glovebox on constant resuscitation, for making chemistry possible and reliable. You were integral members of the Grotjahn group; he will be lucky to have more people like you to work for him. Dr. Reji Nair, high five, buddy! No more is needed. Andrea Rodriguez, one day you will save the world. Caline Abadjian, unicorn is a legendary animal from European folklore, Cherrielee, Forsythia, Baby Fifi, Star Swirl, Twist and Rarity are among the many unicorns of my little pony. How about that for random facts, but I bet you already knew. You are my favorite person to spend Valentine's, next time we should just go watch PBR in real life. Miss Caseypants, can you believe? You are the most unexpected friend of mine, wouldn't have thought of it in a million years that you would be one of the few people would end up knowing me so well. I admire your joy for life and your pure excitement about trivial things in life. You helped me appreciate small moments, hope your enthusiasm never changes, but I can't wait to see who you'll be when you grow up! Thank you for getting me through the day, for being the person who has my back. We have come so far. Your friendship is invaluable and what has made this experience even better is how we work well together; sharing ideas and information. Casey Larsen, I am so proud of you. Dave Marelius, Jayneil Kamdar, Evan Darrow, thank you for making this year fun. All the rest of Grotjahn Group members I had the chance to work with; Farhana Barmare, Zephen Specht, Adria Lombardo, David Catrone, Erik Paulson, Lily Cao, Maulen Utiliyev, Ariana Perez, Khoi Le, Abhi Sharma, Swetha Neravetla, Ruth Mendez, Ian Neel, Jeff

Rafalski, Christoff van Niekerk, Paul Lee, Marly De Gracia, Christie Shulte, Xi Zeng, Elijah Kragulj, Joanna Cuevas, Alice Lu, Meng Zhou. It has been fun!

The contents of Chapter 2 are similar to the material published in the following papers: Grotjahn, Douglas B.; Larsen, Casey; Erdogan, Gulin; Gustafson, Jeffrey; Sharma, Abhinandini; Nair, Reji. "Bifunctional catalysis of alkene isomerization and its applications" Chemical Industries (Boca Raton, FL, United States) **2009**, *123*, 379-387. Grotjahn, Douglas B; Larsen, Casey, R; Gustafson, Jeffery, L; Nair, Reji; Sharma, Abhinandini. "Extensive isomerization of alkenes using a bifunctional catalyst: an alkene zipper". *Journal of the American Chemical Society* **2007**, *129*, 9592-9593. The dissertation author was the primary researcher for the data presented and co-author on the papers included. The co-authors listed in these publications also participated in the research.

Chapter 3, in part is currently being prepared for submission for publication of the material. Erdogan, Gulin; Grotjahn, Douglas B. "Polystyrene-Supported Imidazolylphosphine Ligands and Cyclopentadienylruthenium Complexes for Highly Selective Alkene Isomerization, Facile Product Purification, and Sequential Isomerization / Metathesis" The dissertation author was the primary researcher for the data presented.

Chapter 4 contains material are similar to the material published in the following papers: Erdogan, Gulin; Grotjahn, Douglas B. "Catalysis of Selective Hydrogen/Deuterium Exchange at Allylic Positions Using Deuterium Oxide" *Topics in Catalysis* **2010**, 53, 1055, Erdogan, Gulin; Grotjahn, Douglas B. "Mild and Selective Deuteration and Isomerization of Alkenes by a Bifunctional Catalyst and Deuterium Oxide" *J. Am. Chem. Soc.*, **2009**, 131, 30, 10354, and Grotjahn, Douglas B; Larsen,

Casey R.; Erdogan, Gulin; Gustafson, Jeffery L.; Nair, Reji; Sharma, Abhinandini "Bifunctional Catalysis of Alkene Isomerization and Its Applications", *Catalysis of Organic Reactions* **2009**, 123, 379. The dissertation author was the primary researcher for the data presented.

Chapter 5, in part is currently being prepared for submission for publication of the material. Nair, Reji; Erdogan, Gulin; van Niekerk, Christoffel, Golen, James; Rheingold, Arnold; Grotjahn, Douglas. The dissertation author was the primary researcher for the data presented.

Cheryl and all the Severtsons; Lys, Anne, Maren; Todd Chamoy and the little ones; Navah and Ilan. I am truly blessed to be welcomed in your family. Cheryl, you have given me a sense of stability and belonging, made your home, my home. All of you supported me through all these years and encouraged me on the days that you didn't even know how low I felt. I hope to make it Thursday night family dinner for years to come.

Isabelle and Andrew Lerario, and James Caldwell my very first friends in San Diego! We had great time hiking, camping and all the trips we took looking for the trestle in the middle of nowhere. James, thank you for helping me get my first car and all the help to navigate through life in the United States. Isabelle and Andrew thank you for having me crash on your couch numerous times and making me always feel welcome and at home. I am looking forward to many more days to spend together in happy San Diego, finally enjoying the sunshine to the last drip!

Finally, I'd like to thank all my family for their confidence and trust in me. For letting me explore and supporting my decisions without doubt and quandary. My sister Mine, thank you for all the wonderful trips around the world and keeping me connected

to 41° N, 29° E. My sister Sema and cousin Senem, thank you for welcoming me home every time I visit.

CURRICULUM VITA

2005	B.S., Chemistry Bogazici University, Istanbul, Turkey
2011	M.A., Chemistry San Diego State University, San Diego, CA,
2012	Ph.D., Chemistry University of California, San Diego

PUBLICATIONS

Erdogan, Gulin; Grotjahn, Douglas B. "Catalysis of Selective Hydrogen/Deuterium Exchange at Allylic Positions Using Deuterium Oxide" *Topics in Catalysis* **2010**, 53, 1055.

Erdogan, Gulin; Grotjahn, Douglas B. "Mild and Selective Deuteration and Isomerization of Alkenes by a Bifunctional Catalyst and Deuterium Oxide" *J. Am. Chem. Soc.*, **2009**, 131, 30, 10354.

Grotjahn, Douglas B; Larsen, Casey R.; Erdogan, Gulin; Gustafson, Jeffery L.; Nair, Reji; Sharma, Abhinandini "Bifunctional Catalysis of Alkene Isomerization and Its Applications", *Catalysis of Organic Reactions* **2009**, 123, 379.

Grotjahn Douglas B; Miranda-Soto Valentin; Kragulj Elijah J; Lev Daniel A; Erdogan Gulin; Zeng Xi; Cooksy Andrew L., "Hydrogen-Bond Acceptance of Bifunctional

Ligands in an Alkyne-Metal pi Complex" *Journal of the American Chemical Society* **2008**, 130(1), 20.

Ata Akın, Uzay E. Emir, Didem Bilensoy, Gulin Erdogan, Selcuk Candansyar, Hayrunnisa Bolay, "fNIRS measurements in migraine", Proc. SPIE, Photonics West **2005,** 5693, 417.

ORAL PRESENTATIONS

Erdogan, Gulin; Grotjahn, Douglas B. "Bifunctional Complexes for Alkene Isomerization and Hydrogen-Deuterium Exchange" 243rd American Chemical Society National Meeting & Exposition, Anaheim, CA, USA, March 2012.

Erdogan, Gulin; Grotjahn, Douglas B. "Development of Bifunctional Phosphines and Their Metal Complexes: Applications in Alkene Isomerization, Hydrogen-Deuterium Exchange and Polymer-Immobilization" 5th Annual San Diego State University Student Seminar Symposium, San Diego, CA, USA, March 2012.

Erdogan, Gulin; Grotjahn, Douglas B. "Development of Bifunctional Phosphines and Their Metal Complexes: Applications in Hydrogen-Deuterium Exchange and Alkene Isomerization" Bogazici University Chemistry Department Seminars, Istanbul, Turkey, January 2012.

Erdogan, Gulin; Grotjahn, Douglas B. "Bifunctional Catalysis of Alkene Isomerization / Deuteration" 17th International Symposium on Olefin Metathesis and Related Chemistry (ISOM XVII), Pasadena, CA, USA, August 2008.

POSTER PRESENTATIONS

Erdogan, Gulin; Grotjahn, Douglas B. "Polystyrene Based Bifunctional Ligands and Their Applications in Catalytic Alkene Isomerization" Organometallic Chemistry Gordon Research Seminar and Organometallic Chemistry Gordon Research Conference, Salve Regina University, Newport, RI, USA, July 2011.

Erdogan, Gulin; Grotjahn, Douglas B. "Synthesis of Syndiotactic Polystyrene Based Bifunctional Ligands and Their Applications in Catalysis" 241st American Chemical Society National Meeting & Exposition, Anaheim, CA, USA, March 2011.

Erdogan, Gulin; Grotjahn, Douglas B. "Bifunctional alkene isomerization catalysts on polymer support " 239th American Chemical Society National Meeting & Exposition, San Francisco, CA, USA, March 2010.

Erdogan, Gulin; Grotjahn, Douglas B. "Catalysis of Selective Hydrogen/Deuterium Exchange at Allylic Positions Using Deuterium Oxide " 23rd Organic Reactions Catalysis Society Conference, Monterey, CA, USA, March 2010.

Erdogan, Gulin; Grotjahn, Douglas B. "Polymer Supported Alkene Isomerization Catalysts " 237th American Chemical Society National Meeting & Exposition, Salt Lake City, UT, USA, 2009.

Erdogan, Gulin; Grotjahn, Douglas B. "Bifunctional Catalysis of Alkene Isomerization / Deuteration" 17th International Symposium on Olefin Metathesis and Related Chemistry (ISOM XVII), Pasadena, CA, USA, August 2008.

Erdogan, Gulin; Grotjahn, Douglas B. "Progress in: Bifunctional Catalysis of Alkene Isomerization / Deuteration" 41st Annual Western Regional Meeting of the American Chemical Society, San Diego, CA, USA, November 2007.

Erdogan, Gulin; Grotjahn, Douglas B. " Alkene Isomerization and Deuteration" VI Simposio Internacional: Investigación Química EN LA Frontera Tijuana, B. C. México, 2006.

Erdogan, Gulin; Grotjahn, Douglas B. " Alkene Isomerization and Deuteration" 232nd American Chemical Society National Meeting & Exposition San Francisco, CA USA, 2006.

AWARDS

Inamori Fellowship 2011-2012.

Center for Enabling New Technologies Through Catalysis (CENTC) Summer School Attendance, 2010.

International Precious Metals Institute (IPMI) Outstanding Student Award, 2010.

North American Catalysis Society (NACS) Student Travel Award for Organic Reactions Catalysis Society (ORCS) Conference Participation, 2010.

MAJOR FIELDS OF STUDY

Major Field: Chemistry (Organic and Inorganic)

Studies in Synthesis and Organometallic Catalysis.
Professor Douglas B. Grotjahn

ABSTRACT OF THE DISSERTATION

Metal Complexes with Bifunctional Imidazolyl Phosphines for Catalytic Organic Transformations: Applications in Homogeneous and Polymer Supported Alkene Isomerization, and Hydrogen Deuterium Exchange

by

Gulin Erdogan

Doctor of Philosophy in Chemistry

University of California, San Diego, 2012

San Diego State University, 2012

Professor Douglas B. Grotjahn, Chair

The research covered in this thesis involves studying and understanding the behavior of bifunctional ligands, specifically imidazolylphoshines. The major field of study is reaction of cyclopentadienyl ruthenium complexes with olefins, namely alkene isomerization. In these complexes, the basic nitrogen of the imidazolylphosphine is thought to deprotonate coordinated alkene intermediates reversibly, facilitating isomerization of terminal alkenes to yield internal alkenes selectively. The CpRu alkene isomerization catalyst is capable of moving double bonds as far as 30 positions; further mechanistic studies in presence of deuterium labeling as a tool, has led to development of hydrogen deuterium exchange of olefins at allylic positions. This finding supports the

proposed mechanism and provides and outstanding deuteration at positions accessible by isomerization. The alkene isomerization catalyst can be used in a two-phase setting where the catalyst is dissolved in the organic layer and the non-toxic, non-flammable isotopic source (D_2O) is immiscible with the organic layer. Using biphasic settings one can literally wash out reactive protons on the substrate without using organic solvents.

In order to control high activity of alkene isomerization catalyst in absence of steric bulk provided by the substrate, bulkier phosphine ligands were synthesized and the activity of their metal complexes toward linear olefins was investigated. As a result, a family of catalysts that is capable of isomerizing unsubstituted linear alkenes to various mixtures have been established, where one can choose a complex to fit the needs of the process at hand. Further investigation with terminal alkenes bearing functional groups can be carried out to investigate whether mono-isomerization will still be the major transformation taking place, which is expected to give access to high-value 2-alkenes.

To provide easy product-catalyst separation and potential wider application, the first syntheses of polymer-supported imidazolylphophines were developed, and the alkene isomerization catalyst was thus immobilized on polystyrene-based Merrifield resin. Compared to the homogeneous catalyst, the immobilized catalysts give the same high (*E*)-selectivity and conversion in isomerizations of terminal olefins to internal olefins with very low metal leaching from the insoluble support. Furthermore, use of organic solvents can be excluded and isomerization can be carried out in neat liquid organic substrates.

CHAPTER 1

BIFUNCTIONAL CATALYSIS

Berzelius first introduced the term catalyst in 1835 and today the contribution of catalysis towards the global gross domestic product is about 35 %.[1] More than 90% of chemical and refining processes use catalysts[2] and the world is dependent on catalysts for food, fuel, plastics, synthetic fibers, and many other everyday commodities. The global demand for catalysts in 2010 was estimated at approximately 29.5 billion US dollars and ~850,000 tons in 2007. The worldwide annual demand for catalysts has been projected to increase by 3.5-4% annually through 2012.[3]

A catalyst accelerates a reaction without being consumed in the process, ensuring more efficient use of resources, and maximizing and optimizing the output of a process. Catalysis is essential to our ability to control chemical reactions, including those involved in energy-related transformations. Catalysis is therefore integral to solving current and future energy problems and a key to our sustainability.

Catalysts vary in composition from solid metal surfaces to gases. Traditionally, heterogeneous catalysts have been used for the large-scale production of commodity chemicals due to their robust nature and ease of separation. In contrast, homogenous catalysts offer high selectivity, the ability to produce pure products in high yield and are easier to modify in order to control a reaction. Although the broad use of soluble metal complexes did not begin until the 1940s their superiority mentioned above led to extensive use of homogenous catalysis in industry for syntheses of organic compounds. Today homogenous catalysis is responsible for worldwide production of commodities

like adiponitrile via but-1,3-diene hydrocyanation (Du Pont), detergent range alkenes via Shell Higher Olefins Process (SHOP), poly(ethylene terephtalate) (PET) via polycondensation of terephtalic acid with ethylene glycol.[4]

The wider application of homogenous catalysis is closely related to in-depth understanding of the chemistry involved. The ease of the mechanistic investigation of homogeneous catalysts is a distinct advantage, opening rational ways to develop novel and superior catalysts. In conventional metal-based homogeneous catalysts, catalysis is essentially performed at the metal center, with the ligands not actively participating in bond-making and -breaking of the substrate(s). However, there is a special class of catalysts that operates by cooperation between the metal center and surrounding ligands, referred to as bifunctional catalysts.

Examples of bifunctional catalysts are widely found in biological systems. Liver alcohol dehydrogenase (ADH) catalyzes the oxidation of primary and secondary alcohols and can also catalyze the reverse reaction, reduction of respective aldehydes and ketones. In humans, alcohol dehydrogenase exists as a dimer, in multiple forms divided into five classes. The enzyme is present in the liver and the lining of the stomach in high concentrations. The active enzyme is a dimer of identical subunits and each subunit has two domains, the catalytic active-site domain and the coenzyme-binding domain.[5]

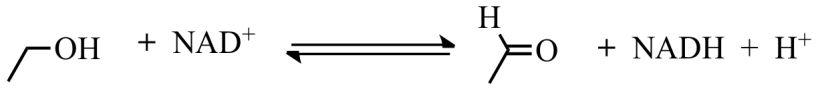

Figure 1.1 Reaction catalyzed by LADH, oxidation of ethanol

The active site (Figure 1.2) consists of a zinc atom, His67, Cys174, Cys46, Ser48, His51, Ile269, Val292, Ala317, and Phe319. The zinc is coordinated by Cys46, Cys174,

and His67 along with a water molecule, which is thought to be displaced by the alcohol substrate. Phe319, Ala317, His51, Ile269 and Val292 appear to stabilize NAD^+ by forming hydrogen bonds. Zinc is considered to act as a Lewis acid on the complexed alcohol molecule or carbonyl group of the aldehyde, facilitating the deprotonation of alcohol or nucleophilic attack on a carbonyl group. In the classical mechanism, the alcohol is thought to be deprotonated by Ser48 and the proton transported out of the active site via a hydrogen bond network involving NAD^+ and His51. Hydride transfer from the α-carbon of alcohol to NAD^+ would result in zinc-bound aldehyde or ketone and NADH, and release of these products are considered the final steps in the catalytic cycle.[5,6]

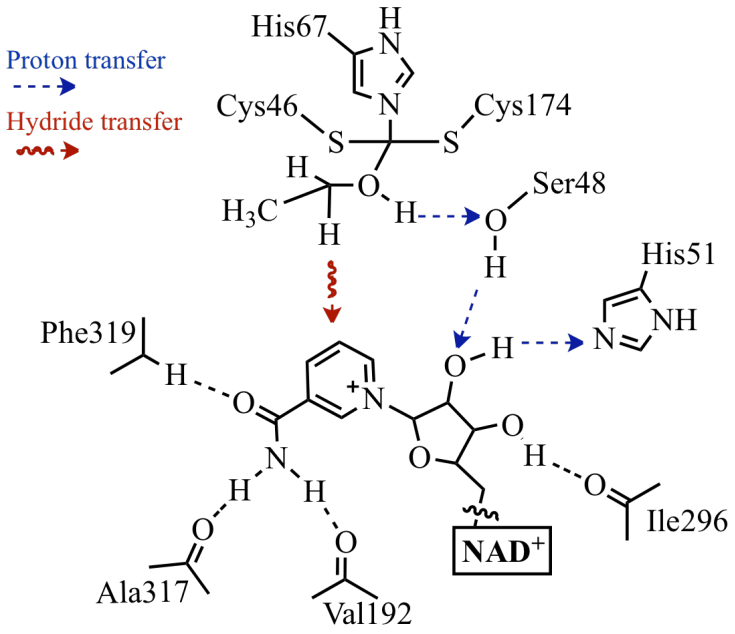

Figure 1.2. Alcohol dehydrogenase mechanism of action in active site

Another example of a bifunctional catalyst is galactose oxidase, a fungal secretory enzyme which is one of the best-characterized free-radical enzymes. Galactose oxidase

has found use in quantitative determination of galactose in blood and other biological fluids.[7-9] The overall reaction catalyzed (Figure 1.3) is oxidation of a primary alcohol to aldehyde coupled with reduction of oxygen to hydrogen peroxide.

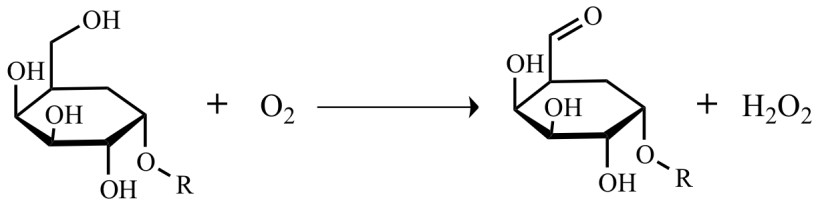

Figure 1.3. Oxidation of D-galactose to D-galacto-hexodialdose

The crystal structure of galactose oxidase[10] shows (Figure 1.4) that the Cu(II) center is bound to two histidine and two tyrosine residues and a water molecule in a square pyramidal fashion. One of the tyrosine ligands is bound axially and can act as a general base, while the other is cross-linked to a cysteine residue, forming a Tyr-Cys dimer. A tryptophan residue is stacked over the Tyr-Cys dimer and is thought to contribute stabilization of the free radical formed.

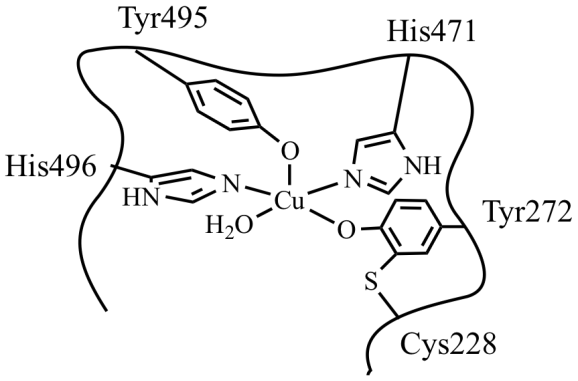

Figure 1.4. Organization of the galactose oxidase active site

The mechanism proposed (Figure 1.5) predicts that galactose replaces the water molecule in the equatorial position and proton from the alcohol is transferred to the axial

tyrosinate (Tyr495). Next, a hydrogen atom is transferred from the substrate to the equatorial Tyr-Cys dimer radical and resulting species is oxidized through electron transfer to the copper center yielding Cu(I) and aldehyde. Finally, Cu(I) and tyrosine are reoxidized by oxygen to regenerate Cu(II) and give hydrogen peroxide. The oxygen reduction half reaction is less well-characterized and proposed to involve a hydroperoxide adduct (F) which may be protonated at the proximal oxygen (G) and give the hydrogen peroxide product.[11,12]

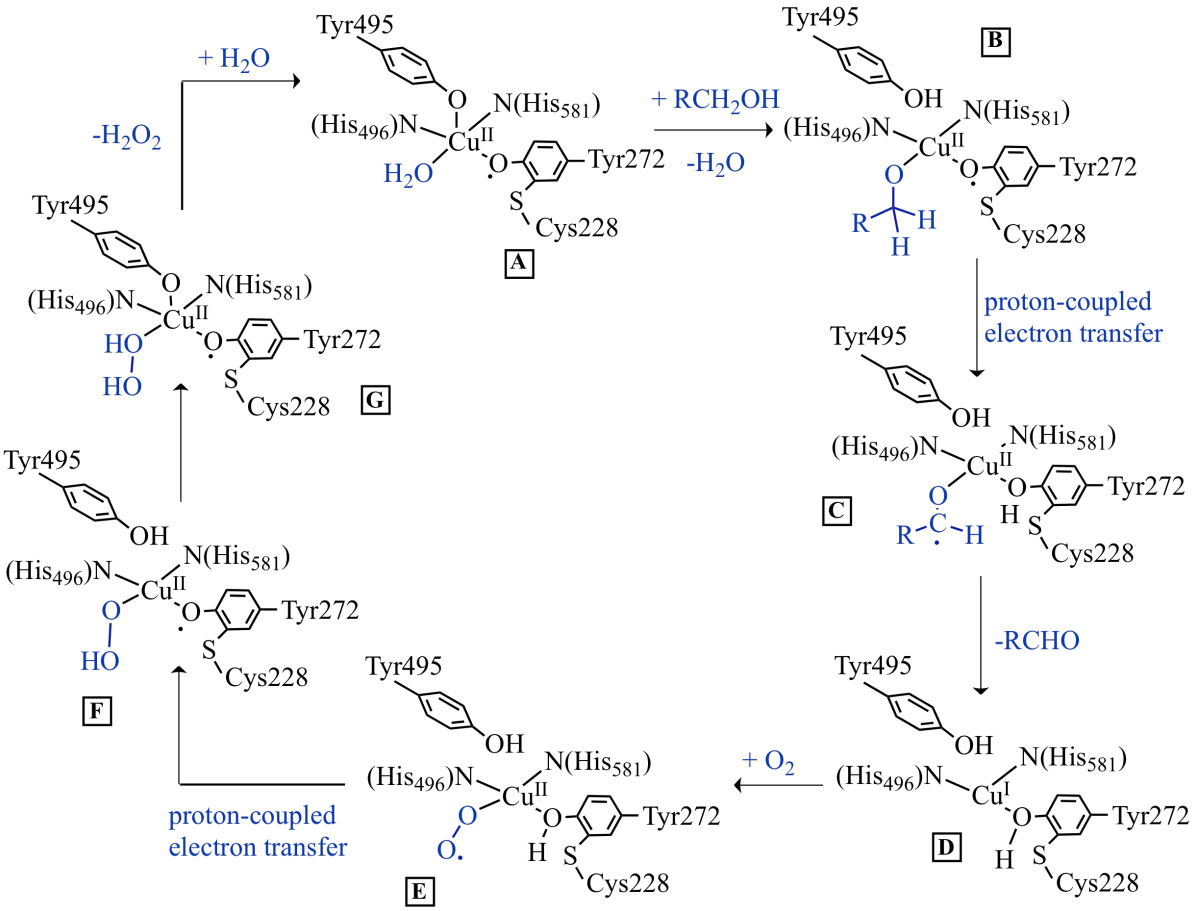

Figure 1.5. Reaction mechanism proposed for galactose oxidase

The design of synthetic bifunctional catalysts has frequently been based on mimicking biological systems.[13-21] Shvo's hydride catalyst[22,23] reported in 1985 is one of

the earlier examples of metal-ligand cooperating bifunctional catalyst. The diruthenium complex is activated by heat and dissociates into two catalytically active monoruthenium complexes, an 18 e^- complex that can be isolated and a 16 e^- complex that has never been directly observed, these two species are thought to interconvert throughout the catalytic cycle. The 18 e^- complex is proposed to simultaneously transfer hydride from the metal center and a proton from the hydroxyl group on the cyclopentadiene ligand to hydrogenate a ketone or imine. Subsequently, the 16 e^- species formed would act as a dehydrogenation catalyst to give a new molecule of 18 e^- complex. The mechanism has been extensively studied and recent reviews have been published on applications[24-27] and mechanism[26,28,29] of Shvo's catalyst and related species.

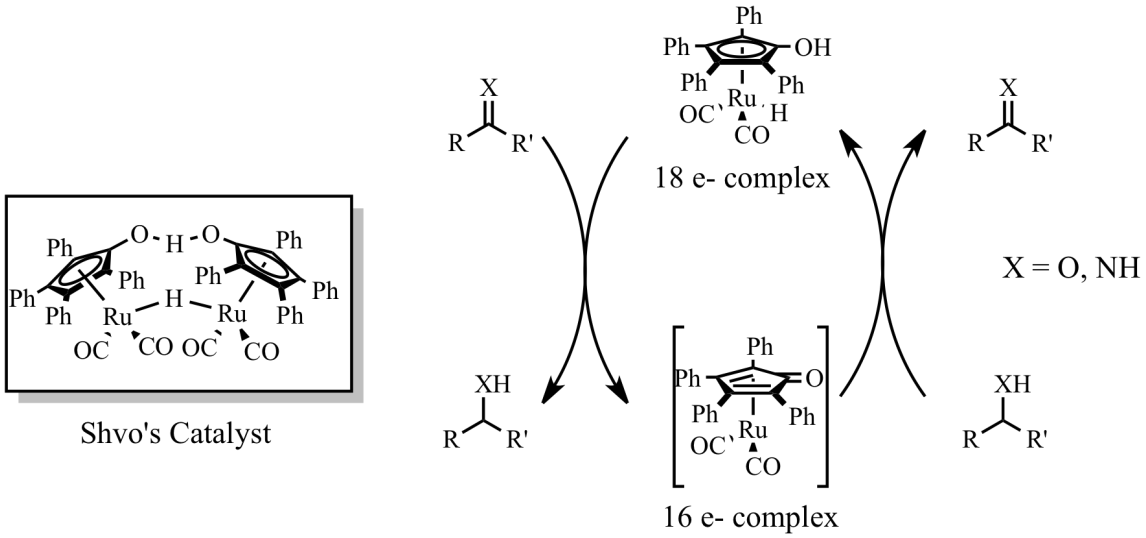

Figure 1.6. Shvo's catalyst and proposed bifunctional mechanism

The Nobel Prize recipient in 2001, Ryoji Noyori, developed a bifunctional ruthenium catalyst based on metal and N-H acid base cooperation for asymmetric hydrogenation of ketones and imines. The hydrogen transfer between an alcohol and a ketone is thought to take place reversibly through a six-membered pericyclic transition

state (Figure 1.7). The amido Ru complex would dehydrogenate an alcohol leading to the amine hydrido complex, which in turn would react with carbonyl compounds to transfer the hydride and a proton to the carbonyl yielding the alcohol product. When formic acid is used for the asymmetric reduction, the reaction proceeds irreversibly with kinetic enantioselection, in principle 100% conversion.[18,30-33]

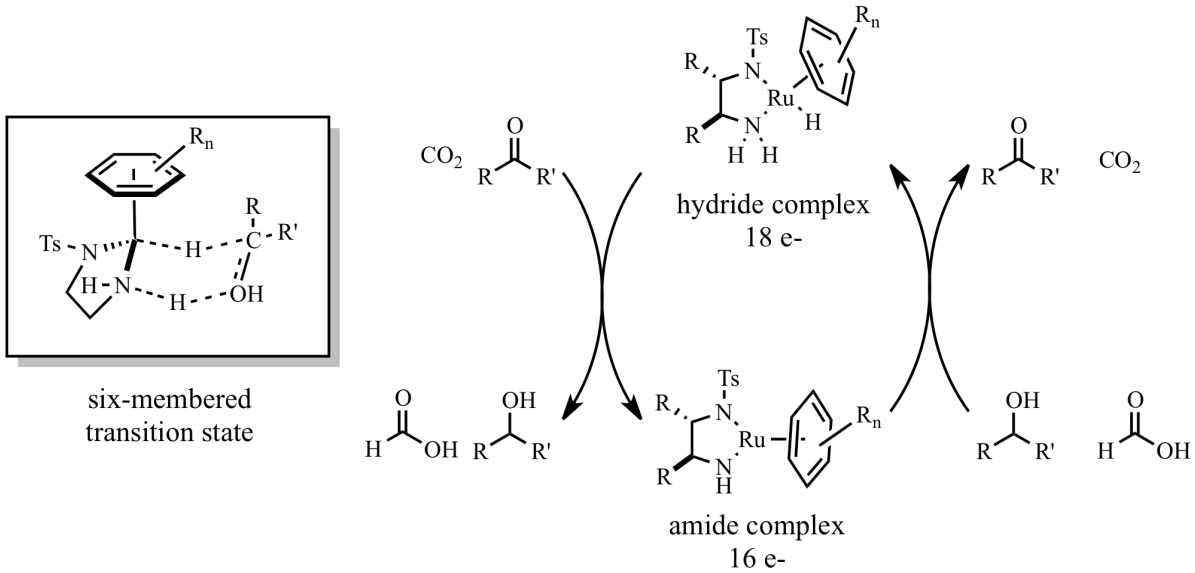

Figure 1.7. Noyori's catalyst and proposed bifunctional mechanism

More recently, Milstein reported a new mode of bond activation by metal-ligand cooperation based on dearomatization-aromatization of pyridine- and acridine-based heteroaromatic pincer complexes (Figure 1.8). Deprotonation of a pyridinyl methylene of the pincer ligand can lead to dearomatization, and the resulting complex can activate a chemical bond H-Y where Y can be H, OR, NR_2 or C, by cooperation between the ligand and the metal, without changing the oxidation state of the metal. These types of complexes can be catalytically used in conversion of alcohols into esters and dihydrogen,[34] synthesis of amides from alcohols and amines,[35] coupling of alcohols with

amines to form imines and dihydrogen,[36] selective synthesis of primary amines from alcohols and ammonia,[37] hydrogenation of esters to alcohols,[38] and hydrogenation of carbon dioxide to formate salts.[39]

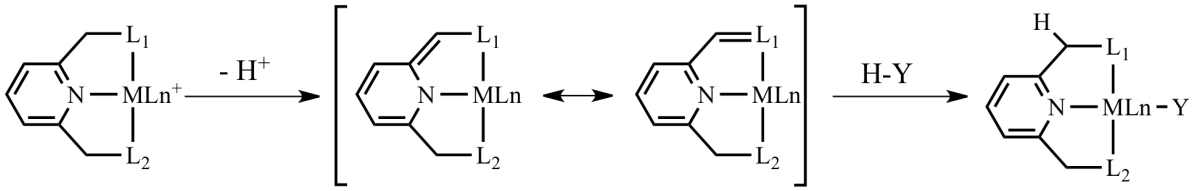

Figure 1.8. Dearomatization and aromatization of Milstein's complexes

Catalysis research in the Grotjahn group focuses on complexes bearing a potential hydrogen acceptor or donor present in the ligands. The bifunctional ligands most studied in the Grotjahn lab are heteroaryl-substituted phosphines, in which the heteroaryl ring is either five- or six-membered and includes one or more nitrogens, e.g. imidazole, pyridine, pyrimidine, or pyrazole rings.[40-47]

In 2004, Lev[44] et al. reported that cyclopentadienyl ruthenium complex **1.6** (Figure 1.9) developed in the Grotjahn group (now commercially available from Strem Chemicals) catalyzes *anti*-Markovnikov alkyne hydration at 70 ^{o}C with initial TOF of 23.8 mol aldehyde per mol catalyst per hour. When the alkyne hydration is uncatalyzed (70 ^{o}C, 5 equivalents of H_2O), 1-nonyne did not hydrate to the ketone or the aldehyde after 28 days.

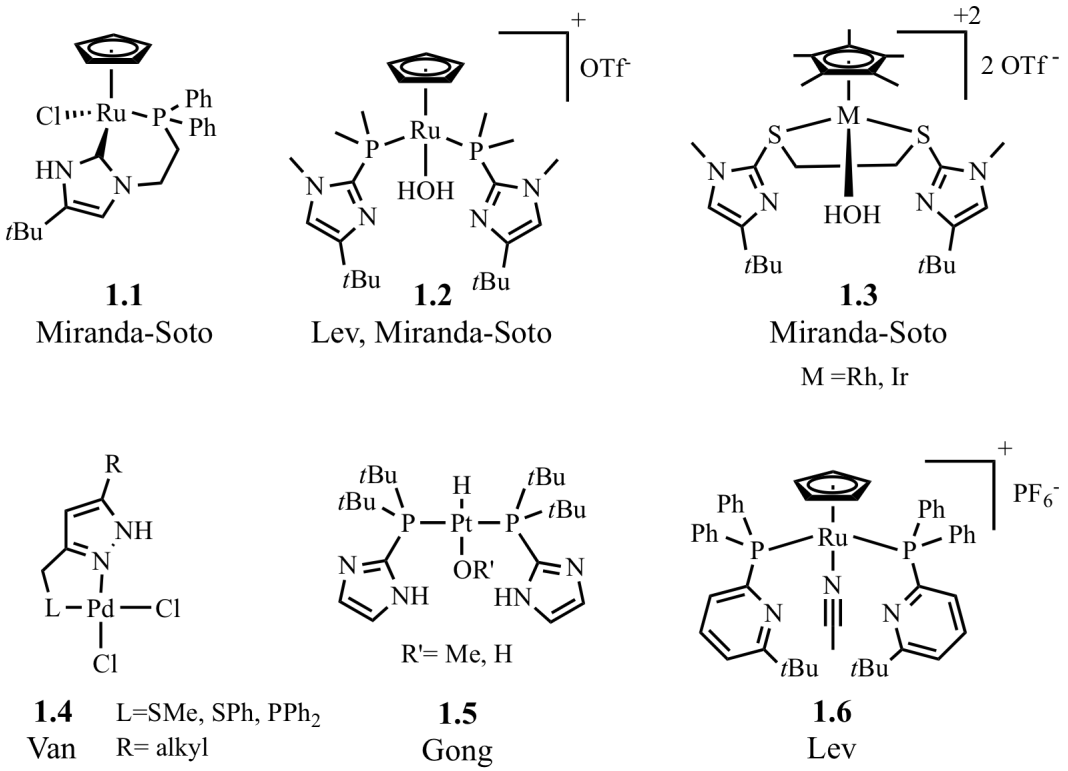

Figure 1.9. Representative bifunctional complexes developed in the Grotjahn lab

The detection limit of this reaction was estimated to be 2 ppm; therefore, the rate of the uncatalyzed reaction is less than 3 x 10^{-9} mol per hour, giving a half-life of at least 20,000 years. When hydration is catalyzed with a Brønsted-Lowry acid, e.g. $HNTf_2$, the ratio of ketone produced with respect to aldehyde is 33 to 1. Thus an upper bound for the rate of aldehyde formation is 1 x 10^{-10} mol per hour. A half-life for aldehyde formation of at least 600 000 years is estimated from the observation that under protic conditions the appearance of aldehyde is 33 times slower than of the ketone. Since **1.6** gives initial TOF of 23.8 mol aldehyde per mol catalyst per hour, a catalytic rate acceleration of >2.4 x 10^{11} was calculated. As for selectivity, there is no detectable ketone from the hydration of 1-nonyne by **1.6** under conditions where one could detect one part ketone in the presence of

10,000 parts aldehyde. Thus, compared with protic catalysis, **1.6** changes the selectivity of alkyne hydration by a factor of over 300 000.

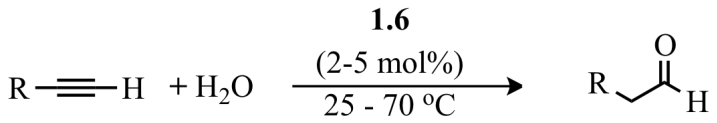

Figure 1.10. *Anti*-Markovnikov alkyne hydration

In studying the origin of remarkable rate enhancements in alkyne hydration, the presence of C-H-N hydrogen bonding in an alkyne π complex was revealed using NMR coupling information, from both data within the alkyne ligand as well as between alkyne and pyridine ($^{2h}J_{CN}$) (Figure 1.11). Scalar coupling across a hydrocarbon C-H bond ($^{2h}J_{CN}$ = 3 Hz) was part of showing that the C-H was engaged in a hydrogen bond with a ligand nitrogen. Comparison made with the complex lacking the pendant nitrogens revealed the difference in couplings observed involving the alkyne hydrogens. The $^{1}J_{CC}$ values of both **1.7** and **1.9** are pointing to identical the similar electronic nature of both phosphine ligands. The difference in $^{1}J_{CH}$ **1.7** and **1.9,** combined with observation of $^{2h}J_{CN}$ of **1.7** strongly suggests presence of hydrogen bonding.[48]

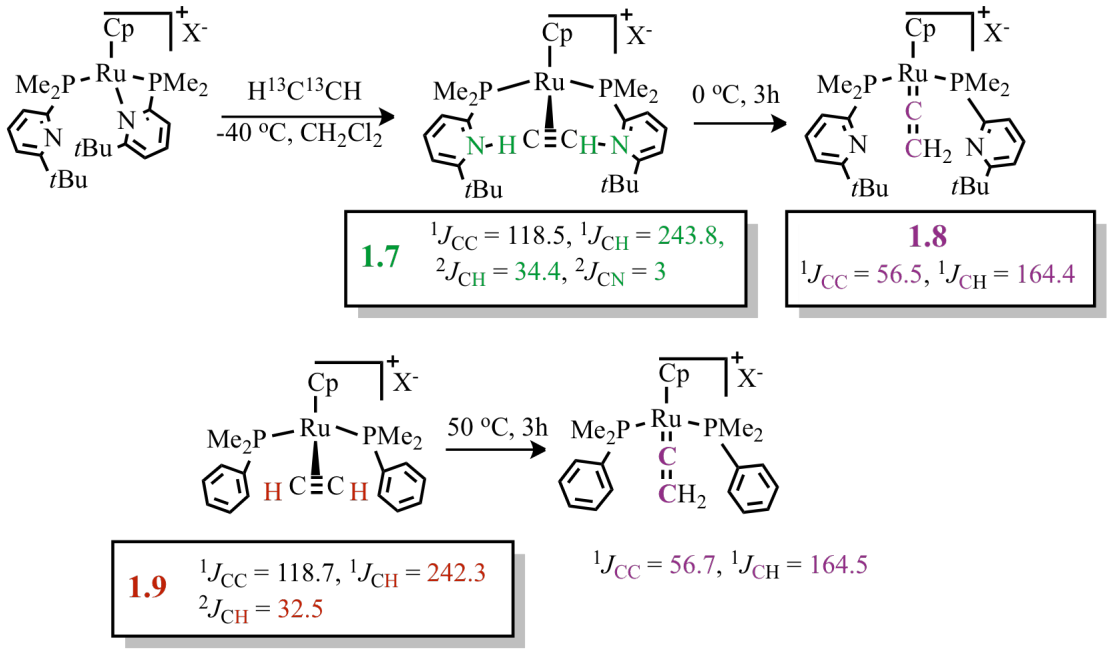

Figure 1.11. Alkyne hydrogen bonding in intermediates related to *anti*-Markovnikov hydration

Hydrogen-bonding networks have been observed with complexes **1.2** and **1.3**; in the case of rhodium and iridium analogue of **1.3**, X-ray structural data also supports the binding of water and the hydrogen bonding to imidazole nitrogens. Both of these complexes show moderate activity in base-free transfer hydrogenation of acetphenone by 2-propanol.[45]

Another lesson learned from *anti*-Markovnikov alkyne hydration is the importance of steric bulk in close proximity to basic nitrogen on heterocycle. Comparison of complex **1.10** and its analogue **1.11** where C6 is bearing a hydrogen atom instead of *tert*-butyl, aquo complex of **1.11** is not formed even upon heating up to 70 °C when 1000 equivalent of water is present. Where as, **1.10-aquo** is formed and **1.10** is quickly consumed with as little as 5 equivalents of water at room temperature.[49,50]

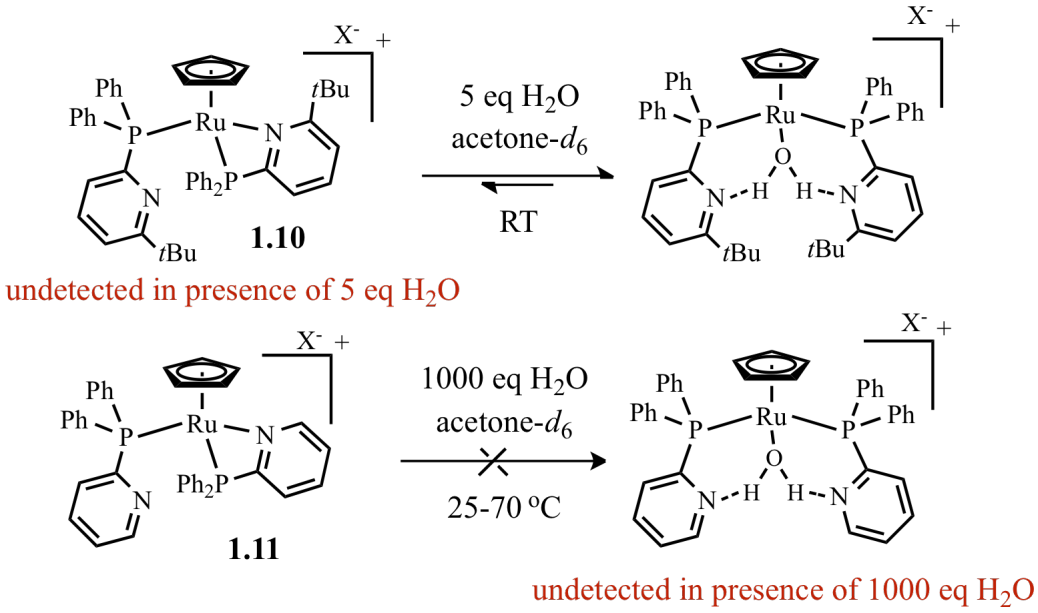

Figure 1.12. Importance of pendant base substituents on structure and reactivity

In accordance to this observation, when hydration equilibrium of **1.2** analogues **1.12** and **1.13** was studied, the equilibrium shifts by 50-fold, from favoring chelation in the case of **1.7** (K_{eq} ~ 400 M^{-1}) to aquo complex formation when C4 is substituted in **1.8** (K_{eq} ~ 20,000 M^{-1}).[49]

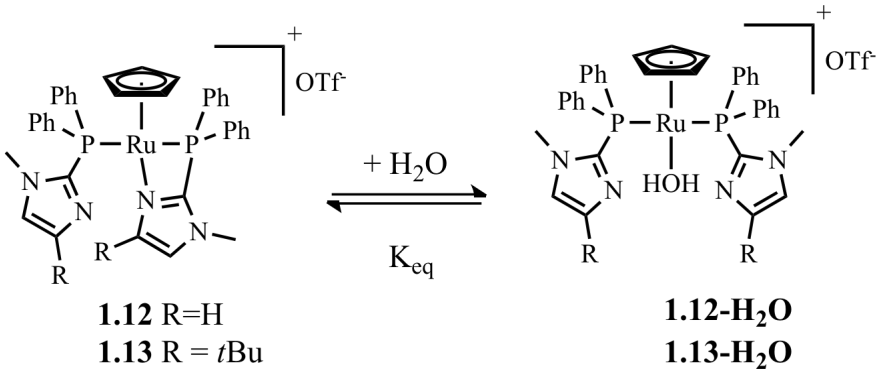

Figure 1.13. Hydration equilibrium of CpRu imidazolyl comlexes 1.12 and 1.13

Comparing carbonylation of **1.11** to **1.12** the observed half-lives are 15 minutes and one day for imidazolyl pendant base and pyridyl pendant base, respectively. The

conclusion that can be drawn is, that the imizadole chleate opens more readily than the pyridine chelate under the same conditions in absence of steric bulk around the chelating basic nitrogen.

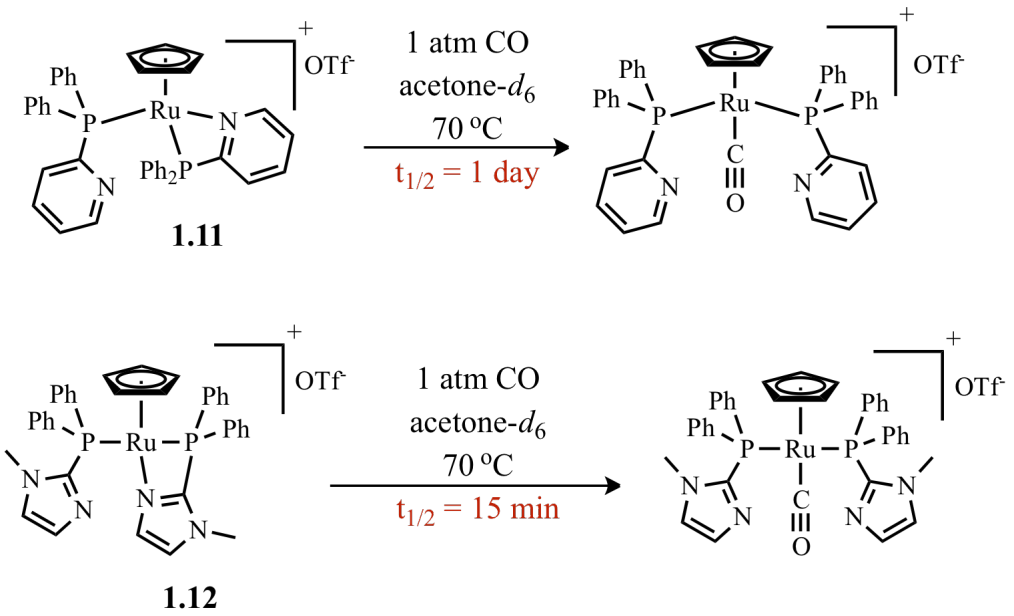

Figure 1.14. Comparison of pyridine and imidazole pendant base effect on chelate opening

The research covered in this thesis involves studying and understanding the behavior of bifunctional ligands, specifically imidazolylphoshines, applying the lessons learned from *anti*-Markovnikov alkyne hydration and looking for reactivity with cyclopentadienyl ruthenium complexes with olefins is the major subject studied. The mechanistic studies using deuterium labeling as a tool, has led to development of hydrogen deuterium exchange of olefins at allylic positions. Unique activity and selectivity of alkene isomerization catalyst, (Figure 1.15), has made it attractive for organic transformations and as of April 2012 it is commercially available through Strem Chemicals. The CpRu alkene isomerization catalyst (Figure 1.15) is capable of moving

double bonds as far as 30 positions; in order to tame its high activity in absence of steric bulk provided by the substrate, bulkier phosphine ligands were synthesized and the activity of catalysts made with them toward linear olefins has been investigated (Chapter 2). To provide easy separation and potential wider application, the alkene isomerization catalyst has been immobilized on polystyrene-based Merrifield resin (Chapter 3). In the search for new catalysts for arylamination, imidazolyl phophine complexes have been used to investigate coupling reactions between halotoluenes and morpholine (Chapter 5).

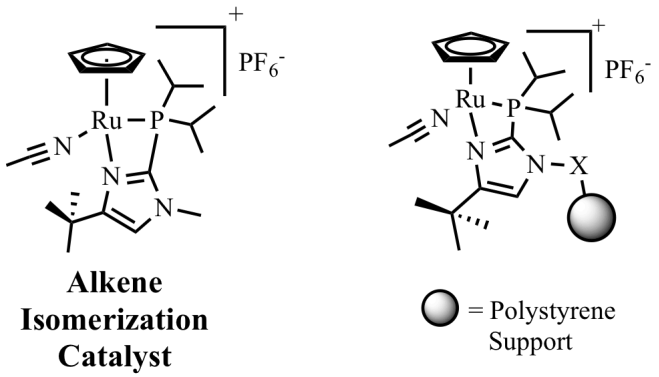

Figure 1.15. Homogenous phase and polymer-supported alkene isomerization catalyst

REFERENCES

(1) Adams, C. *Chem Ind-London* **1999**, 740.

(2) In *R&D Magazine* 2005; Vol. September.

(3) *Market Reports: World Catalyst Market*, 2008.

(4) Whyman, R. *Applied organometallic chemistry and catalysis*; Oxford University Press: Oxford ; New York, 2001.

(5) Dolega, A. *Coordin Chem Rev* **2010**, *254*, 916.

(6) Hammes-Schiffer, S.; Benkovic, S. J. *Annu Rev Biochem* **2006**, *75*, 519.

(7) Frings, C. S.; Pardue, H. L. *Anal Chem* **1964**, *36*, 2477.

(8) Roth, H.; Segal, S.; Bertoli, D. *Anal Biochem* **1965**, *10*, 32.

(9) Hankin, L. *J Assoc Off Ana Chem* **1967**, *50*, 1342.

(10) Firbank, S. J.; Rogers, M. S.; Wilmot, C. M.; Dooley, D. M.; Halcrow, M. A.; Knowles, P. F.; McPherson, M. J.; Phillips, S. E. V. *P Natl Acad Sci USA* **2001**, *98*, 12932.

(11) Que, L.; Tolman, W. B. *Nature* **2008**, *455*, 333.

(12) Whittaker, J. W. *Arch Biochem Biophys* **2005**, *433*, 227.

(13) Breslow, R. *Accounts Chem Res* **1995**, *28*, 146.

(14) Steinhagen, H.; Helmchen, G. *Angewandte Chemie-International Edition in English* **1996**, *35*, 2339.

(15) van den Beuken, E. K.; Feringa, B. L. *Tetrahedron* **1998**, *54*, 12985.

(16) Rowlands, G. J. *Tetrahedron* **2001**, *57*, 1865.

(17) Clapham, S. E.; Hadzovic, A.; Morris, R. H. *Coordin Chem Rev* **2004**, *248*, 2201.

(18) Ikariya, T.; Murata, K.; Noyori, R. *Org Biomol Chem* **2006**, *4*, 393.

(19) Das, S.; Brudvig, G. W.; Crabtree, R. H. *Chem Commun* **2008**, 413.

(20) Natale, D.; Mareque-Rivas, J. C. *Chem Commun* **2008**, 425.

(21) Grotjahn, D. B. *Chem-Eur J* **2005**, *11*, 7146.

(22) Blum, Y.; Shvo, Y. *Israel J Chem* **1984**, *24*, 144.

(23) Blum, Y.; Czarkie, D.; Rahamim, Y.; Shvo, Y. *Organometallics* **1985**, *4*, 1459.

(24) Shvo, Y.; Czarkie, D.; Rahamim, Y.; Chodosh, D. F. *J Am Chem Soc* **1986**, *108*, 7400.

(25) Karvembu, R.; Prabhakaran, R.; Natarajan, K. *Coordin Chem Rev* **2005**, *249*, 911.

(26) Conley, B. L.; Pennington-Boggio, M. K.; Boz, E.; Williams, T. J. *Chemical Reviews* **2010**, *110*, 2294.

(27) Samec, J. S. M. B., J. E. In *Encyclopedia of Reagents for Organic Synthesis*; Wiley: New York, 2008.

(28) Samec, J. S. M.; Backvall, J. E.; Andersson, P. G.; Brandt, P. *Chem Soc Rev* **2006**, *35*, 237.

(29) Comas-Vives, A.; Ujaque, G.; Lledos, A. *J Mol Struc-Theochem* **2009**, *903*, 123.

(30) Noyori, R.; Yamakawa, M.; Hashiguchi, S. *J Org Chem* **2001**, *66*, 7931.

(31) Koike, T.; Ikariya, T. *Adv Synth Catal* **2004**, *346*, 37.

(32) Fujii, A.; Hashiguchi, S.; Uematsu, N.; Ikariya, T.; Noyori, R. *J Am Chem Soc* **1996**, *118*, 2521.

(33) Uematsu, N.; Fujii, A.; Hashiguchi, S.; Ikariya, T.; Noyori, R. *J Am Chem Soc* **1996**, *118*, 4916.

(34) Zhang, J.; Leitus, G.; Ben-David, Y.; Milstein, D. *J Am Chem Soc* **2005**, *127*, 12429.

(35) Gunanathan, C.; Ben-David, Y.; Milstein, D. *Science* **2007**, *317*, 790.

(36) Gnanaprakasam, B.; Zhang, J.; Milstein, D. *Angew Chem Int Edit* **2010**, *49*, 1468.

(37) Gunanathan, C.; Milstein, D. *Angew Chem Int Edit* **2008**, *47*, 8661.

(38) Zhang, J.; Leitus, G.; Ben-David, Y.; Milstein, D. *Angew Chem Int Edit* **2006**, *45*, 1113.

(39) Ben-Ari, E.; Leitus, G.; Shimon, L. J. W.; Milstein, D. *J Am Chem Soc* **2006**, *128*, 15390.

(40) Grotjahn, D. B.; Brown, D. B.; Martin, J. K.; Marelius, D. C.; Abadjian, M. C.; Tran, H. N.; Kalyuzhny, G.; Vecchio, K. S.; Specht, Z. G.; Cortes-Llamas, S. A.; Miranda-Soto, V.; van Niekerk, C.; Moore, C. E.; Rheingold, A. L. *J Am Chem Soc* **2011**, *133*, 19024.

(41) Grotjahn, D. B. *Dalton Trans* **2008**, 6497.

(42) Grotjahn, D. B.; Gong, Y.; DiPasquale, A. G.; Zakharov, L. N.; Rheingold, A. L. *Organometallics* **2006**, *25*, 5693.

(43) Grotjahn, D. B.; Van, S.; Combs, D.; Lev, D. A.; Schneider, C.; Rideout, M.; Meyer, C.; Hernandez, G.; Mejorado, L. *J Org Chem* **2002**, *67*, 9200.

(44) Grotjahn, D. B.; Lev, D. A. *J Am Chem Soc* **2004**, *126*, 12232.

(45) Miranda-Soto, V.; Parra-Hake, M.; Morales-Morales, D.; Toscano, R. A.; Boldt, G.; Koch, A.; Grotjahn, D. B. *Organometallics* **2005**, *24*, 5569.

(46) Miranda-Soto, V.; Grotjahn, D. B.; Cooksy, A. L.; Golen, J. A.; Moore, C. E.; Rheingold, A. L. *Angew Chem Int Edit* **2011**, *50*, 631.

(47) Miranda-Soto, V.; Grotjahn, D. B.; DiPasquale, A. G.; Rheingold, A. L. *J Am Chem Soc* **2008**, *130*, 13200.

(48) Grotjahn, D. B.; Miranda-Soto, V.; Kragulj, E. J.; Lev, D. A.; Erdogan, G.; Zeng, X.; Cooksy, A. L. *J Am Chem Soc* **2008**, *130*, 20.

(49) Lev, D. A., University of California, San Diego and San Diego State University, 2004.

(50) Grotjahn, D. B. *Pure Appl Chem* **2010**, *82*, 635.

CHAPTER 2

DEVELOPMENT OF NEW BIFUNCTIONAL CYCLOPENTADIENYL RUTHENIUM IMIDAZOLYL PHOSPHINE COMPLEXES FOR CONTROLLED ALKENE ISOMERIZATION

INTRODUCTION

This chapter describes some of my experimental and computational efforts to improve selectivity of bifunctional alkene isomerization catalysts developed in the Grotjahn lab, followed by an overview of alkene isomerization challenges and scope. Alkene isomerization is an atom-efficient reaction an a key step in major industrial processes.[1] It is used for in petrochemical refining processes and in the synthesis of linear olefins in the SHOP process or adiponitrile preparation from butadiene and HCN, where two isomerization steps are involved.[2] Carbon-carbon double bond shift is also largely employed in the synthesis of pharmaceuticals and fine chemicals such as flavors and fragrances.[3-6] Significant examples (Figure 2.1) are (i) enantioselective isomerization of (*E*)- and (*Z*)-diethylgeranylamine to (*R*)-citronellal-(*E*)-enamine as the key enantiodetermining step in synthesis of (-)-menthol on the scale of 3,000 tons per year by Takasago International Corporation,[7] (ii) 6-methyl-6-hepten-2-one isomerization in vitamin A synthesis used by BASF,[8] and (iii) the isomerization of allyl benzene derivatives such as safrole, estragole, and eugenol to the corresponding internal alkenes which are used to enhance flavor in food or beverages in industry.[2]

Isomerization step in (-)-menthol synthesis

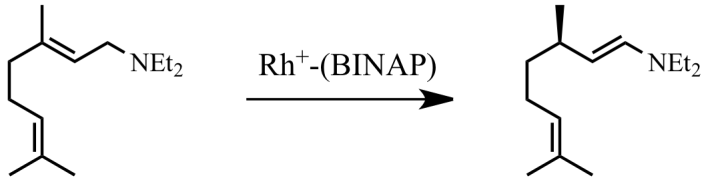

Isomerization step in vitamin A synthesis

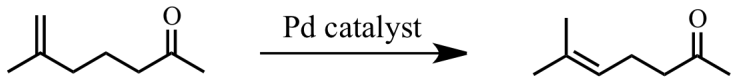

Isomerization for (*E*)-anethole synthesis

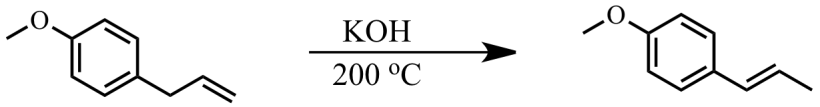

Figure 2.1. Selected alkene isomerizations involved in industrial processes

In the isomerization of allyl benzene derivatives, high selectivity for the (*E*)-isomer is an important challenge since (*Z*)-isomers are characterized by an unpleasant taste and sometimes a toxic nature, so highly pure (*E*)-products are required for market (less than 1% (*Z*)-isomer content for human use). Currently, tedious purification steps are required to separate the isomers, therefore there is an increasing interest in the development of highly selective isomerization processes to reduce production costs. At present, industrial isomerization of 4-allylanisole (estragole) to (*E*)-anethole is performed with potassium hydroxide (KOH) at high temperatures (200 ^{o}C) with moderate yields of about 56% and (*E*) to (*Z*) ratio of 82:18, while most fragrances reported above are still obtained by extractions from natural sources with an overall annual production of several million metric tons.[9] Many more processes of alkene isomerization are a topic of interest,[10-22] hence selective olefin isomerization under mild conditions is a goal that

deserves increased attention from organometallic chemists.

Transition metal-catalyzed olefin isomerization in organic chemistry can be achieved with many metals, across the periodic table. To name a few metals, Fe,[23-30] Ir,[30-36] Pd,[37-39] Ti,[40-43] Ni,[44-47] Rh,[30,34,48-51] and Ru complexes are capable of carbon-carbon double bond isomerization. Wilkins88on's catalyst $RhCl(PPh_3)_3$, **2.1** (Figure 2.2), can be employed in isomerization of allylic ethers to give enol ethers, which can hydrolyze to give free alcohol and a carbonyl compound, becoming a method for removing the allyl protecting group for alcohols.[52-54]

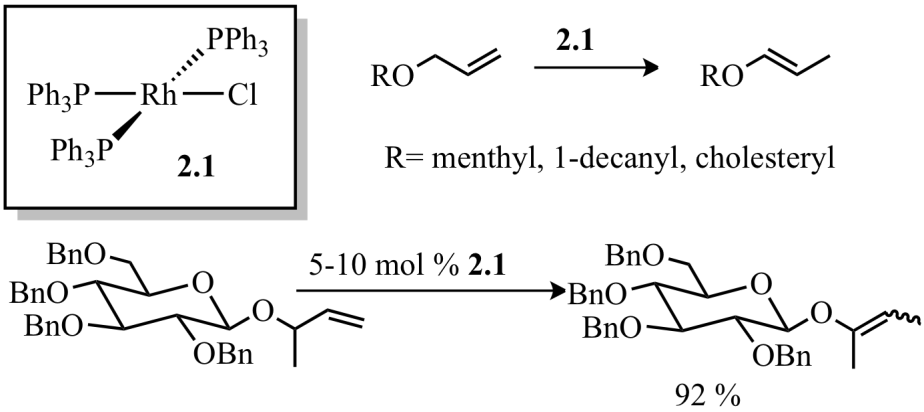

Figure 2.2. Isomerization by Wilkinson's catalyst

Emerson and Pettit proposed the first examples of iron-catalyzed allyl alcohol isomerization to propanal.[55] Since then, many reports of alkene isomerization using iron complexes, especially $Fe(CO)_5$, have been published. Besides allylic alcohols, allyl ethers, allyl benzene derivatives[23] and homoallylic compounds that bear a variety functional groups can be isomerized with $Fe(CO)_5$.[24] Recently, Beller et al. reported $Fe_3(CO)_{12}$ enabling selective isomerization of terminal olefins to corresponding beta-olefins in presence of other internal double bonds (80-100 ^oC, 3N KOH).[56]

Ruthenium based catalysts developed by Grubbs et al. have been widely used for alkene metathesis, and isomerization of alkenes has been observed as a side reaction caused by catalyst degradation. Ruthenium hydrides generated from **2.2** (Figure 2.3) can effectively isomerize allylic bonds to the adjacent position under mild conditions. Although the ruthenium hydride, **2.2-H**, has been isolated by Nolan[57] and Grubbs,[58] it hasn't been exploited as an alkene isomerization catalyst. Later, studies by Nishida,[59] Hanessian,[60] and Rosa[61,62] proved that **2.2-H** can be successfully used for synthetic transformations.

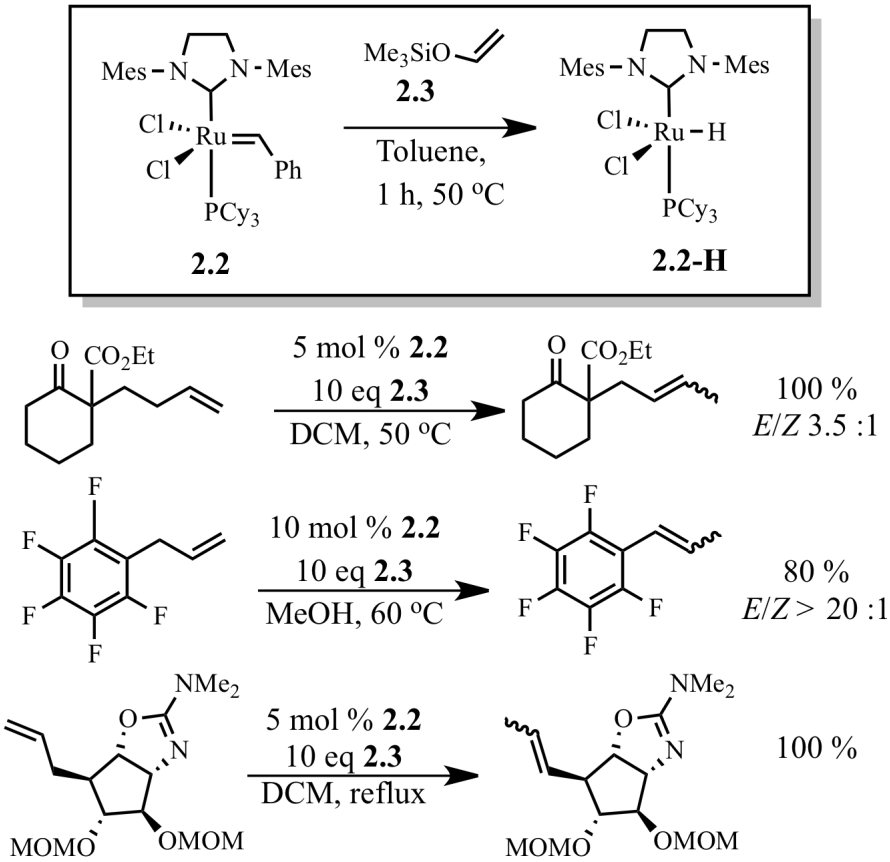

Figure 2.3. Isomerization of allyl groups by metathesis catalyst 2.2

Isomerization of allylic alcohols to corresponding aldehydes and ketones has been extensively investigated heavily with rhodium and ruthenium complexes. A variety of derivatives of ruthenium complexes were employed in early applications, for example $Ru(CO)_3(PPH_3)_2$ and $RuCl_2(PPh_3)_3$, but a breakthrough was made by $CpRu(PPh_3)_2Cl$ and the corresponding indenyl complex in combination with Et_3NHPF_6 investigated by Trost et al.[63,64] As seen in Figure 2.4 and Table 2.1, the indenyl system **2.5** is more active than the cyclopentadienyl system **2.4** possibly due to lowered energy of ring slippage from η^5 to η^3. Modifications of conditions were also explored to obtain amore active catalyst, for example use of AgOTs instead of Et_3NHPF_6 for ionizing the chloride ligand resulted in a turnover frequency number of 200,000 h^{-1}.[65] Isomerization of allylic alcohols proceeded smoothly and isolated double bonds were not affected. Contrary to Trost's suggestion, unfunctionalized alkenes could also be isomerized with this system, although at a much lower rate, for example, 1-octene can was isomerized to a mixture of 2-, 3-, and 4-octene.[65]

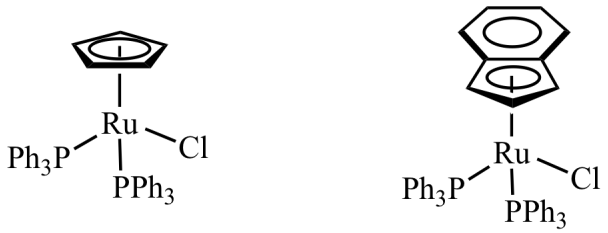

2.4 **2.5**

Figure 2.3. Trost's ruthenium complexes for allylic alcohol isomerization

Table 2.1. Isomerization of allylic alcohols by 2.4 and 2.5 at 100 ^{o}C in 1,4-dioxane with 10 mol% Et_3NHPF_6

Substrate	Catalyst (5 mol %)	Time (h)	Yield (%)
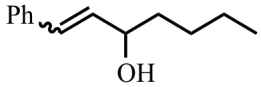	**2.4**	9	23
	2.5	2	83
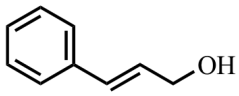	**2.4**	8	90
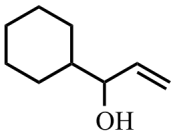	**2.4**	1.5	92
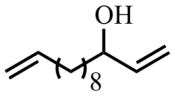	**2.4**	1	87
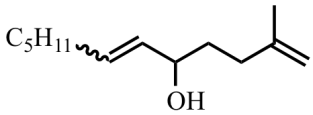	**2.5**	3	82
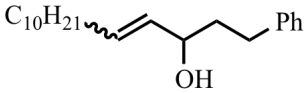	**2.4**	24	53
	2.5	3	81

Slugovc et al.[66] improved the activity of Trost's cyclopentadienyl system by exchanging the chloride ligand for a more labile acetonitrile ligand, which could exchange for alkene substrate more readily (Figure 2.4). The use of **2.6** reduced reaction times, for example in the case of 3-phenyl-2-propenol, complex **2.6** yielded the corresponding carbonyl compound with TON = 760, TOF = 1815 h^{-1} (in 25 min with 0.12 mol % loading) while **2.4** performed with TON = 20 and TOF = 2.5 h^{-1} under similar conditions. Another study done by Slugovc was varying the alkyl groups on the

phosphine ligands from phenyl to methyl and cyclohexyl, which showed the overall better performance of alkyl phosphines. See several examples reported in Table 2.2.

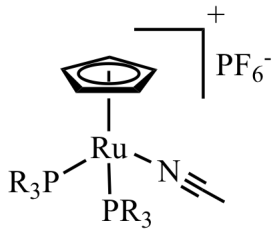

2.6 R = Ph
2.7 R = Me
2.8 R = Cy

Figure 2.4. Improved cyclopentadienyl ruthenium complexes for allylic alcohol isomerization by Slugovc.

Table 2.2. Isomerization of allylic alcohols by 2.4 and 2.5 at 57 ^{o}C in chloroform-*d*

Substrate	Catalyst (1 mol %)	Time	Yield (%)
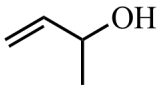	**2.6**	30 min	>98
	2.7	8 min	>98
	2.8	5 min	>98
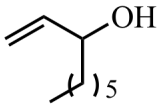	**2.6**	3 min	>98
	2.7	90 min	>98
	2.8	3 min	>98
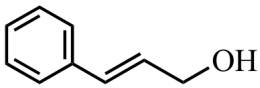	**2.6**	17 h	91
	2.7	15 h	87
	2.8	17 h	-

Although modifications introduced by Slugovc reduced reaction times, substrates where the double bond was located further than allylic positions were not accessible or in the absence of alcohol functionality, and oligomerization side products of the carbonyl compounds were observed. In order to move double bonds over longer carbon chains

(nine or more positions) it has been necessary to use either stoichiometric or 0.9 equivalent of the metal per alkene in systems reported by Iranpoor[67] and Gibson.[68]

In 2007, the Grotjahn group reported the discovery and development of a cyclopentadienyl ruthenium complex that bears a nitrogen-containing heterocyclic substituent on the phosphine ligand.[69]

Metal complexes containing hybrid P-N donor ligands have been extensively investigated due to their potential hemilability. The combination of fundamentally distinguished a P-ligand part which is a soft donor that exhibits π-acceptor properties stabilizing low or medium oxidation state metals and a N-ligand part, which is a hard donor, dominantly acting as a σ-donor more suitable for metals with higher oxidation states. Many metal complexes with mixed donor ligands containing phosphorus as well as sp^2-N donors within heterocycles are known.[70] The main focus has been on ligands with phosphine-pyridine[71-73] and phosphine-oxazoline donors,[74-77] and only a limited number of complexes containing bidentate phosphine-imidazolyl[78-86] or phosphine-imidazoline[87-89] donors have been reported. Applications of metal complexes containing phosphine imidazolyl or phosphine-imidazoline donor ligands in catalysis include the Heck coupling reactions[78,79] and the hydrogenation of alkenes[87] and imines.[89]

Besides the attractive features mentioned above, the synthesis of imidazolyl phosphines by S_N2 replacement by 2-lithioimidazoles on commercially available chlorophosphines could be performed with high yields in nearly all reactions, and pyridyl phosphines are accessible from nucleophilic substitution with metallated pyridines, therefore preparation of different analogues and library construction is straightforward.

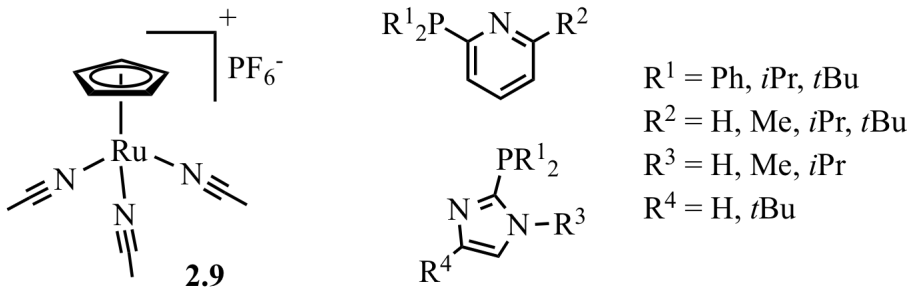

Figure 2.5. CpRu precursor, pyridylphosphines and imidazolylphosphines used for catalytic alkene isomerization screening

In the Grotjahn group, catalytic alkene isomerization was screened with a library of imidazolyl and pyridyl phosphine ligands (Figure 2.5) along with traditional monofunctional phosphines such as PMe_3, PCy_3, PPh_3, and P*i*Pr_2Ph, all using cyclopentadienyl tris(acetonitrile)ruthenium(II) hexafluorophosphate, $[CpRu(CH_3CN)_3]PF_6$, **2.9**, as the metal precursor and ^{1}H NMR spectroscopy as the detection technique. The two prototypical organic substrates 1-pentene and 4-penten-1-ol were chosen to find catalysts that are capable of isomerizing alkenols that have the alcohol functionality further than homoallylic position as well as isomerizing double bonds that lack the potential thermodynamic stabilization provided by formation of a new functional group (formation of aldehyde in this case). Reactions of the chosen substrates were relatively easy to monitor with ^{1}H NMR spectroscopy (there being only two positional isomers for 1-pentene and three for 4-penten-1-ol) and previously reported complexes, **2.4-2.8,** were not successful at isomerizing these substrates.

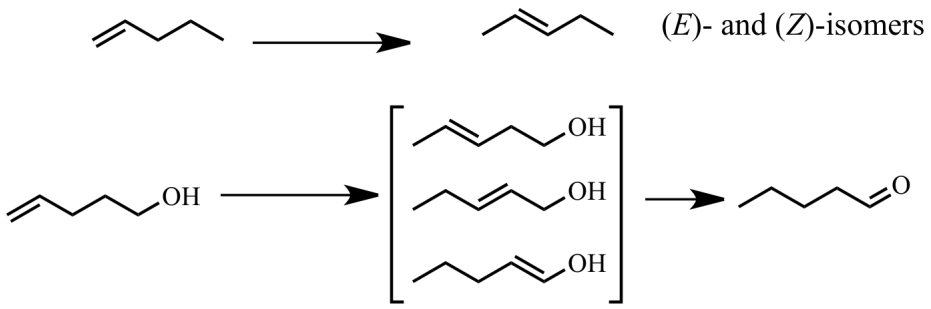

Figure 2.6. Organic substrates used in catalytic alkene isomerization screening

Results of the screening revealed that several pyridyl- and imidazolylphosphines were capable of isomerizing 1-pentene but not all the systems were capable of isomerizing 4-penten-1-ol. The best ligand screened featured the imidazolylphosphine with isopropyl groups on the phosphine and *tert*-butyl group on *C*4 and methyl on *N*1 of the imidazole group (Figure 3.7). Details of this screening can be found in other theses from the Grotjahn group.[90,91] The resulting alkene isomerization catalyst **2.10** selectively converts terminal alkenes to (*E*)-internal alkenes. In case of alkenols, substrates with various chain lengths can be isomerized, culminating in achieving the world record to date of moving an alkene over 30 bonds to form the corresponding ketone from the starting alkenol.[69,92]

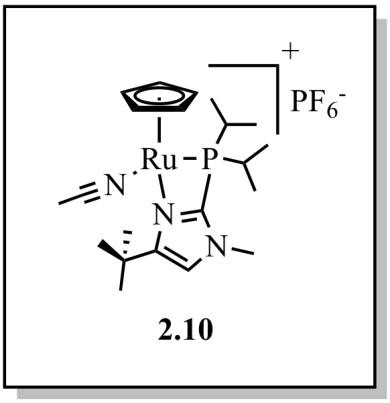

Figure 2.7. Alkene isomerization catalyst developed in Grotjahn research group

Table 2.3 shows substrates that represent the some of the scope of the alkene isomerization catalyst. In all cases, **2.10** presents high selectivity towards formation of (*E*)-alkenes, isomerization of allyl ether (Table 2.2, entry 4) gave (*E*, *E*)-propenyl ether in high yield without Claisen rearrangement of the intermediate allyl propenyl ether[93,94] and without any detectable (*Z*, *E*)-isomer.

Table 2.3. Scope of alkene isomerization catalyst 2.10[a]

Substrate	Product	2.10 (mol %)	Time	Temp (°C)	Yield (%)
	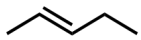	2	15 min	25	95
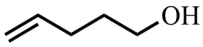	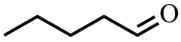	2 5	1 h 1 d	70 25	95 95
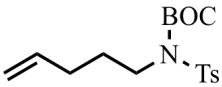	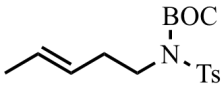	2	4 h	25	75
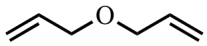	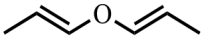	2	40 min	25	96
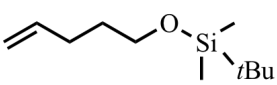	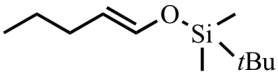	5	4 h	70	90
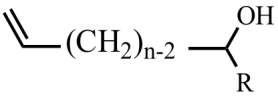 n = 9, R = Me	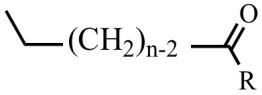	5	4 h	70	97
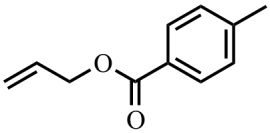	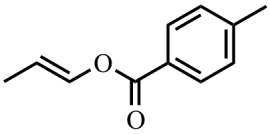	2	2 h	70	96
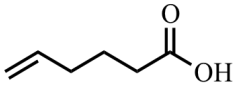	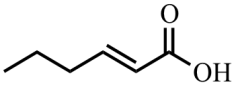	5	2 h	25	86
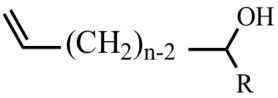 n = 30, R = Me	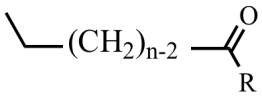	30	3 d	70	81

[a] Acetone or acetone-d_6 as solvent.

There are two major mechanisms which have been proposed for alkene isomerization: (1) an alkene insertion mechanism that involves metal hydrides and goes through alkyl intermediates (Figure 2.8) and (2) an allyl-hydride mechanism, which involves π-allyl intermediates (Figure 2.9) formed through C-H activation. Both routes are reversible; therefore, the products will reach thermodynamic equilibrium eventually.

In the alkene insertion route, a metal hydride binds to the alkene and undergoes insertion to yield a metal alkyl complex (primary and/or secondary), then β-hydrogen elimination from the metal-secondary alkyl complex can give both (*E*)- and (*Z*)-isomer of the internal alkene. The initial (*E*)- to (*Z*) ratio (kinetic product) depends on the nature of the catalyst but the final ratio depends on the thermodynamics. $Ni(OPEt_3)_4$[44] $RhCl_3$[95] and $RhCl(PPh_3)_3$ [96-98] are examples of complexes that have been shown to behave in a manner consistent with the alkene insertion mechanism.

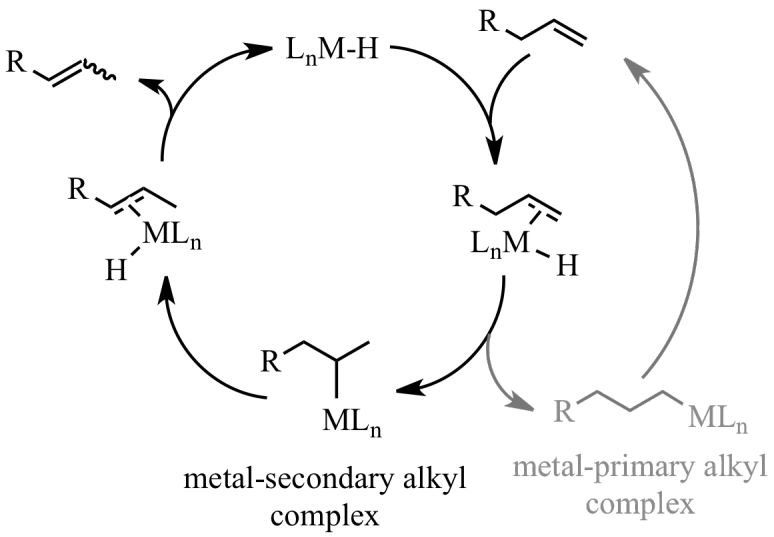

Figure 2.8. Catalytic cycle for alkene insertion mechanism of isomerization

In the allyl-hydride route, the proposed mechanism involves π-allyl intermediates formed by cleavage of an allylic C-H bond. This mechanism has been established for

$Fe_3(CO)_{12}$ and $PdCl_2(NCPh)_2$,[99] a number of detailed mechanisms have been proposed but the simplest is a 1,3-suprafacial shift in which an allylic hydrogen moves from *C*1 to *C*3 in a coordinated olefin by way of direct metal-hydride interaction.

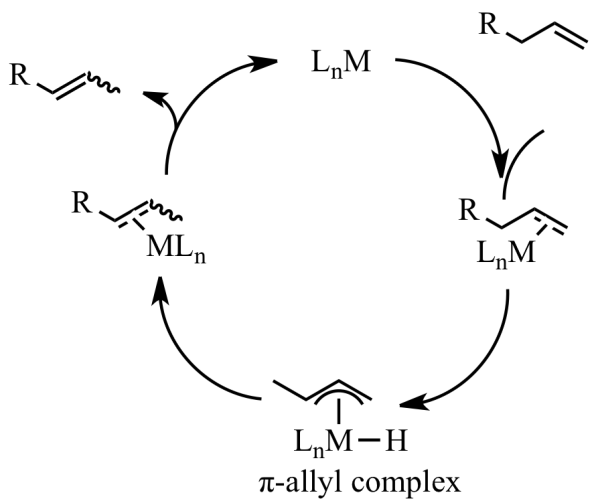

Figure 2.9. Catalytic cycle for allyl mechanism of alkene isomerization

The mechanism proposed for alkene isomerization proposed for **2.10** (Figure 2.10) starts with dissociation of the acetonitrile ligand, demonstrated by the observation of ethylene binding (to form an ethylene analog of **2.11**) when 25 equiv were added in acetone-d_6, displacing the nitrile but leaving the P,N-chelate is still intact. In the case of alkenes with allylic hydrogens, formation of π-allyl complex is thought to be facilitated by the nitrogen on the imidazole on the phosphine ligand, a concept supported by the observation that a complex which lacks the pendant base is 330 times slower at isomerizing 1-pentene and about 10,000 times slower in the case of 4-penten-1-ol.[92] Also bubbling propene into a solution of **2.10** in presence of deuterium oxide leads to H/D exchange at the terminal positions but not the internal position (Chapter 4). The internal

hydrogen stays intact even after extended reaction times in the presence of active catalyst, a fact that renders the alkene insertion mechanism highly unlikely, because it would require an unprecedentedly high preference for forming a metal-primary alkyl intermediate rather than the secondary isomer.

Figure 2.10 also explains the high (*E*)-selectivity observed, because intermediates **2.12-*Z*** and **2.13-*Z*** will be relatively higher in energy than **2.12-*E*** and **2.13-*E*** due to steric constraints. Moreover, when terminal alkenes are isomerized to internal (*E*)-alkenes or (*E*)-2-butene was left in presence of **2.10** some (*Z*)-isomer is observed after extended periods (>>10 x more than the time reaction required; in one case, more than 3,000,000 times longer than the time of reaction required[91]) (Chapter 4).

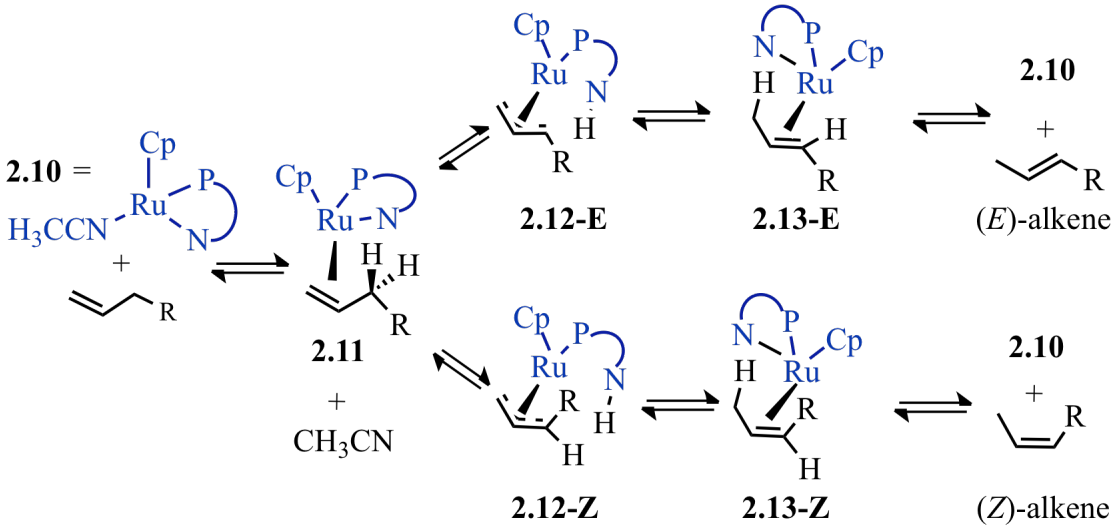

Figure 2.10 Proposed mechanism of alkene isomerization with 2.10

Recent density functional calculations reported by Tao et al.[100] proposed the involvement of an allyl-hydride mechanism but still steps where hydrogen transfer may occur via pendant nitrogen (Figure 2.11). The authors only consider the formation of (*E*)-alkene, so do not address the origins of kinetic selectivity summarized above. Essentially,

the computed mechanism proceeds via **2.11**, **2.12-E**, and **2.13-E**, but the steps between **2.12-E** and the two other species named are thought to differ from the steps shown in Figure 2.10. According to this study isomerization of 1-pentene proceeds as follows: (1) formation of agostic intermediate **2.14** and then the β-H elimination to generate a Ru-H intermediate (**2.15**), (2) (formally) reductive transfer of the hydridic hydrogen to the pendant base N and produce a π-allyl intermediate (**2.12-E**), (3) rotation to place the N-H moiety at the other end of the π-allyl system, (4) oxidative transfer of the NH to Ru to generate corresponding Ru-H intermediate (**2.17**), (5) reductive elimination to eventually generate 2-pentene. It is proposed that the function of the imidazole pendant base is transportation of H between hydride intermediates but the transition state of allylic proton transfer directly to the pendant nitrogen was not located. These calculations do not explain the geometric

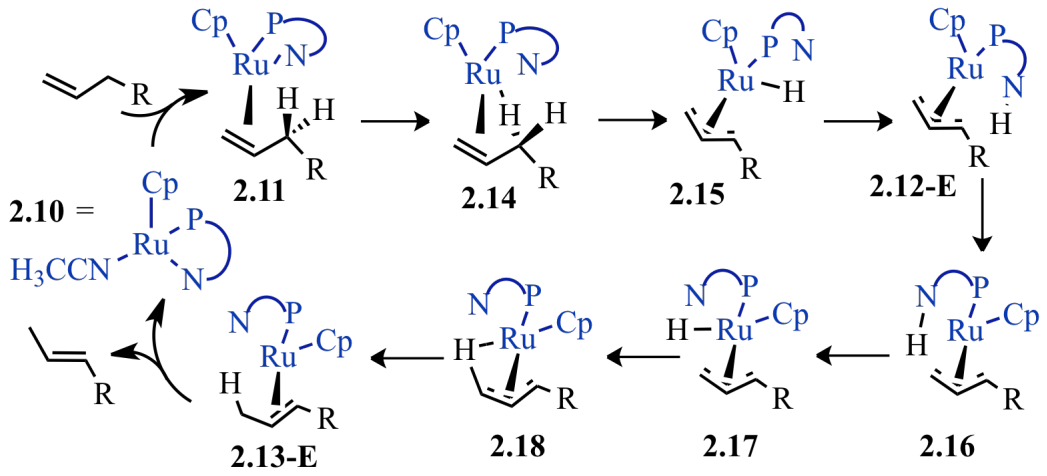

Figure 2.11. Proposed mechanism by Tao et al.

selectivity towards (*E*)-alkenes but still explain the acceleration experimentally observed due to presence of pendant base.

Part of my thesis research seeks to improve or tailor the selectivity of **2.10** through ligand design. Efforts to rationalize the alkene isomerization mechanism through computational mechanistic studies are ongoing in the Grotjahn research group. Looking at preliminary calculations, which I performed, the geometric selectivity can be explained by *iso*-propyl groups on the phosphine ligand occupying the space that would likely to be occupied by a (*Z*)-alkene formed. In contrast, the upper left quadrant is sterically open for the forming (*E*)-alkene to fit. A complete explanation of geometric selectivity would involve calculations with a bound alkene (e.g 1-pentene) in all possible conformations, not just the one shown.

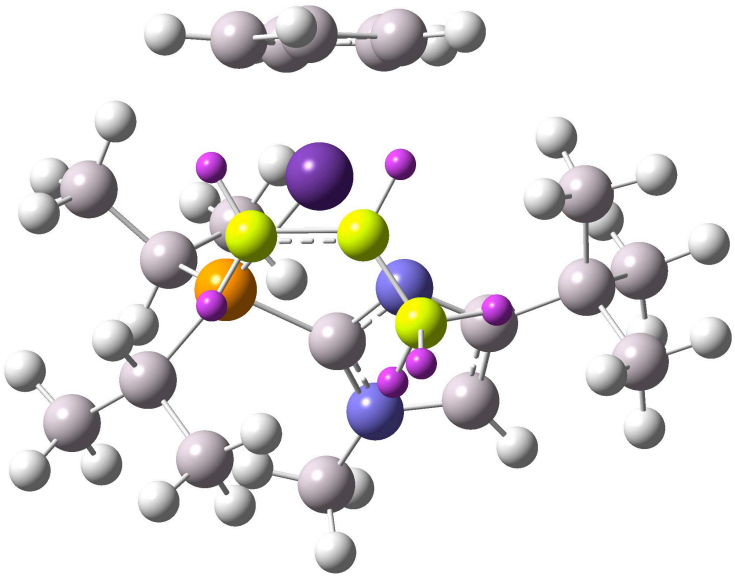

Figure 2.12. Computational model of propene (shown with yellow colored carbons) formed after loss of CH_3CN from alkene isomerization catalyst 2.10

Taking into consideration the steric constraints *iso*-propyl groups on phosphine would impose during isomerization, analogues of **2.10** with bulkier phosphorus substituents could be anticipated to be slower catalysts. This is consistent with

observations in earlier screening of catalytic alkene isomerization: when *tert*-butyl groups were present on the phosphine only a trace amount of 2-pentene was observed at room temperature after 24 h,.[90,91] whereas **2.10** completes this process within 15 min. Thus, bulky groups R^1 on phosphorus may impede alkene binding, as just mentioned; alternatively, it is known from work of Yi Gong in the Grotjahn lab that large R^1 groups impede opening of (imidazolyl)phosphine chelates, likely through an analog of the Thorpe-Ingold effect.[101,102]

Along with the phosphine substituents R^1 (Figure 2.13), imidazole substituents can be used to tune the catalyst by introducing variations in key positions. The α-position to the basic nitrogen provides steric control by introducing bulky groups (R^3) that should influence access to the basic lone pair (see Chapter 1, Figure 1.12, 1.13 and related discussion). The basicity of the lone pair can also be altered by substitutions (R^2) of the non-basic nitrogen of imidazole. Substitution of the non-basic nitrogen can also provide further remote steric control of the corresponding metal complex formed.[103]

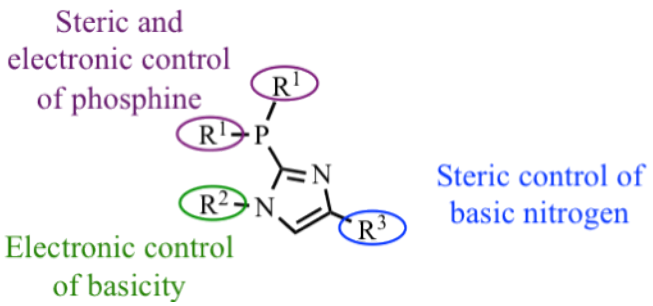

Figure 2.13. Sites for tuning of imidazolylphosphine ligands and catalysts

The effect of increased steric hindrance at the phosphorus (Figure 2.13, R^1), and *C*4 position of imizadole (R^3), was investigated with a series of imidazolylphosphines including four new examples which I made with cyclohexyl, *tert*-butyl, and adamantyl

groups with 4-*tert*-butyl-1-methyl-imidazole that were synthesized along with *iso*-propyl and *tert*-butyl phosphines of 4-adamantyl-1-methyl-imidazole. Facile complexation with $[CpRu(CH_3CN)_3]PF_6$ in acetone at room temperature yielded yellow-brown solids after removal of solvents in good yields.

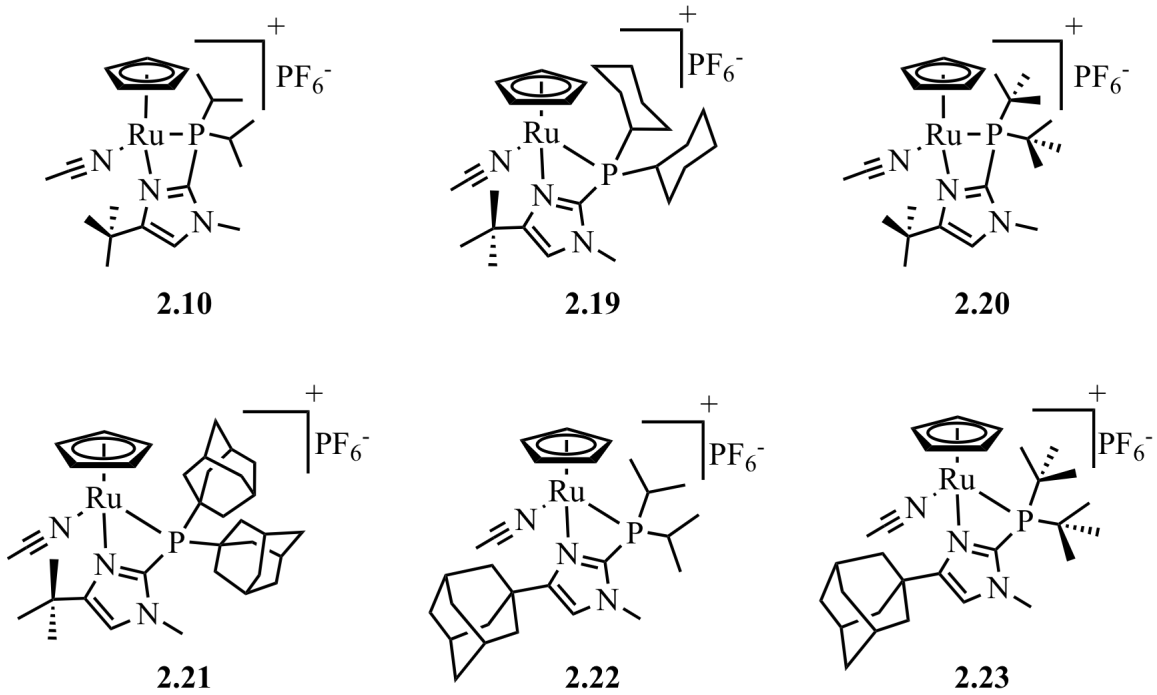

Figure 2.14. Alkene isomerization catalyst and its more sterically hindered analogues

In order to assess the effects of ligand sterics on structure, X-ray structures of close analogs of **2.19** and **2.20** were obtained. Crystals suitable for diffraction were obtained by using anion exchange: **2.19** was converted to **2.26** using tetrakis(3,5-bis(trifluoromethyl)phenyl)borate $[B[3,5\text{-}(CF_3)_2C_6H_3]_4^-]$ and **2.20** converted to **2.27** using tetrakis(pentafluorophenyl)borate $[B(C_6F_5)_4^-]$. Chelation of the basic imidazole nitrogen was observed as in **2.10**. Having *tert*-butyl groups on the phosphorus lengthens the ruthenium phosphorus bond (Ru - P), and perhaps in compensation shortens the

chelate bond length, Ru – N_{Im} and lengthens the bond length between phosphorus and imidazole *C*2 carbon (P - C_{Im}). The biggest change seen with bond angles is the narrowing of the angles around phosphorus in chelate, complementary to the changes in bond lengths mentioned (Table 2.4).

Table 2.4. Important bond lengths and angles for 2.10, 2.26, and 2.27

Bond Length	**2.10** (P*i*Pr$_2$)	**2.26** (PCy$_2$)	**2.27** (P*t*Bu$_2$)
P - C_{Im}	1.808(4)	1.807(5)	1.814(4), 1.828(4)
Ru - N_{Im}	2.202(4)	2.212(4)	2.194(3), 2.175(3)
Ru – P	2.3440(12)	2.330(6)	2.3957(9), 2.4183(9)
Ru - $N_{Acetonitrile}$	2.064(4)	2.057(4)	2.055(4), 2.056(4)
Ru – $Cp_{centeroid}$	1.799	1.799	1.803, 1.811
Bond Angles	**2.10** (P*i*Pr$_2$)	**2.26** (PCy$_2$)	**2.27** (P*t*Bu$_2$)
N_{Im} - Ru - P	67.46(9)	66.75(10)	66.95, 66.68 (8)
Ru - P - C_{Im}	83.83(14)	84.09(15)	82.75(12), 82.09(12)
Ru - N_{Im} - C_{Im}	102.0(2)	101.9(3)	102.9(2), 105.1(3)
P - C_{Im} - N_{Im}	106.1(3)	105.3(3)	106.1(3), 106.0(3)

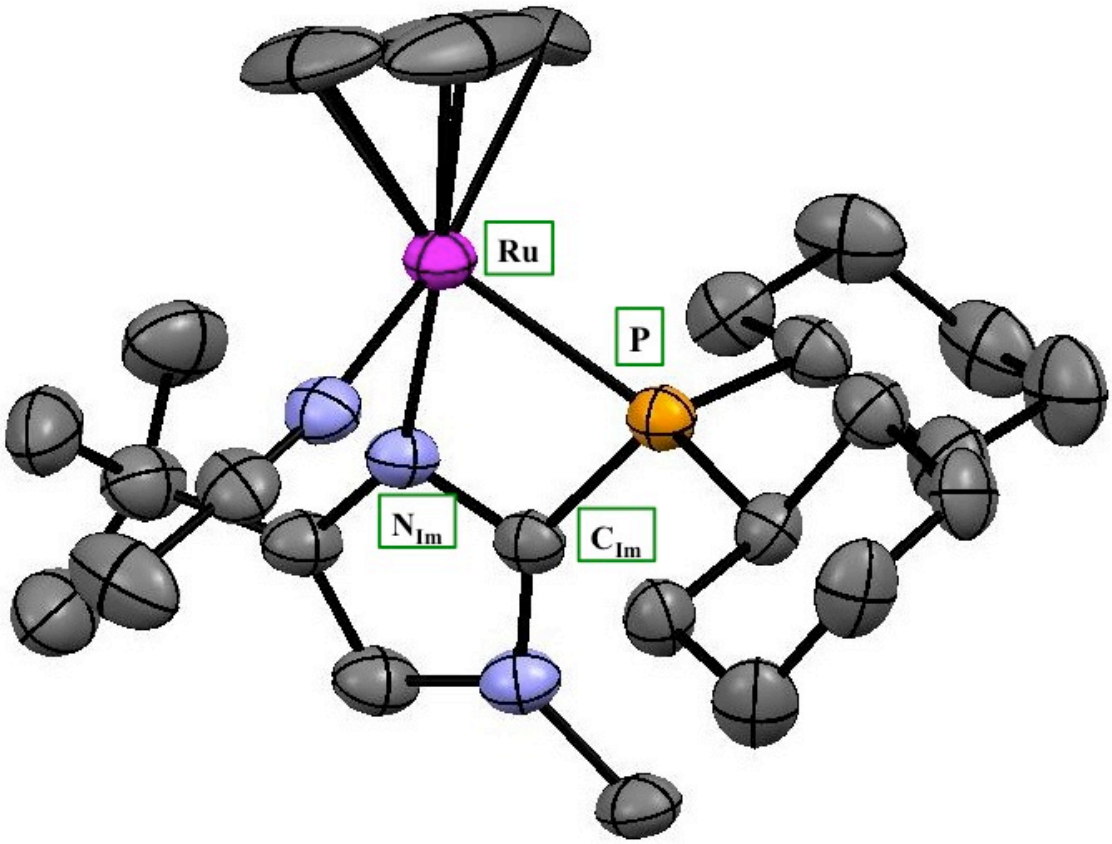

Figure 2.15. X-ray crystal structure of 2.26, hydrogens and counter anion hidden for clarity

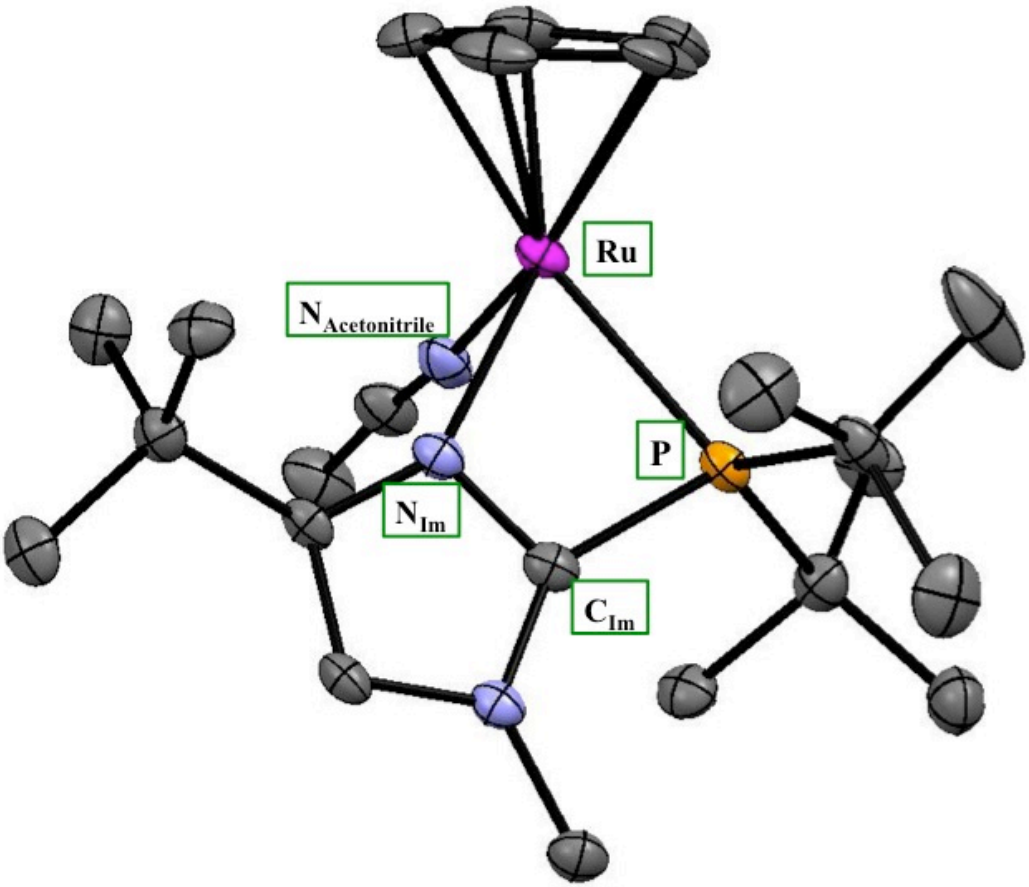

Figure 2.16. X-ray crystal structure of 2.27, hydrogens and counter anion hidden for clarity

Selective isomerization of terminal alkenes to 2-alkenes is a valuable technique, because 2-alkenes are of higher commercial value than terminal alkenes and they are naturally scarce.[104,105] Also, commercially more valuable even-numbered terminal alkenes can be produced from odd-numbered terminal alkenes by selective mono-isomerization followed by ethenolysis. For example, 1-nonene can be isomerized to 2-nonene and ethenolysis of 2-nonene will give two commercially viable products, 1-octene and propane.[106] Moreover, alkene chains of various lengths can be accessed after metathesis of the isomerized alkene. Controlled mono-isomerization of linear alkenes devoid of functional groups have been achieved by few systems[107-111] and most recently,

Jennerjahn et al. have demonstrated use of 1 mol % $Fe_3(CO)_{12}$ in presence of H_2O/KOH in diglyme at 80 ^oC for isomerization of 1-octene to 2-octene, but the geometric selectivity is poor (*E*/*Z* = 5).[56]

In order to investigate controlled mono-isomerization of alkenes in absence of any functional group influence, 1-heptene was studied instead of 1-hexene or 1-octene, because: (1) heptene has only three positional isomers instead of four positional isomers like octene, which makes identification of reaction mixture easier, and (2) heptene isomers have a greater difference of product distribution between the positional isomers than hexene. Product distribution based on enthalpies of heptene isomers was reported previously (Table 2.5).[112] If only the terminal isomer and the two internal (*E*) isomers are possible, the proportion of the three components in this system would be 0.9, 54.1, and 45.0 % (last column of Table 2.5).

Table 2.5. Calculated product distribution of heptenes

Isomers	ΔH_f (kcal mol^{-1})	Calculated (%)	Experimental (%)	System of only 1-, (*E*)-2- and (*E*)-3- (%, calculated from experimental)
1-heptene	-23.35	0.427	0.728	0.9
(*E*)-2-heptene	-25.31	11.743	12.724	54.1
(*Z*)-2-heptene	-26.15	48.525	43.254	
(*E*)-3-heptene	-25.00	6.939	7.262	45.0
(*Z*)-3-heptene	-25.91	32.366	36.032	

Isomerization of 1-heptene (0.5 mmol) was carried out with complexes, **2.10**, **2.19 - 2.23** with 2 mol % catalytic loading at room temperature and at 70 ^oC with total reaction

volume of 1 mL acetone-d_6 in a resealable J. Young NMR tube. At room temperature, terminal alkene 1-heptene was converted to (*E*)-2-heptene selectively with **2.10** and **2.19** (Table 2.6) with similar rate and both systems reached thermodynamic equilibrium in about 30-40 min (entries 2 and 3). In sharp contrast, **2.20** and **2.23** (room temperature data in Table 2.17 and 2.22, respectively) transformed about less than 2 % 1-heptene to 2-heptene, showing that expansion to *tert*-butyl groups from *iso*-propyl groups have a dramatic effect on rate of isomerization.

When isomerization was carried out at 70 ^{o}C with **2.20**, 18 % 2-heptene (*E*/*Z* ~10) and less than 1 % of 3-heptene was observed in one hour with 83 % 1-heptene still present. After 23 h, the mixture still hadn't reached thermodynamic equilibrium among positional isomers (86 % 2-heptene, about 11 % 3-heptene and 4 % 1-heptene), although the ratio of (*E*)- to (*Z*)-2-heptene had decreased from 10 : 1 to 6 : 1, showing a very slow approach to the thermodynamic ratio of 3.4 : 1. The amounts of isomers were calculated from ^{1}H NMR integrations of peaks that were assigned to positions labeled in the structures in Figure 2.17. Experimentally, it was impossible to discriminate the (*E*)- and (*Z*)-isomers of 3-heptene, but it was possible to see separate (though closely spaced) peaks for isomers of 2-heptene. The estimation of (*Z*)-2-heptene can be overestimated about 5 % due to partial overlap of allylic methyl peaks.

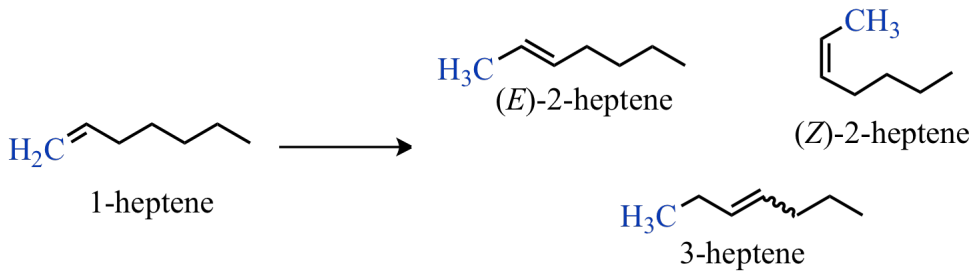

Figure 2.17. Heptene isomers with CH_3 or CH_2 groups used for NMR integrations highlighted

Comparing entry 6 with entry 4, isomerization of 1-heptene sped up to 52 % 2-heptene (*E*/*Z* ~ 9.5) and 3 % 3-heptene formation with 44 % of 1-heptene (20 min) when steric bulk of groups on phosphine was increased from *tert*-butyl (**2.20**) to adamantyl (complex **2.21**, Table 2.6). The thermodynamic ratio of positional isomers was not attained in 35 h (2 % 1-heptene, 76 % 2-heptene, 23 % 3-heptene) at 70 ^{o}C, although the ratio of (*E*)- to (*Z*)-2-heptene had increased from 9.5 : 1 to 4 : 1 (versus theromodynamic ratio of 3.4 : 1). Possibly, the increased steric bulk of phosphine ligand had increased the strain of the chelate, which may lead to relatively more facile opening of the chelate, therefore isomerization. The loss of geometric selectivity of the (*E*)-isomer may be explained by possible lengthening of the P-Ru and bond, which may affect the spatial arrangement of the active site and alleviate crowding so that there is space for the (*Z*)-isomer to fit.

The presence of *iso*-propyl and *iso*-propyl like groups (e.g. cyclohexyl) on phosphorus consistently leads to (*E*)-selective isomerization of 1-heptene, use of **2.22** where *tert*-butyl group on *C*4 position of the imidazole group on the phosphine ligand was replaced with an adamantyl group, 79 % (*E*)-2-heptene, and 18 % 3-heptene was formed, with 2 % 1-heptene still present in 9 minutes at room temperature.

Thermodynamic ratio of positional isomers was reached in 50 minutes (Table 2.6).

Table 2.6. Collective isomerization data of 1-heptene, and equilibrium composition predicted from Table 2.5

Catalyst	$(R^1)_2P$	R^3 on Im	Temp (^oC)	Entry	Time	1- (%)	2- (%)	2- (*E*:*Z*)	3- (%)
Predicted if all 5 isomers are at equilibrium						0.7	56.0	3.4 : 1	43.3
Predicted if only 1-, (*E*)-2- and (*E*)-3- are at equilibrium						0.9	54.1	-	45.0
2.10	*i*-Pr	*t*-Bu	25	**1**	15 min	1.4	67.7	>20 : 1-	28.5
				2	40 min	1.2	54.1	>20 : 1-	42.5
2.19	Cy	*t*-Bu	25	**3**	30 min	1.2	60.1	>20: 1	36.5
2.20	*t*-Bu	*t*-Bu	70	**4**	1 h	82.6	17.7	9.7 : 1	<1
				5	23 h	3.5	85.1	6.0 : 1	11.3
2.21	Ad	*t*-Bu	70	**6**	20 min	43.6	52.1	9.5 : 1	3.2
				7	35 h	1.6	76.0	4 :1	23.3
2.22	*i*-Pr	Ad	25	**8**	9 min	1.6	79.0	> 20 : 1	17.8
				9	12 min	1.5	75.4	> 20 : 1	22.0
				10	50 min	1.2	55.3	> 20 : 1	43.0
2.23	*t*-Bu	Ad	70	**11**	20 min	11.4	79.0	9.7 : 1	10.0
				12	11 h	1.8	77.3	5.8 : 1	22.1

Some difference in activity between **2.10** and **2.22** (R^3 on imidazole = *tert*-butyl versus adamantyl, respectively) can be acknowledged when looking at the isomerization of 1-heptene at early stages (Table 2.6): using **2.10**, in 15 min, the reaction mixture composition was 2 % 1-heptene, 68 % 2-heptene, and 29 % 3-heptene in which the

thermodynamic ratio of positional isomers was reached in 40 min. In contrast, using **2.22**, in a similar time frame (12 min) afforded 2 % 1-heptene, 76 % 2-heptene, and 22 % 3-heptene, and the thermodynamic ratio of positional isomers was reached in 50 min. More rapid conversion of 2-heptene in case of **2.22** compared to **2.10** could be explained by the adamantyl group rendering the N-chelate more labile due to steric bulk in close proximity, though the differences are modest.

Finally, when comparison of **2.20** and **2.23** is made, where *tert*-butyl group on *C*4 position of the imidazole group on the phosphine ligand was replaced with an adamantyl group, reactions at 70 ^{o}C show stark difference. Starting 1-heptene is quickly consumed by **2.23** (entry 11), but **2.20** holds on to the terminal alkene for over **1 h** (entry 4): 83 % and 3 % 1-heptene is present at one-hour mark with **2.20** and **2.23**, respectively. Distinctive (*E*)- and (*Z*)-heptene ratios were observed: although one can obtain 79 % 2-heptene with 9.7 *E*/*Z* ratio in 20 min with **2.23** (entry 11), complex **2.20** (entry 5) after nearly one day provides a higher yield of 2-heptene (85 %) with a mixture of *E*/*Z* ratio of 6 to 1.

In summary, from all of the entries in Table 2.6, it appears that the most promising ones as far as maximal amount of (*E*)-2-heptene are entries 5, 11, and 8, with the first two (both featuring catalysts with *tert*-butyl on P) being the most favorable.

Alkene isomerization of 1-hexene and 1-decene with **2.20** at 70 ^{o}C is consistent with 1-heptene isomerization, as well as 1-hexene isomerization with **2.23** at room temperature.

In conclusion, mono-isomerization of linear alkenes were investigated with a group of CpRu complexes bearing imidazolyl phosphine ligands with varying steric

hindrance at the phosphorus and imidazole *C*4 positions. Cyclohexyl groups on phosphorus behave very much like isopropyl groups; similar rate of isomerization and (*E*)-selectivity is observed. Alkene isomerization is slower and more selective towards mono-isomerization when the phosphorus atom bears *tert*-butyl groups, but modification to bigger substituents leads to acceleration of isomerization arguably due to increased strain applied to chelate ring formed by increased length of Ru-P bond distance. Effect of *C*4 substitution is observed in form of acceleration of isomerization when the substituent is so sterically big that the Ru-N chelate opening is quicker due to elongated Ru-N distance. As a result, a family of catalysts that is capable of isomerizing alkenes to various mixtures have been established, where one can choose a complex to fit the needs of the process at hand.

Further investigation with terminal alkenes bearing functional groups can be carried out with **2.20** to investigate whether mono-isomerization will still be the major transformation taking place, which is expected to give access to high-value 2-alkenes.

The next chapters deal with very different optimizations of the bifunctional alkene isomerization catalysts, fully exploring a novel heterogenized version of **2.10** in Chapter 3 and the ability of homogeneous catalyst **2.10** to perform H/D exchange in Chapter 4.

EXPERIMENTAL SECTION

Manipulations were carried out in a nitrogen-filled glovebox or using Schlenk techniques. Acetone-d_6 from Cambridge Isotope Laboratories, Inc. was further deoxygenated by bubbling N_2 gas through the liquid prior to use. Chloroform-*d* was dried by stirring over calcium hydride for 1 d and vacuum transfer followed by freeze-thaw cycles to degas. THF and ethyl ether were distilled over sodium metal and benzophenone indicator and deoxygenated by bubbling N_2 gas through them. NMR spectra were obtained at 30 °C on either a 500-MHz INOVA (500 MHz listed below for ^{1}H = 499.940 MHz and 125.7 MHz for ^{13}C = 125.718 MHz), a 400-MHz Varian NMR-S (400 MHz listed below for ^{1}H = 399.763 MHz and 100 MHz for ^{13}C = 100.525 MHz) spectrometer. ^{1}H NMR chemical shifts are reported in parts per million downfield from tetramethylsilane and referenced to solvent resonances (^{1}H NMR: 2.05 ppm for acetone-d_6). ^{1}H NMR signals are given followed by multiplicity, coupling constants *J* in Hertz, integration in parentheses. For complex coupling patterns, the first coupling constant listed corresponds to the first splitting listed, e.g. for (dt, *J* = 3.2, 7.9, 1 H) the doublet exhibits the 3.2 Hz coupling. Tetrakis(trimethylsilyl) methane or 1,4-dioxane were used as internal standards for accurate integration. All ^{1}H NMR spectra were acquired using 16 scans with 20 sec relaxation delay and 15° pulse width. ^{31}P NMR chemical shifts were referenced to an external 85 % $H_3PO_{4\ (aq)}$ capillary placed in the solvent. Elemental analyses were performed at NuMega Laboratories (San Diego). X-Ray crystallographic data were obtained at UCSD Chemistry and Biochemistry X-Ray facility.

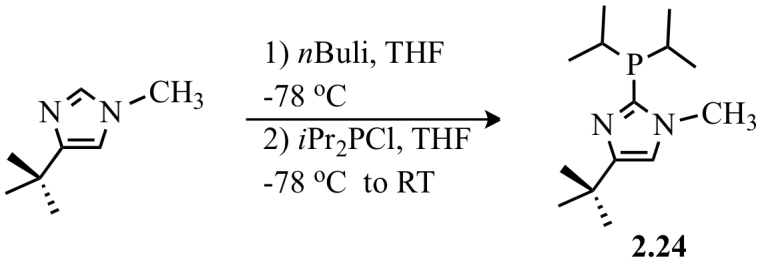

Figure 2.18. Synthesis of 4-(*tert*-Butyl)-2-(di-*iso*-propylphosphino)-1-methyl-1*H*--imidazole

4-(*tert*-butyl)-2-(di-*iso*-propylphosphino)-1-methyl-1*H*-imidazole (2.24). In a Schlenk flask equipped with magnetic stirbar, 4-(*tert*-butyl)-1-methyl-1*H*-imidazole (8.4675 g, 0.0613 mol) was dissolved in 100 mL dry and deoxygenated THF and the flask was placed in an acetone-Dry Ice bath at -78 °C. Using a syringe, an addition funnel was charged with *n*BuLi in hexanes (42 mL of 1.52 M, 0.0638 mol) and the contents were added to the reaction dropwise over 2.5 h. After 30 min, di-*iso*-propylchlorophosphine (9.4256 g, 0.618 mol) was added dropwise using the addition funnel over 4.5 h. The reaction was allowed to warm to room temperature and was quenched with deoxygenated methanol until solution became clear yellow. Solvents were removed on a vacuum line and the resulting solid was suspended in hexanes and the mixture filtered in the glovebox through Celite. The filtrates were concentrated and the residue distilled under oil pump vacuum, collecting the fraction distilling at 110 °C. Pure ligand was obtained as a clear colorless liquid in 74.7 % yield (11.6451 g, 0.0458 mol). ^{1}H NMR (400 MHz, acetone-d_6) δ 0.95 (dd, J = 7.0, 11.5, 6H), 1.05 (dd, J = 7.0, 16.0, 6H), 1.24 (s, 9H), 2.38 (sep of d, J = 2.0, 7.0, 2H), 3.74 (d, J = 1.0, 3H), 6.83 (d, J = 2.0, 1H). ^{31}P NMR (202 MHz, acetone-d_6) δ -18.5 (s) ppm.

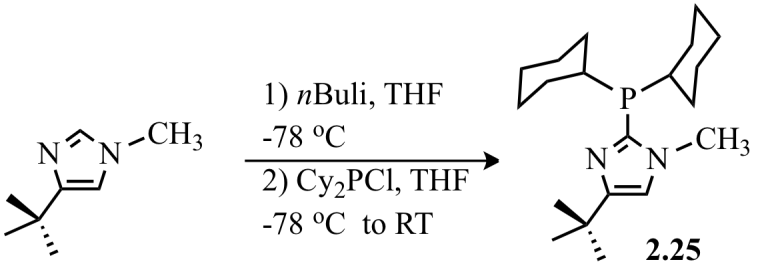

Figure 2.19. Synthesis of 4-(*tert*-Butyl)-2-(di-cyclohexylphosphino)-1-methyl-1*H*--imidazole

4-(*tert*-butyl)-2-(di-cyclohexylphosphino)-1-methyl-1*H*-imidazole (2.25). In a Schlenk flask equipped with magnetic stirbar, 4-(*tert*-butyl)-1-methyl-1*H*-imidazole (140.8 mg, 1.02 mmol) was dissolved in dry and deoxygenated THF (10 mL) and the flask was placed in an acetone-Dry Ice bath at -78 °C. Using a syringe, *n*BuLi in hexanes (640 μL of 1.6M, 1.03 mmol) was added to the reaction dropwise over 10 min. After 1 h, di-cyclohexylchlorophosphine (262.8 mg, 1.13 mmol) was added dropwise using a gas tight syringe over 25 min. The reaction was allowed to warm to room temperature and was quenched with deoxygenated methanol until solution became clear and pale yellow. Solvents were removed on a vacuum line and the resulting solid was suspended in hexanes and the mixture filtered in the glovebox through Celite plug and fractions were collected. Pure compound was obtained as a white solid, which was combined with the product from a second run on identical scale. The total amount obtained was 315.9 mg (47% yield). ^{1}H NMR (400 MHz, acetone-d_6) δ 1.24 (s, 9H), 1.90-1.00 (m, 30H), 2.2-2.08 (m, 2H), 3.72 (d, J = 1.0, 3H), 6.81 (d, J = 2.0, 1H). ^{31}P NMR (162 MHz, acetone-d_6) δ -27.4 (s) ppm. Elemental calculated for $C_{20}H_{35}N_2P$ (334.48) C, 71.82; H, 10.55; N, 8.38. Found C, 71.87; H, 10.38; N, 8.18.

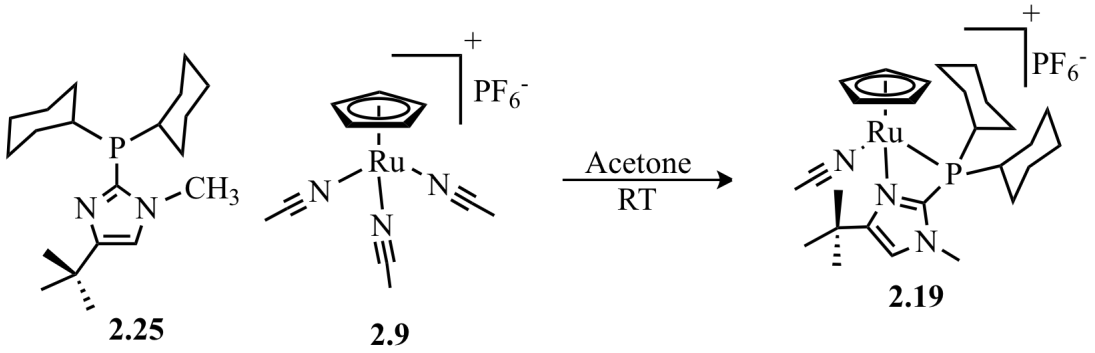

Figure 2.20. Complexation of 2.25 to give 2.19

Complexation of 2.25 to give [CpRu (4-(*tert*-butyl)-2-(di-cyclohexylphosphino)-1-methyl-1*H*-imidazole)(acetonitrile)]PF_6 (2.19) In a glove box, ruthenium precursor $[CpRu(CH_3CN)_3]PF_6$ (217.3 mg, 0.500 mmol) was combined in a scintillation vial equipped with a magnetic stir bar and deoxygenated acetone (4 mL). The phosphine, **2.25** (167.3 mg, 0.500 mmol) was added dropwise in deoxygenated acetone (3 mL), and the resulting solution was allowed to stir overnight at room temperature under an atmosphere of nitrogen. The solvent was removed in vacuo, without stirring, and the residue left under vacuum until a flaky powder remained. The product was obtained as yellow colored powder in 94.4% yield (360.5 mg, ~16 % bis-acetonitrile complex is present). ^{1}H NMR (500 MHz, acetone-d_6) δ 1.37 (s, 9 H), 1.52-1.25 (m obscured by neighboring peak, 10H), 1.96-1.68 (m, 8H), 2.25-2.12 (m, 2H), 2.51 (d, J = 1.5, 3 H), 2.60-2.54 (m obscured by neighboring peak, 1 H), 2.94-2.82 (m, 1H), 3.81 (s, 3 H), 4.60 (s, 5 H), 7.03 (s, 1 H) ppm. ^{31}P NMR (202 MHz, acetone-d_6) δ 27.42 (s) ppm. Elemental calculated for $C_{27}H_{43}F_6N_3P_2Ru$ (686.66) C, 47.23; H, 6.31; N, 6.12. Found C, 47.32; H, 5.99; N, 6.60.

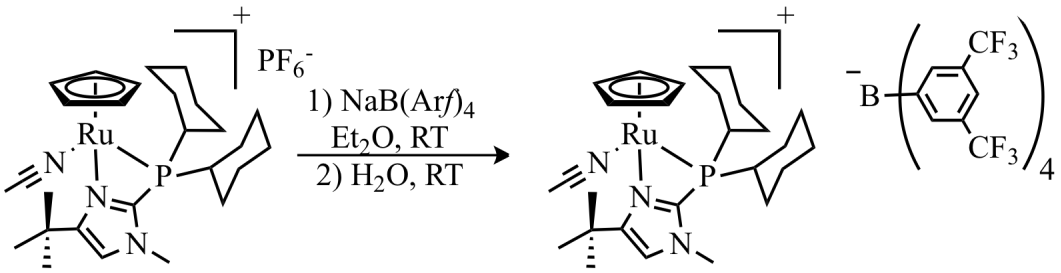

2.19 **2.26**

Figure 2.21. Anion exchange of 2.19

Synthesis of [CpRu (4-(*tert*-butyl)-2-(di-cyclohexylphosphino)-1-methyl-1*H*-imidazole)(acetonitrile)]B[(3,5-(CF_3)$_2$$C_6H_3$)]$_4$ (2.26) In a glove box, ruthenium complex **2.19** (70.2 mg, 0.102 mmol) was combined in a scintillation vial equipped with a magnetic stir bar and deoxygenated ethyl ether (4 mL). The salt, sodium tetrakis(3,5-bis(trifluoromenthyl)phenyl)borate (93.1 mg, 0.105 mmol) was added dropwise in deoxygenated ethyl ether (3 mL), and the resulting solution was allowed to stir overnight at room temperature under an atmosphere of nitrogen. Deoxygenated water (8 mL) was added to dissolve sodium hexafluorophosphate and excess sodium tetrakis(3,5-bis(trifluoromenthyl)phenyl)borate, and the mixture was allowed to stir for 90 min. The organic layer was separated and aqueous layer was washed with ethyl ether (3 x 5 mL). The solvent was removed from combined organic layers in vacuo, without stirring, and the residue left under vacuum until a flaky powder remained. The product was obtained as yellow colored powder in 85.7 % yield (124.0 mg). Single crystals were obtained from hexanes diffusion into THF solution of **3.26** at room temperature. X-ray analysis of crystals revealed the structure. ^{1}H NMR (400 MHz, acetone-d_6) δ 1.36 (s, 9 H), 1.52-1.25 (m obscured by neighboring peak, 10H), 1.94-1.64 (m, 8H), 2.25-2.10 (m, 2H), 2.50 (s, 3 H), 2.60-2.54 (m obscured by neighboring peak, 1 H), 2.94-2.82 (m, 1H), 3.81 (s, 3 H),

4.60 (s, 5 H), 7.01 (s, 1 H) ppm, 7.66 (s, 4H), 7.79-7.78 (m, 8H). ^{31}P NMR (162 MHz, acetone-d_6) δ 27.39 (s) ppm. ^{19}F NMR (376 MHz, acetone-d_6) δ -63.32 (s) ppm.

Table 2.7. Crystal data and structure refinement for 2.26

Empirical formula	C_{59} H_{55} B F_{24} N_3 P Ru
Formula weight	1404.91
Temperature	100(2) K
Wavelength	1.54178 Å
Crystal system	Monoclinic
Space group	C2/c
Unit cell dimensions	a = 19.0519(12) Å α= 90° b = 16.8814(10) Å β= 94.238(4)° c = 38.694(2) Å γ = 90°
Volume	12410.8(13) Å^3
Z	8
Density (calculated)	1.504 g/cm^3
Absorption coefficient	3.302 mm^{-1}
F(000)	5680
Crystal size	0.08 x 0.02 x 0.01mm^3
Crystal color, habit	Yellow plate
Theta range for data collection	3.63 to 69.31°
Index ranges	-22<=h<=22, -20<=k<=19, -36<=l<=46
Reflections collected	38189
Independent reflections	10849 [R(int) = 0.0358]

Table 2.7 Continued

Completeness to theta = 65.00°	97.0 %
Absorption correction	Multi-scan
Refinement method	Full-matrix least-squares on F^2
Data / restraints / parameters	10849 / 0 / 975
Goodness-of-fit on F^2	1.027
Final R indices [I>2sigma(I)]	R1 = 0.0641, wR2 = 0.1653
R indices (all data)	R1 = 0.0777, wR2 = 0.1782
Largest diff. peak and hole	2.032 and -0.485 e $Å^{-3}$

Table 2.8. Atomic coordinates (x 10^4) and equivalent isotropic displacement parameters ($Å^2$x 10^3) for 2.26. U(eq) is defined as one third of the trace of the orthogonalized U^{ij} tensor.

	x	y	z	U(eq)
Ru(1)	2666(1)	4053(1)	1083(1)	36(1)
P(1)	2297(1)	4732(1)	1561(1)	34(1)
F(31)	3613(4)	12257(4)	2087(3)	71(3)
F(31')	3800(30)	11840(60)	2019(9)	140(30)
F(32)	3226(5)	11747(7)	2538(2)	71(3)
F(32')	3190(30)	12080(50)	2436(18)	130(30)
F(33)	3897(3)	11093(4)	2241(2)	63(2)
F(33')	3650(40)	11040(30)	2390(20)	150(30)
F(34)	367(5)	11357(6)	1950(5)	91(5)

Table 2.8. Continued

	x	y	z	U(eq)
F(34')	255(6)	11337(11)	1692(7)	97(7)
F(35)	868(4)	12454(6)	2003(3)	70(4)
F(35')	579(11)	11810(20)	2143(3)	134(14)
F(36)	593(5)	12005(8)	1513(2)	73(4)
F(36')	743(9)	12423(12)	1696(11)	156(17)
F(41)	4349(2)	11571(3)	796(1)	87(1)
F(42)	4107(2)	11512(3)	247(1)	90(1)
F(43)	4434(2)	10496(2)	531(1)	66(1)
F(44)	1102(2)	10974(2)	75(1)	89(2)
F(45)	961(2)	11793(2)	480(1)	69(1)
F(46)	1609(2)	12095(2)	78(1)	74(1)
F(51)	-250(8)	7554(12)	1597(3)	106(6)
F(51')	130(30)	7319(12)	1668(11)	145(15)
F(52)	-161(8)	8701(6)	1802(3)	81(4)
F(52')	-448(14)	8320(30)	1652(12)	129(18)
F(53)	606(7)	7868(8)	1945(4)	82(5)
F(53')	480(20)	8200(40)	1992(8)	146(19)
F(54)	613(3)	7267(3)	415(1)	56(2)
F(54')	10(13)	7920(16)	337(6)	141(14)
F(55)	-63(5)	8248(7)	348(4)	89(5)
F(55')	328(8)	9013(8)	214(3)	93(5)
F(56)	961(9)	8356(11)	207(4)	107(7)
F(56')	1072(12)	8181(18)	189(8)	76(8)
F(61)	3773(7)	7718(11)	587(4)	75(4)
F(61')	3820(20)	6860(30)	860(17)	149(19)
F(62)	4726(7)	7693(12)	903(5)	98(6)
F(62')	3920(30)	7930(40)	591(8)	140(17)
F(63)	4006(11)	6786(7)	926(3)	87(5)
F(63')	4744(17)	7590(30)	936(10)	102(15)
F(64)	4300(4)	7496(6)	2202(2)	80(4)
F(64')	4398(13)	8140(30)	2259(5)	105(19)

Table 2.8. Continued

	x	y	z	U(eq)
F(65)	3215(4)	7573(8)	2274(2)	99(5)
F(65')	3790(30)	7178(11)	2195(5)	113(19)
F(66)	3860(7)	8571(4)	2354(2)	88(4)
F(66')	3390(20)	8200(30)	2369(5)	110(20)
N(1)	2333(2)	5283(2)	963(1)	34(1)
N(2)	2151(2)	6365(2)	1259(1)	40(1)
N(3)	3639(2)	4583(2)	1093(1)	40(1)
C(1)	1909(4)	3254(5)	847(4)	104(4)
C(2)	2449(6)	3297(4)	633(2)	82(3)
C(3)	3034(4)	3029(5)	818(3)	101(4)
C(4)	2873(9)	2822(4)	1136(3)	126(5)
C(5)	2170(10)	2950(6)	1157(3)	134(6)
C(7)	2286(3)	5795(3)	340(2)	53(1)
C(8)	2270(4)	6600(4)	163(2)	69(2)
C(9)	1638(4)	5308(4)	211(2)	75(2)
C(10)	2954(4)	5374(4)	260(2)	65(2)
C(11)	2257(3)	5903(3)	727(1)	42(1)
C(12)	2147(3)	6566(3)	914(1)	46(1)
C(13)	2270(2)	5577(3)	1274(1)	34(1)
C(14)	2048(3)	6896(3)	1550(2)	48(1)
C(15)	1367(2)	4577(3)	1665(1)	43(1)
C(16)	1130(3)	5069(4)	1961(2)	56(1)
C(17)	358(3)	4866(5)	2022(2)	70(2)
C(18)	-130(3)	4965(4)	1703(2)	64(2)
C(19)	120(3)	4475(4)	1407(2)	66(2)
C(20)	876(3)	4706(4)	1335(2)	50(1)
C(21)	2798(2)	4945(3)	1974(1)	37(1)
C(22)	2829(3)	4173(3)	2194(1)	46(1)
C(23)	3228(3)	4305(4)	2541(1)	48(1)
C(24)	3967(3)	4628(4)	2498(2)	56(1)
C(25)	3941(3)	5376(4)	2283(2)	55(1)

Table 2.8. Continued

	x	y	z	U(eq)
C(26)	3537(3)	5238(3)	1928(1)	44(1)
C(27)	4162(3)	4870(3)	1045(2)	47(1)
C(28)	4830(3)	5234(4)	970(2)	74(2)
C(31)	2219(2)	10332(2)	1573(1)	31(1)
C(32)	1577(2)	10723(3)	1607(1)	34(1)
C(33)	1522(2)	11372(3)	1820(1)	36(1)
C(34)	2093(3)	11657(3)	2021(1)	36(1)
C(35)	2735(2)	11275(3)	1996(1)	35(1)
C(36)	2795(2)	10640(3)	1776(1)	32(1)
C(37)	3369(3)	11589(3)	2211(1)	44(1)
C(38)	824(3)	11781(3)	1830(1)	46(1)
C(41)	2473(2)	10221(2)	940(1)	30(1)
C(42)	1930(2)	10612(3)	741(1)	35(1)
C(43)	2057(3)	11146(3)	485(1)	37(1)
C(44)	2743(3)	11321(3)	411(1)	39(1)
C(45)	3291(3)	10953(3)	603(1)	37(1)
C(46)	3159(2)	10419(2)	863(1)	32(1)
C(47)	4041(3)	11135(3)	544(2)	48(1)
C(48)	1422(3)	11512(3)	282(1)	45(1)
C(51)	1588(2)	9141(2)	1186(1)	32(1)
C(52)	1382(2)	8875(3)	855(1)	39(1)
C(53)	799(3)	8373(3)	788(2)	47(1)
C(54)	416(3)	8120(3)	1055(2)	48(1)
C(55)	617(2)	8366(3)	1387(1)	43(1)
C(56)	1188(2)	8868(3)	1453(1)	36(1)
C(57)	196(3)	8100(4)	1683(2)	54(1)
C(58)	579(4)	8111(6)	427(2)	80(2)
C(61)	2916(2)	9014(2)	1368(1)	28(1)
C(62)	3100(2)	8775(2)	1703(1)	29(1)
C(63)	3587(2)	8173(3)	1781(1)	34(1)
C(64)	3897(2)	7779(3)	1520(1)	36(1)

Table 2.8. Continued

	x	y	z	U(eq)
C(65)	3714(2)	7998(3)	1182(1)	37(1)
C(66)	3238(2)	8604(3)	1106(1)	33(1)
C(67)	4060(3)	7578(4)	896(2)	57(2)
C(68)	3753(3)	7943(3)	2150(1)	42(1)
B(1)	2300(2)	9676(3)	1269(1)	30(1)

Table 2.9. Anisotropic displacement parameters ($Å^2 x 10^3$) for 2.26. The anisotropic displacement factor exponent takes the form: $-2p^2[h^2 a^{*2} U^{11} + ... + 2 h k a^* b^* U^{12}]$

	U^{11}	U^{22}	U^{33}	U^{23}	U^{13}	U^{12}
Ru(1)	42(1)	26(1)	40(1)	-1(1)	3(1)	1(1)
P(1)	31(1)	34(1)	37(1)	0(1)	2(1)	-1(1)
F(31)	69(4)	55(4)	86(6)	12(3)	-19(4)	-28(3)
F(31')	90(30)	260(80)	71(18)	-70(40)	36(19)	-130(40)
F(32)	54(4)	113(7)	45(3)	-28(4)	-1(3)	-3(4)
F(32')	100(30)	150(50)	130(50)	-120(40)	-70(30)	40(30)
F(33)	42(3)	58(4)	85(5)	-30(4)	-24(3)	14(2)
F(33')	140(50)	140(40)	140(50)	50(30)	-110(40)	-50(30)
F(34)	46(5)	64(6)	169(14)	38(7)	55(8)	20(4)
F(34')	35(5)	95(11)	161(17)	-52(13)	3(9)	26(6)
F(35)	49(4)	63(6)	96(7)	-42(5)	-15(4)	33(4)
F(35')	91(12)	260(40)	52(7)	-21(12)	3(7)	108(18)
F(36)	56(5)	109(9)	52(4)	-6(4)	-9(3)	55(6)
F(36')	74(11)	73(13)	330(50)	120(20)	60(20)	41(10)
F(41)	60(2)	95(3)	108(3)	-41(3)	14(2)	-43(2)
F(42)	60(2)	109(3)	101(3)	57(3)	17(2)	-14(2)
F(43)	45(2)	63(2)	93(3)	8(2)	22(2)	-3(2)
F(44)	91(3)	57(2)	107(3)	-14(2)	-64(3)	16(2)

Table 2.9. Continued

	U^{11}	U^{22}	U^{33}	U^{23}	U^{13}	U^{12}
F(45)	59(2)	78(2)	69(2)	16(2)	2(2)	33(2)
F(46)	73(2)	73(2)	74(2)	38(2)	-7(2)	10(2)
F(51)	98(9)	129(13)	97(6)	-35(7)	43(6)	-89(9)
F(51')	180(30)	49(9)	230(30)	14(13)	140(30)	-22(15)
F(52)	81(7)	78(5)	90(6)	13(4)	50(5)	22(5)
F(52')	62(12)	170(40)	160(30)	80(30)	50(15)	38(17)
F(53)	61(5)	112(8)	77(8)	47(7)	25(5)	13(6)
F(53')	140(30)	240(40)	65(11)	-10(20)	15(17)	-130(30)
F(54)	57(3)	49(3)	62(4)	-24(2)	0(2)	-10(2)
F(54')	160(20)	190(20)	73(12)	43(15)	-48(14)	-140(20)
F(55)	73(6)	112(9)	74(6)	-26(6)	-46(5)	38(7)
F(55')	107(10)	85(9)	81(9)	8(7)	-30(7)	-8(8)
F(56)	162(15)	117(11)	39(5)	2(6)	-11(7)	-94(11)
F(56')	54(8)	102(15)	73(12)	-29(9)	4(7)	8(9)
F(61)	84(7)	90(8)	46(6)	-31(6)	-22(4)	53(5)
F(61')	69(16)	120(30)	260(40)	-130(30)	34(18)	-14(15)
F(62)	48(7)	165(13)	84(10)	-63(9)	25(6)	-6(8)
F(62')	270(40)	120(30)	35(12)	13(12)	48(19)	140(30)
F(63)	135(13)	43(5)	83(7)	-12(5)	18(6)	50(7)
F(63')	70(18)	180(30)	55(13)	-7(14)	4(10)	90(20)
F(64)	74(6)	113(9)	51(3)	22(4)	-1(3)	65(6)
F(64')	75(16)	180(40)	58(12)	42(18)	-34(11)	-70(20)
F(65)	68(4)	170(13)	58(4)	64(6)	-5(3)	-29(6)
F(65')	230(60)	44(10)	64(12)	28(8)	-20(20)	18(16)
F(66)	151(11)	68(4)	40(4)	1(3)	-24(5)	21(5)
F(66')	140(30)	160(40)	48(12)	43(19)	39(17)	130(30)
N(1)	38(2)	28(2)	36(2)	0(2)	-3(2)	-1(2)
N(2)	38(2)	33(2)	47(2)	-4(2)	-1(2)	4(2)
N(3)	37(2)	33(2)	51(2)	-3(2)	7(2)	5(2)
C(1)	56(4)	54(4)	200(12)	-60(6)	-7(6)	-12(3)
C(2)	153(9)	42(3)	48(4)	-19(3)	-11(4)	-16(4)

Table 2.9. Continued

	U^{11}	U^{22}	U^{33}	U^{23}	U^{13}	U^{12}
C(3)	69(5)	56(4)	178(11)	-68(6)	16(6)	4(4)
C(4)	243(15)	30(4)	92(7)	-4(4)	-69(9)	20(6)
C(5)	265(16)	48(5)	102(7)	-30(5)	108(10)	-80(8)
C(7)	72(4)	42(3)	43(3)	5(2)	-6(3)	-2(3)
C(8)	101(5)	51(3)	54(4)	8(3)	6(3)	7(3)
C(9)	96(5)	66(4)	59(4)	-8(3)	-16(4)	-11(4)
C(10)	99(5)	53(3)	46(3)	5(3)	18(3)	6(3)
C(11)	49(3)	31(2)	44(3)	1(2)	-4(2)	1(2)
C(12)	52(3)	33(2)	50(3)	5(2)	-5(2)	2(2)
C(13)	28(2)	33(2)	41(3)	-1(2)	2(2)	-2(2)
C(14)	50(3)	32(2)	61(3)	-10(2)	8(2)	2(2)
C(15)	33(2)	41(3)	55(3)	4(2)	5(2)	-3(2)
C(16)	37(3)	69(4)	64(4)	-4(3)	11(2)	0(3)
C(17)	40(3)	94(5)	78(5)	2(4)	20(3)	0(3)
C(18)	28(2)	67(4)	99(5)	7(4)	11(3)	1(2)
C(19)	34(3)	66(4)	96(5)	-2(4)	-7(3)	-4(3)
C(20)	33(2)	59(3)	57(3)	-8(3)	-3(2)	3(2)
C(21)	38(2)	39(2)	35(2)	-2(2)	3(2)	4(2)
C(22)	42(3)	47(3)	49(3)	2(2)	4(2)	-1(2)
C(23)	52(3)	58(3)	33(3)	11(2)	3(2)	4(2)
C(24)	41(3)	82(4)	42(3)	-3(3)	-7(2)	2(3)
C(25)	39(3)	72(4)	51(3)	-4(3)	-5(2)	-10(3)
C(26)	41(3)	52(3)	38(3)	0(2)	2(2)	-6(2)
C(27)	46(3)	37(3)	60(3)	3(2)	8(2)	12(2)
C(28)	39(3)	57(4)	125(6)	15(4)	15(3)	6(3)
C(31)	27(2)	28(2)	37(2)	4(2)	2(2)	3(2)
C(32)	30(2)	34(2)	37(2)	2(2)	-2(2)	4(2)
C(33)	36(2)	36(2)	38(2)	3(2)	5(2)	10(2)
C(34)	44(3)	33(2)	32(2)	-1(2)	2(2)	9(2)
C(35)	36(2)	32(2)	38(2)	-1(2)	3(2)	1(2)
C(36)	28(2)	30(2)	37(2)	3(2)	4(2)	2(2)

Table 2.9. Continued

	U^{11}	U^{22}	U^{33}	U^{23}	U^{13}	U^{12}
C(37)	47(3)	42(3)	43(3)	-10(2)	-1(2)	0(2)
C(38)	44(3)	50(3)	44(3)	-8(2)	1(2)	14(2)
C(41)	31(2)	21(2)	36(2)	-4(2)	-4(2)	0(2)
C(42)	33(2)	31(2)	40(3)	0(2)	-2(2)	1(2)
C(43)	43(3)	29(2)	38(3)	2(2)	-5(2)	2(2)
C(44)	54(3)	28(2)	35(2)	4(2)	0(2)	-5(2)
C(45)	43(2)	29(2)	40(3)	-5(2)	2(2)	-9(2)
C(46)	34(2)	25(2)	37(2)	0(2)	-5(2)	-1(2)
C(47)	49(3)	38(3)	57(3)	1(2)	9(2)	-10(2)
C(48)	58(3)	37(3)	39(3)	4(2)	-8(2)	2(2)
C(51)	23(2)	26(2)	46(3)	-4(2)	-5(2)	5(2)
C(52)	29(2)	41(3)	46(3)	-2(2)	0(2)	2(2)
C(53)	36(2)	43(3)	61(3)	-11(2)	-5(2)	-4(2)
C(54)	32(2)	42(3)	68(4)	-4(3)	0(2)	-8(2)
C(55)	31(2)	36(2)	61(3)	1(2)	4(2)	1(2)
C(56)	30(2)	33(2)	46(3)	5(2)	1(2)	4(2)
C(57)	46(3)	54(3)	64(4)	5(3)	12(3)	-9(3)
C(58)	57(4)	113(6)	68(5)	-24(5)	0(3)	-31(4)
C(61)	22(2)	24(2)	38(2)	1(2)	-1(2)	-2(2)
C(62)	23(2)	29(2)	36(2)	1(2)	2(2)	0(2)
C(63)	26(2)	35(2)	42(3)	3(2)	0(2)	-1(2)
C(64)	29(2)	30(2)	49(3)	3(2)	-3(2)	7(2)
C(65)	32(2)	33(2)	46(3)	-4(2)	-1(2)	6(2)
C(66)	31(2)	30(2)	36(2)	-2(2)	-4(2)	0(2)
C(67)	56(3)	58(4)	55(4)	-12(3)	-6(3)	27(3)
C(68)	43(3)	43(3)	41(3)	11(2)	0(2)	8(2)
B(1)	22(2)	27(2)	39(3)	2(2)	-3(2)	3(2)

Table 2.10. Bond lengths and angles for 2.26

Ru(1)-N(3)	2.057(4)	F(35')-C(38)	1.331(15)
Ru(1)-C(5)	2.117(7)	F(36)-F(36')	1.02(4)
Ru(1)-C(4)	2.122(7)	F(36)-C(38)	1.327(9)
Ru(1)-C(1)	2.130(7)	F(36')-C(38)	1.208(13)
Ru(1)-C(3)	2.153(6)	F(41)-C(47)	1.322(7)
Ru(1)-C(2)	2.172(6)	F(42)-C(47)	1.329(7)
Ru(1)-N(1)	2.212(4)	F(43)-C(47)	1.316(7)
Ru(1)-P(1)	2.3306(12)	F(44)-C(48)	1.329(6)
P(1)-C(13)	1.807(5)	F(45)-C(48)	1.299(7)
P(1)-C(21)	1.836(5)	F(46)-C(48)	1.325(6)
P(1)-C(15)	1.864(5)	F(51)-F(51')	0.85(4)
F(31)-F(31')	0.84(9)	F(51)-C(57)	1.280(10)
F(31)-C(37)	1.323(8)	F(51)-F(52')	1.37(4)
F(31)-F(32')	1.65(8)	F(51')-C(57)	1.32(2)
F(31')-C(37)	1.23(3)	F(51')-F(53)	1.64(5)
F(31')-F(33)	1.53(9)	F(52)-F(52')	1.00(5)
F(32)-F(32')	0.69(9)	F(52)-C(57)	1.324(10)
F(32)-C(37)	1.340(9)	F(52)-F(53')	1.62(5)
F(32)-F(33')	1.57(9)	F(52')-C(57)	1.280(19)
F(32')-C(37)	1.27(4)	F(53)-F(53')	0.64(7)
F(33)-F(33')	0.79(10)	F(53)-C(57)	1.294(15)
F(33)-C(37)	1.308(8)	F(53')-C(57)	1.29(3)
F(33')-C(37)	1.26(4)	F(54)-C(58)	1.428(11)
F(34)-F(34')	1.007(17)	F(54)-F(54')	1.61(3)
F(34)-F(35')	1.12(2)	F(54')-F(55)	0.57(3)
F(34)-C(38)	1.243(9)	F(54')-C(58)	1.16(2)
F(34')-C(38)	1.392(15)	F(55)-C(58)	1.261(12)
F(34')-F(36)	1.49(2)	F(55)-F(55')	1.597(19)
F(35)-F(36')	1.20(4)	F(55')-F(56)	1.64(2)
F(35)-C(38)	1.319(8)	F(55')-C(58)	1.781(17)
F(35)-F(35')	1.35(3)	F(56)-C(58)	1.233(16)

Table 2.10. Continued

F(56')-C(58)	1.37(3)	C(7)-C(8)	1.522(8)
F(61)-C(67)	1.298(14)	C(7)-C(9)	1.535(9)
F(61')-C(67)	1.30(4)	C(11)-C(12)	1.359(7)
F(62)-C(67)	1.282(14)	C(15)-C(16)	1.510(8)
F(62')-C(67)	1.33(4)	C(15)-C(20)	1.540(7)
F(63)-C(67)	1.348(14)	C(16)-C(17)	1.546(7)
F(63')-C(67)	1.30(3)	C(17)-C(18)	1.498(10)
F(64)-F(65')	1.11(4)	C(18)-C(19)	1.519(10)
F(64)-F(64')	1.13(4)	C(19)-C(20)	1.539(7)
F(64)-C(68)	1.289(7)	C(21)-C(26)	1.515(7)
F(64')-C(68)	1.315(17)	C(21)-C(22)	1.555(7)
F(64')-F(66)	1.33(4)	C(22)-C(23)	1.509(8)
F(65)-F(66')	1.17(4)	C(23)-C(24)	1.531(8)
F(65)-C(68)	1.321(8)	C(24)-C(25)	1.512(9)
F(65)-F(65')	1.33(4)	C(25)-C(26)	1.543(7)
F(65')-C(68)	1.303(18)	C(27)-C(28)	1.462(8)
F(66)-F(66')	1.10(5)	C(31)-C(36)	1.401(6)
F(66)-C(68)	1.331(8)	C(31)-C(32)	1.405(6)
F(66')-C(68)	1.219(18)	C(31)-B(1)	1.630(7)
N(1)-C(13)	1.316(6)	C(32)-C(33)	1.381(7)
N(1)-C(11)	1.389(6)	C(33)-C(34)	1.376(7)
N(2)-C(13)	1.349(6)	C(33)-C(38)	1.501(6)
N(2)-C(12)	1.376(7)	C(34)-C(35)	1.393(6)
N(2)-C(14)	1.465(6)	C(35)-C(36)	1.379(6)
N(3)-C(27)	1.134(7)	C(35)-C(37)	1.511(7)
C(1)-C(5)	1.366(16)	C(41)-C(46)	1.403(6)
C(1)-C(2)	1.369(13)	C(41)-C(42)	1.408(6)
C(2)-C(3)	1.356(13)	C(41)-B(1)	1.624(7)
C(3)-C(4)	1.339(16)	C(42)-C(43)	1.374(7)
C(4)-C(5)	1.363(18)	C(43)-C(44)	1.389(7)
C(7)-C(10)	1.509(9)	C(43)-C(48)	1.525(7)
C(7)-C(11)	1.513(8)	C(44)-C(45)	1.383(7)

Table 2.10. Continued

C(45)-C(46)	1.387(7)	C(55)-C(57)	1.512(8)
C(45)-C(47)	1.497(7)	C(61)-C(62)	1.380(6)
C(51)-C(52)	1.386(7)	C(61)-C(66)	1.406(6)
C(51)-C(56)	1.405(7)	C(61)-B(1)	1.645(6)
C(51)-B(1)	1.643(6)	C(62)-C(63)	1.394(6)
C(52)-C(53)	1.406(7)	C(63)-C(64)	1.378(7)
C(53)-C(54)	1.375(8)	C(63)-C(68)	1.489(7)
C(53)-C(58)	1.494(9)	C(64)-C(65)	1.382(7)
C(54)-C(55)	1.379(8)	C(65)-C(66)	1.385(6)
C(55)-C(56)	1.388(7)	C(65)-C(67)	1.504(7)
N(3)-Ru(1)-C(5)	142.3(6)	N(3)-Ru(1)-P(1)	95.41(12)
N(3)-Ru(1)-C(4)	105.3(5)	C(5)-Ru(1)-P(1)	99.2(2)
C(5)-Ru(1)-C(4)	37.5(5)	C(4)-Ru(1)-P(1)	118.0(4)
N(3)-Ru(1)-C(1)	149.9(3)	C(1)-Ru(1)-P(1)	114.6(3)
C(5)-Ru(1)-C(1)	37.5(5)	C(3)-Ru(1)-P(1)	154.4(4)
C(4)-Ru(1)-C(1)	62.4(4)	C(2)-Ru(1)-P(1)	151.0(3)
N(3)-Ru(1)-C(3)	92.0(2)	N(1)-Ru(1)-P(1)	66.75(10)
C(5)-Ru(1)-C(3)	61.5(4)	C(13)-P(1)-C(21)	111.7(2)
C(4)-Ru(1)-C(3)	36.5(4)	C(13)-P(1)-C(15)	105.0(2)
C(1)-Ru(1)-C(3)	61.4(3)	C(21)-P(1)-C(15)	106.3(2)
N(3)-Ru(1)-C(2)	113.0(3)	C(13)-P(1)-Ru(1)	84.09(15)
C(5)-Ru(1)-C(2)	62.1(3)	C(21)-P(1)-Ru(1)	128.35(16)
C(4)-Ru(1)-C(2)	61.7(3)	C(15)-P(1)-Ru(1)	116.70(17)
C(1)-Ru(1)-C(2)	37.1(4)	F(31')-F(31)-C(37)	65(3)
C(3)-Ru(1)-C(2)	36.5(4)	F(31')-F(31)-F(32')	111(4)
N(3)-Ru(1)-N(1)	80.73(15)	C(37)-F(31)-F(32')	49(2)
C(5)-Ru(1)-N(1)	137.0(6)	F(31)-F(31')-C(37)	77(3)
C(4)-Ru(1)-N(1)	171.4(3)	F(31)-F(31')-F(33)	123(4)
C(1)-Ru(1)-N(1)	109.3(3)	C(37)-F(31')-F(33)	55(3)
C(3)-Ru(1)-N(1)	138.8(4)	F(32')-F(32)-C(37)	69(4)
C(2)-Ru(1)-N(1)	110.5(2)	F(32')-F(32)-F(33')	117(5)

Table 2.10. Continued

C(37)-F(32)-F(33')	50(2)	F(51)-F(51')-F(53)	111(3)
F(32)-F(32')-C(37)	80(5)	C(57)-F(51')-F(53)	50.4(15)
F(32)-F(32')-F(31)	125(5)	F(52')-F(52)-C(57)	65.2(14)
C(37)-F(32')-F(31)	52(3)	F(52')-F(52)-F(53')	107(2)
F(33')-F(33)-C(37)	69(4)	C(57)-F(52)-F(53')	50.7(16)
F(33')-F(33)-F(31')	117(4)	F(52)-F(52')-C(57)	70(2)
C(37)-F(33)-F(31')	51(2)	F(52)-F(52')-F(51)	123(2)
F(33)-F(33')-C(37)	76(4)	C(57)-F(52')-F(51)	57.5(12)
F(33)-F(33')-F(32)	122(5)	F(53')-F(53)-C(57)	75(4)
C(37)-F(33')-F(32)	55(3)	F(53')-F(53)-F(51')	118(4)
F(34')-F(34)-F(35')	136(2)	C(57)-F(53)-F(51')	52.0(14)
F(34')-F(34)-C(38)	75.6(11)	F(53)-F(53')-C(57)	76(4)
F(35')-F(34)-C(38)	68.3(12)	F(53)-F(53')-F(52)	128(5)
F(34)-F(34')-C(38)	59.9(9)	C(57)-F(53')-F(52)	52.8(17)
F(34)-F(34')-F(36)	111.5(14)	C(58)-F(54)-F(54')	44.5(7)
C(38)-F(34')-F(36)	54.6(8)	F(55)-F(54')-C(58)	86(3)
F(36')-F(35)-C(38)	57.2(9)	F(55)-F(54')-F(54)	146(3)
F(36')-F(35)-F(35')	107.8(12)	C(58)-F(54')-F(54)	59.6(14)
C(38)-F(35)-F(35')	59.7(8)	F(54')-F(55)-C(58)	67(3)
F(34)-F(35')-C(38)	60.2(7)	F(54')-F(55)-F(55')	130(4)
F(34)-F(35')-F(35)	114.6(14)	C(58)-F(55)-F(55')	76.1(9)
C(38)-F(35')-F(35)	58.8(11)	F(55)-F(55')-F(56)	79.6(9)
F(36')-F(36)-C(38)	60.2(12)	F(55)-F(55')-C(58)	43.4(5)
F(36')-F(36)-F(34')	108.0(15)	F(56)-F(55')-C(58)	42.0(6)
C(38)-F(36)-F(34')	58.8(8)	C(58)-F(56)-F(55')	75.1(12)
F(36)-F(36')-F(35)	137.9(15)	F(65')-F(64)-F(64')	127(2)
F(36)-F(36')-C(38)	72.5(13)	F(65')-F(64)-C(68)	65.3(13)
F(35)-F(36')-C(38)	66.6(14)	F(64')-F(64)-C(68)	65.4(14)
F(51')-F(51)-C(57)	74(2)	F(64)-F(64')-C(68)	63.1(10)
F(51')-F(51)-F(52')	129(3)	F(64)-F(64')-F(66)	117.3(15)
C(57)-F(51)-F(52')	57.6(13)	C(68)-F(64')-F(66)	60.5(13)
F(51)-F(51')-C(57)	68.1(17)	F(66')-F(65)-C(68)	58.3(12)

Table 2.10. Continued

F(66')-F(65)-F(65')	108.1(17)	C(1)-C(5)-Ru(1)	71.7(4)
C(68)-F(65)-F(65')	58.8(12)	C(10)-C(7)-C(11)	110.6(5)
F(64)-F(65')-C(68)	63.9(13)	C(10)-C(7)-C(8)	108.5(5)
F(64)-F(65')-F(65)	119.0(17)	C(11)-C(7)-C(8)	109.7(5)
C(68)-F(65')-F(65)	60.2(12)	C(10)-C(7)-C(9)	110.7(6)
F(66')-F(66)-F(64')	111.1(16)	C(11)-C(7)-C(9)	107.5(5)
F(66')-F(66)-C(68)	59.4(13)	C(8)-C(7)-C(9)	110.0(5)
F(64')-F(66)-C(68)	59.3(10)	C(12)-C(11)-N(1)	106.4(4)
F(66)-F(66')-F(65)	135.5(18)	C(12)-C(11)-C(7)	130.2(5)
F(66)-F(66')-C(68)	69.9(18)	N(1)-C(11)-C(7)	123.4(4)
F(65)-F(66')-C(68)	67.2(16)	C(11)-C(12)-N(2)	108.8(4)
C(13)-N(1)-C(11)	107.8(4)	N(1)-C(13)-N(2)	111.0(4)
C(13)-N(1)-Ru(1)	101.9(3)	N(1)-C(13)-P(1)	105.3(3)
C(11)-N(1)-Ru(1)	149.3(3)	N(2)-C(13)-P(1)	143.3(4)
C(13)-N(2)-C(12)	106.0(4)	C(16)-C(15)-C(20)	110.7(4)
C(13)-N(2)-C(14)	126.9(4)	C(16)-C(15)-P(1)	115.3(4)
C(12)-N(2)-C(14)	127.1(4)	C(20)-C(15)-P(1)	109.3(4)
C(27)-N(3)-Ru(1)	169.4(5)	C(15)-C(16)-C(17)	109.6(5)
C(5)-C(1)-C(2)	108.1(9)	C(18)-C(17)-C(16)	112.9(6)
C(5)-C(1)-Ru(1)	70.7(5)	C(17)-C(18)-C(19)	110.6(5)
C(2)-C(1)-Ru(1)	73.1(4)	C(18)-C(19)-C(20)	110.3(5)
C(3)-C(2)-C(1)	106.8(9)	C(19)-C(20)-C(15)	109.5(5)
C(3)-C(2)-Ru(1)	71.0(4)	C(26)-C(21)-C(22)	109.9(4)
C(1)-C(2)-Ru(1)	69.8(4)	C(26)-C(21)-P(1)	112.8(3)
C(4)-C(3)-C(2)	109.6(9)	C(22)-C(21)-P(1)	108.0(3)
C(4)-C(3)-Ru(1)	70.5(5)	C(23)-C(22)-C(21)	111.0(4)
C(2)-C(3)-Ru(1)	72.5(4)	C(22)-C(23)-C(24)	111.3(4)
C(3)-C(4)-C(5)	107.9(9)	C(25)-C(24)-C(23)	111.3(5)
C(3)-C(4)-Ru(1)	73.0(5)	C(24)-C(25)-C(26)	111.0(5)
C(5)-C(4)-Ru(1)	71.1(5)	C(21)-C(26)-C(25)	110.5(4)
C(4)-C(5)-C(1)	107.6(8)	N(3)-C(27)-C(28)	178.0(7)
C(4)-C(5)-Ru(1)	71.4(5)	C(36)-C(31)-C(32)	115.1(4)

Table 2.10. Continued

C(36)-C(31)-B(1)	123.0(4)	F(36')-C(38)-F(34)	127.3(9)
C(32)-C(31)-B(1)	121.1(4)	F(36')-C(38)-F(35)	56.3(18)
C(33)-C(32)-C(31)	122.3(4)	F(34)-C(38)-F(35)	109.1(8)
C(34)-C(33)-C(32)	121.6(4)	F(36')-C(38)-F(36)	47.3(18)
C(34)-C(33)-C(38)	119.3(4)	F(34)-C(38)-F(36)	108.5(9)
C(32)-C(33)-C(38)	119.1(4)	F(35)-C(38)-F(36)	103.1(7)
C(33)-C(34)-C(35)	117.4(4)	F(36')-C(38)-F(35')	108.6(16)
C(36)-C(35)-C(34)	121.1(4)	F(34)-C(38)-F(35')	51.5(13)
C(36)-C(35)-C(37)	120.9(4)	F(35)-C(38)-F(35')	61.4(14)
C(34)-C(35)-C(37)	117.9(4)	F(36)-C(38)-F(35')	135.8(7)
C(35)-C(36)-C(31)	122.5(4)	F(36')-C(38)-F(34')	104.3(15)
F(31')-C(37)-F(33')	108(4)	F(34)-C(38)-F(34')	44.5(8)
F(31')-C(37)-F(32')	114(3)	F(35)-C(38)-F(34')	132.7(7)
F(33')-C(37)-F(32')	103(3)	F(36)-C(38)-F(34')	66.6(11)
F(31')-C(37)-F(33)	74(5)	F(35')-C(38)-F(34')	93.1(13)
F(33')-C(37)-F(33)	36(5)	F(36')-C(38)-C(33)	119.1(9)
F(32')-C(37)-F(33)	127(3)	F(34)-C(38)-C(33)	113.1(5)
F(31')-C(37)-F(31)	38(5)	F(35)-C(38)-C(33)	112.7(5)
F(33')-C(37)-F(31)	133(3)	F(36)-C(38)-C(33)	109.9(5)
F(32')-C(37)-F(31)	79(4)	F(35')-C(38)-C(33)	114.2(7)
F(33)-C(37)-F(31)	106.8(6)	F(34')-C(38)-C(33)	114.2(7)
F(31')-C(37)-F(32)	134(2)	C(46)-C(41)-C(42)	115.5(4)
F(33')-C(37)-F(32)	74(5)	C(46)-C(41)-B(1)	123.3(4)
F(32')-C(37)-F(32)	31(4)	C(42)-C(41)-B(1)	120.7(4)
F(33)-C(37)-F(32)	104.6(6)	C(43)-C(42)-C(41)	122.7(4)
F(31)-C(37)-F(32)	105.9(6)	C(42)-C(43)-C(44)	120.4(4)
F(31')-C(37)-C(35)	109.5(16)	C(42)-C(43)-C(48)	117.5(4)
F(33')-C(37)-C(35)	110(2)	C(44)-C(43)-C(48)	122.0(4)
F(32')-C(37)-C(35)	111(2)	C(45)-C(44)-C(43)	118.6(4)
F(33)-C(37)-C(35)	113.7(5)	C(44)-C(45)-C(46)	120.8(4)
F(31)-C(37)-C(35)	112.8(5)	C(44)-C(45)-C(47)	121.3(4)
F(32)-C(37)-C(35)	112.4(6)	C(46)-C(45)-C(47)	117.9(4)

Table 2.10. Continued

C(45)-C(46)-C(41)	122.0(4)	F(52')-C(57)-F(51')	101.6(17)
F(43)-C(47)-F(41)	105.2(5)	F(53')-C(57)-F(51')	102(2)
F(43)-C(47)-F(42)	105.6(5)	F(53)-C(57)-F(51')	78(2)
F(41)-C(47)-F(42)	107.8(5)	F(51)-C(57)-F(52)	107.1(8)
F(43)-C(47)-C(45)	113.0(4)	F(52')-C(57)-F(52)	45(2)
F(41)-C(47)-C(45)	112.3(5)	F(53')-C(57)-F(52)	76(3)
F(42)-C(47)-C(45)	112.4(5)	F(53)-C(57)-F(52)	104.7(9)
F(45)-C(48)-F(46)	107.5(4)	F(51')-C(57)-F(52)	136.6(13)
F(45)-C(48)-F(44)	107.7(5)	F(51)-C(57)-C(55)	113.5(7)
F(46)-C(48)-F(44)	106.3(5)	F(52')-C(57)-C(55)	113.6(11)
F(45)-C(48)-C(43)	112.9(4)	F(53')-C(57)-C(55)	117.1(14)
F(46)-C(48)-C(43)	111.7(5)	F(53)-C(57)-C(55)	111.0(7)
F(44)-C(48)-C(43)	110.3(4)	F(51')-C(57)-C(55)	108.5(12)
C(52)-C(51)-C(56)	116.2(4)	F(52)-C(57)-C(55)	110.6(6)
C(52)-C(51)-B(1)	122.1(4)	F(54')-C(58)-F(56)	118.1(15)
C(56)-C(51)-B(1)	121.4(4)	F(54')-C(58)-F(55)	27.0(16)
C(51)-C(52)-C(53)	122.1(5)	F(56)-C(58)-F(55)	112.4(13)
C(54)-C(53)-C(52)	120.3(5)	F(54')-C(58)-F(56')	119.5(19)
C(54)-C(53)-C(58)	118.8(5)	F(56)-C(58)-F(56')	15.3(19)
C(52)-C(53)-C(58)	120.9(6)	F(55)-C(58)-F(56')	121.4(15)
C(53)-C(54)-C(55)	118.8(5)	F(54')-C(58)-F(54)	75.9(16)
C(54)-C(55)-C(56)	120.9(5)	F(56)-C(58)-F(54)	106.3(11)
C(54)-C(55)-C(57)	119.3(5)	F(55)-C(58)-F(54)	102.8(8)
C(56)-C(55)-C(57)	119.7(5)	F(56')-C(58)-F(54)	91.5(14)
C(55)-C(56)-C(51)	121.7(5)	F(54')-C(58)-C(53)	123.7(15)
F(51)-C(57)-F(52')	65(2)	F(56)-C(58)-C(53)	114.0(9)
F(51)-C(57)-F(53')	123.9(16)	F(55)-C(58)-C(53)	112.0(8)
F(52')-C(57)-F(53')	112(2)	F(56')-C(58)-C(53)	116.4(14)
F(51)-C(57)-F(53)	109.6(11)	F(54)-C(58)-C(53)	108.5(7)
F(52')-C(57)-F(53)	132.9(17)	F(54')-C(58)-F(55')	83.4(14)
F(53')-C(57)-F(53)	29(3)	F(56)-C(58)-F(55')	62.9(12)
F(51)-C(57)-F(51')	38.0(19)	F(55)-C(58)-F(55')	60.5(9)

Table 2.10. Continued

F(56')-C(58)-F(55')	77.7(13)	F(61)-C(67)-C(65)	114.4(7)
F(54)-C(58)-F(55')	148.1(7)	F(62')-C(67)-C(65)	111.8(15)
C(53)-C(58)-F(55')	103.2(7)	F(63)-C(67)-C(65)	111.3(8)
C(62)-C(61)-C(66)	116.1(4)	F(66')-C(68)-F(64)	126.6(10)
C(62)-C(61)-B(1)	123.0(4)	F(66')-C(68)-F(65')	107(2)
C(66)-C(61)-B(1)	120.6(4)	F(64)-C(68)-F(65')	50.8(19)
C(61)-C(62)-C(63)	122.4(4)	F(66')-C(68)-F(64')	104(2)
C(64)-C(63)-C(62)	120.6(4)	F(64)-C(68)-F(64')	51.4(18)
C(64)-C(63)-C(68)	120.1(4)	F(65')-C(68)-F(64')	100(2)
C(62)-C(63)-C(68)	119.3(4)	F(66')-C(68)-F(65)	55(2)
C(63)-C(64)-C(65)	118.3(4)	F(64)-C(68)-F(65)	107.8(7)
C(64)-C(65)-C(66)	121.0(4)	F(65')-C(68)-F(65)	61.0(19)
C(64)-C(65)-C(67)	118.5(4)	F(64')-C(68)-F(65)	137.5(9)
C(66)-C(65)-C(67)	120.5(5)	F(66')-C(68)-F(66)	51(2)
C(65)-C(66)-C(61)	121.7(4)	F(64)-C(68)-F(66)	106.7(7)
F(62)-C(67)-F(61')	118(2)	F(65')-C(68)-F(66)	134.9(11)
F(62)-C(67)-F(63')	10(3)	F(64')-C(68)-F(66)	60.3(18)
F(61')-C(67)-F(63')	111(3)	F(65)-C(68)-F(66)	104.4(8)
F(62)-C(67)-F(61)	109.9(13)	F(66')-C(68)-C(63)	118.8(9)
F(61')-C(67)-F(61)	87(3)	F(64)-C(68)-C(63)	114.5(5)
F(63')-C(67)-F(61)	117.2(19)	F(65')-C(68)-C(63)	113.1(10)
F(62)-C(67)-F(62')	95(3)	F(64')-C(68)-C(63)	111.6(9)
F(61')-C(67)-F(62')	106(3)	F(65)-C(68)-C(63)	110.8(5)
F(63')-C(67)-F(62')	104(3)	F(66)-C(68)-C(63)	112.0(5)
F(61)-C(67)-F(62')	20(4)	C(41)-B(1)-C(31)	102.5(3)
F(62)-C(67)-F(63)	103.2(11)	C(41)-B(1)-C(51)	111.8(4)
F(61')-C(67)-F(63)	19(3)	C(31)-B(1)-C(51)	113.2(4)
F(63')-C(67)-F(63)	95(2)	C(41)-B(1)-C(61)	112.5(4)
F(61)-C(67)-F(63)	103.3(10)	C(31)-B(1)-C(61)	113.4(4)
F(62')-C(67)-F(63)	120(3)	C(51)-B(1)-C(61)	103.7(3)
F(62)-C(67)-C(65)	113.6(8)		
F(61')-C(67)-C(65)	110.7(19)		
F(63')-C(67)-C(65)	113.1(17)		

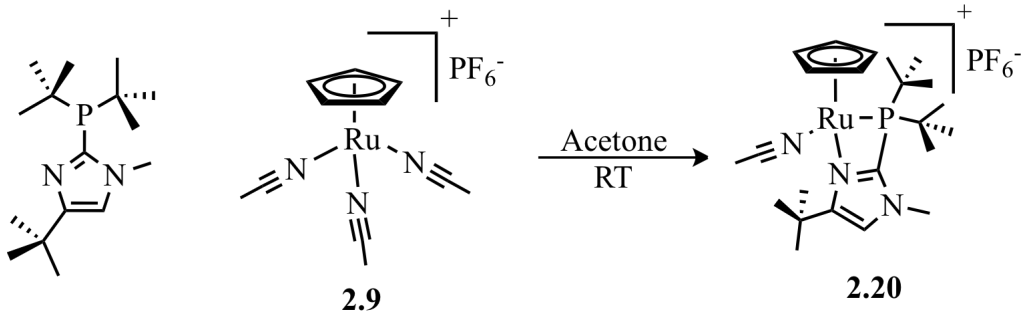

Figure 2.22. Synthesis of 2.20

Synthesis of [CpRu (4-(*tert*-butyl)-2-(di-*tert*-butylphosphino)-1-methyl-1*H*-imidazole)(acetonitrile)]PF_6 (2.20) In a glove box, ruthenium precursor $[CpRu(CH_3CN)_3]PF_6$ (108.7 mg, 0.250 mmol) was combined in a scintillation vial equipped with a magnetic stir bar and deoxygenated acetone (4 mL). The phosphine 4-(*tert*-butyl)-2-(di-*tert*-butylphosphino)-1-methyl-1*H*-imidazole, (70.7 mg, 0.250 mmol) was added dropwise in deoxygenated acetone (3 mL), and the resulting solution was allowed to stir overnight at room temperature under an atmosphere of nitrogen. The solvent was removed in vacuo, without stirring, and the residue left under vacuum until a flaky powder. The product was obtained as yellow colored powder in 101.6 % yield (161.1 mg, ~4 mol% acetone is present). ^{1}H NMR (500 MHz, acetone-d_6) δ 1.41 (s, 9 H), 1.46 (broad d, J = 14.5, 18H), 2.44 (s, 3 H), 3.86 (s, 3 H), 4.58 (s, 5 H), 7.05 (s, 1 H) ppm. ^{31}P NMR (202 MHz, acetone-d_6) δ 58.59 (s) ppm. Elemental calculated for $C_{23}H_{39}F_6N_3P_2Ru$ (634.58) C, 43.53; H, 6.19; N, 6.62. Found C, 42.66; H, 5.94; N, 6.33.

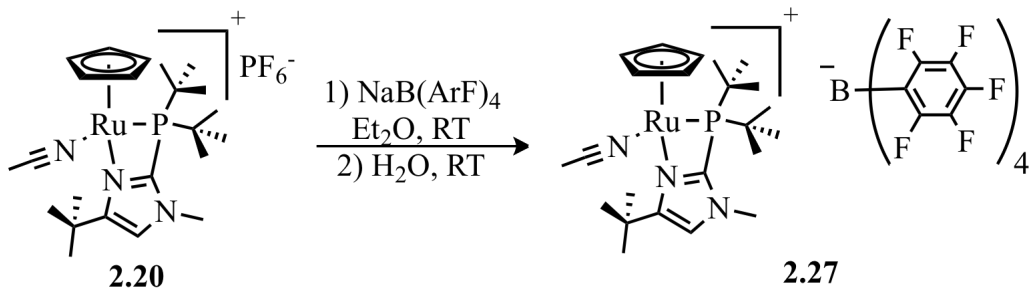

Figure 2.23. Anion exchange of 2.20

Synthesis of [CpRu (4-(*tert*-butyl)-2-(di-*tert*-butylphosphino)-1-methyl-1*H*-imidazole)(acetonitrile)]B[(C_6F_5)]$_4$ (2.27) In a glove box, ruthenium complex **2.20** (63.5 mg, 0.100 mmol) was combined in a scintillation vial equipped with a magnetic stir bar and deoxygenated ethyl ether (2 mL). The salt, potassium tetrakis(pentafluorophenyl)borate, (71.8 mg, 0.100 mmol) was added dropwise in deoxygenated ethyl ether (3 mL), and the resulting solution was allowed to stir overnight at room temperature under an atmosphere of nitrogen. Deoxygenated water (4 mL) was added to dissolve potassium hexafluorophosphate and excess potassium tetrakis(pentafluorophenyl)borate, and the mixture was allowed to stir for 3 h. The organic layer was separated and aqueous layer was washed with ethyl ether (2 x 2 mL). The solvent was removed from combined organic layers in vacuo, without stirring, and the residue left under vacuum until a flaky powder remained. The product was obtained as a yellow colored powder in 95.2 % yield (111.3 mg, ethyl ether present). Single crystals were obtained from pentane diffusion into THF solution of **2.27** at room temperature. X-ray analysis of crystals revealed the structure. ^{1}H NMR (400 MHz, acetone-d_6) δ 1.41 (s, 9 H), 1.46 (broad d, J = 14.5, 18H), 2.44 (s, 3 H), 3.86 (s, 3 H), 4.58 (s, 5 H), 7.05 (s, 1 H) ppm. ^{31}P NMR (162 MHz, acetone-d_6) δ 58.58 (s) ppm. ^{19}F

NMR (376 MHz, acetone-d_6) δ -133.04 (s), -164.52 (t, J = 20), -168.45 (t, J = 17.5) ppm.

Table 2.11. Crystal data and structure refinement for 2.27

Empirical formula	C_{47} H_{39} B F_{20} N_3 P Ru
Formula weight	1168.66
Temperature	100(2) K
Wavelength	1.54184 Å
Crystal system	Triclinic
Space group	P1
Unit cell dimensions	a = 13.4597(10) Å α = 65.352(2)° b = 13.7879(7) Å β = 66.222(3)° c = 16.0133(11) Å γ = 62.597(2)°
Volume	2314.3(3) $Å^3$
Z	2
Density (calculated)	1.677 Mg/m^3
Absorption coefficient	4.161 mm^{-1}
F(000)	1172
Crystal size	0.25 x 0.25 x 0.15 mm^3
Crystal color, habit	Orange block
Theta range for data collection	3.15 to 65.90°
Index ranges	-15<=h<=15, -16<=k<=16, -18<=l<=18
Reflections collected	11493
Independent reflections	11493 [R(int) = 0.0491]

Table 2.11. Continued

Completeness to theta = 65.00°	99.0 %
Absorption correction	Multi-scan
Refinement method	Full-matrix least-squares on F^2
Data / restraints / parameters	11493 / 3 / 1370
Goodness-of-fit on F^2	1.046
Final R indices [I>2sigma(I)]	R1 = 0.0277, wR2 = 0.0694
R indices (all data)	R1 = 0.0278, wR2 = 0.0695
Largest diff. peak and hole	0.640 and -0.788 e.Å^{-3}
Absolute structure parameter	0.002(4)

Table 2.12. Atomic coordinates (x 10^4) and equivalent isotropic displacement parameters (Å^{2}x 10^3) for 2.27. U(eq) is defined as one third of the trace of the orthogonalized U^{ij} tensor

	x	y	z	U(eq)
Ru(1)	3382(1)	6724(1)	2305(1)	18(1)
Ru(1')	6665(1)	3332(1)	7329(1)	17(1)
P(1)	1681(1)	8392(1)	2538(1)	17(1)
P(1')	8274(1)	1624(1)	7686(1)	17(1)
N(1)	3753(3)	8049(3)	2397(2)	20(1)
N(2)	2864(3)	9733(3)	2640(2)	19(1)
N(3)	3366(3)	6020(3)	3721(3)	23(1)
N(1')	8129(3)	3659(3)	7299(2)	18(1)

Table 2.12. Continued

	x	y	z	U(eq)
N(2')	9754(3)	2685(3)	7750(2)	19(1)
N(3')	6055(3)	3453(3)	8696(3)	23(1)
B(1)	4560(4)	964(4)	4853(4)	20(1)
B(1')	946(4)	4706(4)	9814(4)	18(1)
F(1)	6059(2)	413(2)	2962(2)	27(1)
F(2)	7451(2)	1478(2)	1631(2)	36(1)
F(3)	7838(2)	3075(3)	1924(2)	42(1)
F(4)	6737(2)	3586(2)	3617(2)	36(1)
F(5)	5297(2)	2549(2)	4961(2)	26(1)
F(6)	3729(2)	1873(2)	3196(2)	23(1)
F(7)	1995(2)	3761(2)	2723(2)	27(1)
F(8)	794(2)	5203(2)	3844(2)	29(1)
F(9)	1305(2)	4592(2)	5520(2)	25(1)
F(10)	2927(2)	2638(2)	6068(2)	21(1)
F(11)	6413(2)	-1175(2)	4751(2)	27(1)
F(12)	6287(3)	-3074(2)	4799(2)	41(1)
F(13)	4258(2)	-3102(2)	4854(2)	36(1)
F(14)	2362(2)	-1166(2)	4808(2)	28(1)
F(15)	2435(2)	711(2)	4788(2)	24(1)
F(16)	2751(2)	492(2)	6519(2)	22(1)
F(17)	2891(2)	-654(2)	8296(2)	29(1)
F(18)	4909(2)	-1383(2)	8762(2)	32(1)
F(19)	6769(2)	-906(2)	7391(2)	32(1)
F(20)	6660(2)	224(2)	5613(2)	28(1)
F(1')	1700(2)	3784(2)	8228(2)	25(1)
F(2')	3407(2)	1888(2)	7929(2)	34(1)
F(3')	4799(2)	565(2)	9135(2)	43(1)
F(4')	4405(2)	1216(2)	10672(2)	35(1)
F(5')	2636(2)	3033(2)	11043(2)	23(1)
F(6')	-953(2)	6823(2)	9430(2)	23(1)

Table 2.12. Continued

	x	y	z	U(eq)
F(7')	-2975(2)	7144(2)	9251(2)	30(1)
F(8')	-3481(2)	5329(2)	9477(2)	33(1)
F(9')	-1842(2)	3213(2)	9765(2)	30(1)
F(10')	205(2)	2879(2)	9849(2)	24(1)
F(11')	346(2)	2959(2)	11476(2)	22(1)
F(12')	-657(2)	3040(2)	13260(2)	32(1)
F(13')	-1203(2)	4950(2)	13725(2)	36(1)
F(14')	-621(2)	6748(2)	12336(2)	32(1)
F(15')	385(2)	6687(2)	10558(2)	26(1)
F(16')	2650(2)	5219(2)	10060(2)	26(1)
F(17')	3846(2)	6556(2)	8806(2)	36(1)
F(18')	3480(2)	7715(2)	7038(2)	37(1)
F(19')	1891(2)	7462(2)	6567(2)	33(1)
F(20')	667(2)	6172(2)	7807(2)	26(1)
C(1)	4503(4)	6505(4)	907(3)	28(1)
C(2)	3367(4)	6622(4)	985(3)	30(1)
C(3)	3068(4)	5730(4)	1744(3)	31(1)
C(4)	4017(4)	5036(3)	2159(3)	29(1)
C(5)	4920(4)	5511(3)	1642(3)	28(1)
C(6)	2732(3)	8855(3)	2576(3)	19(1)
C(7)	4033(3)	9430(3)	2516(3)	21(1)
C(8)	4589(3)	8396(3)	2361(3)	23(1)
C(9)	5894(4)	7744(4)	2113(4)	31(1)
C(10)	6184(4)	6523(4)	2790(4)	35(1)
C(11)	6518(4)	8376(4)	2189(4)	35(1)
C(12)	6278(4)	7684(5)	1096(4)	43(1)
C(13)	2006(4)	10815(3)	2803(3)	23(1)
C(14)	1177(4)	9389(3)	1428(3)	25(1)
C(15)	697(4)	8788(4)	1137(3)	30(1)

Table 2.12. Continued

	x	y	z	U(eq)
C(16)	230(4)	10547(3)	1528(4)	32(1)
C(17)	2258(4)	9604(4)	656(3)	33(1)
C(18)	420(3)	8496(3)	3625(3)	22(1)
C(19)	847(4)	7533(3)	4469(3)	27(1)
C(20)	-517(4)	8281(4)	3490(3)	31(1)
C(21)	-86(4)	9611(3)	3889(3)	28(1)
C(22)	3463(3)	5535(3)	4477(3)	22(1)
C(23)	3549(4)	4961(3)	5458(3)	30(1)
C(24)	5619(3)	1397(3)	4049(3)	20(1)
C(25)	6200(3)	1177(3)	3183(3)	22(1)
C(26)	6948(3)	1724(4)	2466(3)	25(1)
C(27)	7134(4)	2524(4)	2612(3)	28(1)
C(28)	6574(4)	2791(3)	3470(3)	26(1)
C(29)	5847(3)	2225(3)	4152(3)	19(1)
C(30)	3428(3)	2127(3)	4665(3)	19(1)
C(31)	3131(3)	2505(3)	3804(3)	21(1)
C(32)	2247(3)	3490(3)	3544(3)	20(1)
C(33)	1620(4)	4211(3)	4109(3)	21(1)
C(34)	1884(3)	3897(3)	4962(3)	21(1)
C(35)	2758(3)	2878(3)	5214(3)	18(1)
C(36)	4442(3)	-114(3)	4752(3)	18(1)
C(37)	5391(4)	-1132(3)	4760(3)	22(1)
C(38)	5343(4)	-2121(3)	4796(3)	27(1)
C(39)	4312(4)	-2141(3)	4824(3)	28(1)
C(40)	3363(4)	-1171(3)	4805(3)	22(1)
C(41)	3442(3)	-193(3)	4777(3)	20(1)
C(42)	4678(3)	445(3)	5959(3)	19(1)
C(43)	5686(3)	50(3)	6243(3)	21(1)
C(44)	5761(4)	-549(3)	7175(3)	24(1)

Table 2.12. Continued

	x	y	z	U(eq)
C(45)	4838(4)	-800(3)	7863(3)	24(1)
C(46)	3823(3)	-430(3)	7631(3)	22(1)
C(47)	3774(3)	167(3)	6702(3)	21(1)
C(1')	6325(4)	4366(4)	5936(3)	32(1)
C(2')	5363(4)	4789(3)	6664(3)	26(1)
C(3')	4928(3)	3901(4)	7248(3)	29(1)
C(4')	5592(4)	2934(4)	6903(4)	33(1)
C(5')	6467(4)	3232(4)	6084(4)	35(1)
C(6')	8842(3)	2612(3)	7645(3)	18(1)
C(7')	9579(3)	3823(3)	7477(3)	19(1)
C(8')	8581(3)	4432(3)	7185(3)	17(1)
C(9')	8104(3)	5701(3)	6716(3)	22(1)
C(10')	6786(4)	6200(3)	7130(3)	28(1)
C(11')	8711(4)	6312(3)	6844(3)	26(1)
C(12')	8354(4)	5878(4)	5654(3)	27(1)
C(13')	10723(3)	1778(3)	8116(3)	23(1)
C(14')	9290(3)	1008(3)	6658(3)	24(1)
C(15')	8663(5)	471(6)	6457(5)	58(2)
C(16')	10456(4)	108(4)	6822(4)	37(1)
C(17')	9534(4)	1990(4)	5810(3)	39(1)
C(18')	8214(4)	481(3)	8854(3)	23(1)
C(19A)	9219(8)	-674(8)	8991(7)	31(2)
C(20A)	8125(7)	986(6)	9636(6)	24(2)
C(21A)	7076(8)	308(7)	9140(7)	30(2)
C(19B)	9308(8)	-144(9)	9162(8)	39(2)
C(20B)	7237(8)	985(7)	9590(7)	33(2)
C(21B)	7887(7)	-378(7)	8691(7)	28(2)
C(22')	5631(3)	3580(3)	9437(3)	24(1)
C(23')	5153(4)	3666(4)	10404(3)	30(1)

Table 2.12. Continued

	x	y	z	U(eq)
C(24')	2026(3)	3495(3)	9673(3)	19(1)
C(25')	2314(3)	3155(3)	8892(3)	20(1)
C(26')	3222(4)	2173(3)	8697(3)	25(1)
C(27')	3929(4)	1508(3)	9306(3)	27(1)
C(28')	3715(3)	1835(3)	10072(3)	25(1)
C(29')	2781(3)	2803(3)	10258(3)	20(1)
C(30')	-240(3)	4847(3)	9624(3)	19(1)
C(31')	-1128(3)	5898(3)	9501(3)	19(1)
C(32')	-2188(3)	6080(4)	9431(3)	25(1)
C(33')	-2438(3)	5181(4)	9528(3)	24(1)
C(34')	-1613(4)	4105(4)	9677(3)	24(1)
C(35')	-542(3)	3968(3)	9715(3)	21(1)
C(36')	450(3)	4804(3)	10912(3)	18(1)
C(37')	131(3)	3924(3)	11654(3)	20(1)
C(38')	-403(3)	3950(3)	12584(3)	23(1)
C(39')	-673(3)	4906(4)	12824(3)	24(1)
C(40')	-382(3)	5808(3)	12120(3)	24(1)
C(41')	158(3)	5743(3)	11196(3)	20(1)
C(42')	1560(3)	5643(3)	9033(3)	18(1)
C(43')	2409(3)	5791(3)	9204(3)	21(1)
C(44')	3032(4)	6472(3)	8577(3)	25(1)
C(45')	2867(4)	7058(3)	7673(3)	26(1)
C(46')	2049(4)	6924(3)	7455(3)	23(1)
C(47')	1432(3)	6242(3)	8105(3)	21(1)

Table 2.13. Anisotropic displacement parameters ($Å^2$x 10^3) for 2.27. The anisotropic displacement factor exponent takes the form: $-2\pi^2[h^2 a^{*2}U^{11} + ... + 2 h k a^* b^* U^{12}]$

	U^{11}	U^{22}	U^{33}	U^{23}	U^{13}	U^{12}
Ru(1)	19(1)	24(1)	14(1)	-9(1)	1(1)	-11(1)
Ru(1')	15(1)	23(1)	15(1)	-6(1)	-2(1)	-10(1)
P(1)	19(1)	21(1)	13(1)	-3(1)	-2(1)	-11(1)
P(1')	16(1)	21(1)	15(1)	-6(1)	0(1)	-11(1)
N(1)	20(2)	24(2)	17(2)	-6(1)	0(1)	-14(1)
N(2)	23(2)	23(1)	18(2)	-6(1)	-5(1)	-12(1)
N(3)	19(2)	27(2)	22(2)	-11(2)	-4(1)	-6(1)
N(1')	18(2)	22(1)	16(2)	-6(1)	-3(1)	-10(1)
N(2')	20(2)	23(1)	15(2)	-5(1)	-4(1)	-10(1)
N(3')	19(2)	27(2)	29(2)	-11(2)	-6(2)	-11(1)
B(1)	24(2)	26(2)	18(3)	-8(2)	-5(2)	-13(2)
B(1')	22(2)	19(2)	17(2)	-5(2)	-6(2)	-9(2)
F(1)	29(1)	32(1)	22(1)	-13(1)	1(1)	-14(1)
F(2)	31(1)	54(1)	19(1)	-11(1)	6(1)	-22(1)
F(3)	39(2)	54(2)	31(2)	1(1)	0(1)	-35(1)
F(4)	38(1)	38(1)	42(2)	-10(1)	-4(1)	-28(1)
F(5)	29(1)	32(1)	24(1)	-14(1)	-2(1)	-16(1)
F(6)	25(1)	28(1)	18(1)	-9(1)	-5(1)	-9(1)
F(7)	29(1)	34(1)	20(1)	-5(1)	-10(1)	-12(1)
F(8)	23(1)	27(1)	29(1)	-7(1)	-10(1)	-1(1)
F(9)	24(1)	28(1)	24(1)	-12(1)	-2(1)	-9(1)
F(10)	24(1)	26(1)	16(1)	-8(1)	-4(1)	-10(1)
F(11)	23(1)	25(1)	37(2)	-11(1)	-14(1)	-5(1)
F(12)	47(2)	24(1)	59(2)	-14(1)	-32(2)	-1(1)
F(13)	55(2)	26(1)	43(2)	-4(1)	-21(1)	-24(1)
F(14)	34(1)	38(1)	22(1)	0(1)	-9(1)	-27(1)
F(15)	20(1)	31(1)	24(1)	-8(1)	-6(1)	-12(1)
F(16)	18(1)	31(1)	20(1)	-6(1)	-4(1)	-12(1)
F(17)	25(1)	34(1)	18(1)	-3(1)	0(1)	-12(1)

Table 2.13. Continued

	U^{11}	U^{22}	U^{33}	U^{23}	U^{13}	U^{12}
F(18)	35(1)	36(1)	18(1)	-1(1)	-10(1)	-9(1)
F(19)	27(1)	40(1)	33(2)	-2(1)	-17(1)	-14(1)
F(20)	21(1)	37(1)	27(1)	-5(1)	-7(1)	-15(1)
F(1')	26(1)	33(1)	21(1)	-11(1)	-8(1)	-10(1)
F(2')	32(1)	39(1)	36(2)	-25(1)	0(1)	-12(1)
F(3')	34(1)	33(1)	47(2)	-20(1)	-3(1)	2(1)
F(4')	22(1)	34(1)	31(1)	0(1)	-7(1)	-4(1)
F(5')	21(1)	29(1)	16(1)	-5(1)	-3(1)	-9(1)
F(6')	22(1)	21(1)	25(1)	-8(1)	-4(1)	-7(1)
F(7')	21(1)	34(1)	27(1)	-9(1)	-7(1)	-2(1)
F(8')	19(1)	59(2)	29(1)	-18(1)	-1(1)	-20(1)
F(9')	32(1)	43(1)	28(1)	-12(1)	0(1)	-28(1)
F(10')	25(1)	23(1)	27(1)	-7(1)	-5(1)	-13(1)
F(11')	25(1)	22(1)	20(1)	-5(1)	-2(1)	-13(1)
F(12')	33(1)	40(1)	17(1)	1(1)	0(1)	-22(1)
F(13')	33(1)	59(2)	19(1)	-20(1)	3(1)	-18(1)
F(14')	36(1)	38(1)	30(1)	-21(1)	-6(1)	-11(1)
F(15')	35(1)	23(1)	23(1)	-7(1)	-5(1)	-15(1)
F(16')	30(1)	34(1)	18(1)	-1(1)	-8(1)	-20(1)
F(17')	38(1)	51(1)	33(2)	-12(1)	-4(1)	-32(1)
F(18')	51(2)	43(1)	22(1)	-6(1)	6(1)	-38(1)
F(19')	46(2)	37(1)	12(1)	2(1)	-5(1)	-22(1)
F(20')	32(1)	35(1)	14(1)	-2(1)	-8(1)	-17(1)
C(1)	32(2)	37(2)	15(2)	-14(2)	8(2)	-18(2)
C(2)	32(2)	42(2)	25(2)	-22(2)	-1(2)	-15(2)
C(3)	32(2)	45(2)	33(3)	-27(2)	0(2)	-20(2)
C(4)	37(2)	22(2)	29(3)	-16(2)	0(2)	-11(2)
C(5)	24(2)	30(2)	26(2)	-18(2)	5(2)	-10(2)
C(6)	23(2)	22(2)	14(2)	-3(2)	0(2)	-15(2)
C(7)	23(2)	30(2)	12(2)	-4(2)	0(2)	-18(2)

Table 2.13. Continued

	U^{11}	U^{22}	U^{33}	U^{23}	U^{13}	U^{12}
C(8)	23(2)	36(2)	14(2)	-8(2)	2(2)	-20(2)
C(9)	22(2)	45(2)	36(3)	-24(2)	2(2)	-18(2)
C(10)	22(2)	37(2)	49(3)	-21(2)	-8(2)	-7(2)
C(11)	22(2)	47(2)	41(3)	-20(2)	1(2)	-16(2)
C(12)	29(2)	70(3)	43(3)	-34(3)	16(2)	-35(2)
C(13)	30(2)	20(2)	21(2)	0(2)	-9(2)	-13(2)
C(14)	31(2)	29(2)	19(2)	0(2)	-11(2)	-16(2)
C(15)	39(2)	35(2)	24(2)	-3(2)	-13(2)	-19(2)
C(16)	45(3)	26(2)	35(3)	1(2)	-25(2)	-16(2)
C(17)	48(3)	45(2)	12(2)	8(2)	-11(2)	-32(2)
C(18)	19(2)	26(2)	20(2)	-7(2)	3(2)	-12(2)
C(19)	26(2)	29(2)	20(2)	-6(2)	3(2)	-13(2)
C(20)	24(2)	35(2)	33(3)	-6(2)	-3(2)	-17(2)
C(21)	25(2)	28(2)	26(2)	-8(2)	1(2)	-12(2)
C(22)	26(2)	22(2)	26(2)	-9(2)	-9(2)	-10(2)
C(23)	43(2)	29(2)	27(2)	1(2)	-18(2)	-20(2)
C(24)	21(2)	22(2)	19(2)	-7(2)	-7(2)	-6(2)
C(25)	20(2)	27(2)	19(2)	-8(2)	-4(2)	-8(2)
C(26)	20(2)	33(2)	20(2)	-9(2)	-2(2)	-9(2)
C(27)	27(2)	36(2)	18(2)	1(2)	-3(2)	-21(2)
C(28)	27(2)	27(2)	29(2)	-3(2)	-9(2)	-16(2)
C(29)	17(2)	25(2)	14(2)	-5(2)	0(2)	-12(2)
C(30)	18(2)	24(2)	19(2)	-5(2)	-2(2)	-13(2)
C(31)	20(2)	30(2)	15(2)	-8(2)	0(2)	-14(2)
C(32)	22(2)	26(2)	13(2)	-3(2)	-6(2)	-10(2)
C(33)	19(2)	24(2)	18(2)	-4(2)	-6(2)	-6(2)
C(34)	19(2)	25(2)	19(2)	-9(2)	0(2)	-11(2)
C(35)	22(2)	23(2)	11(2)	-1(2)	-4(2)	-13(2)
C(36)	23(2)	23(2)	10(2)	-5(2)	-2(2)	-10(2)

Table 2.13. Continued

	U^{11}	U^{22}	U^{33}	U^{23}	U^{13}	U^{12}
C(37)	25(2)	26(2)	17(2)	-6(2)	-7(2)	-10(2)
C(38)	34(2)	21(2)	26(2)	-3(2)	-14(2)	-7(2)
C(39)	44(3)	23(2)	23(2)	-1(2)	-12(2)	-18(2)
C(40)	29(2)	33(2)	11(2)	-2(2)	-4(2)	-20(2)
C(41)	26(2)	29(2)	9(2)	-3(2)	0(2)	-19(2)
C(42)	20(2)	20(2)	18(2)	-6(2)	-4(2)	-9(2)
C(43)	20(2)	25(2)	21(2)	-6(2)	-6(2)	-9(2)
C(44)	26(2)	26(2)	27(2)	-9(2)	-13(2)	-6(2)
C(45)	30(2)	24(2)	16(2)	-5(2)	-7(2)	-8(2)
C(46)	23(2)	22(2)	16(2)	-7(2)	2(2)	-10(2)
C(47)	21(2)	22(2)	23(2)	-9(2)	-8(2)	-6(2)
C(1')	29(2)	52(3)	19(2)	1(2)	-12(2)	-22(2)
C(2')	26(2)	26(2)	25(2)	-1(2)	-15(2)	-5(2)
C(3')	18(2)	44(2)	27(2)	-11(2)	-8(2)	-11(2)
C(4')	32(2)	37(2)	45(3)	-12(2)	-19(2)	-16(2)
C(5')	23(2)	60(3)	37(3)	-31(2)	-13(2)	-7(2)
C(6')	16(2)	25(2)	12(2)	-6(2)	0(2)	-10(2)
C(7')	23(2)	24(2)	15(2)	-6(2)	-3(2)	-15(2)
C(8')	17(2)	22(2)	15(2)	-5(2)	0(2)	-14(2)
C(9')	20(2)	23(2)	24(2)	-4(2)	-4(2)	-12(2)
C(10')	26(2)	28(2)	26(2)	-8(2)	1(2)	-13(2)
C(11')	30(2)	27(2)	20(2)	-5(2)	1(2)	-19(2)
C(12')	29(2)	28(2)	23(2)	1(2)	-9(2)	-14(2)
C(13')	19(2)	28(2)	24(2)	-8(2)	-5(2)	-9(2)
C(14')	18(2)	34(2)	27(2)	-18(2)	1(2)	-12(2)
C(15')	39(3)	94(4)	74(4)	-71(4)	18(3)	-35(3)
C(16')	30(2)	40(2)	31(3)	-19(2)	7(2)	-9(2)
C(17')	36(3)	48(3)	22(3)	-14(2)	4(2)	-12(2)
C(18')	21(2)	23(2)	25(2)	-4(2)	-4(2)	-10(2)

Table 2.13. Continued

	U^{11}	U^{22}	U^{33}	U^{23}	U^{13}	U^{12}
C(19A)	34(5)	25(4)	35(6)	-8(4)	-9(4)	-12(4)
C(20A)	28(4)	24(3)	19(4)	0(3)	-8(3)	-12(3)
C(21A)	30(5)	34(4)	29(5)	2(4)	-5(4)	-26(4)
C(19B)	28(5)	40(5)	34(6)	7(5)	-16(4)	-9(4)
C(20B)	35(5)	32(4)	22(5)	-4(4)	1(4)	-16(4)
C(21B)	24(4)	24(4)	29(5)	0(4)	4(4)	-17(3)
C(22')	16(2)	33(2)	26(2)	-13(2)	-2(2)	-11(2)
C(23')	25(2)	47(2)	22(2)	-18(2)	1(2)	-14(2)
C(24')	21(2)	19(2)	16(2)	-2(2)	-2(2)	-12(2)
C(25')	13(2)	25(2)	23(2)	-7(2)	-1(2)	-10(2)
C(26')	28(2)	27(2)	27(2)	-13(2)	0(2)	-16(2)
C(27')	19(2)	21(2)	33(3)	-10(2)	2(2)	-6(2)
C(28')	18(2)	22(2)	26(2)	0(2)	-1(2)	-11(2)
C(29')	17(2)	24(2)	16(2)	-5(2)	0(2)	-10(2)
C(30')	20(2)	25(2)	10(2)	-4(2)	0(2)	-12(2)
C(31')	18(2)	27(2)	14(2)	-8(2)	0(2)	-10(2)
C(32')	21(2)	35(2)	15(2)	-11(2)	-3(2)	-5(2)
C(33')	19(2)	42(2)	15(2)	-9(2)	-1(2)	-15(2)
C(34')	26(2)	36(2)	17(2)	-11(2)	4(2)	-20(2)
C(35')	21(2)	25(2)	15(2)	-7(2)	-1(2)	-10(2)
C(36')	18(2)	22(2)	19(2)	-6(2)	-7(2)	-9(2)
C(37')	15(2)	24(2)	23(2)	-6(2)	-6(2)	-8(2)
C(38')	19(2)	30(2)	19(2)	-3(2)	-3(2)	-12(2)
C(39')	18(2)	42(2)	15(2)	-13(2)	0(2)	-13(2)
C(40')	19(2)	32(2)	28(2)	-16(2)	-6(2)	-7(2)
C(41')	20(2)	23(2)	20(2)	-4(2)	-6(2)	-10(2)
C(42')	21(2)	18(2)	16(2)	-5(2)	-3(2)	-9(2)
C(43')	24(2)	26(2)	14(2)	-7(2)	-3(2)	-10(2)
C(44')	24(2)	34(2)	24(2)	-15(2)	3(2)	-18(2)

Table 2.13. Continued

	U^{11}	U^{22}	U^{33}	U^{23}	U^{13}	U^{12}
C(45')	34(2)	26(2)	19(2)	-8(2)	6(2)	-20(2)
C(46')	30(2)	27(2)	11(2)	-4(2)	0(2)	-15(2)
C(47')	24(2)	25(2)	14(2)	-5(2)	-3(2)	-11(2)

Table 2.14. Bond lengths and angles for 2.27

Ru(1)-N(3)	2.056(4)	N(1)-C(8)	1.385(5)
Ru(1)-C(4)	2.160(4)	N(2)-C(6)	1.351(5)
Ru(1)-C(3)	2.175(4)	N(2)-C(7)	1.379(5)
Ru(1)-N(1)	2.175(3)	N(2)-C(13)	1.457(5)
Ru(1)-C(5)	2.175(4)	N(3)-C(22)	1.141(6)
Ru(1)-C(2)	2.185(4)	N(1')-C(6')	1.342(5)
Ru(1)-C(1)	2.191(4)	N(1')-C(8')	1.373(5)
Ru(1)-P(1)	2.4183(9)	N(2')-C(6')	1.356(5)
Ru(1')-N(3')	2.055(4)	N(2')-C(7')	1.371(5)
Ru(1')-C(3')	2.138(4)	N(2')-C(13')	1.453(5)
Ru(1')-C(4')	2.164(4)	N(3')-C(22')	1.140(6)
Ru(1')-C(2')	2.173(4)	B(1)-C(30)	1.644(6)
Ru(1')-C(5')	2.180(4)	B(1)-C(36)	1.644(6)
Ru(1')-C(1')	2.189(4)	B(1)-C(24)	1.645(7)
Ru(1')-N(1')	2.194(3)	B(1)-C(42)	1.656(6)
Ru(1')-P(1')	2.3957(9)	B(1')-C(42')	1.649(6)
P(1)-C(6)	1.828(4)	B(1')-C(36')	1.651(6)
P(1)-C(18)	1.880(4)	B(1')-C(30')	1.653(6)
P(1)-C(14)	1.894(4)	B(1')-C(24')	1.663(6)
P(1')-C(6')	1.814(4)	F(1)-C(25)	1.350(5)
P(1')-C(18')	1.878(4)	F(2)-C(26)	1.340(5)
P(1')-C(14')	1.892(4)	F(3)-C(27)	1.346(5)
N(1)-C(6)	1.321(5)	F(4)-C(28)	1.336(5)

Table 2.14. Continued

F(5)-C(29)	1.352(5)	F(17')-C(44')	1.349(5)
F(6)-C(31)	1.337(5)	F(18')-C(45')	1.334(5)
F(7)-C(32)	1.347(5)	F(19')-C(46')	1.355(5)
F(8)-C(33)	1.335(5)	F(20')-C(47')	1.351(5)
F(9)-C(34)	1.337(5)	C(1)-C(2)	1.420(7)
F(10)-C(35)	1.355(4)	C(1)-C(5)	1.433(7)
F(11)-C(37)	1.344(5)	C(1)-H(1)	0.9500
F(12)-C(38)	1.343(5)	C(2)-C(3)	1.402(7)
F(13)-C(39)	1.340(5)	C(2)-H(2)	0.9500
F(14)-C(40)	1.342(5)	C(3)-C(4)	1.422(7)
F(15)-C(41)	1.355(5)	C(3)-H(3)	0.9500
F(16)-C(47)	1.353(5)	C(4)-C(5)	1.435(7)
F(17)-C(46)	1.345(5)	C(4)-H(4)	0.9500
F(18)-C(45)	1.342(5)	C(5)-H(5)	0.9500
F(19)-C(44)	1.350(5)	C(7)-C(8)	1.348(6)
F(20)-C(43)	1.348(5)	C(7)-H(1N)	0.9500
F(1')-C(25')	1.359(5)	C(8)-C(9)	1.527(6)
F(2')-C(26')	1.340(5)	C(9)-C(12)	1.523(7)
F(3')-C(27')	1.331(5)	C(9)-C(11)	1.525(6)
F(4')-C(28')	1.349(5)	C(9)-C(10)	1.541(7)
F(5')-C(29')	1.340(5)	C(10)-H(10A)	0.9800
F(6')-C(31')	1.353(5)	C(10)-H(10B)	0.9800
F(7')-C(32')	1.349(5)	C(10)-H(10C)	0.9800
F(8')-C(33')	1.355(5)	C(11)-H(11A)	0.9800
F(9')-C(34')	1.340(5)	C(11)-H(11B)	0.9800
F(10')-C(35')	1.352(5)	C(11)-H(11C)	0.9800
F(11')-C(37')	1.354(5)	C(12)-H(12A)	0.9800
F(12')-C(38')	1.351(5)	C(12)-H(12B)	0.9800
F(13')-C(39')	1.341(5)	C(12)-H(12C)	0.9800
F(14')-C(40')	1.341(5)	C(13)-H(13A)	0.9800
F(15')-C(41')	1.355(5)	C(13)-H(13B)	0.9800
F(16')-C(43')	1.352(5)	C(13)-H(13C)	0.9800

Table 2.14. Continued

C(14)-C(17)	1.541(6)	C(27)-C(28)	1.387(7)
C(14)-C(16)	1.541(6)	C(28)-C(29)	1.376(6)
C(14)-C(15)	1.541(6)	C(30)-C(35)	1.384(6)
C(15)-H(15A)	0.9800	C(30)-C(31)	1.410(6)
C(15)-H(15B)	0.9800	C(31)-C(32)	1.369(6)
C(15)-H(15C)	0.9800	C(32)-C(33)	1.372(6)
C(16)-H(16A)	0.9800	C(33)-C(34)	1.392(6)
C(16)-H(16B)	0.9800	C(34)-C(35)	1.381(6)
C(16)-H(16C)	0.9800	C(36)-C(41)	1.382(6)
C(17)-H(17A)	0.9800	C(36)-C(37)	1.396(6)
C(17)-H(17B)	0.9800	C(37)-C(38)	1.370(6)
C(17)-H(17C)	0.9800	C(38)-C(39)	1.383(7)
C(18)-C(20)	1.530(6)	C(39)-C(40)	1.358(6)
C(18)-C(19)	1.531(6)	C(40)-C(41)	1.383(6)
C(18)-C(21)	1.533(6)	C(42)-C(47)	1.387(6)
C(19)-H(19A)	0.9800	C(42)-C(43)	1.398(6)
C(19)-H(19B)	0.9800	C(43)-C(44)	1.391(6)
C(19)-H(19C)	0.9800	C(44)-C(45)	1.361(6)
C(20)-H(20A)	0.9800	C(45)-C(46)	1.369(6)
C(20)-H(20B)	0.9800	C(46)-C(47)	1.379(6)
C(20)-H(20C)	0.9800	C(1')-C(5')	1.411(7)
C(21)-H(21A)	0.9800	C(1')-C(2')	1.425(7)
C(21)-H(21B)	0.9800	C(1')-H(1')	0.9500
C(21)-H(21C)	0.9800	C(2')-C(3')	1.408(6)
C(22)-C(23)	1.460(6)	C(2')-H(2')	0.9500
C(23)-H(23A)	0.9800	C(3')-C(4')	1.414(6)
C(23)-H(23B)	0.9800	C(3')-H(3')	0.9500
C(23)-H(23C)	0.9800	C(4')-C(5')	1.423(7)
C(24)-C(25)	1.373(6)	C(4')-H(4')	0.9500
C(24)-C(29)	1.394(6)	C(5')-H(5')	0.9500
C(25)-C(26)	1.394(6)	C(7')-C(8')	1.367(6)
C(26)-C(27)	1.360(6)	C(7')-H(7')	0.9500

Table 2.14. Continued

C(8')-C(9')	1.516(5)	C(18')-C(21B)	1.579(9)
C(9')-C(11')	1.527(6)	C(18')-C(20A)	1.612(9)
C(9')-C(12')	1.527(6)	C(19A)-H(19D)	0.9800
C(9')-C(10')	1.539(5)	C(19A)-H(19E)	0.9800
C(10')-H(10D)	0.9800	C(19A)-H(19F)	0.9800
C(10')-H(10E)	0.9800	C(20A)-H(20D)	0.9800
C(10')-H(10F)	0.9800	C(20A)-H(20E)	0.9800
C(11')-H(11D)	0.9800	C(20A)-H(20F)	0.9800
C(11')-H(11E)	0.9800	C(21A)-H(21D)	0.9800
C(11')-H(11F)	0.9800	C(21A)-H(21E)	0.9800
C(12')-H(12D)	0.9800	C(21A)-H(21F)	0.9800
C(12')-H(12E)	0.9800	C(19B)-H(19G)	0.9800
C(12')-H(12F)	0.9800	C(19B)-H(19H)	0.9800
C(13')-H(13D)	0.9800	C(19B)-H(19I)	0.9800
C(13')-H(13E)	0.9800	C(20B)-H(20G)	0.9800
C(13')-H(13F)	0.9800	C(20B)-H(20H)	0.9800
C(14')-C(17')	1.517(7)	C(20B)-H(20I)	0.9800
C(14')-C(16')	1.530(6)	C(21B)-H(21G)	0.9800
C(14')-C(15')	1.535(6)	C(21B)-H(21H)	0.9800
C(15')-H(15D)	0.9800	C(21B)-H(21I)	0.9800
C(15')-H(15E)	0.9800	C(22')-C(23')	1.451(6)
C(15')-H(15F)	0.9800	C(23')-H(23D)	0.9800
C(16')-H(16D)	0.9800	C(23')-H(23E)	0.9800
C(16')-H(16E)	0.9800	C(23')-H(23F)	0.9800
C(16')-H(16F)	0.9800	C(24')-C(25')	1.367(6)
C(17')-H(17D)	0.9800	C(24')-C(29')	1.395(6)
C(17')-H(17E)	0.9800	C(25')-C(26')	1.394(6)
C(17')-H(17F)	0.9800	C(26')-C(27')	1.377(7)
C(18')-C(20B)	1.481(10)	C(27')-C(28')	1.359(7)
C(18')-C(19B)	1.490(10)	C(28')-C(29')	1.392(6)
C(18')-C(21A)	1.513(9)	C(30')-C(35')	1.384(6)
C(18')-C(19A)	1.542(9)	C(30')-C(31')	1.387(6)

Table 2.14. Continued

C(31')-C(32')	1.374(6)	N(3)-Ru(1)-C(1)	140.29(15)
C(32')-C(33')	1.361(7)	C(4)-Ru(1)-C(1)	64.04(17)
C(33')-C(34')	1.376(6)	C(3)-Ru(1)-C(1)	63.55(17)
C(34')-C(35')	1.389(6)	N(1)-Ru(1)-C(1)	102.29(15)
C(36')-C(41')	1.384(5)	C(5)-Ru(1)-C(1)	38.32(17)
C(36')-C(37')	1.391(6)	C(2)-Ru(1)-C(1)	37.86(17)
C(37')-C(38')	1.376(6)	N(3)-Ru(1)-P(1)	94.73(9)
C(38')-C(39')	1.373(6)	C(4)-Ru(1)-P(1)	145.09(13)
C(39')-C(40')	1.377(6)	C(3)-Ru(1)-P(1)	110.39(12)
C(40')-C(41')	1.382(6)	N(1)-Ru(1)-P(1)	66.68(8)
C(42')-C(43')	1.390(6)	C(5)-Ru(1)-P(1)	162.40(13)
C(42')-C(47')	1.405(6)	C(2)-Ru(1)-P(1)	101.38(12)
C(43')-C(44')	1.361(6)	C(1)-Ru(1)-P(1)	124.10(12)
C(44')-C(45')	1.384(7)	N(3')-Ru(1')-C(3')	90.30(16)
C(45')-C(46')	1.386(6)	N(3')-Ru(1')-C(4')	115.31(17)
C(46')-C(47')	1.365(6)	C(3')-Ru(1')-C(4')	38.38(17)
		N(3')-Ru(1')-C(2')	101.42(15)
N(3)-Ru(1)-C(4)	89.61(16)	C(3')-Ru(1')-C(2')	38.14(17)
N(3)-Ru(1)-C(3)	113.82(17)	C(4')-Ru(1')-C(2')	64.38(17)
C(4)-Ru(1)-C(3)	38.28(18)	N(3')-Ru(1')-C(5')	152.57(16)
N(3)-Ru(1)-N(1)	84.47(14)	C(3')-Ru(1')-C(5')	63.60(17)
C(4)-Ru(1)-N(1)	148.20(15)	C(4')-Ru(1')-C(5')	38.2(2)
C(3)-Ru(1)-N(1)	161.70(16)	C(2')-Ru(1')-C(5')	63.82(17)
N(3)-Ru(1)-C(5)	102.75(15)	N(3')-Ru(1')-C(1')	138.38(16)
C(4)-Ru(1)-C(5)	38.66(17)	C(3')-Ru(1')-C(1')	63.39(18)
C(3)-Ru(1)-C(5)	64.24(17)	C(4')-Ru(1')-C(1')	63.74(18)
N(1)-Ru(1)-C(5)	112.69(15)	C(2')-Ru(1')-C(1')	38.15(18)
N(3)-Ru(1)-C(2)	150.81(16)	C(5')-Ru(1')-C(1')	37.68(19)
C(4)-Ru(1)-C(2)	63.43(18)	N(3')-Ru(1')-N(1')	83.67(13)
C(3)-Ru(1)-C(2)	37.50(18)	C(3')-Ru(1')-N(1')	151.41(15)
N(1)-Ru(1)-C(2)	124.24(15)	C(4')-Ru(1')-N(1')	160.91(16)
C(5)-Ru(1)-C(2)	63.73(18)	C(2')-Ru(1')-N(1')	115.94(14)

Table 2.14. Continued

C(5')-Ru(1')-N(1')	123.21(16)	C(6')-N(2')-C(13')	129.1(3)
C(1')-Ru(1')-N(1')	103.98(15)	C(7')-N(2')-C(13')	124.3(3)
N(3')-Ru(1')-P(1')	92.95(9)	C(22')-N(3')-Ru(1')	174.4(3)
C(3')-Ru(1')-P(1')	141.47(13)	C(30)-B(1)-C(36)	111.1(3)
C(4')-Ru(1')-P(1')	107.94(12)	C(30)-B(1)-C(24)	100.9(3)
C(2')-Ru(1')-P(1')	165.54(12)	C(36)-B(1)-C(24)	115.8(3)
C(5')-Ru(1')-P(1')	102.35(12)	C(30)-B(1)-C(42)	114.7(3)
C(1')-Ru(1')-P(1')	127.99(13)	C(36)-B(1)-C(42)	100.1(3)
N(1')-Ru(1')-P(1')	66.95(8)	C(24)-B(1)-C(42)	114.9(3)
C(6)-P(1)-C(18)	110.27(19)	C(42')-B(1')-C(36')	114.3(3)
C(6)-P(1)-C(14)	106.18(18)	C(42')-B(1')-C(30')	114.4(3)
C(18)-P(1)-C(14)	110.3(2)	C(36')-B(1')-C(30')	101.1(3)
C(6)-P(1)-Ru(1)	82.09(12)	C(42')-B(1')-C(24')	100.6(3)
C(18)-P(1)-Ru(1)	127.16(13)	C(36')-B(1')-C(24')	114.4(3)
C(14)-P(1)-Ru(1)	114.92(14)	C(30')-B(1')-C(24')	112.7(3)
C(6')-P(1')-C(18')	111.55(18)	C(2)-C(1)-C(5)	107.6(4)
C(6')-P(1')-C(14')	105.18(17)	C(2)-C(1)-Ru(1)	70.8(2)
C(18')-P(1')-C(14')	111.53(19)	C(5)-C(1)-Ru(1)	70.2(2)
C(6')-P(1')-Ru(1')	82.75(12)	C(2)-C(1)-H(1)	126.2
C(18')-P(1')-Ru(1')	124.11(13)	C(5)-C(1)-H(1)	126.2
C(14')-P(1')-Ru(1')	115.99(14)	Ru(1)-C(1)-H(1)	124.3
C(6)-N(1)-C(8)	108.1(3)	C(3)-C(2)-C(1)	109.1(4)
C(6)-N(1)-Ru(1)	105.1(3)	C(3)-C(2)-Ru(1)	70.8(2)
C(8)-N(1)-Ru(1)	146.9(3)	C(1)-C(2)-Ru(1)	71.3(2)
C(6)-N(2)-C(7)	106.5(3)	C(3)-C(2)-H(2)	125.4
C(6)-N(2)-C(13)	130.3(3)	C(1)-C(2)-H(2)	125.4
C(7)-N(2)-C(13)	123.2(3)	Ru(1)-C(2)-H(2)	124.0
C(22)-N(3)-Ru(1)	172.5(3)	C(2)-C(3)-C(4)	108.0(4)
C(6')-N(1')-C(8')	107.9(3)	C(2)-C(3)-Ru(1)	71.7(2)
C(6')-N(1')-Ru(1')	102.9(2)	C(4)-C(3)-Ru(1)	70.3(2)
C(8')-N(1')-Ru(1')	148.6(2)	C(2)-C(3)-H(3)	126.0
C(6')-N(2')-C(7')	106.5(3)	C(4)-C(3)-H(3)	126.0

Table 2.14. Continued

Ru(1)-C(3)-H(3)	123.7	H(10A)-C(10)-H(10C)	109.5
C(3)-C(4)-C(5)	108.1(4)	H(10B)-C(10)-H(10C)	109.5
C(3)-C(4)-Ru(1)	71.4(2)	C(9)-C(11)-H(11A)	109.5
C(5)-C(4)-Ru(1)	71.2(2)	C(9)-C(11)-H(11B)	109.5
C(3)-C(4)-H(4)	125.9	H(11A)-C(11)-H(11B)	109.5
C(5)-C(4)-H(4)	125.9	C(9)-C(11)-H(11C)	109.5
Ru(1)-C(4)-H(4)	123.1	H(11A)-C(11)-H(11C)	109.5
C(1)-C(5)-C(4)	107.1(4)	H(11B)-C(11)-H(11C)	109.5
C(1)-C(5)-Ru(1)	71.4(2)	C(9)-C(12)-H(12A)	109.5
C(4)-C(5)-Ru(1)	70.1(2)	C(9)-C(12)-H(12B)	109.5
C(1)-C(5)-H(5)	126.4	H(12A)-C(12)-H(12B)	109.5
C(4)-C(5)-H(5)	126.4	C(9)-C(12)-H(12C)	109.5
Ru(1)-C(5)-H(5)	123.7	H(12A)-C(12)-H(12C)	109.5
N(1)-C(6)-N(2)	110.0(3)	H(12B)-C(12)-H(12C)	109.5
N(1)-C(6)-P(1)	106.0(3)	N(2)-C(13)-H(13A)	109.5
N(2)-C(6)-P(1)	143.7(3)	N(2)-C(13)-H(13B)	109.5
C(8)-C(7)-N(2)	108.5(4)	H(13A)-C(13)-H(13B)	109.5
C(8)-C(7)-H(1N)	125.7	N(2)-C(13)-H(13C)	109.5
N(2)-C(7)-H(1N)	125.7	H(13A)-C(13)-H(13C)	109.5
C(7)-C(8)-N(1)	106.9(3)	H(13B)-C(13)-H(13C)	109.5
C(7)-C(8)-C(9)	128.0(4)	C(17)-C(14)-C(16)	108.6(4)
N(1)-C(8)-C(9)	124.9(4)	C(17)-C(14)-C(15)	110.6(4)
C(12)-C(9)-C(11)	109.7(4)	C(16)-C(14)-C(15)	107.9(3)
C(12)-C(9)-C(8)	108.5(4)	C(17)-C(14)-P(1)	106.2(3)
C(11)-C(9)-C(8)	109.1(3)	C(16)-C(14)-P(1)	115.3(3)
C(12)-C(9)-C(10)	109.0(4)	C(15)-C(14)-P(1)	108.3(3)
C(11)-C(9)-C(10)	110.0(4)	C(14)-C(15)-H(15A)	109.5
C(8)-C(9)-C(10)	110.5(4)	C(14)-C(15)-H(15B)	109.5
C(9)-C(10)-H(10A)	109.5	H(15A)-C(15)-H(15B)	109.5
C(9)-C(10)-H(10B)	109.5	C(14)-C(15)-H(15C)	109.5
H(10A)-C(10)-H(10B)	109.5	H(15A)-C(15)-H(15C)	109.5
C(9)-C(10)-H(10C)	109.5	H(15B)-C(15)-H(15C)	109.5

Table 2.14. Continued

C(14)-C(16)-H(16A)	109.5	H(21A)-C(21)-H(21B)	109.5
C(14)-C(16)-H(16B)	109.5	C(18)-C(21)-H(21C)	109.5
H(16A)-C(16)-H(16B)	109.5	H(21A)-C(21)-H(21C)	109.5
C(14)-C(16)-H(16C)	109.5	H(21B)-C(21)-H(21C)	109.5
H(16A)-C(16)-H(16C)	109.5	N(3)-C(22)-C(23)	177.3(4)
H(16B)-C(16)-H(16C)	109.5	C(22)-C(23)-H(23A)	109.5
C(14)-C(17)-H(17A)	109.5	C(22)-C(23)-H(23B)	109.5
C(14)-C(17)-H(17B)	109.5	H(23A)-C(23)-H(23B)	109.5
H(17A)-C(17)-H(17B)	109.5	C(22)-C(23)-H(23C)	109.5
C(14)-C(17)-H(17C)	109.5	H(23A)-C(23)-H(23C)	109.5
H(17A)-C(17)-H(17C)	109.5	H(23B)-C(23)-H(23C)	109.5
H(17B)-C(17)-H(17C)	109.5	C(25)-C(24)-C(29)	113.6(4)
C(20)-C(18)-C(19)	107.8(4)	C(25)-C(24)-B(1)	126.7(4)
C(20)-C(18)-C(21)	110.8(3)	C(29)-C(24)-B(1)	118.7(3)
C(19)-C(18)-C(21)	106.9(4)	F(1)-C(25)-C(24)	121.1(4)
C(20)-C(18)-P(1)	108.3(3)	F(1)-C(25)-C(26)	115.0(4)
C(19)-C(18)-P(1)	107.3(3)	C(24)-C(25)-C(26)	123.9(4)
C(21)-C(18)-P(1)	115.5(3)	F(2)-C(26)-C(27)	120.7(4)
C(18)-C(19)-H(19A)	109.5	F(2)-C(26)-C(25)	119.7(4)
C(18)-C(19)-H(19B)	109.5	C(27)-C(26)-C(25)	119.6(4)
H(19A)-C(19)-H(19B)	109.5	F(3)-C(27)-C(26)	120.6(4)
C(18)-C(19)-H(19C)	109.5	F(3)-C(27)-C(28)	119.6(4)
H(19A)-C(19)-H(19C)	109.5	C(26)-C(27)-C(28)	119.7(4)
H(19B)-C(19)-H(19C)	109.5	F(4)-C(28)-C(29)	121.5(4)
C(18)-C(20)-H(20A)	109.5	F(4)-C(28)-C(27)	120.3(4)
C(18)-C(20)-H(20B)	109.5	C(29)-C(28)-C(27)	118.2(4)
H(20A)-C(20)-H(20B)	109.5	F(5)-C(29)-C(28)	115.4(3)
C(18)-C(20)-H(20C)	109.5	F(5)-C(29)-C(24)	119.6(3)
H(20A)-C(20)-H(20C)	109.5	C(28)-C(29)-C(24)	125.0(4)
H(20B)-C(20)-H(20C)	109.5	C(35)-C(30)-C(31)	113.0(3)
C(18)-C(21)-H(21A)	109.5	C(35)-C(30)-B(1)	128.2(4)
C(18)-C(21)-H(21B)	109.5	C(31)-C(30)-B(1)	118.5(3)

Table 2.14. Continued

F(6)-C(31)-C(32)	116.7(4)	C(36)-C(41)-C(40)	124.5(4)
F(6)-C(31)-C(30)	119.2(3)	C(47)-C(42)-C(43)	112.8(4)
C(32)-C(31)-C(30)	124.1(4)	C(47)-C(42)-B(1)	119.4(4)
F(7)-C(32)-C(31)	120.0(4)	C(43)-C(42)-B(1)	126.7(4)
F(7)-C(32)-C(33)	119.6(3)	F(20)-C(43)-C(44)	115.8(3)
C(31)-C(32)-C(33)	120.5(4)	F(20)-C(43)-C(42)	121.1(4)
F(8)-C(33)-C(32)	121.3(4)	C(44)-C(43)-C(42)	123.1(4)
F(8)-C(33)-C(34)	120.4(4)	F(19)-C(44)-C(45)	119.9(4)
C(32)-C(33)-C(34)	118.3(4)	F(19)-C(44)-C(43)	119.5(4)
F(9)-C(34)-C(35)	120.8(4)	C(45)-C(44)-C(43)	120.5(4)
F(9)-C(34)-C(33)	119.7(3)	F(18)-C(45)-C(44)	120.7(4)
C(35)-C(34)-C(33)	119.4(4)	F(18)-C(45)-C(46)	120.2(4)
F(10)-C(35)-C(34)	114.8(3)	C(44)-C(45)-C(46)	119.1(4)
F(10)-C(35)-C(30)	120.4(3)	F(17)-C(46)-C(45)	120.5(4)
C(34)-C(35)-C(30)	124.8(4)	F(17)-C(46)-C(47)	120.5(4)
C(41)-C(36)-C(37)	113.5(4)	C(45)-C(46)-C(47)	119.0(4)
C(41)-C(36)-B(1)	126.9(3)	F(16)-C(47)-C(46)	115.9(4)
C(37)-C(36)-B(1)	119.0(4)	F(16)-C(47)-C(42)	118.7(4)
F(11)-C(37)-C(38)	116.8(4)	C(46)-C(47)-C(42)	125.4(4)
F(11)-C(37)-C(36)	119.5(4)	C(5')-C(1')-C(2')	108.4(4)
C(38)-C(37)-C(36)	123.7(4)	C(5')-C(1')-Ru(1')	70.8(3)
F(12)-C(38)-C(37)	121.0(4)	C(2')-C(1')-Ru(1')	70.3(2)
F(12)-C(38)-C(39)	119.3(4)	C(5')-C(1')-H(1')	125.8
C(37)-C(38)-C(39)	119.7(4)	C(2')-C(1')-H(1')	125.8
F(13)-C(39)-C(40)	120.6(4)	Ru(1')-C(1')-H(1')	124.7
F(13)-C(39)-C(38)	120.2(4)	C(3')-C(2')-C(1')	106.7(4)
C(40)-C(39)-C(38)	119.2(4)	C(3')-C(2')-Ru(1')	69.6(2)
F(14)-C(40)-C(39)	120.1(4)	C(1')-C(2')-Ru(1')	71.5(2)
F(14)-C(40)-C(41)	120.6(4)	C(3')-C(2')-H(2')	126.7
C(39)-C(40)-C(41)	119.3(4)	C(1')-C(2')-H(2')	126.7
F(15)-C(41)-C(36)	121.4(3)	Ru(1')-C(2')-H(2')	123.9
F(15)-C(41)-C(40)	114.2(4)	C(2')-C(3')-C(4')	109.9(4)

Table 2.14. Continued

C(2')-C(3')-Ru(1')	72.3(2)	C(9')-C(10')-H(10D)	109.5
C(4')-C(3')-Ru(1')	71.8(2)	C(9')-C(10')-H(10E)	109.5
C(2')-C(3')-H(3')	125.1	H(10D)-C(10')-H(10E)	109.5
C(4')-C(3')-H(3')	125.1	C(9')-C(10')-H(10F)	109.5
Ru(1')-C(3')-H(3')	122.4	H(10D)-C(10')-H(10F)	109.5
C(3')-C(4')-C(5')	106.6(4)	H(10E)-C(10')-H(10F)	109.5
C(3')-C(4')-Ru(1')	69.8(2)	C(9')-C(11')-H(11D)	109.5
C(5')-C(4')-Ru(1')	71.5(2)	C(9')-C(11')-H(11E)	109.5
C(3')-C(4')-H(4')	126.7	H(11D)-C(11')-H(11E)	109.5
C(5')-C(4')-H(4')	126.7	C(9')-C(11')-H(11F)	109.5
Ru(1')-C(4')-H(4')	123.7	H(11D)-C(11')-H(11F)	109.5
C(1')-C(5')-C(4')	108.4(4)	H(11E)-C(11')-H(11F)	109.5
C(1')-C(5')-Ru(1')	71.5(2)	C(9')-C(12')-H(12D)	109.5
C(4')-C(5')-Ru(1')	70.3(3)	C(9')-C(12')-H(12E)	109.5
C(1')-C(5')-H(5')	125.8	H(12D)-C(12')-H(12E)	109.5
C(4')-C(5')-H(5')	125.8	C(9')-C(12')-H(12F)	109.5
Ru(1')-C(5')-H(5')	124.1	H(12D)-C(12')-H(12F)	109.5
N(1')-C(6')-N(2')	109.8(3)	H(12E)-C(12')-H(12F)	109.5
N(1')-C(6')-P(1')	106.1(3)	N(2')-C(13')-H(13D)	109.5
N(2')-C(6')-P(1')	143.7(3)	N(2')-C(13')-H(13E)	109.5
C(8')-C(7')-N(2')	108.7(3)	H(13D)-C(13')-H(13E)	109.5
C(8')-C(7')-H(7')	125.6	N(2')-C(13')-H(13F)	109.5
N(2')-C(7')-H(7')	125.6	H(13D)-C(13')-H(13F)	109.5
C(7')-C(8')-N(1')	107.0(3)	H(13E)-C(13')-H(13F)	109.5
C(7')-C(8')-C(9')	128.1(4)	C(17')-C(14')-C(16')	107.7(4)
N(1')-C(8')-C(9')	124.6(3)	C(17')-C(14')-C(15')	110.7(5)
C(8')-C(9')-C(11')	109.9(3)	C(16')-C(14')-C(15')	108.6(4)
C(8')-C(9')-C(12')	107.8(3)	C(17')-C(14')-P(1')	107.1(3)
C(11')-C(9')-C(12')	108.9(3)	C(16')-C(14')-P(1')	115.4(3)
C(8')-C(9')-C(10')	111.3(3)	C(15')-C(14')-P(1')	107.5(3)
C(11')-C(9')-C(10')	109.9(3)	C(14')-C(15')-H(15D)	109.5
C(12')-C(9')-C(10')	109.0(3)	C(14')-C(15')-H(15E)	109.5

Table 2.14. Continued

H(15D)-C(15')-H(15E)	109.5	C(19B)-C(18')-P(1')	115.9(5)
C(14')-C(15')-H(15F)	109.5	C(21A)-C(18')-P(1')	106.8(4)
H(15D)-C(15')-H(15F)	109.5	C(19A)-C(18')-P(1')	121.6(5)
H(15E)-C(15')-H(15F)	109.5	C(21B)-C(18')-P(1')	103.7(4)
C(14')-C(16')-H(16D)	109.5	C(20A)-C(18')-P(1')	107.4(4)
C(14')-C(16')-H(16E)	109.5	C(18')-C(19A)-H(19D)	109.5
H(16D)-C(16')-H(16E)	109.5	C(18')-C(19A)-H(19E)	109.5
C(14')-C(16')-H(16F)	109.5	C(18')-C(19A)-H(19F)	109.5
H(16D)-C(16')-H(16F)	109.5	C(18')-C(20A)-H(20D)	109.5
H(16E)-C(16')-H(16F)	109.5	C(18')-C(20A)-H(20E)	109.5
C(14')-C(17')-H(17D)	109.5	C(18')-C(20A)-H(20F)	109.5
C(14')-C(17')-H(17E)	109.5	C(18')-C(21A)-H(21D)	109.5
H(17D)-C(17')-H(17E)	109.5	C(18')-C(21A)-H(21E)	109.5
C(14')-C(17')-H(17F)	109.5	C(18')-C(21A)-H(21F)	109.5
H(17D)-C(17')-H(17F)	109.5	C(18')-C(19B)-H(19G)	109.5
H(17E)-C(17')-H(17F)	109.5	C(18')-C(19B)-H(19H)	109.5
C(20B)-C(18')-C(19B)	111.3(7)	H(19G)-C(19B)-H(19H)	109.5
C(20B)-C(18')-C(21A)	61.0(6)	C(18')-C(19B)-H(19I)	109.5
C(19B)-C(18')-C(21A)	136.1(6)	H(19G)-C(19B)-H(19I)	109.5
C(20B)-C(18')-C(19A)	128.5(6)	H(19H)-C(19B)-H(19I)	109.5
C(19B)-C(18')-C(19A)	36.4(6)	C(18')-C(20B)-H(20G)	109.5
C(21A)-C(18')-C(19A)	110.8(6)	C(18')-C(20B)-H(20H)	109.5
C(20B)-C(18')-C(21B)	107.6(5)	H(20G)-C(20B)-H(20H)	109.5
C(19B)-C(18')-C(21B)	109.3(6)	C(18')-C(20B)-H(20I)	109.5
C(21A)-C(18')-C(21B)	48.0(5)	H(20G)-C(20B)-H(20I)	109.5
C(19A)-C(18')-C(21B)	73.2(5)	H(20H)-C(20B)-H(20I)	109.5
C(20B)-C(18')-C(20A)	46.5(5)	C(18')-C(21B)-H(21G)	109.5
C(19B)-C(18')-C(20A)	71.1(6)	C(18')-C(21B)-H(21H)	109.5
C(21A)-C(18')-C(20A)	106.0(6)	H(21G)-C(21B)-H(21H)	109.5
C(19A)-C(18')-C(20A)	103.2(6)	C(18')-C(21B)-H(21I)	109.5
C(21B)-C(18')-C(20A)	144.7(5)	H(21G)-C(21B)-H(21I)	109.5
C(20B)-C(18')-P(1')	108.4(4)	H(21H)-C(21B)-H(21I)	109.5

Table 2.14. Continued

N(3')-C(22')-C(23')	176.0(4)	F(7')-C(32')-C(31')	120.5(4)
C(22')-C(23')-H(23D)	109.5	C(33')-C(32')-C(31')	119.7(4)
C(22')-C(23')-H(23E)	109.5	F(8')-C(33')-C(32')	121.2(4)
H(23D)-C(23')-H(23E)	109.5	F(8')-C(33')-C(34')	119.4(4)
C(22')-C(23')-H(23F)	109.5	C(32')-C(33')-C(34')	119.3(4)
H(23D)-C(23')-H(23F)	109.5	F(9')-C(34')-C(33')	120.1(4)
H(23E)-C(23')-H(23F)	109.5	F(9')-C(34')-C(35')	121.0(4)
C(25')-C(24')-C(29')	113.8(3)	C(33')-C(34')-C(35')	118.9(4)
C(25')-C(24')-B(1')	120.8(4)	F(10')-C(35')-C(30')	121.8(3)
C(29')-C(24')-B(1')	125.1(4)	F(10')-C(35')-C(34')	113.8(4)
F(1')-C(25')-C(24')	120.5(3)	C(30')-C(35')-C(34')	124.4(4)
F(1')-C(25')-C(26')	114.4(4)	C(41')-C(36')-C(37')	113.0(4)
C(24')-C(25')-C(26')	125.1(4)	C(41')-C(36')-B(1')	127.5(4)
F(2')-C(26')-C(27')	120.7(3)	C(37')-C(36')-B(1')	119.0(3)
F(2')-C(26')-C(25')	120.6(4)	F(11')-C(37')-C(38')	115.8(4)
C(27')-C(26')-C(25')	118.6(4)	F(11')-C(37')-C(36')	119.4(4)
F(3')-C(27')-C(28')	121.6(4)	C(38')-C(37')-C(36')	124.8(4)
F(3')-C(27')-C(26')	119.7(4)	F(12')-C(38')-C(39')	120.0(4)
C(28')-C(27')-C(26')	118.7(4)	F(12')-C(38')-C(37')	120.4(4)
F(4')-C(28')-C(27')	120.3(3)	C(39')-C(38')-C(37')	119.6(4)
F(4')-C(28')-C(29')	118.8(4)	F(13')-C(39')-C(38')	120.4(4)
C(27')-C(28')-C(29')	120.9(4)	F(13')-C(39')-C(40')	121.1(4)
F(5')-C(29')-C(28')	116.0(4)	C(38')-C(39')-C(40')	118.5(4)
F(5')-C(29')-C(24')	121.4(3)	F(14')-C(40')-C(39')	119.8(4)
C(28')-C(29')-C(24')	122.6(4)	F(14')-C(40')-C(41')	120.2(4)
C(35')-C(30')-C(31')	113.1(4)	C(39')-C(40')-C(41')	120.0(4)
C(35')-C(30')-B(1')	126.0(3)	F(15')-C(41')-C(40')	115.1(3)
C(31')-C(30')-B(1')	120.1(4)	F(15')-C(41')-C(36')	120.8(4)
F(6')-C(31')-C(32')	116.6(3)	C(40')-C(41')-C(36')	124.2(4)
F(6')-C(31')-C(30')	118.9(3)	C(43')-C(42')-C(47')	112.7(4)
C(32')-C(31')-C(30')	124.5(4)	C(43')-C(42')-B(1')	121.0(4)
F(7')-C(32')-C(33')	119.8(4)	C(47')-C(42')-B(1')	125.7(4)

Table 2.14. Continued

F(16')-C(43')-C(44')	116.1(4)	C(44')-C(45')-C(46')	117.3(4)
F(16')-C(43')-C(42')	118.4(3)	F(19')-C(46')-C(47')	120.1(4)
C(44')-C(43')-C(42')	125.5(4)	F(19')-C(46')-C(45')	118.6(4)
F(17')-C(44')-C(43')	121.3(4)	C(47')-C(46')-C(45')	121.3(4)
F(17')-C(44')-C(45')	118.9(4)	F(20')-C(47')-C(46')	115.9(4)
C(43')-C(44')-C(45')	119.8(4)	F(20')-C(47')-C(42')	120.8(4)
F(18')-C(45')-C(44')	121.2(4)	C(46')-C(47')-C(42')	123.4(4)
F(18')-C(45')-C(46')	121.6(4)		

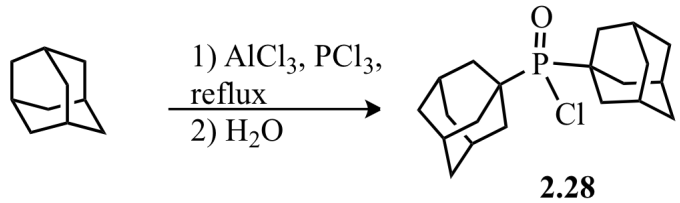

Figure 2.24. Synthesis of di-1-adamantylphosphinic chloride

Synthesis of di-1-adamantylphosphinic chloride[113] (2.28) In a 2 L pear shaped flask equipped with magnetic stirring bar and distilling column, a mixture of adamantane (54.8782 g, 0.403 mol), aluminum (III) chloride (61.9397 g, 0.464 mol), and of phosphorus (III) chloride (180 mL, 2.06 mol) was refluxed for 7 h under positive nitrogen atmosphere. Then the excess of phosphorus (III) chloride was distilled off until about 150 mL liquid had been collected, leaving a viscous substance residue. After cooling to room temperature, dichloromethane (350 mL) was added to reaction flask and the flask cooled in an ice-water bath. The resulting suspension was cautiously hydrolyzed with ice-water mixture (~250 mL) and stirred overnight at 0 ^{o}C. White sticky solid separated out of the mixture overnight leaving an orange suspension on top. Vacuum filtration of the mixture resulted in two immiscible liquid layers, where the upper organic layer was separated and dried over $MgSO_4$. After filtration, removal of solvents from the filtrate using a rotary evaporator and drying in a desiccator under oil pump vacuum overnight resulted in mostly white solid in 97.4 % yield (69.2311 g). ^{1}H NMR (400 MHz, chloroform-*d*) δ 1.74 (broad s, 12H), 2.04 (broad s, 6H), 2.14 (broad s, 12H). ^{31}P NMR (162 MHz, chloroform-*d*) δ 85.8 (s) ppm.

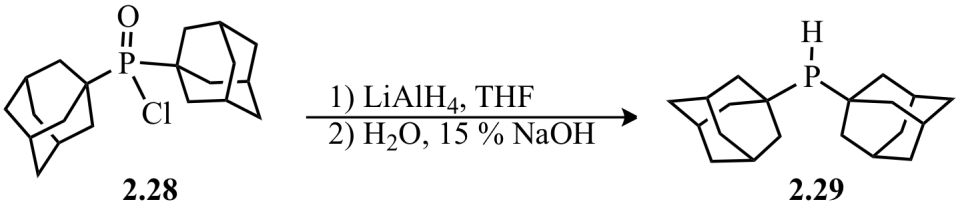

Figure 2.25. Synthesis of di-1-adamantylphosphine

Synthesis of di-1-adamantylphosphine[113] (2.29) In a 2 L pear shaped flask equipped with magnetic stirring bar, di-1-adamantylphosphinic chloride (21.2345 g, 60.2 mmol) was dissolved in freshly distilled THF (300 mL) and flask was cooled in an ice-water bath while stirring the solution under nitrogen atmosphere. Lithium aluminum hydride (5.7471 g, 151.4 mmol) was added in 1 g portions over 90 min. After warming to room temperature overnight, the reaction mixture was cooled to 0 ^{o}C in an ice-water bath, and hydrolyzed with 16 mL H_2O:THF mixture (6 + 10 mL) followed by 3 M NaOH (12 mL) and DI-H_2O (18 mL). After stirring for 5 h, the suspension was vacuum filtered and filtrate was reduced to half volume using a rotary evaporator. White solid separated out and was vacuum filtered and dried in a desiccator over phosphorus pentaoxide, under oil pump vacuum, leaving the product as white solid (14.3864 g, 79.1 % yield) ^{1}H NMR (500 MHz, chloroform-*d*) δ 1.72 (broad s, 12H), 1.89 (broad s, 6H), 1.94 (broad s, 12H), 2.79 (d, J = 200, 1H). ^{31}P NMR (202 MHz, chloroform-*d*) δ 17.8 (s) ppm.

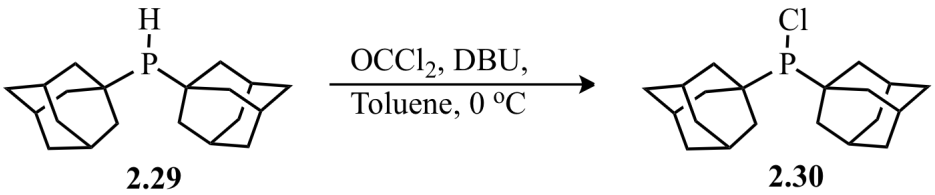

Figure 2.26. Synthesis of di-1-adamantylchlorophosphine

Synthesis of di-1-adamantylchlorophosphine[113] (2.30) In a 500 mL Schlenk flask equipped with magnetic stirring bar, di-1-adamantylphosphine (4.0951 g, 13.5 mmol) and 1,8-diazabicyclo[5.4.0]undec-7-ene, DBU, (2.41 g, 15.8 mmol) was dissolved in dry and deoxygenated toluene (300 mL) and the flask was cooled to 0 ^{o}C in ice-water bath under nitrogen atmosphere. Phosgene in toluene (12 mL of 20 % solution, 2.2 g, 22.6 mmol phosgene) was added over 15 min via gas tight syringe through the septum. The color of the solution turned pale yellow with white solid (presumed DBU.HCl) formation. Reaction progress was monitored using ^{31}P NMR spectroscopic analysis of aliquots over 4 h and nitrogen gas was bubbled through to ensure removal of excess phosgene. After vacuum filtration in glovebox, solvents were removed in vacuo at 25-30 ^{o}C on a Schlenk line outside the glovebox. The resulting white chalky solid was washed with hexanes and dried under oil pump vacuum, leaving white solid (3.58 g, 79.2 % yield). ^{1}H NMR (400 MHz, dry chloroform-*d*) δ 2.0-1.6 (m, 30H). ^{31}P NMR (202 MHz, chloroform-*d*) δ 139.9 (s) ppm.

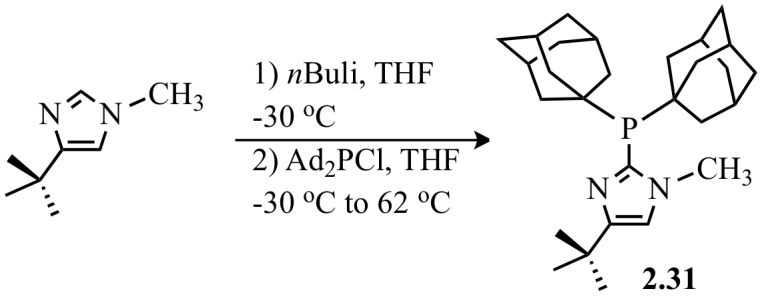

Figure 2.27. Synthesis of 4-(*tert*-butyl)-2-(di-1-adamatylphosphino)-1-methyl-1*H*-imidazole

4-(*tert*-butyl)-2-(di-1-adamatylphosphino)-1-methyl-1*H*-imidazole (2.31). In a Schlenk flask equipped with magnetic stirbar, 4-(*tert*-butyl)-1-methyl-1*H*-imidazole

(207.5 mg, 1.501 mmol) was dissolved in dry and deoxygenated THF (30 mL) and the flask was placed in an acetonitrile-Dry Ice bath intended to be at -30 °C. Using a syringe, *n*BuLi in hexanes (620 µL of 2.5 M, 1.53 mmol) was added to the reaction dropwise over 30 min. After 1 h, di-1-adamantylchlorophosphine (505.3 mg, 1.5 mmol) solution in dry and deoxygenated THF (30 mL) was added dropwise using syringes over 15 min. After addition was complete, the reaction was allowed to warm to room temperature and heated in oil bath at 50 ^{o}C for 4 h and 62 ^{o}C for 2.5 h while aliquots taken from the reaction were analyzed using ^{1}H and ^{31}P NMR spectroscopy. After the reaction stirred at room temperature overnight, it was quenched by adding deoxygenated methanol (0.5 mL). Solvents were removed on a vacuum line and the 107.7 mg of the resulting off-white solid was recrystallized from aqueous ethanol. Pure compound was obtained as a white solid (59.6 mg, 0.14 mmol, 55.3 % yield). ^{1}H NMR (500 MHz, acetone-d_6) δ 1.30 (s, 9H), 1.74-1.64 (m, 12H), 1.86-1.76 (m, 6H), 1.92-1.86 (m, 6H), 2.24-2.14 (m, 6H), 3.76 (s, 3H), 6.85 (d, J = 3.0, 1 H) ppm. ^{31}P NMR (202 MHz, acetone-d_6) δ 1.8 (s) ppm. Elemental calculated for $C_{23}H_{39}N_2P$ (438.63) C, 76.67; H, 9.88; N, 6.39.

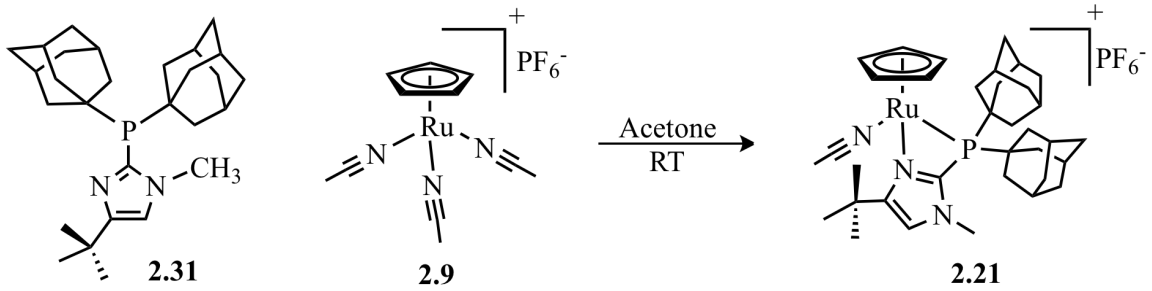

Figure 2.28. Synthesis of 2.21

Synthesis of [CpRu (4-(*tert*-butyl)-2-(di-1-adamantylphosphino)-1-methyl-1*H*-imidazole)(acetonitrile)]PF_6 (2.21) In a glove box, ruthenium precursor $[CpRu(CH_3CN)_3]PF_6$ (5.2 mg, 0.011 mmol) was combined in a Schlenk flask equipped with a magnetic stir bar and dry, deoxygenated THF (~0.5 mL). The phosphine 4-(*tert*-butyl)-2-(di-1-adamantylphosphino)-1-methyl-1*H*-imidazole (5.1 mg, 0.011 mmol) was added dropwise in dry, deoxygenated THF (0.5 mL), and the resulting solution was allowed to stir overnight at room temperature. The solvent was removed in vacuo, without stirring, and the residue left under vacuum until a flaky powder remained. The product was obtained as yellow colored powder (10.6 mg, 2 mol% bis-acetonitrile complex present, 101.9 % yield). ^{1}H NMR (500 MHz, acetone-d_6) δ 1.41 (s, 9 H), 1.86-1.70 (m, 12H), 2.32-2.00 (m, 18H), 2.44 (s, 3 H), 3.92 (s, 3 H), 4.63 (s, 5 H), 7.06 (s, 1 H) ppm. ^{31}P NMR (202 MHz, acetone-d_6) δ 52.05 (s) ppm.

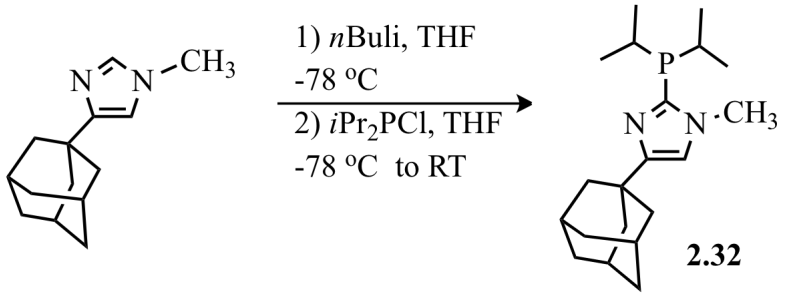

Figure 2.29. Synthesis of 4-(1-adamantyl)-2-(di-*iso*-propylphosphino)-1-methyl-1*H*-imidazole

4-(1-adamantyl)-2-(di-*iso*-propylphosphino)-1-methyl-1*H*-imidazole (2.32). In a Schlenk flask equipped with magnetic stirbar, 4-(1-adamantyl)-1-methyl-1*H*-imidazole (331.0 mg, 1.53 mmol) was dissolved in dry and deoxygenated THF (20 mL) and the flask was placed in an water-ice bath. Using a syringe, *n*BuLi in hexanes (650 μL of 2.5

M, 1.6 mmol) was added to the reaction dropwise over 20 min. After 2 h, di-*iso*-propylchlorophosphine (246.5 mg, 1.615 mmol) was added dropwise using a gas tight syringe over 30 min. The reaction was allowed to warm to room temperature overnight and was quenched with deoxygenated methanol (0.8 mL) until solution became clear (yellow-brown). Solvents were removed on a vacuum line and the resulting solid was suspended in hexanes and the mixture filtered in the glovebox through a Celite plug. Pure compound was obtained after passing the crude product through a silica plug, eluting with hexanes/ethylacetate containing triethyl amine; after concentration and storage of the residue under Teflon diaphram pump, product was obtained as yellow clear liquid (314.9 mg, 0.95 mmol, 61.9 % yield). ^{1}H NMR (500 MHz, acetone-d_6) δ 0.71 (dd, J = 7.0, 12.0, 6H), 0.82 (dd, J = 7.0, 15.5, 6H), 1.67-1.61 (m, 6H), 1.78-1.72 (m, 3H), 1.90-1.82 (m, 3H), 2.25 (sep of d, J = 1.5, 7.0, 2 H), 3.52 (s, 3 H), 6.55 (s, 1 H) ppm. ^{31}P NMR (202 MHz, acetone-d_6) δ -18.42 (s) ppm. Elemental calculated for $C_{20}H_{33}N_2P$ (684.64) C, 72.25; H, 10.00; N, 8.43. Found C, 71.94; H, 9.85; N, 7.96.

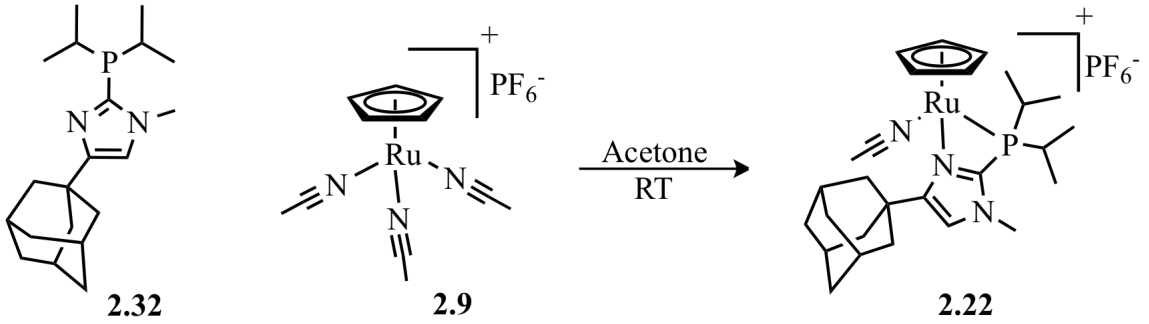

Figure 2.30. Complexation of 2.32 to give 2.22

Complexation of 2.32 to give [CpRu (4-(1-adamantyl)-2-(di-*iso*-propylphosphino)-1-methyl-1*H*-imidazole)(acetonitrile)]PF$_6$ (2.22) In a glove box, ruthenium precursor

$[CpRu(CH_3CN)_3]PF_6$ (145.8 mg, 0.336 mmol) was combined in a scintillation vial equipped with a magnetic stir bar and deoxygenated acetone (4 mL). The phosphine, **2.32** (111.7 mg, 0.336 mmol) was added dropwise in deoxygenated acetone (8 mL), and the resulting solution was allowed to stir overnight at room temperature under an atmosphere of nitrogen. The solvent was removed in vacuo, without stirring, and the residue left under vacuum until a flaky powder remained. The product was obtained as yellow colored powder (243.9 mg, acetonitrile is present, 100.2% yield). ^{1}H NMR (500 MHz, acetone-d_6) δ 1.09 (dd, J = 7.0, 16.0, 3H), 1.19 (dd, J = 7.5, 16.5, 3H), 1.36 (dd, J = 7.0, 18.0, 3H), 1.49 (dd, J = 7.0, 17.5, 3H), 2.19-2.10 (m, 6H), 2.00-1.95 (m, 3H), 1.88-1.80 (m, 6H), 2.47 (s, 3 H), 2.85-2.78 (m, 1 H), 3.03-3.10 (m, 1H), 3.82 (s, 3 H), 4.62 (s, 5 H), 6.96 (s, 1 H) ppm. ^{31}P NMR (202 MHz, acetone-d_6) δ 37.62 (s) ppm. Elemental calculated for $C_{27}H_{41}F_6N_3P_2Ru$ (684.64) C, 47.37; H, 6.04; N, 6.14. Found C, 46.96; H, 5.83; N, 6.30.

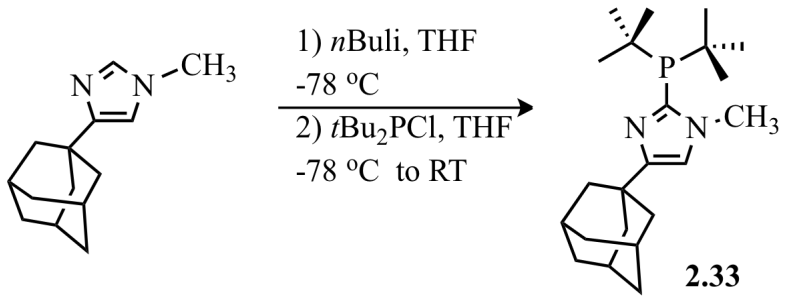

Figure 2.31. Synthesis of 4-(1-adamantyl)-2-(di-*tert*-butylphosphino)-1-methyl-1*H*-imidazole

4-(1-adamantyl)-2-(di-*tert*-butylphosphino)-1-methyl-1*H*-imidazole (2.33). In a Schlenk flask equipped with magnetic stirbar, 4-(1-adamantyl)-1-methyl-1*H*-imidazole (300.3 mg, 1.39 mmol) was dissolved in dry and deoxygenated THF (20 mL) and the flask was placed in an acetone-Dry Ice bath at -78 °C. Using a syringe, *n*BuLi in hexanes

(580 μL of 2.5 M, 1.42 mmol) was added to the reaction dropwise over 15 min. After 2 h, di-*tert*-butylchlorophosphine (317.0 mg, 1.75 mmol) was added dropwise using a gas tight syringe over 25 min. The reaction was allowed to warm to room temperature and was quenched with deoxygenated methanol until solution became clear and orange. Solvents were removed on a vacuum line and the resulting solid was suspended in hexanes and the mixture filtered in the glovebox through Celite. Column chromatography with hexanes and ethyl acetate (5:1) containing triethyl amine yielded pure compound was obtained as a yellow sticky solid (320.1 mg, 0.89 mmol, 64 % yield). ^{1}H NMR (500 MHz, acetone-d_6) δ 1.18 (d, J = 12.0, 18H), 1.84-1.72 (m, 6H), 1.94-1.90 (m, 6H), 2.02-1.98 (m, 3H), 3.79 (s, 3 H), 6.81 (s, 1 H) ppm. ^{31}P NMR (202 MHz, acetone-d_6) δ 1.23 (s) ppm. Elemental calculated for $C_{22}H_{37}N_2P$ (360.52) C, 73.29; H, 10.34; N, 7.77. Found C, 72.90; H, 9.96; N, 7.53.

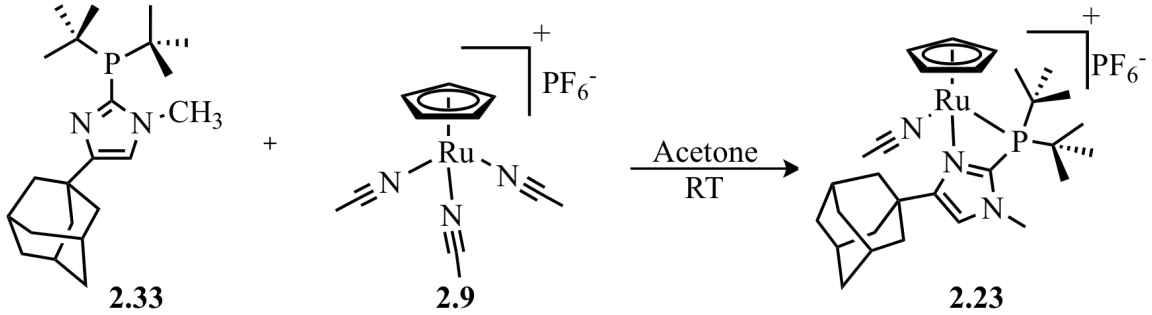

Figure 2.32. Complexation of 2.33 to give 2.23

Complexation of 2.33 to give [CpRu (4-(1-adamantyl)-2-(di-*tert*-butylphosphino)-1-methyl-1*H*-imidazole)(acetonitrile)]PF$_6$ (2.23) In a glove box, ruthenium precursor [CpRu(CH$_3$CN)$_3$]PF$_6$ (217.3 mg, 0.500 mmol) was combined in a scintillation vial equipped with a magnetic stir bar and deoxygenated acetone (5 mL). The phosphine, **2.33** (180.3 mg, 0.500 mmol) was added dropwise in deoxygenated acetone (2 mL), and

the resulting solution was allowed to stir overnight at room temperature under an atmosphere of nitrogen. The solvent was removed in vacuo, without stirring, and the residue left under vacuum until a flaky powder remained. The product was obtained as yellow-orange colored powder (368.1 mg, acetone is present, 103.3% yield). ^{1}H NMR (500 MHz, acetone-d_6) δ 1.48 (broad d, J = 11.0, 18H), 1.90-1.82 (m, 6H), 2.20-2.10 (m, 6H), 2.50-2.32 (m, 3H), 2.69 (s, 3 H), 3.90 (s, 3 H), 4.62 (s, 5 H), 7.02 (s, 1 H) ppm. ^{31}P NMR (202 MHz, acetone-d_6) δ 58.71 (s) ppm. Elemental calculated for $C_{29}H_{45}F_6N_3P_2Ru$ (712.70) C, 48.87; H, 6.36; N, 5.90. Found C, 48.24; H, 6.20; N, 5.49.

General procedure for catalytic isomerization reactions of 1-heptene

In a glove box, internal standard $(Me_3Si)_4C$ (small weighed amount) and substrate (0.50 mmol) were combined with acetone-d_6 (~700 μL), and an initial NMR spectrum was acquired. Back in the glovebox, to this mixture was added catalyst **2.10, 2.19-2.23** (0.01 mmol; 2 mol%) followed by enough acetone-d_6 to reach a final volume of 1.0 mL. If the mixture was heated at 70 ^{o}C in an oil bath it was done so for the times given, spectra were acquired at NMR probe temperature of 30 ^{o}C. The value of the integral for the singlet due to the internal standard, $C(Me_3Si)_4$, was set equal to 100.00 integral units in each case. Data were acquired with eight 15° pulses and 20 sec delays between pulses.

1-heptene isomerization with 2.10 at room temperature. (Table 2.15) General procedure was followed using 1-heptene (49.1 mg, 0.50 mmol), $C(Me_3Si)_4$ (0.9 mg, 2.9 μmol) and **2.10** (6.1 mg, 0.01 mmol) in acetone-d_6 (1 mL).

Table 2.15. 1-heptene Isomerization with 2 mol % 2.10 in NMR probe

Time (min)	1-Heptene (%)	2-Heptene (%)	3-Heptene (%)
15	1.4	67.7	28.5
24	1.2	59.5	36.9
32	1.1	55.7	40.8
40	1.2	54.1	42.5
50	0.9	52.5	44.2
60	1.1	52.3	44.8
65	1.2	52.3	44.7
70	1.0	51.6	44.6
75	1.1	51.9	44.9
80	1.1	51.5	45.3
90	1.0	51.2	45.3

1-heptene isomerization with 2.19 at room temperature. (Table 2.16) General procedure was followed using 1-heptene (49.1 mg, 0.50 mmol), $C(Me_3Si)_4$ (0.8 mg, 2.6 μmol) and **2.19** (6.9 mg, 0.01 mmol) in acetone-d_6 (1 mL).

Table 2.16. 1-heptene Isomerization with 2 mol % 2.19 at RT

Time (h)	1-Heptene (%)	2-Heptene (%)	3-Heptene (%)
1	1.4	60.1	37.3
2	1.5	53.7	44.3
5	0.9	51.9	45.5
24	1.1	52.8	45.0

1-heptene isomerization with 2.19 at room temperature. (Table 2.17) General procedure was followed using 1-heptene (49.2 mg, 0.50 mmol), $C(Me_3Si)_4$ (1.1 mg, 3.6 μmol) and **2.19** (6.9 mg, 0.01 mmol) in acetone-d_6 (1 mL).

Table 2.17. 1-heptene Isomerization with 2 mol % 2.19 in NMR probe

Time (min)	1-Heptene (%)	2-Heptene (%)	3-Heptene (%)
5	1.7	86.3	11.5
10	1.3	82.5	14.5
15	1.2	60.1	36.5
30	1.2	57.5	41.3
60	0.6	52.0	46.6
90	1.0	51.2	46.9
120	1.1	51.3	46.5

1-heptene isomerization with 2.20 at room temperature. (Table 2.18) General procedure was followed using 1-heptene (49.2 mg, 0.50 mmol), $C(Me_3Si)_4$ (0.8 mg, 2.6 μmol) and **2.20** (6.4 mg, 0.01 mmol) in acetone-d_6 (1 mL).

Table 2.18. 1-heptene Isomerization with 2 mol % 2.20 at RT

Time (h)	1-Heptene (%)	2-Heptene (%)	3-Heptene (%)
1	96.6	0.6	-
10	93.4	2.1	<1
24	3.1	4.6	<1

1-heptene isomerization with 2.20 70 ^{o}C. (Table 2.19) General procedure was followed using 1-heptene (49.3 mg, 0.50 mmol), $C(Me_3Si)_4$ (1.7 mg, 5.6 μmol) and **2.20** (6.4 mg, 0.01 mmol) in acetone-d_6 (1 mL) and the J. Young NMR tube was placed in an oil bath at 70 ^{o}C.

Table 2.19. 1-heptene isomerization with 2 mol % 2.20 at 70 ^{o}C

Time	1-Heptene (%)	2-Heptene (%)	(*E*:*Z*)	3-Heptene (%)
20 min	94.3	5.3	-	<1
40 min	88.7	11.5	-	<1
1 h	82.6	17.7	9.7 : 1	<1
1.5 h	73.6	25.1	10.8 : 1	1.4
2 h	62.4	34.1	11 : 1	1.7
11 h	8.6	84.3	6.6 : 1	7.7
23 h	3.5	85.1	6.0 : 1	11.3

1-heptene isomerization with 2.21 at 70 ^{o}C. (Table 2.20) General procedure was followed using 1-heptene (63.7 mg, 0.66 mmol), $C(Me_3Si)_4$ (1.5 mg, 4.9 μmol) and **2.21** (10.5 mg, 0.0132 mmol) in acetone-d_6 (1.4 mL) and placed the J. Young NMR tube in oil bath at 70 ^{o}C.

Table 2.20. 1-heptene isomerization with 2 mol % 2.21 at 70 ^{o}C

Time	1-Heptene (%)	2-Heptene (%)	(*E*:*Z*)	3-Heptene (%)
20 min	43.6	52.1	9.5 : 1	3.2
40 min	5.9	81.1	9 : 1	12.5
1 h	2.6	79.9	8.6 : 1	17.6
1.5 h	1.9	78.1	6.8 : 1	20.6
2 h	1.8	76.8	6.7 : 1	21.5
3 h	1.7	77.1	6 : 1	22.2
11 h	1.5	76.0	4.6 : 1	23.1
23 h	1.6	76.3	4 : 1	22.9
35 h	1.6	76.0	3.9 :1	23.4

1-heptene isomerization with 2.22 at room temperature. (Table 2.21) General procedure was followed using 1-heptene (49.3 mg, 0.50 mmol), $C(Me_3Si)_4$ (1.7 mg, 5.6 μmol) and **2.22** (6.8 mg, 0.01 mmol) in acetone-d_6 (1 mL).

Table 2.21. 1-heptene isomerization with 2 mol % 2.22 at RT

Time (min)	1-Heptene (%)	2-Heptene (%)	3-Heptene (%)
9	1.6	79.0	17.8
12	1.5	75.4	22.0
28	1.2	62.8	34.7
32	1.1	59.9	38.9
37	1.2	58.2	39.6
50	1.2	55.3	43.0
60	1.1	54.7	43.9
70	1.1	53.5	44.2
80	1.2	53.0	45.2
92	1.3	52.5	45.8

1-heptene isomerization with 2.23 at room temperature. (Table 2.22) General procedure was followed using 1-heptene (49.2 mg, 0.50 mmol), $C(Me_3Si)_4$ (1.2 mg, 3.9 μmol) and **2.23** (7.1 mg, 0.01 mmol) in acetone-d_6 (1 mL).

Table 2.22. 1-heptene isomerization with 2 mol % 2.23 at RT ge715

Time (h)	1-Heptene (%)	2-Heptene (%)	(*E* : *Z*)	3-Heptene (%)
1	97.6	1.3	-	-
10	95.2	1.5	-	-
24	86.3	11.6	5.3 : 1	<1

1-heptene isomerization with 2.23 at 70 °C. (Table 2.21) General procedure was followed using 1-heptene (49.8 mg, 0.51 mmol), $C(Me_3Si)_4$ (1.8 mg, 5.9 μmol) and **2.23**

(7.0 mg, 0.01 mmol) in acetone-d_6 (1 mL) and placed the J. Young NMR tube in oil bath at 70 ^{o}C.

Table 2.23. 1-heptene isomerization with 2 mol % 2.23 at 70 ^{o}C

Time (h)	1-Heptene (%)	2-Heptene (%)	(*E*:*Z*)	3-Heptene (%)
1 h	2.8	78.8	10 : 1	15.4
14 h	1.8	76.7	6.2 : 1	21.5
36 h	1.3	75.9	4.1 : 1	22.4

1-heptene isomerization with 2.23 at 70 ^{o}C (repeat with spectra taken at shorter intervals). (Table 2.21) General procedure was followed using 1-heptene (49.3 mg, 0.50 mmol), $C(Me_3Si)_4$ (1.7 mg, 5.6 μmol) and **2.23** (6.4 mg, 0.01 mmol) in acetone-d_6 (1 mL) and placed the J. Young NMR tube in oil bath at 70 ^{o}C.

Table 2.24. 1-heptene isomerization with 2 mol % 2.23 at 70 ^{o}C

Time	1-Heptene (%)	2-Heptene (%)	(*E*:*Z*)	3-Heptene (%)
20 min	11.4	79.0	9.7 : 1	10.0
40 min	4.3	81.9	9.4 : 1	15.0
60 min	2.6	79.7	9.1 :1	17.0
90 min	2.7	79.7	9.3 :1	18.5
2 h	2.2	78.9	8.4 :1	19.4
11h	1.8	77.3	5.8 : 1	22.1
23 h	1.8	76.0	6.1 : 1	22.2

1-hexene isomerization with 2.20 at room temperature. (Table 2.25 entry 1, 2) General procedure used for 1-heptene was followed using 1-hexene (25.3 mg, 0.50 mmol), $C(Me_3Si)_4$ (3.3 mg, 5.6 μmol) and **2.20** (3.8 mg, μmol) in acetone-d_6 (1 mL).

1-hexene isomerization with 2.20 at 70 ^{o}C. (Table 2.25, entry 3) General procedure used for 1-heptene was followed using 1-hexene (28.6 mg, 0.34 mmol), 1,4-dioxane as internal standard (9.9 mg, 0.11 mmol) and **2.20** (4.3 mg, 6.8 μmol) in acetone-d_6 (1 mL) and placed the J. Young NMR tube in oil bath at 70 ^{o}C.

Table 2.25. 1-hexene isomerization with 2 mol % 2.20 at RT and 70 ^{o}C

Time (h)	1-Hexene (%)	2-Hexene (%)	3-Hexene (%)
24, RT	100	-	-
66, RT	92.8	7.0	<1
24, 70 ^{o}C	18.3	70.0	6.0

1-decene isomerization with 2.20 at 70 ^{o}C. (Table 2.26) General procedure used for 1-heptene was followed using 1-decene (28.8 mg, 0.20 mmol), $C(Me_3Si)_4$ (1.1 mg, 3.6 μmol) and **2.20** (2.5 mg, 4.2 μmol) in acetone-d_6 (1 mL) and placed the J. Young NMR tube in oil bath at 70 ^{o}C.

Table 2.26. 1-decene isomerization with 2 mol % 2.20 at 70 ^{o}C

Time (h)	1-decene (%)	2-decene (%)	3- and 4-decene (%)
1	90.5	6.2	<1
5	81.4	15.4	<1
36	49.6	44.8	4
48	43.1	49.5	10

1-hexene isomerization with 2.23 at 70 ^{o}C. (Table 2.27) General procedure used for 1-heptene was followed using 1-hexene (12.6 mg, 0.15 mmol), $C(Me_3Si)_4$ (0.9 mg, 2.9

μmol) and **2.23** (2.1 mg, μmol) in acetone-d_6 (1 mL) and placed the J. Young NMR tube in oil bath at 70 ^{o}C.

Table 2.27. 1-hexene isomerization with 2 mol % 2.23 at RT

Time (min)	1-Hexene (%)	2-Hexene (%)	3-Hexene (%)
7	94.3	6.2	<1
45	71.3	26.0	2.4
65	51.9	41.9	4.0
90	31.9	58.7	7.6
123	14.0	68.3	11.1
150	2.0	72.1	20.5
180	1.5	68.0	23.5
42 h	1.7	61.2	22.7

The part of the contents of Chapter 2 are similar to the material published in the following papers: Grotjahn, Douglas B.; Larsen, Casey; Erdogan, Gulin; Gustafson, Jeffrey; Sharma, Abhinandini; Nair, Reji. "Bifunctional catalysis of alkene isomerization and its applications" Chemical Industries (Boca Raton, FL, United States) **2009**, *123*, 379-387. Grotjahn, Douglas B; Larsen, Casey, R; Gustafson, Jeffery, L; Nair, Reji; Sharma, Abhinandini. "Extensive isomerization of alkenes using a bifunctional catalyst: an alkene zipper". *Journal of the American Chemical Society* **2007**, *129*, 9592-9593. The dissertation author was the primary researcher for the data presented and co-author on the papers included. The co-authors listed in these publications also participated in the research.

REFERENCES

(1) Leeuwen, P. W. N. M. v. *Homogeneous catalysis : understanding the art*; Kluwer Academic Publishers: Dordrecht ; Boston, 2004.

(2) Parshall, G. W.; Ittel, S. D. *Homogeneous catalysis : the applications and chemistry of catalysis by soluble transition metal complexes*; 2nd ed.; Wiley: New York, 1992.

(3) Cornils, B.; Herrmann, W. A. *Applied homogeneous catalysis with organometallic compounds : a comprehensive handbook in three volumes*; 2nd, completely rev. and enlarged ed.; Wiley-VCH: Weinheim, 2002.

(4) Surburg, H.; Panten, J.; Bauer, K. *Common fragrance and flavor materials : preparation, properties and uses*; 5th completely rev. and enl. ed.; Wiley-VCH: Weinheim, 2006.

(5) Kraft, P.; Swift, K. A. D.; Royal Society of Chemistry (Great Britain); Society of Chemical Industry (Great Britain) *Current topics in flavor and fragrance research*; Wiley-VCH: Weinheim ; Chichester, 2008.

(6) Chapuis, C.; Jacoby, D. *Appl Catal a-Gen* **2001**, *221*, 93.

(7) Inoue, S.; Takaya, H.; Tani, K.; Otsuka, S.; Sato, T.; Noyori, R. *J Am Chem Soc* **1990**, *112*, 4897.

(8) Pommer, H.; Nurrenbach, A. *Pure Appl Chem* **1975**, *43*, 527.

(9) Sharma, S. K.; Srivastava, V. K.; Jasra, R. V. *J Mol Catal a-Chem* **2006**, *245*, 200.

(10) Evans, D.; Osborn, J. A.; Wilkinso.G *J Chem Soc A* **1968**, 3133.

(11) Bergbreiter, D. E.; Parsons, G. L. *J Organomet Chem* **1981**, *208*, 47.

(12) Casey, C. P.; Cyr, C. R. *J Am Chem Soc* **1973**, *95*, 2248.

(13) Akita, M.; Yasuda, H.; Nagasuna, K.; Nakamura, A. *B Chem Soc Jpn* **1983**, *56*, 554.

(14) Wakamatsu, H.; Nishida, M.; Adachi, N.; Mori, M. *J Org Chem* **2000**, *65*, 3966.

(15) Hsing, H. H.; Tenneco Oil Co., USA . 1984, p 32 pp.

(16) O'Young, C. L.; Browne, J. E.; Matteo, J. F.; Sawicki, R. A.; Hazen, J.; Texaco Inc., USA . 1993, p 15 pp.

(17) Timm, D.; Oehlmann, G.; Fricke, R.; Roost, U.; Zubowa, H. L.; Becker, K.; Striegler, H.; Leuna-Werke A.-G., Germany . 1993, p 8 pp.

(18) Dong, J.; Xuan, D.; Liu, S.; Wang, Y.; China Petroleum & Chemical Corp., Peop. Rep. China; Shanghai Research Institute of Petrochemical Engineering, SINOPEC . 2011, p 6pp.

(19) Saruwatari, T.; Yamane, H.; Idemitsu Kosan Co., Ltd., Japan . 2011, p 6pp.; Chemical Indexing Equivalent to 145:166849 (WO).

(20) Koenigsmann, L.; Schwab, E.; Hahn, T.; Kons, G.; BASF SE, Germany . 2011, p 15pp.

(21) Butler, J. R.; Fina Technology, Inc., USA . 2011, p 6pp.

(22) Ramachandran, B.; Choi, S.; Gartside, R. J.; Greene, M. I.; Lummus Technology Inc., USA . 2011, p 17pp.; Chemical Indexing Equivalent to 154:159003 (WO).

(23) Jolly, P. W.; Stone, F. G. A.; Mackenzie, K. *Journal of the Chemical Society (Resumed)* **1965**, 6416.

(24) Damico, R.; Logan, T. *The Journal of Organic Chemistry* **1967**, *32*, 2356.

(25) Damico, R. *The Journal of Organic Chemistry* **1968**, *33*, 1550.

(26) Iranpoor, N.; Mottaghinejad, E. *J Organomet Chem* **1992**, *423*, 399.

(27) Cherkaoui, H.; Soufiaoui, M.; Grée, R. *Tetrahedron* **2001**, *57*, 2379.

(28) Mayer, M.; Welther, A.; Jacobi von Wangelin, A. *ChemCatChem* **2011**, *3*, 1567.

(29) Corriu, R. J. P.; Huynh, V.; Moreau, J. J. E.; Pataud-Sat, M. *J Organomet Chem* **1983**, *255*, 359.

(30) Chin, C. S.; Park, J.; Kim, C.; Lee, S. Y.; Shin, J. H.; Kim, J. B. *Catal Lett* **1988**, *1*, 203.

(31) Crabtree, R. H.; Felkin, H.; Morris, G. E. *Journal of the Chemical Society, Chemical Communications* **1976**, 716.

(32) Baudry, D.; Ephritikhine, M.; Felkin, H. *Journal of the Chemical Society, Chemical Communications* **1978**, 694.

(33) Lu, X. Y.; Lin, Y. R.; Ma, D. W. *Pure Appl Chem* **1988**, *60*, 1299.

(34) Chin, C. S.; Lee, B.; Kim, S.; Chun, J. *Journal of the Chemical Society, Dalton Transactions* **1991**, 443.

(35) Ohmura, T.; Yamamoto, Y.; Miyaura, N. *Chem Commun* **1998**, 1337.

(36) van der Drift, R. C.; Bouwman, E.; Drent, E. *J Organomet Chem* **2002**, *650*, 1.

(37) Jimenez Rodriguez, C.; Foster, D. F.; Eastham, G. R.; Cole-Hamilton, D. J. *Chem Commun* **2004**, 1720.

(38) Gauthier, D.; Lindhardt, A. T.; Olsen, E. P. K.; Overgaard, J.; Skrydstrup, T. *J Am Chem Soc* **2010**, *132*, 7998.

(39) Lim, H. J.; Smith, C. R.; RajanBabu, T. V. *The Journal of Organic Chemistry* **2009**, *74*, 4565.

(40) Cooper, G. D.; Finkbeiner, H. L. *The Journal of Organic Chemistry* **1962**, *27*, 1493.

(41) Finkbeiner, H. L.; Cooper, G. D. *The Journal of Organic Chemistry* **1962**, *27*, 3395.

(42) Averbuj, C.; Eisen, M. S. *J Am Chem Soc* **1999**, *121*, 8755.

(43) Iengo, P.; Aprile, G.; Di Serio, M.; Gazzoli, D.; Santacesaria, E. *Appl Catal a-Gen* **1999**, *178*, 97.

(44) Tolman, C. A. *J Am Chem Soc* **1972**, *94*, 2994.

(45) Lochow, C. F.; Miller, R. G. *J Org Chem* **1976**, *41*, 3020.

(46) Rigo, P.; Bressan, M.; Basato, M. *Inorg Chem* **1979**, *18*, 860.

(47) Bricout, H.; Monflier, E.; Carpentier, J. F.; Mortreux, A. *Eur J Inorg Chem* **1998**, 1739.

(48) Krompiec, S.; Kuźnik, N.; Urbala, M.; Rzepa, J. *Journal of Molecular Catalysis A: Chemical* **2006**, *248*, 198.

(49) Krompiec, S.; Kuźnik, N.; Krompiec, M.; Penczek, R.; Mrzigod, J.; Tórz, A. *Journal of Molecular Catalysis A: Chemical* **2006**, *253*, 132.

(50) Bergens, S. H.; Bosnich, B. *J Am Chem Soc* **1991**, *113*, 958.

(51) Tanaka, K.; Shoji, T. *Org Lett* **2005**, *7*, 3561.

(52) Boons, G.-J.; Burton, A.; Isles, S. *Chem Commun* **1996**, 141.

(53) Corey, E. J.; Suggs, J. W. *The Journal of Organic Chemistry* **1973**, *38*, 3224.

(54) Wuts, P. G. M.; Greene, T. W.; Greene, T. W. *Greene's protective groups in organic synthesis*; 4th ed.; Wiley-Interscience: Hoboken, N.J., 2007.

(55) Emerson, G. F.; Pettit, R. *J Am Chem Soc* **1962**, *84*, 4591.

(56) Jennerjahn, R.; Jackstell, R.; Piras, I.; Franke, R.; Jiao, H.; Bauer, M.; Beller, M. *ChemSusChem* **2012**, *5*, 734.

(57) Lee, H. M.; Smith, D. C.; He, Z. J.; Stevens, E. D.; Yi, C. S.; Nolan, S. P. *Organometallics* **2001**, *20*, 794.

(58) Trnka, T. M.; Morgan, J. P.; Sanford, M. S.; Wilhelm, T. E.; Scholl, M.; Choi, T. L.; Ding, S.; Day, M. W.; Grubbs, R. H. *J Am Chem Soc* **2003**, *125*, 2546.

(59) Arisawa, M.; Terada, Y.; Nakagawa, M.; Nishida, A. *Angew Chem Int Edit* **2002**, *41*, 4732.

(60) Hanessian, S.; Giroux, S.; Larsson, A. *Org Lett* **2006**, *8*, 5481.

(61) Donohoe, T. J.; O'Riordan, T. J. C.; Rosa, C. P. *Angewandte Chemie International Edition* **2009**, *48*, 1014.

(62) Donohoe, T. J.; Rosa, C. P. *Org Lett* **2007**, *9*, 5509.

(63) Trost, B. M.; Kulawiec, R. J. *J Am Chem Soc* **1993**, *115*, 2027.

(64) Trost, B. M.; Kulawiec, R. J. *Tetrahedron Lett* **1991**, *32*, 3039.

(65) van der Drift, R. C.; Vailati, M.; Bouwman, E.; Drent, E. *J Mol Catal a-Chem* **2000**, *159*, 163.

(66) Slugovc, C.; Ruba, E.; Schmid, R.; Kirchner, K. *Organometallics* **1999**, *18*, 4230.

(67) Iranpoor, N.; Mottaghinejad, E. *J Organomet Chem* **1992**, *423*, 399.

(68) Gibson, T.; Tulich, L. *J Org Chem* **1981**, *46*, 1821.

(69) Grotjahn, D. B.; Larsen, C. R.; Gustafson, J. L.; Nair, R.; Sharma, A. *J Am Chem Soc* **2007**, *129*, 9592.

(70) Slone, C. S.; Weinberger, D. A.; Mirkin, C. A. *Prog Inorg Chem* **1999**, *48*, 233.

(71) Espinet, P.; Soulantica, K. *Coordin Chem Rev* **1999**, *193-5*, 499.

(72) Grotjahn, D. B.; Lev, D. A. *J Am Chem Soc* **2004**, *126*, 12232.

(73) Hintermann, L.; Dang, T. T.; Labonne, A.; Kribber, T.; Xiao, L.; Naumov, P. *Chem-Eur J* **2009**, *15*, 7167.

(74) Helmchen, G.; Pfaltz, A. *Accounts Chem Res* **2000**, *33*, 336.

(75) Braunstein, P.; Graiff, C.; Naud, F.; Pfaltz, A.; Tiripicchio, A. *Inorg Chem* **2000**, *39*, 4468.

(76) Guiry, P. J.; Saunders, C. P. *Adv Synth Catal* **2004**, *346*, 497.

(77) Gavrilov, K. N.; Polosukhin, A. I. *Usp Khim+* **2000**, *69*, 721.

(78) Ruther, T.; Done, M. C.; Cavell, K. J.; Peacock, E. J.; Skelton, B. W.; White, A. H. *Organometallics* **2001**, *20*, 5522.

(79) Henriksen, S. T.; Norrby, P. O.; Kaukoranta, P.; Andersson, P. G. *J Am Chem Soc* **2008**, *130*, 10414.

(80) Jalil, M. A.; Fujinami, S.; Senda, H.; Nishikawa, H. *J Chem Soc Dalton* **1999**, 1655.

(81) Jalil, M. A.; Fujinami, S.; Nishikawa, H. *J Chem Soc Dalton* **2001**, 1091.

(82) Jalil, M. A.; Yamada, T.; Fujinami, S.; Honjo, T.; Nishikawa, H. *Polyhedron* **2001**, *20*, 627.

(83) Tejel, C.; Ciriano, M. A.; Jimenez, S.; Oro, L. A.; Graiff, C.; Tiripicchio, A. *Organometallics* **2005**, *24*, 1105.

(84) Espino, G.; Jalon, F. A.; Maestro, M.; Manzano, B. R.; Perez-Manrique, M.; Bacigalupe, A. C. *Eur J Inorg Chem* **2004**, 2542.

(85) Schulz, T.; Torborg, C.; Schaffner, B.; Huang, J.; Zapf, A.; Kadyrov, R.; Borner, A.; Beller, M. *Angew Chem Int Edit* **2009**, *48*, 918.

(86) Milde, B.; Schaarschmidt, D.; Ruffer, T.; Lang, H. *Dalton T* **2012**, *41*, 5377.

(87) Menges, F.; Neuburger, M.; Pfaltz, A. *Org Lett* **2002**, *4*, 4713.

(88) Busacca, C. A.; Grossbach, D.; So, R. C.; O'Brien, E. M.; Spinelli, E. M. *Org Lett* **2003**, *5*, 595.

(89) Guiu, E.; Claver, C.; Benet-Buchholz, J.; Castillon, S. *Tetrahedron-Asymmetr* **2004**, *15*, 3365.

(90) Nair, R., University of California, San Diego and San Diego State University, 2011.

(91) Larsen, C. R., University of California, San Diego and San Diego State University, 2012.

(92) Grotjahn, D. B. L., Casey R.; Erdogan, Gulin; Gustafson, Jeffery L.; Nair, Reji; Sharma, Abhinandini In *Catalysis of Organic Reactions* Prunier, M. L., Ed.; CRC Press: 2009; Vol. 123, p 379.

(93) Trost, B. M.; Zhang, T. *Org Lett* **2006**, *8*, 6007.

(94) Nelson, S. G.; Bungard, C. J.; Wang, K. *J Am Chem Soc* **2003**, *125*, 13000.

(95) Cramer, R. *J Am Chem Soc* **1966**, *88*, 2272.

(96) Tuner, M.; Jouanne, J. V.; Brauer, H. D.; Kelm, H. *J Mol Catal* **1979**, *5*, 425.

(97) Tuner, M.; Jouanne, J. V.; Brauer, H. D.; Kelm, H. *J Mol Catal* **1979**, *5*, 433.

(98) Tuner, M.; Jouanne, J. V.; Kelm, H. *J Mol Catal* **1979**, *5*, 447.

(99) Bingham, D.; Hudson, B.; Webster, D. E.; Wells, P. B. *J Chem Soc Dalton* **1974**, 1521.

(100) Tao, J. C.; Sun, F. S.; Fang, T. *J Organomet Chem* **2012**, *698*, 1.

(101) Grotjahn, D. B.; Gong, Y.; Zakharov, L.; Golen, J. A.; Rheingold, A. L. *J Am Chem Soc* **2006**, *128*, 438.

(102) Grotjahn, D. B. *Dalton Trans* **2008**, 6497.

(103) Lev, D. A., University of California, San Diego and San Diego State University, 2004.

(104) McDonough, J. M.; Gray, L. S., Jr.; Akzona Inc. . 1972, p 14 pp.

(105) Noddings, C. R.; Dow Chemical Co. . 1967, p 4 pp.

(106) Clark, T. P.; Frazier, K. A.; Timmers, F. J.; Kolthammer, B. W.; Dow Global Technologies LLC, USA . 2011, p 13pp.

(107) Sivaramakrishna, A.; Mushonga, P.; Rogers, I. L.; Zheng, F.; Haines, R. J.; Nordlander, E.; Moss, J. R. *Polyhedron* **2008**, *27*, 1911.

(108) Li, G.; Qian, Y.; Huang, Y.-Z.; Chen, S. *J Mol Catal* **1992**, *72*, L15.

(109) McGowan, K. P.; Abboud, K. A.; Veige, A. S. *Organometallics* **2011**, *30*, 4949.

(110) Hu, S. Q.; Liu, D. P.; Li, L. S.; Guo, Z.; Chen, Y. T.; Borgna, A.; Yang, Y. H. *Chem Eng J* **2010**, *165*, 916.

(111) Mirza-Aghayan, M.; Boukherroub, R.; Bolourtchian, M.; Hoseini, M.; Tabar-Hydar, K. *J Organomet Chem* **2003**, *678*, 1.

(112) Morrill, T. C.; D'Souza, C. A. *Organometallics* **2003**, *22*, 1626.

(113) Goerlich, J. R.; Schmutzler, R. *Phosphorus, Sulfur Silicon Relat. Elem.* **1995**, *102*, 211.

CHAPTER 3

POLYMER SUPPORTED ALKENE ISOMERIZATION

INTRODUCTION

Despite the significant advantages of homogeneous catalysis, which include high efficiency and high selectivity, there is still demand for highly active and stable heterogeneous systems due to the tedious and time-consuming purification steps required to remove homogeneous catalysts from reaction mixtures. In organometallic catalysis, where both the product and the catalyst's ligands are small organic molecules, chromatography often represents the best purification option. Here, immobilization of the catalyst may provide an elegant solution to purification problems.[1] Immobilized catalysts can provide faster synthetic procedures, reduce costs, and promote environmentally friendly industrial manufacturing.[2] Fine chemicals production and pharmaceuticals production provide high value commodities from building blocks to drugs that allow us to support the ever-expanding world. Production of these materials require high selectivity in terms of chemo-, regio- and stereo- selectivity which can be provided by homogenous catalysts but separation and purification are among the biggest hindrances to commercialization. Thus, the motivating factors for creating selective yet recoverable catalysts are large.

Homogeneous catalysts provide greater selectivity and controllability due to their molecular nature ensuring the presence of only a single type of active site, whereas heterogeneous catalysts may contain ill-defined surfaces that lead to difficult design and improvement. On the other hand, the inherent difficulty and expense of separating a homogeneous catalyst from the products at the end of the reaction along with easier handling and robust nature of heterogeneous catalysts has often led industry to prefer use

of the latter. An ideal catalyst, therefore, would be one that is: (1) readily separated from the stream of reactants and products, (2) able to be recycled without losing efficiency, (3) equivalent to or better than the best homogeneous catalyst and (4) specific for the desired reaction.[1,3] An immobilized molecular catalyst on an insoluble support could function mechanistically as if in solution and at the same time offer all the engineering and manipulative advantages of heterogeneous catalysts.

The great variety of catalyst solid supports[1,3,4] can be divided into two broad classes, (1) inorganic oxides, and (2) organic polymers. Typical examples of both are listed in Table 3.1. Both exhibit contrasting advantages and disadvantages. One of the most important differences is the degree to which they can be functionalized; organic matrices can be loaded up to 10 meq/g but inorganic matrices cannot be loaded to an extent more than 1-2 meq/g of matrix.[5]

Inorganic supports are superior in thermal and mechanical stability but they lack the chemical stability, inertness and flexibility. They are more resilient to changes in temperature, pressure and solvent polarity compared to organic supports.

Table 3.1. Supports for immobilization

Organic	Inorganic
Polystyrene	Silica
Polyamide	Alumina
Polymethacrylate	Zeolite
Polybutadiene	Clay
Polyvinyl	Carbon
Silicone resins	Metal oxides

The principle advantages of organic polymers are (1) easy modification and functionalization, (2) controllable physical properties, and (3) chemical inertness (except at higher temperatures). Although organic polymers have poor mechanical stability that prevent their use in stirred reactions, this can be overcome by introducing techniques that prevent pulverization. The porous nature of polymers offers the advantage of higher selectivity through control of diffusion, but at the same time the rate of the reaction depends on the accessibility of the catalytic sites within the polymer. The choice of solvent along with temperature can highly affect the swelling, and therefore change the pore size and govern the size of molecules and at which rate they can reach or leave the active sites.

In the work described below, 2% cross-linked polystyrene was chosen as the support for the alkene isomerization catalyst. Since the introduction of the Merrifield resin for peptide synthesis, cross-linked polystyrene-supported catalysts have been adopted for numerous organic reactions to facilitate product purification and catalyst recovery.[6-8] Functionalization of the preformed commercial polymer is practical and can be well adapted from previous literature. For example, Pericas and coworkers reported immobilization of (*E*)-4-hydroxyproline onto Merrifield-type polymers through a copper-mediated 1,3-dipolar cycloaddition.[9]

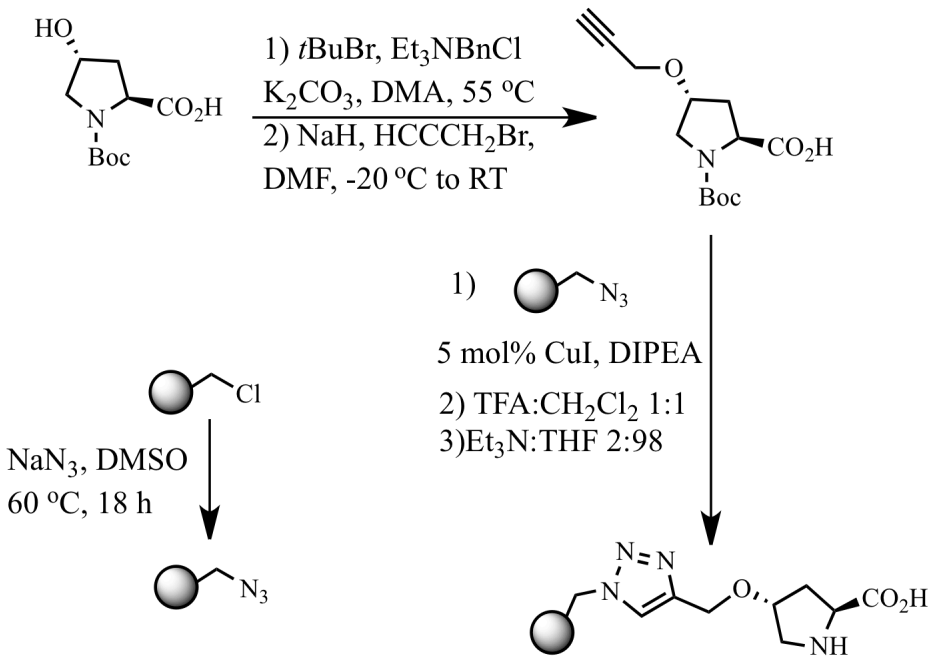

Figure 3.1. Immobilization of (*E*)-4-hydroxyproline

The immobilized proline-derived catalyst in Figure 3.1 can be used (Figure 3.2) for diastereoselective direct aldol reactions, enantioselective alpha-aminoxylation of aldehydes and ketones,[10] and asymmetric Manninch reaction of aldehydes with preformed N-(p-methoxyphenyl)ethyl glyoxylate imine. [11]

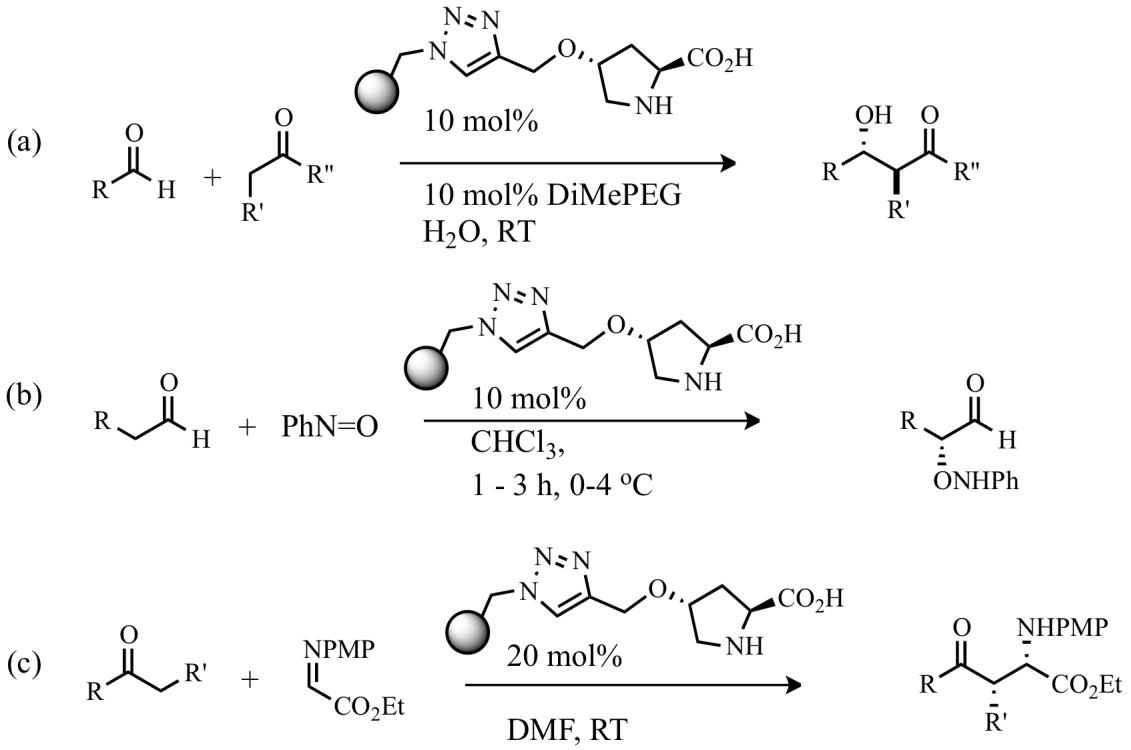

Figure 3.2. Reactions catalyzed by polystyrene immobilized (*E*)-4-hydroxyprline. (a) Diasteroselective direct aldol reactions, (b) Enantioselective alpha-aminoxylation of ketones, (c) Enantioselective Mannich reactions

Metathesis catalysts have received great attention and several attempts to immobilize them on different types of supports have been published. Grela et al. reported immobilizing 2nd generation Hoveyda-Grubbs catalyst on PS-DES (Figure 3.3), which is commercially available and easily accessed by treating Merrifield resin with allylmagnesiumchloride followed by hydrosilylation with diethylsilane.[12]

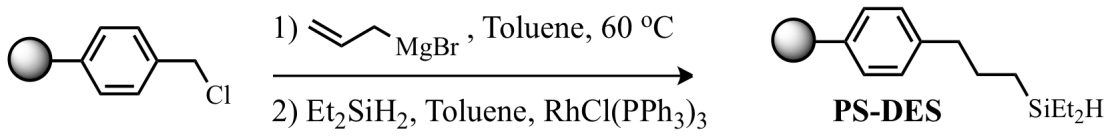

Figure 3.3. PS-DES synthesis from Merrifield resin

Polymer-supported 2nd generation Hoveyda-Grubbs catalyst (**3.4**, Figure 3.4) was successfully recycled up to six cycles without significant loss of activity, and the same batch of recycled catalyst could be used sequentially in different metathesis reactions. [13]

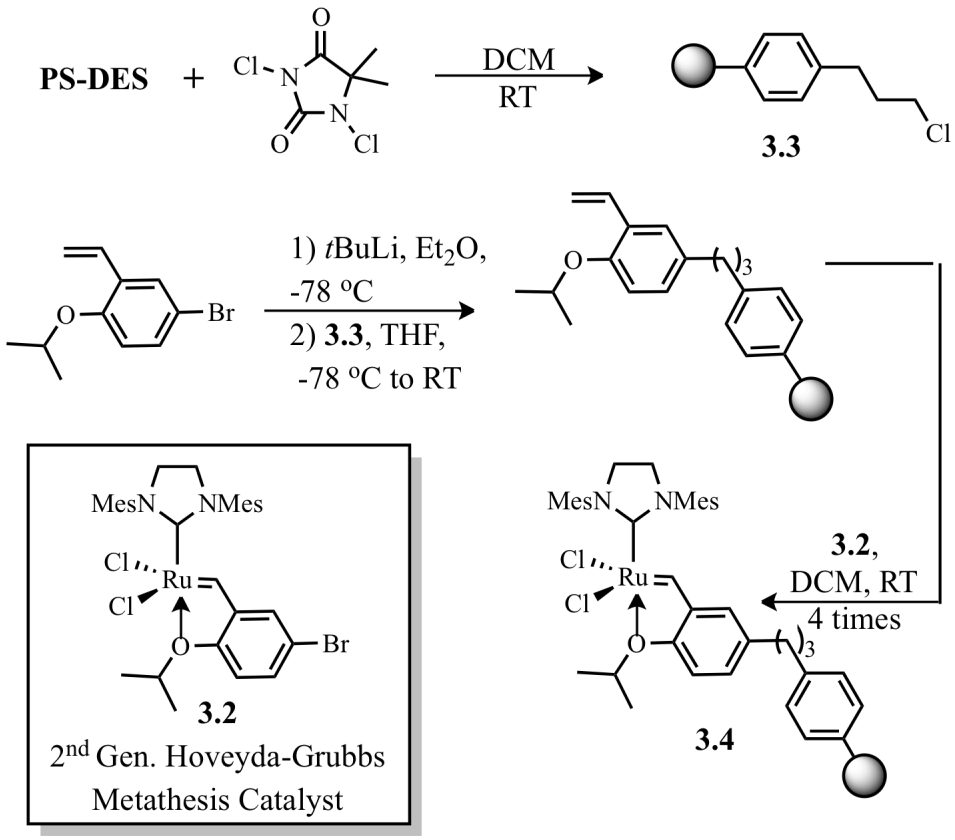

Figure 3.4. Polymer-supported 2nd generation Hoveyda-Grubbs metathesis catalyst

There are different strategies to bind a catalyst to a support; immobilization of proline-derived catalyst is an example of direct immobilization where the pre-built ligand or complex is anchored on the support (Figure 3.1). The approach followed for immobilization of metathesis catalyst (Figure 3.4) is an example of stepwise synthesis where the ligands and complex is added to the polymer in a stepwise fashion. Although the direct immobilization of a preformed metal complex is advantageous because it

reduces the possibility of non-selective metal binding, an alternative strategy involving the stepwise synthesis of ligands on the solid support has the advantage of being able to prepare libraries. Starting with an anchored ligand, different metal complexes can be formed leading greater versatility. When using stepwise solid phase synthesis approach, the characterization of the species formed on the solid support can be hard to characterize and the undesired coordination of the metal to the support along with incomplete ligand formation and complexation should be kept in mind. On the other hand excess reagents ad other products can be removed from the immobilized complex by thorough washes with appropriate solvents.

As mentioned in chapter 3, isomerization of carbon-carbon double bonds is a desirable reaction. Significantly, our search of the literature on heterogeneous[14-23] or heterogenized[24-32] alkene isomerization catalysts revealed a lack of highly selective systems. Some heterogeneous alkene isomerization systems use strong acid[15,18,20] or base [16,17] catalytic sites. Many of the systems require high temperatures and they either suffer from forming positional isomers[14-23,25,29] in thermodynamic ratios and/or mixtures of geometric isomers.[14-31] Heterogeneous systems that use metals[3] as active components provide milder conditions and among these, perhaps the best system is reported by Ley et al. in synthesis of the natural product carpapone, using a polymer-supported form of Felkin's iridium catalyst with (*E*)-olefin selectivity up to >98%.

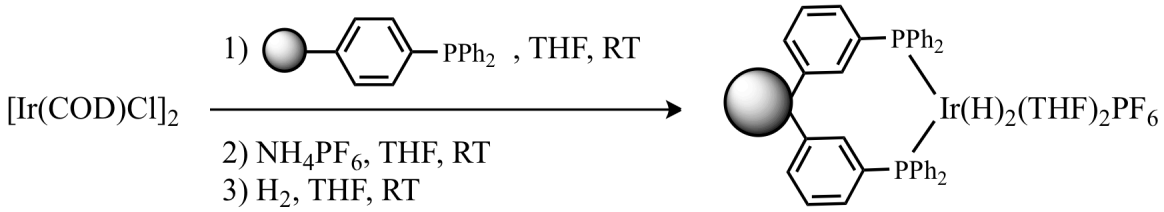

Figure 3.5. Polymer-supported Felkin's iridium catalyst

The isomerization reactions were carried out with about 40 mol% catalytic loading for 24 h at room temperature. Electron-rich arylated allylic systems were successfully isomerized in highly (*E*)-selective fashion, whereas, with electron poor systems only up to 50% isomerization was possible. Allyl ether isomerizations took place with high conversions but essentially equimolar mixtures of (*Z*)- and (*E*)-products were obtained. Regardless of the type of the substrate, up to 4% of the hydrogenated alkene product was present. Also worthy to note that when compared to the homogenous system, the polymer-supported system was reported to be less geometrically selective.[31,32] In summary; (1) immobilized Felkin's iridium catalyst requires catalyst activation with H_2 gas prior to use, (2) polymer-supported system is less (*E*)-selective than the related homogenous catalyst, (3) small amount of hydrogenation products are observed along with minor or equivalent amount of (*Z*)-products in several substrates, (4) use of up to 40 mol % catalytic loadings are used.

Table 3.2. Scope of polymer-supported Felkin's iridium catalyst

Starting Material	Product	(*E*)-(*Z*) Selectivity
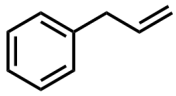	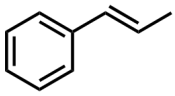	(*E*) only
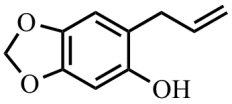	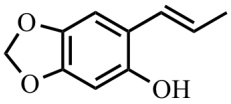	~92% (*E*)
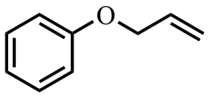	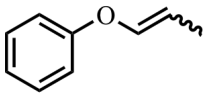	1 :1
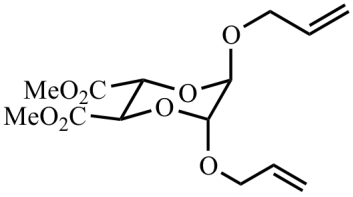	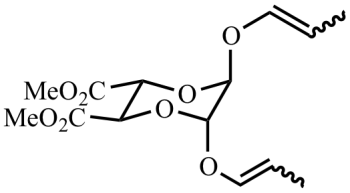	Mixture of (*E*) and (*Z*)
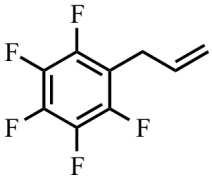	50% Conversion	-
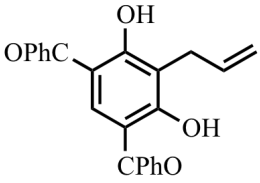	Recovered starting material with <4% isomerized product	-
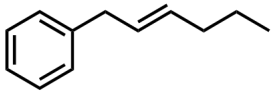	Recovered starting material	-

DESIGN, DEVELOPMENT AND TESTING OF HETEROGENIZED CATALYSTS

Previously reported systems for alkene isomerization lack the high selectivity for (*E*)-isomers and best system reported so far suffers from loss of (*E*)-selectivity upon immobilization. Homogenous alkene isomerization catalyst (chapter 3) reported in the Grotjahn group shows exceptional ability to move double bonds over many positions with functional group tolerance and geometric selectivity towards (E)-alkenes regardless of functional group present. For example, silyl ethers where the (*Z*)-isomers are thermodynamically stable versus unfunctionalized hydrocarbon chains where (*E*)-isomers are more stable.[33] Immobilization of alkene isomerization catalyst **2.10** in the form of began by on Merrifield resin by the sodium salt of 4-(*tert*-butyl)-1*H*-imidazole for **PS-1** followed by installation of phosphine functionality using *n*BuLi, then *i*Pr_2PCl and finally complexation employing $[CpRu(CH_3CN)_3]PF_6$ as precursor. The point of attachment to the resin was chosen as *N1* on the pendant base, which is proposed on the basis of X-ray diffraction studies to be away from the active site of the catalyst.[34]

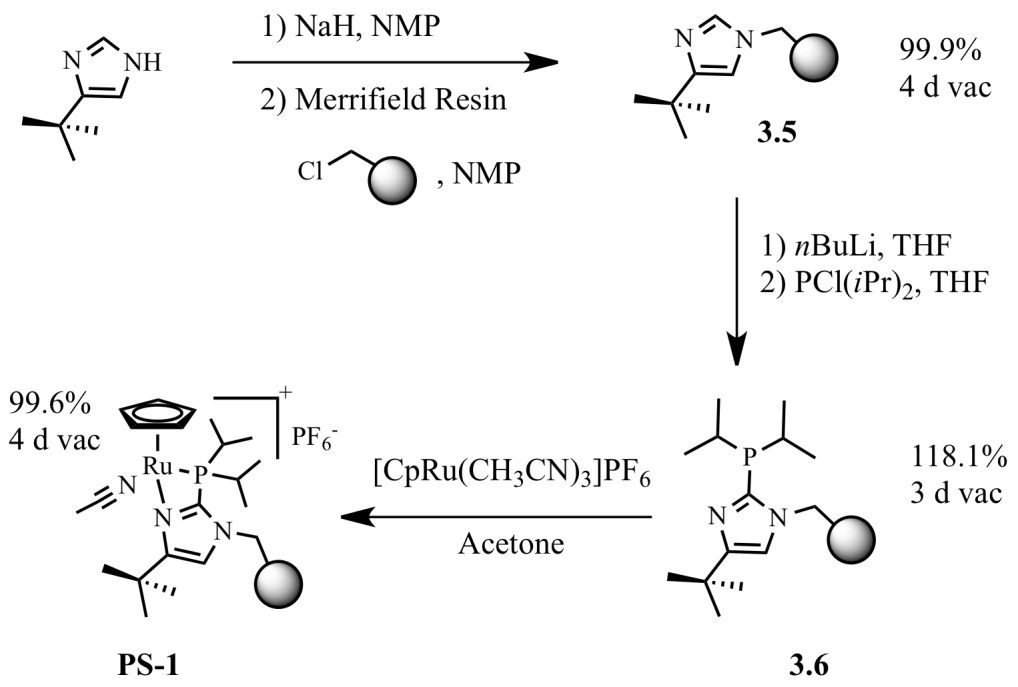

Figure 3.6. Synthesis of polymer-supported alkene isomerization catalyst PS-1

In order to explore the effects of having the active site further away from the resin matrix with possibly improved substrate and product transport rates,[35,36] in addition to **PS-1** a second version of the catalyst (**PSL-1**, Figure 3.7) featuring a tether of five atoms was also envisioned. The longer tether was installed by alkylation of the sodium salt of 4-*t*Bu-imidazole using tetrahydropyran-protected 3-bromopropanol, followed by deprotection of the THP ether to reveal the alcohol. The displacement of chloride on Merrifield resin was accomplished by the alkoxide accessed from deprotonation of **3.9** with sodium hydride. Installation of phosphine functionality and complexation was as followed in **PS-1**. Polymer was extensively washed at each step and composition of the polymer was determined by elemental analysis via nitrogen percent weight.

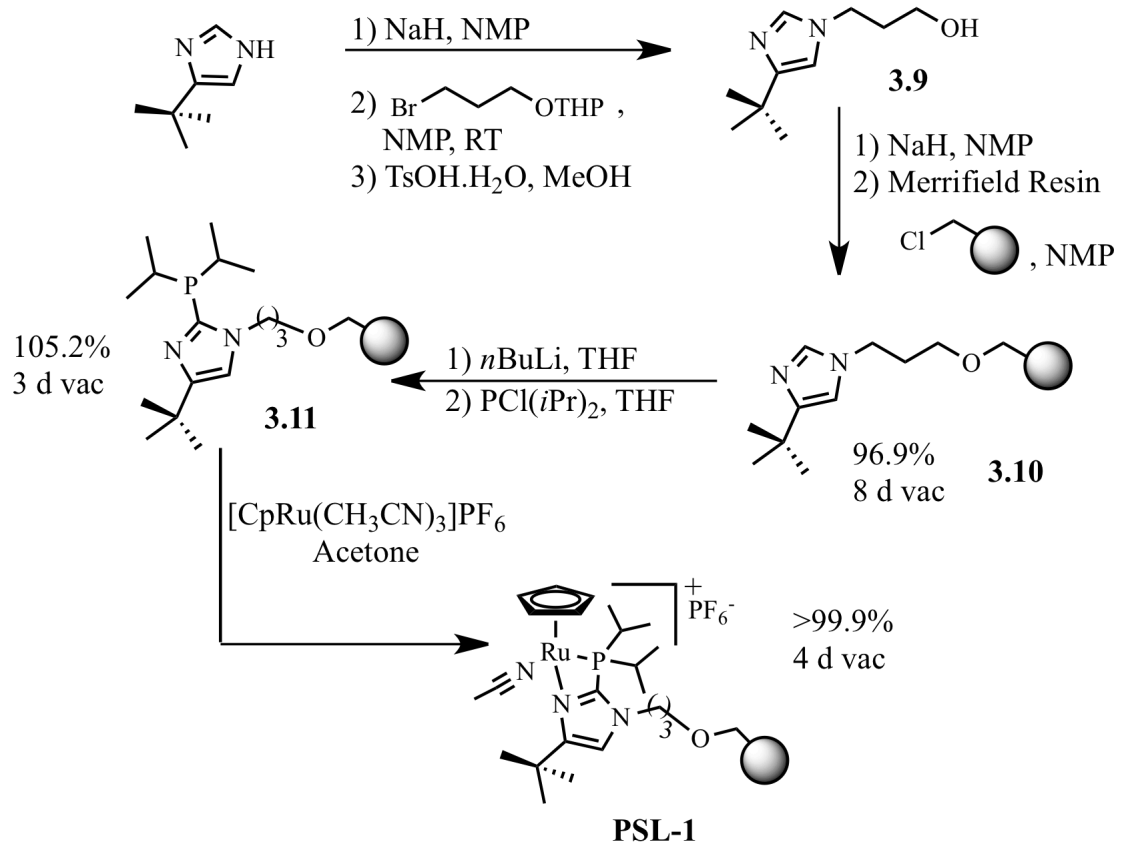

Figure 3.7. Synthesis of polymer-supported alkene isomerization catalyst PSL-1

Compared to their homogenous counterparts, in general, heterogeneous catalysts are generally harder to characterize. Polymer was extensively washed at each step and composition of the polymer was determined by elemental analysis via nitrogen percent weight, but this technique could give direct evidence of ligand or catalyst structure. In order to verify full complexation of $[CpRu(CH_3CN)_3]PF_6$ with polystyrene supported 4-*tert*-butyl-2-(diisopropylphosphino)-1*H*-imidazole and absence of free phosphine, a smaller scale reaction of **PS-1** was carried out in a J. Young NMR tube. ^{31}P NMR data for **PS-2** shows a single peak at -18.7 ppm, which is in agreement with data for the solution-phase imidazolylphosphine (-18.5 ppm in acetone-d_6). Metal complexation was carried out with 1 equivalent of ruthenium precursor $[CpRu(CH_3CN)_3]PF_6$ and the

absence of the peak at -18.7 ppm confirmed that complexation was complete, and the chemical shift of 41.5 ppm suggests that on the resin, **PS-1** was present rather than **PS-2**. The ligands in **PSL-1** and **PS-1** appear to be the first polymer-supported imidazolylphosphines.

Isomerization of alkene substrates was achieved at low (1-2 mol %) catalyst loadings in acetone as solvent, either at room temperature or at 70 °C. At room temperature, reactions were performed in vials with Teflon-lined caps that were placed on a nutator in order to introduce mixing without mechanical destruction of the polymer beads. Reactions at elevated temperatures were conducted in resealable J. Young NMR tubes without mechanical mixing of any kind; further optimization of mixing technique during heating might lead to improved results. The performance of heterogenized catalysts **PS-1** and **PSL-1** was compared with that of soluble catalyst **1** by subjecting substrates to similar conditions and observing the progress of isomerization by ^{1}H NMR spectroscopy.

Table 3.3. Substrate scope of PS-1 and PSL-1

Entry	Starting Material	Product	Catalyst	Mol %	T(oC)	Time	Yield %
1	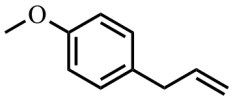	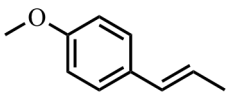	**PS-1**	2	RT	20 min	96.3
			PSL-1	2	RT	20 min	98.6
			2.10	2	RT	10 min	99.2
2	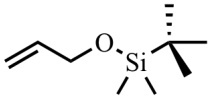	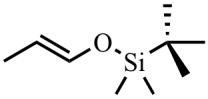	**PS-1**	2	RT	30 min	97.1
			PSL-1	2	RT	30 min	96.5
			2.10	2	RT	4 min	99.8
3	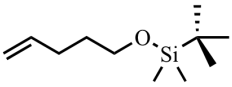	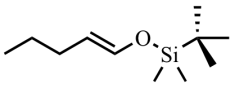	**PS-1**	5	70	24 h	70.5
			PSL-1	5	70	24 h	57.7
			2.10	5	70	4 h	90
4	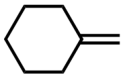	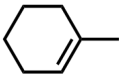	**PS-1**	2	70	48 h	91.2
			PSL-1	2	70	72 h	83.9
			2.10	2	70	1 h	98.0
5	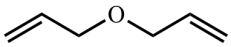	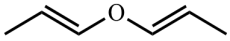	**PS-1**	2	RT	5 h	97.4
			PSL-1	2	RT	5 h	98.6
			2.10	2	RT	40 min	96
6	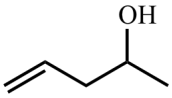	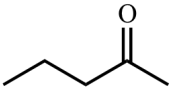	**PS-1**	2	70	2 h	91.2
			PSL-1	2	70	1 h	90.0
			2.10	2	70	1 h	97.0
7	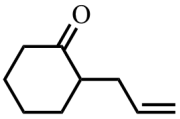	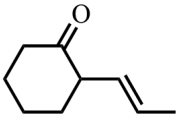	**PS-1**	2	70	1 h	78.1
			PSL-1	2	70	23 h	81.8
			2.10	2	70	45 min	91.6
8	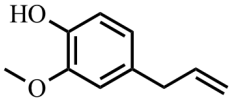	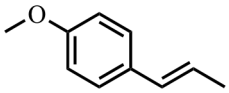	**PS-1**	1	RT	45 min	98.5
			PSL-1	1	RT	52 min	94.4
			2.10	1	RT	4 min	98.8

Isomerization of 4-allyl anisole, eugenol and diallyl ether was achieved at room temperature (Table 3.3). In each case performance of **PS-1** and **PSL-1** was comparable,

where both catalysts retained the very high stereoselectivty of solution phase catalyst **2**.**10** to yield (*E*)-isomers. **PS-1** outperformed **PSL-1** with substrates that require either multiple bond movements or are sterically more challenging.

Solvent-free reactions lead to new environmentally benign procedures that save resources and energy. They reduce the burden of organic solvent disposal and also bring down handling costs by simplifying experimental procedure and work up techniques consequently help saving costs during industrial production.[37] Our attempt to circumvent use of organic solvents lead us to the observation of reversal of the relative performances of **PS-1** and **PSL-1**, though both effective (Figure 3.8). In general, under neat conditions, **PSL-1** isomerizes 4-penten-2-ol, eugenol and 2-allylcyclohexanone in shorter time than does **PS-1**. Isomerization of 4-penten-2-ol was carried out with 2 mol% catalyst at room temperature. In two hours, **PSL-1** produces 90.7 % of corresponding ketone where as **PS-1** reaches same amount of ketone in 5 hours. It is worth noting that in 2 h, **PS-1** yields 19.9 % ketone and only 27.6 % starting alcohol is left, whereas the rest of the reaction mixture contains internal olefins. Eugenol and allylcyclohexanone were isomerized using 1 mol% catalytic loading. Quantitative conversion to (*E*)-isoeugenol was possible over 24 h, although the reactions were possibly complete before this time.

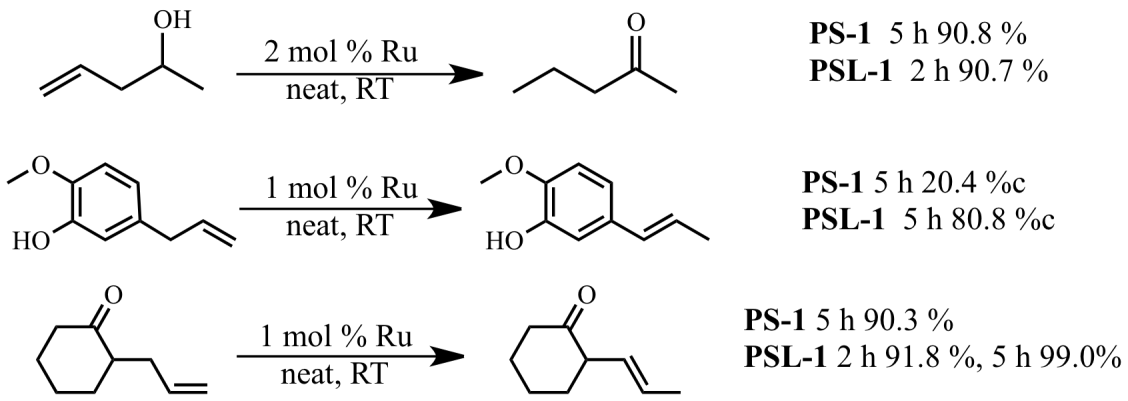

Figure 3.8. Isomerizations with PS-1 and PSL-1 under neat conditions

To further highlight the advantages of an immobilized alkene isomerization catalyst, alkene isomerization and metathesis have been performed in sequence without purification along the way. Stilbenoids, especially resveratrol, have received attention due to their potential value in cancer prevention and therapy[38-40] and they are shown to be accessible by metathesis.[38] Therefore, 4-allyl anisole and TMS-protected eugenol were isomerized with **PS-1.** After filtration, isomerized alkenes were subjected to metathesis reaction with silica-supported 2nd generation Hoveyda-Grubbs catalyst that was prepared according to literature.[41] Metathesis products were isolated in 73.5 and 87 % overall yield, respectively.

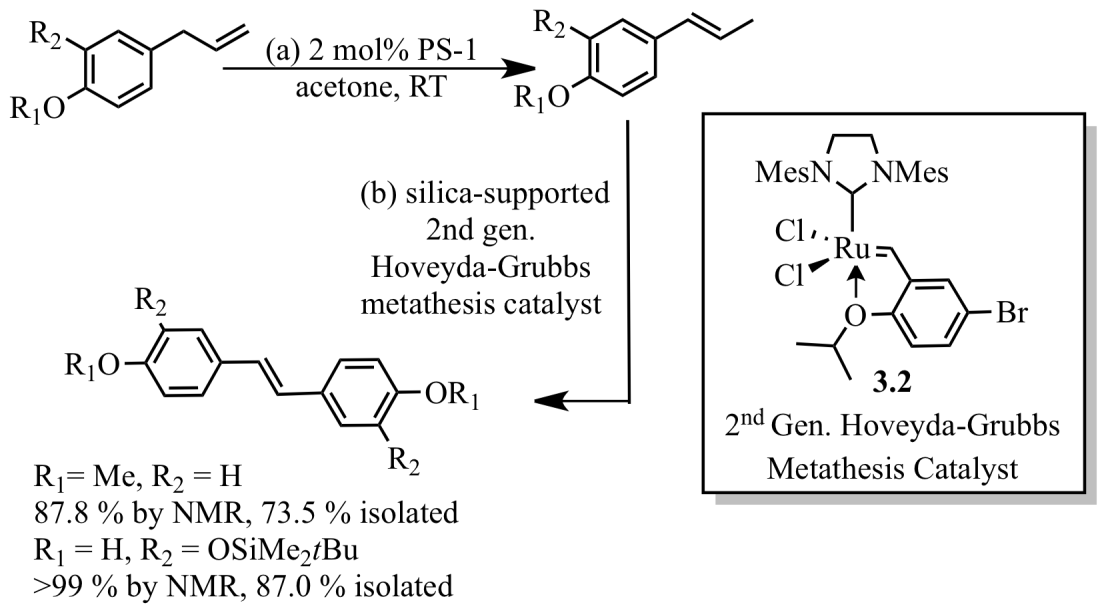

Figure 3.9. Sequential polymer-supported alkene isomerization and silica-supported metathesis

Alkenyl aromatics, like 4-allyl anisole, eugenol and their isomers are used in a wide range of flavoring, cosmetic, fragrance and pharmaceutical applications. Isoeugenol is extracted from natural sources or traditionally generated from eugenol by isomerization using stoichiometric excess KOH in alcoholic solutions at high temperature (200 °C).[42] Recycling and recovery studies were carried out with **PS-1** in the isomerization of eugenol to *E*-isoeugenol because of commercial interest in obtaining the product free of (*Z*)-isomer, as well as free of metal residues. The ruthenium content of combined filtrates and washes from each cycle was determined by inductively coupled plasma optical emission spectroscopy (ICP-OES) analysis.[43-45] The substrate conversion during each of the five cycles is near quantitative and yet in total only about 1.3 % ruthenium of the initial loading is lost, with 0.7% being lost in the first cycle. The higher leaching at the first cycle suggests the presence of more loosely held ruthenium species, perhaps

deposited in the pores of the polymer. In order to reduce metal contamination further, pre-treatment of the polymer-supported catalysts may further reduce the amount of metal leached into product.

Table 3.4. Recycling experiments performed with PS-1 and amount of metal leaching

Cycle #	% Eugenol	% (E)-Isoeugenol	Ru concentration (ppm)
1	0.6	98.1	1.08
2	0.9	99.4	0.51
3	0.3	99.9	0.17
4	0.2	98.4	0.11
5	0.2	97.1	0.07

In conclusion, we find it significant that the very high kinetic selectivity for formation of (*E*)-isomers is completely retained on heterogenization. In general, both **PS-2.10** and **PSL-1** show lower but still very useful activity compared to that of **2**.**10**, probably due to slow diffusion rates, which is a common trait for heterogenized catalysts. Compared to their homogenous counterparts, in general, heterogeneous catalysts are generally harder to characterize and suffer from slower diffusion rates and lower activity.[1,46] **PSL-1** outperforms **PS-1** under neat conditions. The difference in activity may be attributed to easier access to **PSL-1** active site provided by the longer tethering. Faster isomerization with **PSL-1** of the neat liquid substrates examined may also due to this catalyst's ability to swell faster compared to **PS-1** with substrates containing functionalities with oxygen. Overall, **1** is successfully heterogenized as **PS-1** and **PSL-1**;

the selectivity of the catalyst is fully retained with very low metal leaching from the insoluble support. Ongoing work seeks to create faster heterogeneous bifunctional catalysts for a variety of applications.

DESIGN, DEVELOPMENT AND TESTING OF SOLUBLE HETEROGENIZED CATALYSTS

Polymeric supports had become a driving force for lab automation and separation techniques. Increasing number of new polymeric supports have been published and used for supported catalysis. Every polymer has its drawbacks and advantages hence can be utilized for the parameters they offer. As an alternative to insoluble polymeric supports, soluble polymer supports can be used to immobilize catalysts. Soluble supports will allow overcoming disadvantages such as difficult analysis of catalyst composition, or substrate access to active sites. By having the supported catalyst soluble in the reaction medium, the catalyst, in theory, will behave more like its homogenous analogue and will allow for better selectivity, yield and especially reaction rate.[47]

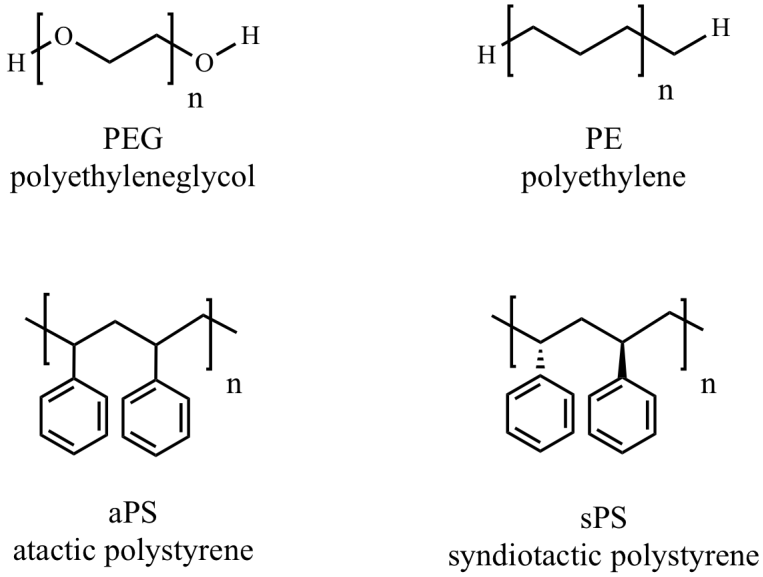

Figure 3.10. Examples of soluble polymers

Changing the temperature and/or polarity profile of the reaction can facilitate precipitation and enable recycling and recovery of a soluble polymer supported catalyst by simple filtration. Polyethyleneglycol (PEG), polyethylene (PE), and linear atactic polystyrenes (aPS) have been widely used as soluble polymer supports. PEG and PE suffer from low loading capacities due to their end-functionalized nature. Attempts to overcome these limitations by branching result in reduced solubility. Linear polystyrenes with low cross linking often times require demanding filtration techniques due their poor precipitation properties.[48] Syndiotactic polystyrene[49] (sPS) is a crystalline material that can be recovered in high yields because of the high stereoregular nature of the main chain. Also various loading capacities can be achieved by changing the functional group levels in the side chain of the polymer just like on any other polystyrene resin.

Bae et al. have demonstrated functionalization of sPS controlled functionalization of sPS through iridium-catalyzed borylation via activation of aromatic C-H bonds in the side chains up to 42 mol% incorporation of pinacolboronate ester (B(pin)) group.[50]

Quantitative recovery of pinacolboronate ester-functionalized sPS (sPS-B(pin)) as a fine powder has been achieved by adding an equal volume of methanol to a 5 mL chloroform solution of 50 mg sPS-B(pin). Under the same conditions, aPS-B(pin) recovery was only 55%, and as a sticky solid.

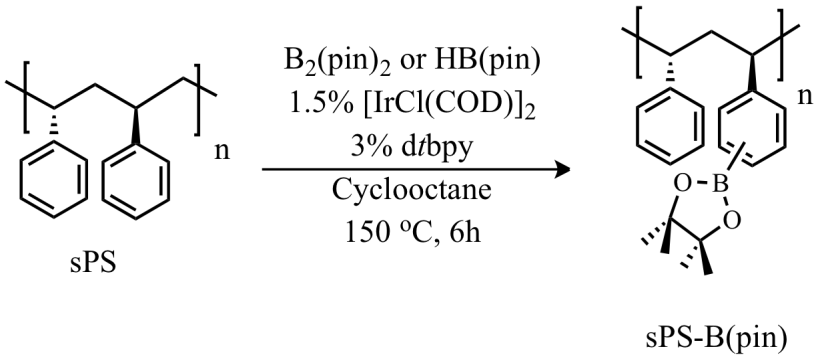

Figure 3.11. Borylation of sPS with Ir-catalyzed C-H activation

Boronate esters are versatile intermediates used in organic synthesis. sPS-B(pin) can be further functionalized, for example, a hydroxyl group can be introduced by oxidation of the ester and through Suzuki-Miyaura cross-coupling different functional groups can be introduced onto sPS. Bae et al. successfully used triphenylphosphine-functionalized sPS (sPS-TPP) in Suzuki-Miyaura coupling of both electron-rich and electron-poor aryl halides. Simple precipitation of the sPS-TPP-supported palladium catalyst was again achieved by methanol recycled over four cycles without loss of activity. Over five cycles sPS-TPP-supported palladium catalyst was recovered quantitatively.[51]

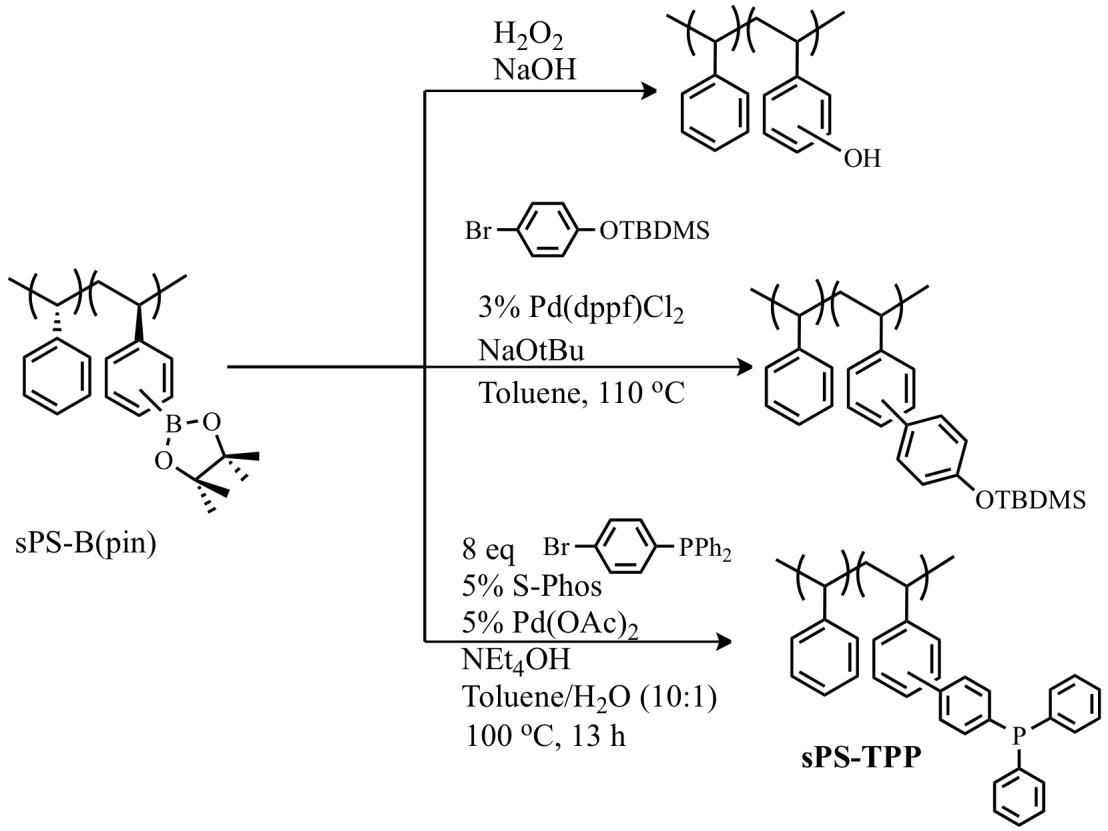

Figure 3.12. Facile functionalization of sPS-B(pin)

Taking this study as precedent, we decided to support alkene isomerization catalyst on sPS. Considering our previous approach to immobilization, we decided the point of attachment to the resin as *N1* on the pendant base, using a benzyl spacer by means of Suzuki-Miyaura coupling conditions. Addition of the phosphine functionality and metal complexation should take place in similar reaction conditions to **PS-1** and **PSL-1**. Different reaction conditions were investigated to establish whether the benzyl spacer can be installed at the desired position with the tertiary butyl group still at the 4-position (Figure 3.13, compound **3.12**). Due to electron delocalization between *N1* and *N3*, the benzylation reaction can occur adjacent to the more hindered nitrogen (**3.13**). Use

of 1-bromo-4-(chloromethyl)benzene with N-methyl-2-pyrrolidone (NMP) as solvent at -18 ^{o}C are the optimal conditions for the best product distribution(Table 3.5).

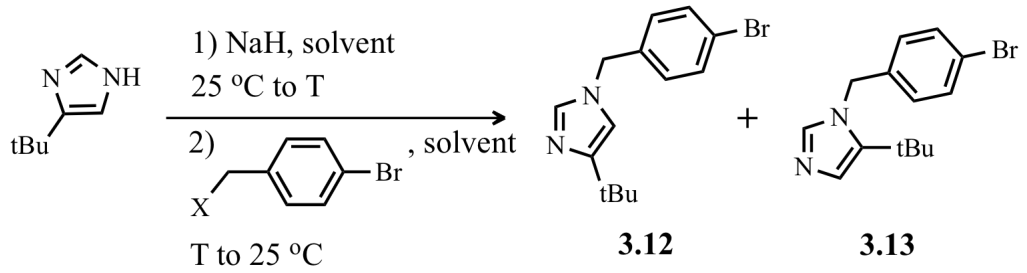

Figure 3.13. Benzyl spacer installment on 4-(*t*Bu)-imidazole

Table 3.5. Reaction conditions for optimal 1-(4-bromobenzyl)-4-(*t*Bu)-imidazole synthesis

Leaving Group	Ratio of Electrophile to Imidazole	Solvent	Temperature (^{o}C)	Product Ratio (3.12 : 3.13)
Br	1 : 1	THF	0	100 :20
Br	1 : 1	THF	25	100 : 18
Br	1 : 1	DMF	0	100 : 10
Br	1 : 1	NMP	0	100 : 8
Br	1 : 0.8	DMF	-42	100 : 8
Cl	1 : 0.8	NMP	-18	100 : 3
Cl	1 : 0.8	DMF	-42	100 : 5

A sample of sPS (from Dow Chemicals and Prof. Gaetano Guerra, Dipartimento di Chimica Università di Salerno Via Ponte Don Melillo) with molecular weight 3.2 x 10^5 g/mol was functionalized according to literature[50] using chloro(1,5-cyclooctadiene)iridium(I) dimer, $[IrCl(COD)]_2$, with 4,4'-di-*tert*-butyl-2,2'-bipyridine as base and bis(pinacolato)diboron as borylating agent in cyclooctane. The amount of B(pin) groups incorporated on the side chains was calculated from ratios of the ^{1}H NMR

(obtained in chloroform-*d*) integrals of the methine peaks from the main chain versus the those of the methyl groups of B(pin). According to these calculations, 1.5 to 2.7 % B(pin) incorporation was achieved by using 3% Ir and different amounts of $B_2(pin)_2$. Before installation of the imidazole on the sPS, the reaction of sPS-B(pin) was tried with bromotoluene as a model. Observance of ^{1}H NMR peaks around 2.4 ppm suggested that the sPS-B(pin) had been arylated under the reaction conditions.

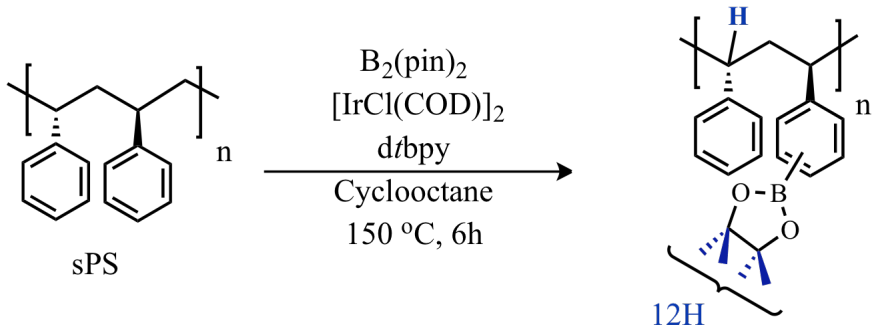

Figure 3.14. Synthesis of sPS-B(pin) and ^{1}H NMR signals used to calculate % incorporation

The incorporation of bromotoluene was successful, when sPS(Bpin) was coupled with 1-(4-bromobenzyl)-4-*tert*-Bu-imidazole under the same conditions, diastereotopic hydrogens of the methylene spacer as a singlet were observed around 5.0 ppm in the ^{1}H NMR spectrum. Changing the base from NMe_4OH to NEt_4OH or NaO*t*Bu didn't improve the reaction.

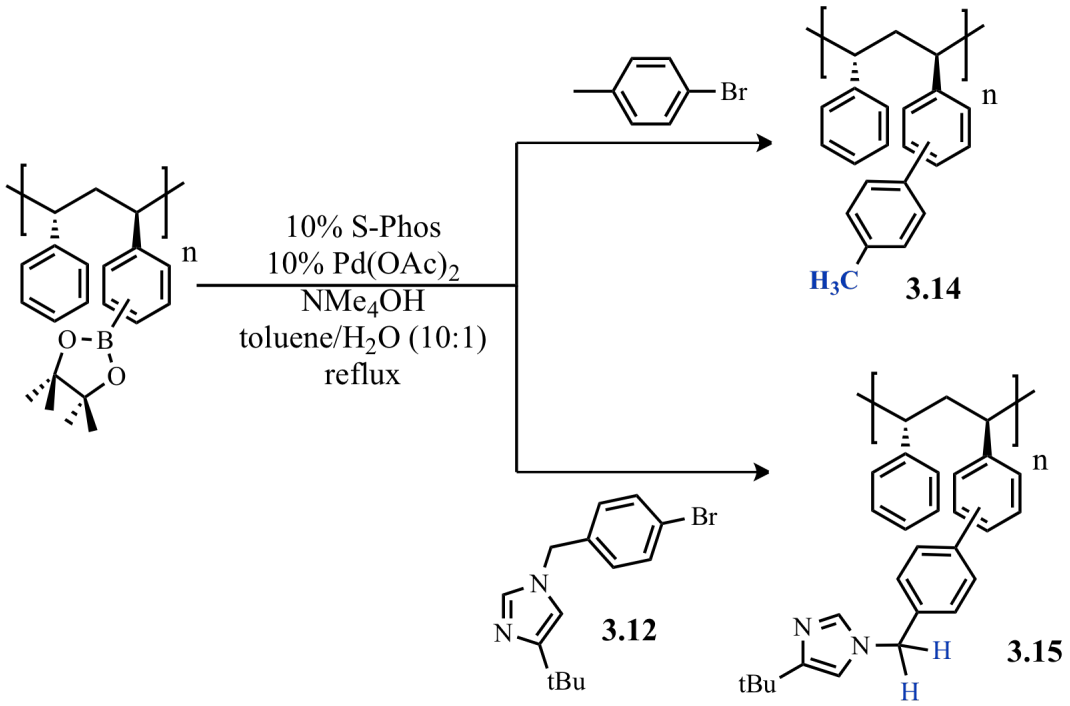

Figure 3.15. Functionalization of sPS-B(pin)

Treatment of **3.15** with BuLi in THF resulted in color change from light yellow to dark yellow. In comparison, the color change at this step starting with **PS-1** and **PSL-1** was from yellow to deep red color with the addition of BuLi and generation of the nucleophile, which faded back to yellow upon treatment with chlorophosphine. **3.16** was obtained as a gray solid, where NMR spectroscopic analysis of a solution in chloroform-*d* showed ^{31}P NMR peaks at -2.2, -50. 7, and -99.1 ppm, and in the ^{1}H NMR spectrum, and an identifiable signal for the diastereotopic hydrogens of the methylene spacer were not observed between 4.8 and 5.2 ppm. Multiple signals seen in the ^{31}P NMR spectra suggested that there was more than one phosphine species formed, where perhaps even deprotonation and phosphination of the methylene spacer had taken place. Attempt to complex this sample with $[CpRu(CH_3)_3]PF_6$ was not successful.

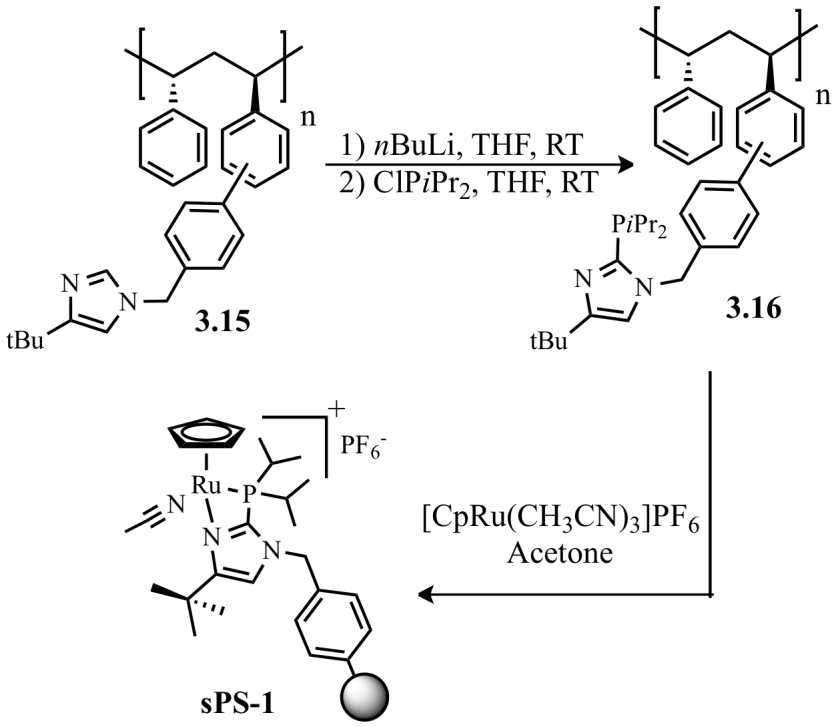

Figure 3.16. Synthesis of sPS-1

EXPERIMENTAL SECTION

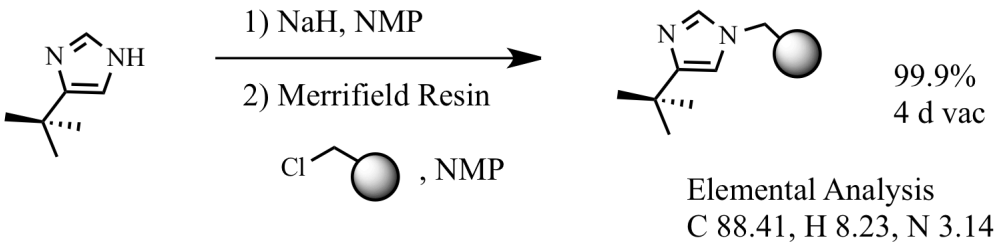

Figure 3.17. Synthesis of polystyrene-supported 4-*tert*-butyl-1-1*H*-imidazole

Polystyrene-supported 4-*tert*-butyl-1*H*-imidazole (3.5): The resin used, Merrifield HL (50-100 mesh) was purchased from Novabiochem and the concentration of reactive chloromethyl groups was assayed by the supplier as 1.1 mmol per gram. In a nitrogen-filled glovebox, using a scintillation vial, NaH (97.1 mg, 2.43 mmol, 60% by weight in mineral oil) was washed with dry hexanes and dried under reduced pressure. A solution of 4-*tert*-butyl-1*H*-imidazole (251.7 mg, 2.03 mmol) in dry NMP (5 mL) was added to NaH. The resulting mixture was stirred for 10 min before the reaction mixture was transferred to a vial containing Merrifield resin (1.0044 g, 1.10 mmol) swelled with dry NMP (~5 mL). The mixture was slowly stirred in a 50 ^{o}C oil bath overnight. The reaction mixture was transferred to a polyethylene syringe equipped with fritted disk and Teflon valve. The liquid was expelled and the resin was rinsed with dry NMP (total of 20 mL in three portions). The resin was washed with methanol (10 mL) then alternating between dichloromethane (10 mL) and methanol, four times each. The resin was stirred with dichloromethane in the syringe overnight before draining the liquid and drying the resin under reduced pressure for ~ 4 days (1.1005 g 99.9 %). Elemental analysis Calculated: N, 2.81; Found: C, 88.41; H, 8.23; N, 3.14.

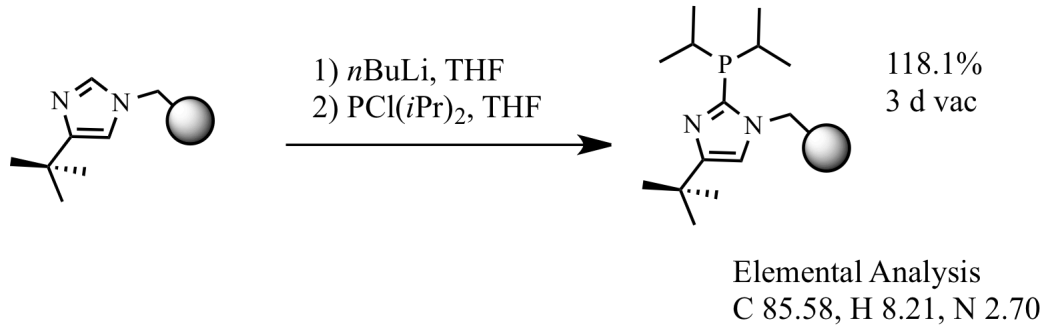

Figure 3.18. Synthesis of 4-*tert*-butyl-2-(diisopropylphosphino)-1*H*-imidazole

Polystyrene-supported 4-*tert*-butyl-2-(diisopropylphosphino)-1*H*-imidazole (3.6): In a nitrogen-filled glovebox, using a polyethylene syringe equipped with fritted disk and Teflon valve, dry THF (~3 mL) was added to polystyrene supported 4-*tert*-butyl-2-(diisopropylphosphino)-1*H*-imidazole (314.6 mg, 379.4 μmol). After 5 h BuLi (325 μL, 1.52 M in hexanes, 494 μmol) was added dropwise. The resin turned cherry red almost immediately. After 10 min of stirring, liquids were expelled and the resin was washed with dry THF (3 x 3 mL). A solution of $ClP(i\text{-}Pr_2)_2$ (69.2 mg, 453 μmol) in dry THF (~1 mL) was added and color of the resin faded to yellow almost immediately. After 2 h of stirring the liquids were expelled and the resin was washed with dry THF (4 x 5 mL). The syringe assembly was placed in a desiccator under reduced pressure for 3 d (395.6 g 118.1 %). Elemental analysis Calculated: N 2.52; Found: C, 85.58; H, 8.21; N, 2.70.

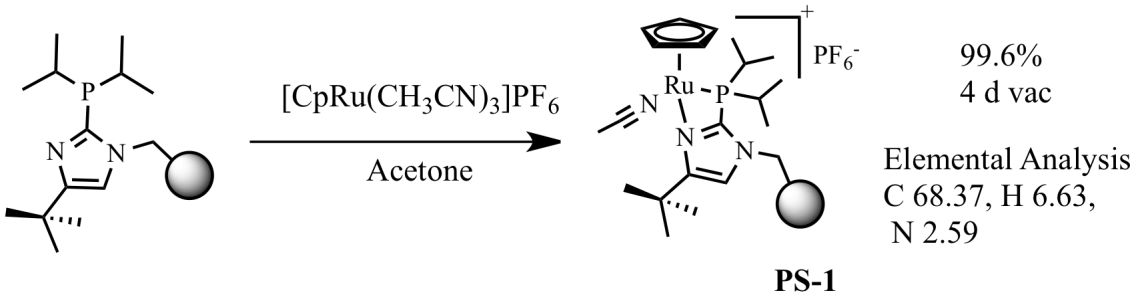

Figure 3.19. Synthesis of PS-1

Polystyrene-supported 2.10 (PS-1): In a nitrogen-filled glovebox, using a polyethylene syringe equipped with fritted disk and Teflon valve, polystyrene-supported 3-(4-*tert*-butyl-2-(diisopropylphosphino)-1*H*-imidazole (359.0 mg, 322.4 μmol) was swelled with acetone (~2 mL). A solution of $[CpRu(CH_3CN)_3]PF_6$ (307.8 mg, 609.4 μmol) in acetone (~4 mL) was added to syringe containing the resin. After stirring for 1 h, liquids were expelled and the resin was washed with acetone (6 x 4 mL). The syringe assembly was placed in a desiccator under reduced pressure for 3 d (456.3 g 96.6 %). Elemental analysis Calculated: N, 2.87; Found: C, 68.37; H, 6.63; N, 2.59.

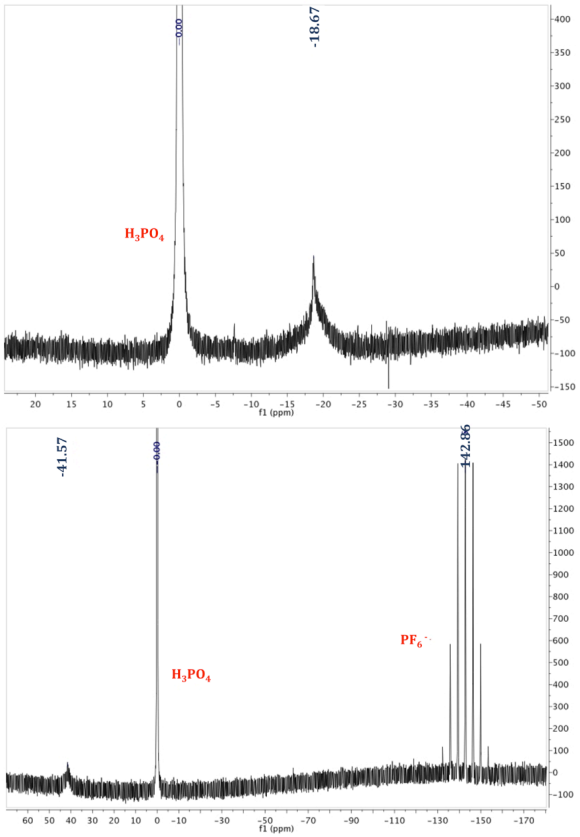

Figure 3.20. ^{31}P NMR spectrum of PS-2 (left) and PS-1 (right)

J. Young scale PS-1 synthesis for NMR analysis was performed in order to verify full complexation of $[CpRu(CH_3CN)_3]PF_6$ with polystyrene supported 4-*tert*-butyl-2-(diisopropylphosphino)-1*H*-imidazole and absence of free phosphine. A J. Young NMR tube was charged with polystyrene supported 4-*tert*-butyl-1*H*-imidazole (115.5 mg, 0.116 mmol), and dry and deoxygenated THF was added until the resin was all wet. A portion of BuLi solution (50.0 µL, 2.5M in hexanes, 0.116 mmol) was added to a 1-dram vial and diluted with THF (0.5 mL). The resulting solution was quantitatively transferred into the J. Young NMR tube dropwise. The color changed from light yellow to cherry red, similar to that observed in a larger-scale reaction (see above). The reaction was left to proceed at room temperature for 1.5 h. A solution of $ClP(i\text{-}Pr_2)_2$ (17.6 mg, 0.116 mmol) in dry THF

was added to the tube quantitative using portions of THF. The color of the resin faded to yellow almost immediately. The J. Young NMR tube was placed on a nutator for reaction to proceed at room temperature for 9 h.

A ^{31}P NMR spectrum[52] was acquired and a single peak at -18.7 ppm was observed with respect to an external 85 % $H_3PO_{4(aq)}$ capillary placed in the tube. This chemical shift is analogous to that of the free imidazolylphosphine **3.6** (-18.5 ppm in acetone-d_6).

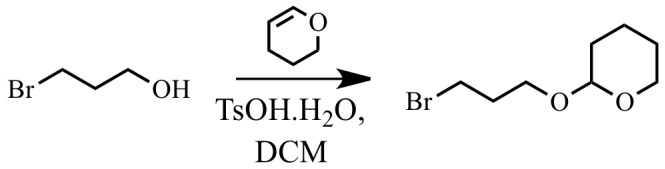

Figure 3.21. Synthesis of 2-(3-bromopropoxy)tetrahydro-2*H*-pyran

2-(3-bromopropoxy)tetrahydro-2*H*-pyran (3.7): In a round bottom flask, a solution of 3-bromopropanol (2.1093 g, 15.2 mmol) and 3,4-dihydro-2*H*-pyran (1.9118 g, 22.7 mmol) in dichloromethane (30 mL) containing p-toluenesulfonic acid mono hydrate (291.0 mg, 1.53 mmol) was stirred overnight at room temperature. The solution was diluted with hexanes and washed with DI H_2O (total of 250 mL in four portions). The aqueous layer was back-extracted with hexanes (2 X 50 mL). Combined organic layers were dried with anhydrous $MgSO_4$, filtered, and after removing the solvents under reduced pressure the crude product was purified by column chromatography over silica, eluting with 4:1 hexanes:diethyl ether, to give the product (3.0269 g, 97.4 %) as a an oil.

^{1}H NMR (500 MHz, chloroform-*d*) δ 4.62-4.59 (m, 1H), 3.89-3.85 (m, 2H), 3.56-3.51 (m, 4H), 2.17-2.13 (m, 2H), 1.84-1.66 (m, 2H), 1.60-1.52 (m, 4H). Data are in accordance with those previously reported.[53,54]

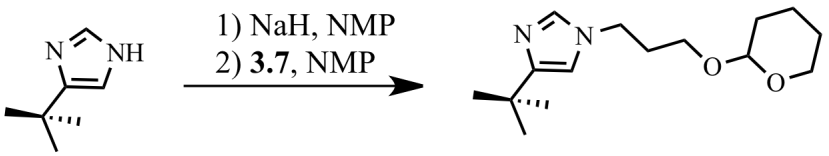

Figure 3.22. Synthesis of 4-*tert*-butyl-1-(3-(tetrahydro-2*H*-*pyran*-2-yloxy)propyl)-1*H*-imidazole

4-*tert*-butyl-1-(3-(tetrahydro-2*H*-pyran-2-yloxy)propyl)-1*H*-imidazole (3.8): In a nitrogen-filled glovebox, using a Schlenk flask NaH (711.2mg, 17.8 mmol, 60% by weight in mineral oil) was washed with dry hexanes and dried under reduced pressure. In a vial 4-*tert*-butyl-1*H*-imidazole (1.8159 g, 14.6 mmol) was dissolved in NMP (5 mL) and the resulting solution transferred to Schlenk flask, which was taken out of the glovebox and connected to a Schlenk line and placed in an ice-water bath. After stirring overnight at room temperature, reaction mixture was diluted with DI H_2O and washed with Et_2O (4 x 50 mL). Combined organic layers were washed with DI H_2O (2 x 50 mL) and dried over anhydrous $MgSO_4$. After filtration and removing the solvents under reduced pressure, the residue was purified by column chromatography over silica, eluting with 1:4 hexanes:ethyl acetate, to give the product (3.4433 g, 94.1 %). ^{1}H NMR (500 MHz, chloroform-*d*) δ 7.39 (d, *J* = 1.0 Hz, 1H), 6.63 (d, *J* = 1.5 Hz, 1H), 4.55-4.54 (m, 1H), 4.05-3.96 (m, 2H), (ddd, *J* = 3.5, 4.0, 11.0 Hz, 1H), 3.87-3.83 (m, 1H), 3.79-3.75 (dt, *J* = 5.5, 10.0 Hz, 1H), 3.53-3.50 (m, 1H), 3.39-3.33 (td, *J* = 6.0, 10.0 Hz, 1H), 2.06-2.01 (dquin, *J* = 1.0, 6.0 Hz, 2H), 1.86-1.82 (m, 1H), 1.76-1.71 (m, 1H), 1.62-1.52 (m, 4H), 1.29 (s, 9H).

Elemental analysis Calculated: C, 67.63; H, 9.84; N, 10.52. Found: C, 64.26; H, 9.81; N, 10.09.

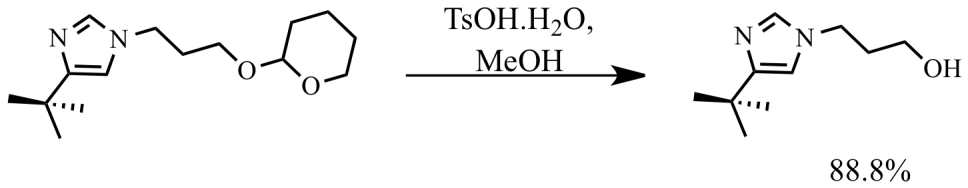

Figure 3.23. 3-(4-*tert*-butyl-1*H*-imidazol-1-yl)propan-1-ol

3-(4-*tert*-butyl-1*H*-imidazol-1-yl)propan-1-ol (3.9):[4] In a round bottom flask, a solution of 4-*tert*-butyl-1-(3-(tetrahydro-2*H*-pyran-2-yloxy)propyl)-1*H*-imidazole (3.3008 g, 12.4 mmol) in methanol (700 mL) containing p-toluenesulfonic acid monohydrate (4.7633 g, 25.0 mmol) was stirred overnight at room temperature. The reaction mixture was quenched with solid NaOH and concentrated under reduced pressure. The residue was dissolved in DI H_2O and washed with diethyl ether until washings showed no TL spots visible above the origin when eluted with 1:4 hexanes:ethyl acetate. Combined organic layers were washed with brine (2 x 50 mL) and dried with anhydrous $MgSO_4$. After filtration, the solvents were removed under reduced pressure to give the product (2.0064 g, 88.8 %) as a yellow solid. ^{1}H NMR (500 MHz, chloroform-*d*) δ 7.40 (d, *J* = 1.5 Hz, 1H), 6.62 (d, *J* = 1.5 Hz, 1H), 4.03 (t, *J* = 7.0 Hz, 1H), 3.65 (t, *J* = 6.0 Hz, 2H), 2.10-1.99 (m, 2H), 1.29 (s, 9H).

Elemental analysis Calculated: C, 65.90; H, 9.95; N, 15.37. Found: C, 65.66; H, 9.98; N, 15.09.

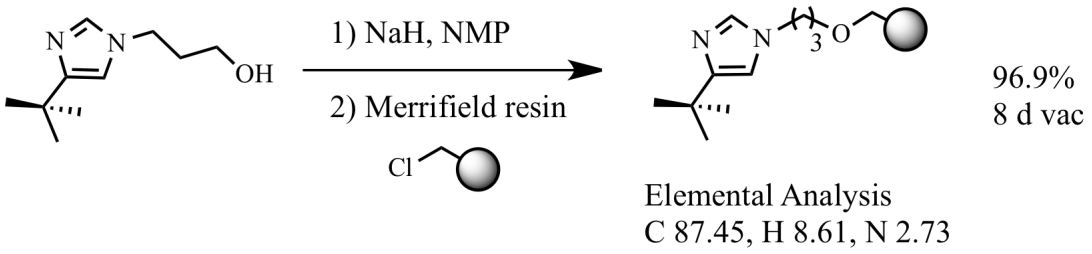

Figure 3.24. Polystyrene-supprted 4-*tert*-butyl-1*H*-imidazol-1-yl group with linker

Polystyrene-supported 4-*tert*-butyl-1*H*-imidazol-1-yl group with linker (3.10): The resin used, Merrifield HL (50-100 mesh) was purchased from Novabiochem and the concentration of reactive chloromethyl groups was assayed by the supplier as 1.1 mmol per gram. In a nitrogen-filled glovebox, using a scintillation vial, NaH (121.3 mg, 3.0 mmol, 60% by weight in mineral oil) was washed with dry hexanes and dried under reduced pressure. A solution of 3-(4-*tert*-butyl-1*H*-imidazol-1-yl) propan-1-ol (546.4 mg, 3.00 mmol) in NMP (2 mL) was added to the NaH, and the resulting mixture was stirred for 10 min before being transferred to a vial containing Merrifield resin (1.4870 g, 1.64 mmol) swelled with NMP (~5 mL). The mixture was slowly stirred in a 50 ^{o}C oil bath overnight. The reaction mixture was transferred to a polyethylene syringe equipped with fritted disk and Teflon valve. The liquid was expelled and the resin was rinsed with dry NMP (total of 20 mL in three portions). The resin was washed with methanol (10 mL) then alternating between dichloromethane (10 mL) and methanol, four times each. The resin was stirred with dichloromethane in the syringe overnight before draining the liquid and drying the resin under reduced pressure with oil-pump vacuum for ~ 8 d (1.5678 g 96.9 %). Elemental analysis Calculated: N, 2.65. Found: C, 87.45; H, 8.61; N, 2.73.

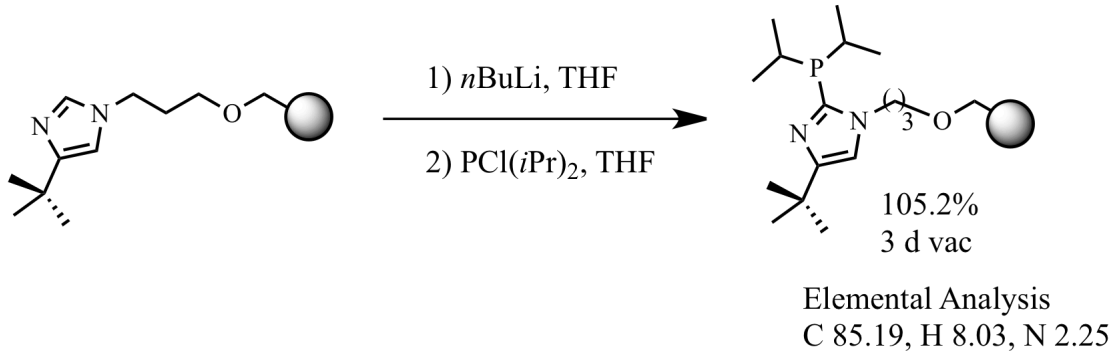

Figure 3.25. Polystyrene-supported 4-*tert*-butyl-2-(diisopropylphosphino-1*H*-imidazole

Polystyrene-supported 4-*tert*-butyl-2-(diisopropylphosphino)-1*H*-imidazole ligand with linker (3.11): In a nitrogen-filled glovebox, using a polyethylene syringe equipped with fritted disk and Teflon, dry THF (~3 mL) was added to polystyrene supported 3-(4-*tert*-butyl-1*H*-imidazol-1-yl)propan-1-ol (400.0 mg, 0.38 mmol). After 5 h, BuLi solution (380 µL, 1.52 M in hexanes, 578 µmol) was added dropwise. The resin turned cherry red almost immediately. After 10 min of stirring, liquids were expelled and resin was washed with dry THF (3 x 3 mL). A solution of $ClP(i\text{-}Pr_2)_2$ (87.9 mg, 576 µmol) in dry THF (~1 mL) was added and color of the resin faded to yellow almost immediately. After 2 h of stirring the liquids were expelled and the resin was washed with dry THF (4 x 5 mL). The syringe assembly was placed in a desiccator under reduced pressure with oil-pump vacuum for 3 d (467.0 mg 105.2 %). Elemental analysis Calculated: N, 2.39. Found: C, 85.19; H, 8.03; N, 2.25.

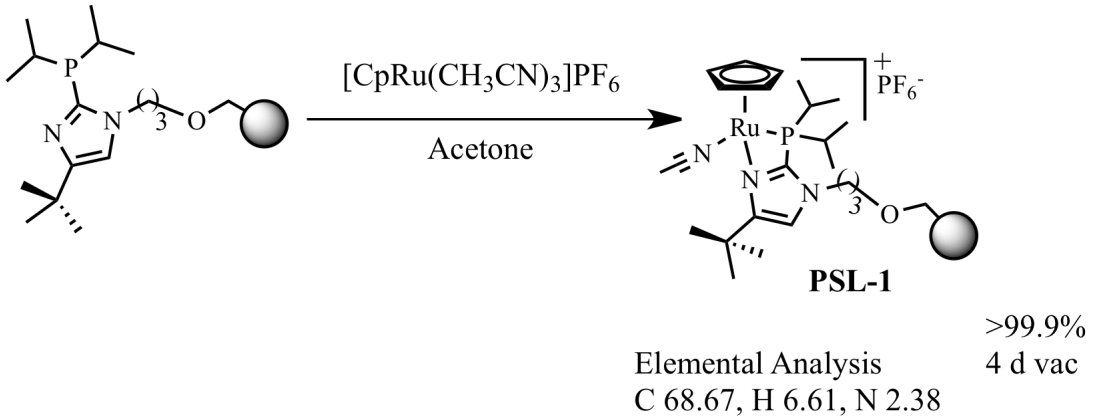

Figure 3.26. Synthesis of PSL-1

Polystyrene-supported 2.10 with linker (PSL-1): In a nitrogen-filled glovebox, using a polyethylene syringe equipped with fritted disk and Teflon, polystyrene supported 3-(4-*tert*-butyl-2-(diisopropylphosphino)-1*H*-imidazol-1-yl)propan-1-ol (443.0 mg, 371.1 μmol) was swelled with acetone (~2 mL). A solution of $CpRu(CH_3CN)_3PF_6$ (226.6 mg, 448.7 μmol) in acetone (~4 mL) was added to the syringe containing the resin. After stirring for 1 h, liquids were expelled and resin was washed with acetone (6 x 5 mL). The syringe assembly was placed in a desiccator under reduced pressure with oil-pump vacuum for 3 d (573.8 mg 100.0 %). Elemental analysis Calculated N 2.72 Found: C, 68.67; H, 6.61; N, 2.38.

General procedures for catalytic isomerization reactions

General Procedure A: In the glovebox, polymer-supported catalyst was weighed in a conical vial and acetone-d_6 is added to swell the polymer supported catalyst. In a separate vial, substrate was weighed and tetrakis(trimethylsilyl)methane or 1,4-dioxane was added as internal standard. Acetone-d_6 was added to ensure complete dissolution of all material. A small sample (<3 μL) was removed by capillary action into the tip of a Pasteur pipette and the sample was analyzed in acetone-d_6 to get an initial ^{1}H NMR spectrum to set the integral values. A solution of substrate and internal standard was added to the conical vial. The substrate vial was washed with additional acetone-d_6 and washings were added to the conical vial. The reaction mixture was stirred with a magnetic stir bar at room temperature. The progress of the reaction was monitored by stopping the stirring briefly and removing a sample by a Pasteur pipette tip from the reaction mixture. Samples were analyzed by ^{1}H NMR.

General Procedure B: Reactions were set up as in General Procedure A, except that either a conical vial or a J. Young NMR tube was used for the reaction. In addition, during the reaction, rather than stirring, a nutator was used to agitate the mixture gently. In the cases where a J. Young NMR tube was used as reaction vessel, NMR spectra could be acquired directly, without the need to remove aliquots.

General Procedure C: Reactions were set up as in General Procedure A, except, the conical vial was immersed in an oil bath at 70°C and the reaction was stirred with a magnetic stirrer.

General Procedure D: Reactions were set up as in General Procedure A, except that either a conical vial or a J. Young NMR tube was used for the reaction. The conical vial or J. Young NMR tube was immersed in an oil bath at 70 ^{o}C. In the cases where a J. Young NMR tube was used as reaction vessel, NMR spectra could be acquired directly, without the need to remove aliquots.

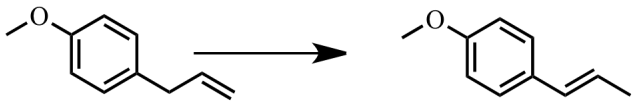

Figure 3.27. Isomerization of 4-allylanisole

Isomerization of 4-allylanisole with PS-1. General procedure B was followed using 4-allylanisole (74.0 mg, 0.50 mmol), **PS-1** (14.7 mg, 0.010 mmol, 2 mol %) and tetrakis(trimethylsilyl)methane (1.5 mg, 4.92 x 10^{-3} mmol). **Starting material** ^{1}H NMR (500 MHz, acetone-d_6) δ 7.10 (~d, AA' of AA'BB', J = 8.8 Hz, 2H), 6.85 (~d, BB' of AA'BB', J = 8.8 Hz, 2H), 5.94 (tdd, J = 6.8, 10.0, 16.8 Hz, 1H), 5.05 (tdd, J = 1.6, 2.0, 17.2 Hz, 1H), 5.00 (tdd, J = 1.2, 2.0, 10.0 Hz, 1H), 3.76 (s, 3H), 3.31 (d, J = 6.8 Hz, 2H). **Product (*E*)-Anethole** ^{1}H NMR at 96 h (500 MHz, acetone-d_6) δ 7.29 (~d, AA' of AA'BB', J = 9.2 Hz, 2H), 6.85 (~d, BB' of AA'BB', J = 8.8 Hz, 2H), 6.37-6.34 (m, 1H), 6.10 (bs, 1H), 3.77 (s, 3H), 1.80-1.75 (m, 2H).

Table 3.6. Isomerization of 4-allylanisole with PS-1

Time (min)	Starting material (%)	Product (%)
2	78.7	25.7
5	51.5	46.5
10	21.5	78.6
20	-	96.3

Isomerization of 4-allylanisole with PSL-1. General procedure B was followed using 4-allylanisole (74.1 mg, 0.50 mmol), **PSL-1** (15.5 mg, 0.010 mmol, 2 mol %) and tetrakis(trimethylsilyl)methane (1.3 mg, 4.26 x 10^{-3} mmol).

Table 3.7. Isomerization of 4-allylanisole with PSL-1

Time (min)	Starting material (%)	Product (%)
2	76.5	20.6
5	49.9	44.7
10	19.1	80.9
20	-	98.6

Isomerization of 4-allylanisole with 2.10. A J. Young NMR tube was charged with tetrakis(trimethylsilyl)methane (1.2 mg), 4-allyl anisole (22.5 mg, 0.15 mmol), in acetone-d_6 (about 0.8 mL). After acquisition of an initial spectrum to set the integral values, **2.10** (1.8 mg, 3.0 x 10^{-3} mmol, 2 mol %) was transferred quantitatively from a vial using acetone-d_6 in several portions into the J. Young NMR tube. Total reaction volume was adjusted to 1 mL by addition of acetone-d_6.

Table 3.8. Isomerization of 4-allylanisole with 2.10

Time (min)	Starting material (%)	Product (%)
10	-	99.2

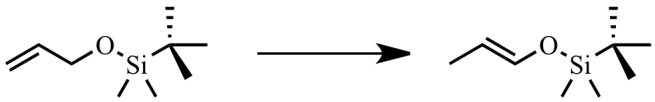

Figure 3.28. Isomerization of allyloxy(*tert*-butyl)dimethylsilane

Isomerization of allyloxy(*tert*-butyl)dimethylsilane with PS-1. General procedure B was followed using allyloxy(*tert*-butyl)dimethylsilane (87.4 mg, 0.51 mmol), **PS-1** (14.7 mg, 0.010 mmol, 2 mol %) and tetrakis(trimethylsilyl)methane (1.6 mg, 5.25 x 10^{-3} mmol). **Starting material** ^{1}H NMR (500 MHz, acetone-d_6) δ 5.92 (tdd, J = 4.4, 10.4, 17.2, 1H), 5.26 (tdd, J = 2.0, 2.0, 17.2, 1H), 5.04 (tdd, J = 1.6, 1.6, 10.4, 1H), (ddd, J = 1.4, 2.0, 4.4, 2H), 0.91 (s, 9H), 0.07 (s, 6H) **Product** ^{1}H NMR (500 MHz, acetone-d_6) δ 6.29 (qd, J = 1.7, 11.9, 1H), 4.94 (qd, J = 6.8, 11.8, 1H), 1.48 (dd, J = 1.6, 6.8, 3H), 0.91 (s, 9H), 0.12 (s, 6H).

Table 3.9. Isomerization of allyloxy(tert-butyl)dimethylsilane with PS-1

Time (min)	Starting material (%)	Product (%)
20	19.7	80.5
30	3.7	97.0
40	<1	97.1

Isomerization of allyloxy(*tert*-butyl)dimethylsilane with PSL-1. General procedure B was followed using allyloxy(*tert*-butyl)dimethylsilane (87.3 mg, 0.51 mmol), **PSL-1** (15.5 mg, 0.010 mmol, 2 mol %) and tetrakis(trimethylsilyl)methane (1.5 mg, 4.92 x 10^{-3} mmol).

Table 3.10. Isomerization of allyloxyallyloxy(tert-butyl)dimethylsilane with PSL-1

Time (min)	Starting material (%)	Product (%)
20	14.4	80.9
30	1.2	96.5
40	<1	97.3

Isomerization of allyloxy(*tert*-butyl)dimethylsilane with 2.10. A J. Young NMR tube was charged with tetrakis(trimethylsilyl)methane (1.0 mg, 3.28 x 10^{-3} mmol) and allyloxy(*tert*-butyl)dimethylsilane (26.1 mg, 0.15 mmol) in acetone-d_6 . After acquisition of an initial spectrum to set the integral values, **2.10** (1.9 mg, 3.1 x 10^{-3} mmol, 2 mol %) was transferred quantitatively from a vial using acetone-d_6 in several portions into the J. Young NMR tube. Total reaction volume was adjusted to 1.2 mL by addition of acetone-d_6.

Table 3.11. Isomerization of allyloxy(tert-butyl)dimethylsilane with 2.10

Time (min)	Starting material (%)	Isomer (%)
4	0.5	99.8

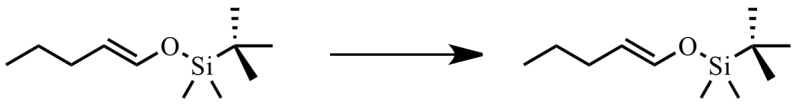

Figure 3.29. Isomerization of *tert*-butyldimethyl(pent-4-enyloxy)silane

Isomerization of *tert*-butyldimethyl(pent-4-enyloxy)silane with 5 mol% PS-1. General procedure D was followed using *tert*-butyldimethyl(pent-4-enyloxy)silane (100.2 mg, 0.50 mmol), **PS-1** (36.6 mg, 0.025 mmol, 5 mol %) and

tetrakis(trimethylsilyl)methane (2.5 mg, 8.20 x 10^{-3} mmol). **Starting material** ^{1}H NMR (500 MHz, acetone-d_6) δ 5.84 (tdd, J = 7.0, 10.0, 17.0, 1H), 4.99 (tdd, J = 1.5, 2.0, 17.0, 1H), 4.92 (tdd, J = 1.0, 2.5, 9.0, 1H), 3.64 (t, J = 6.0, 2H) 2.11 (~tdd, $^{4}J_{H1\text{-}H3}$ = 2.0 Hz, $^{3}J_{H2\text{-}H3}$ = $^{3}J_{H3\text{-}H4}$ = 7.4, 2H), 1.59 (tt, $^{3}J_{H4\text{-}H5}$ = 6.5 $^{3}J_{H3\text{-}H4}$ = 7.5, 2H), 0.90 (s, 9H), 0.05 (s, 6H). **Product** ^{1}H NMR (500 MHz, acetone-d_6) δ 6.29 (td, J = 1.5, 12.0, 1H), 4.94 (td, J = 7.5, 12.0, 1H), 1.86 (qd, J = 1.0, 7.2, 2H), 1.33 (td, J = 7.5, 14.5, 2H), 0.92 (s, 9H), 0.87 (t, J = 7.5, 3H), 0.13 (s, 6H).

Table 3.12. Isomerization of *tert*-butyldimethyl(pent-4-enyloxy)silane with 5 mol% PS-1

Time (h)	Starting material (%)	2- and 3-alkenes (%)	Enol ether (%)
2	7.0	63.4	19.9
5	1.5	50.0	37.8
15	<1	31.3	64.5
24	<1	15.4	70.5

Isomerization of *tert*-butyldimethyl(pent-4-enyloxy)silane with 5 mol% PSL-1. General procedure D was followed using *tert*-butyldimethyl(pent-4-enyloxy)silane (102.2 mg, 0.50 mmol), **PSL-1** (38.6 mg, 0.025 mmol, 5 mol %) and tetrakis(trimethylsilyl)methane (2.3 mg, 7.56 x 10^{-3} mmol).

Table 3.13. Isomerization of *tert*-butyldimethyl(pent-4-enyloxy)silane with 5 mol% PSL-1

Time (h)	Starting material (%)	2- and 3-alkenes (%)	Enol ether (%)
1	36.9	54.3	7.0
2	13.6	63.1	13.1
5	14.4	63.1	12.9
15	<1	38.4	46.8
24	<1	25.5	57.7

Isomerization of *tert*-butyldimethyl(pent-4-enyloxy)silane with 2 mol% PS-1. General procedure D was followed in a J. Young NMR tube using *tert*-butyldimethyl(pent-4-enyloxy)silane (30.8 mg, 0.15 mmol), **PS-1** (4.6 mg, 3.0 x 10^{-3} mmol, 2 mol %) and 1,4-dioxane (9.7 mg, 0.11 mmol).

Table 3.14. Isomerization of *tert*-butyldimethyl(pent-4-enyloxy)silane with 2 mol% PS-1

Time (h)	Starting material (%)	2-alkene (%)	3-alkene (%)	Enol ether (%)
1	13.0	72.5	9.5	8.7
2	9.0	74.6	11.5	15.1
5	3.9	61.4	10.2	28.8
24	1.9	33.8	2.6	60.2
48	0.7	19.2	3.4	71.0

Isomerization of *tert*-butyldimethyl(pent-4-enyloxy)silane with PSL-1. General procedure D was followed in a J. Young NMR tube using *tert*-butyldimethyl(pent-4-enyloxy)silane (33.5 mg, 0.17 mmol), **PSL-1** (5.2 mg, 3.4 x 10^{-3} mmol, 2 mol %) and 1,4-dioxane (8.8 mg, 0.099 mmol).

Table 3.15. Isomerization of *tert*-butyldimethyl(pent-4-enyloxy)silane with 2 mol% PSL-1

Time (h)	Starting material (%)	2-alkene (%)	3-alkene (%)	Enol ether (%)
1	47.0	46.4	4.8	1.3
2	25.4	61.1	7.2	9.1
5	11.1	68.7	9.5	16.4
24	2.8	56.7	9.4	33.8
48	1.6	38.0	6.9	51.7

Isomerization of *tert*-butyldimethyl(pent-4-enyloxy)silane with 2.10 as seen in reference 29 Table 1 entry 8.

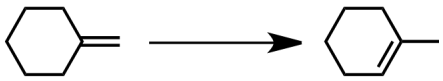

Figure 3.30. Isomerization of methylenecyclohexane

Isomerization of methylenecyclohexane with PS-1. General procedure D was followed using methylenecyclohexane (19.2 mg, 0.20 mmol), **PS-1** (5.8 mg, 4.0x10^{-3} mmol, 2 mol %) and 1,4-dioxane (10.6 mg, 0.12 mmol). **Starting material** ^{1}H NMR (500 MHz, acetone-d_6) δ 4.56 (t, J = 1 Hz, 2H), 2.09-2.12 (br m, 4H), 1.53 ppm (br s, 6H). **1-methyl-cyclohexene** in the mixture: ^{1}H NMR (500 MHz, acetone-d_6) δ 5.36 (qd, J = 2.0, 3.0,

1H), 1.96-1.91 (m, *J* = 2, 2H), 1.86-1.90 (br m, 2H), 1.57-1.62 (m, 5H), 1.49-1.55 ppm (m, 2H).

Table 3.16. Isomerization of methylenecyclohexane with PS-1

Time (h)	Starting material (%)	Isomer (%)
1	86.7	12.0
2	75.5	23.3
5	55.3	42.2
24	16.7	79.6
48	6.4	91.2
72	3.3	93.9

Isomerization of methylenecyclohexane with PSL-1. General procedure D was followed using methylenecyclohexane (19.7 mg, 0.21 mmol), **PSL-1** (6.2 mg, 4.0 x 10^{-3} mmol, 2 mol %) and tetrakis(trimethylsilyl)methane (10.3 mg, 0.12 mmol).

Table 3.17. Isomerization of methylenecyclohexane with PSL-1

Time (h)	Starting material (%)	Isomer (%)
1	87.7	10.6
2	78.6	19.0
5	65.0	32.3
24	33.2	62.2
48	16.3	78.6
72	9.8	83.9

Isomerization of methylenecyclohexane with 2.10. A J. Young NMR tube was charged with tetrakis(trimethylsilyl)methane (1.1 mg, 3.61 x 10^{-3} mmol) and methylenecyclohexane (20.9 mg, 0.22 mmol) in acetone-d_6 (about 1 mL). After acquisition of an initial spectrum to set the integral values, **2.10** (2.6 mg, 4.3 x 10^{-3} mmol, 2 mol %) was transferred quantitatively from a vial using acetone-d_6 in several portions into the J. Young NMR tube. Total reaction volume was adjusted to ca. 1.2 mL by addition of acetone-d_6.

Table 3.18. Isomerization of methylenecyclohexane with 2.10

Time (h)	Starting material (%)	Isomer (%)
1	2.4	98.0
2	1.1	99.2

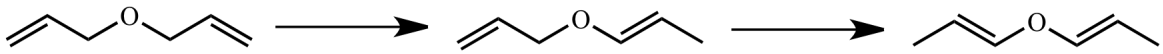

Figure 3.31. Isomerization of allyl ether

Isomerization of allyl ether with PS-1. General procedure A was followed using allyl ether (50.3 mg, 0.51 mmol), 1,4-dioxane (10.9 mg, 0.12 mmol), and **PS-1** (14.7 mg, 0.010 mmol, 2 mol%). **Starting material** ^{1}H NMR (400 MHz, acetone-d_6) δ 5.91 (tdd, J = 3.2, 12.8, 17.6 Hz, 2H), 5.27 (qd, J = 1.8, 17.2 Hz, 2H), 5.13 (qd, J = 1.4, 10.4 Hz, 2H), 3.97 (td, J = 1.6, 6.2 Hz, 4H). **Intermediate** ^{1}H NMR (400 MHz, acetone-d_6) δ 6.26 (dq, J = 1.6, 12.4 Hz, 1H), 5.31 (dq, J = 1.8, 17.4 Hz, 1H), 5.30 (tdd, J = 6.2, 10.4, 17.2 Hz, 1H), 5.17 (dq, J = 1.6, 10.4 Hz, 1H), 4.79 (dq, J = 6.8, 12.8 Hz, 1H), 4.18 (dt, J = 1.6, 5.2

Hz, 2H), 1.52 (dd, J = 1.6, 6.8 Hz, 3H). **Product** ^{1}H NMR (400 MHz, acetone-d_6) δ 6.32 (dq, J = 1.6, 12.2 Hz, 2H), 5.02 (dq, J = 6.8, 12.4 Hz, 2H), 1.55 (dd, J = 1.6, 6.8 Hz, 6H).

Table 3.19. Isomerization of allyl ether with PS-1

Time (h)	Starting material (%)	Intermediate (%)	Product (%)
1	1.2	46.7	53.1
2	-	17.9	79.8
5	-	-	97.4

Isomerization of allyl ether with PSL-1. General procedure A was followed using allyl ether (50.3 mg, 0.51 mmol), 1,4-dioxane (10.9 mg, 0.12 mmol), and **PSL-1** (15.5 mg, 0.010 mmol, 2 mol%).

Table 3.20. Isomerization of allyl ether with PSL-1

Time (min)	Starting material (%)	Intermediate (%)	Product (%)
1	1.5	46.2	52.4
2	-	16.7	81.8
5	-	-	98.6

Isomerization of allyl ether with 2.10 as seen in reference 29 Table 1 entry 2.

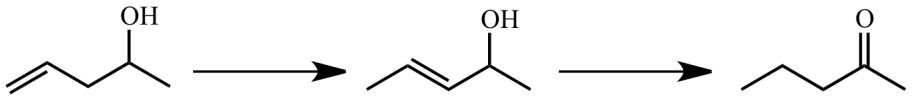

Figure 3.32. Isomerization of 4-penten-2-ol

Isomerization of 4-penten-2-ol with PS-1. General procedure C was followed using 4-penten-2-ol (86.2 mg, 1.00 mmol), **PS-1** (29.4 mg, 0.020 mmol, 2 mol %) and a few

crystals of tetrakis(trimethylsilyl)methane. **Starting material** ^{1}H NMR (400 MHz, acetone-d_6) δ 5.86 (tdd, J = 7.2, 10.0, 17.2, 1H), 5.03 (d, J = 17.5, 1H), 4.98 (d, J = 10.5, 1H), 3.76 (~ septet, $J \approx 6$, 1H), 3.49 (d, J = 4.8, 1H), 2.16 (ttd, J = 1.5, 6.5, 14, 2H), 1.11 ppm (d, J = 6.4, 3H). **Product 2-pentanone in mixture** (400 MHz, acetone-d_6) δ 2.41 (t, J = 7.2, 2H), 2.06 (s, 3H), 1.53 (sextet, J = 7.5, 2H), 0.87 ppm (t, J = 7.5, 3H).

Table 3.21. Isomerization of 4-penten-2-ol with PS-1

Time (h)	Starting material (%)	Isomer (%)	Ketone (%)
1	1	27	80
2	-	-	91.2

Isomerization of 4-penten-2-ol with PSL-1. General procedure C was followed using 4-penten-2-ol (86.2 mg, 1.00 mmol), **PSL-1** (31.0 mg, 0.020 mmol, 2 mol %) and a few crystals of tetrakis(trimethylsilyl)methane.

Table 3.22. Isomerization of 4-penten-2-ol with PSL-1

Time (h)	Starting material (%)	Isomer (%)	Ketone (%)
1	1.8	2.3	90

Isomerization of 4-penten-2-ol with 2.10 as seen in reference 29, Table 1 entry 7.

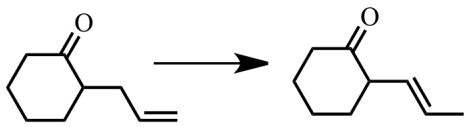

Figure 3.33. Isomerization of 2-allylcyclohexanone

Isomerization of 2-allylcyclohexanone with PS-1. General procedure D was followed using 2-allylcyclohexanone (29.6 mg, 0.21 mmol), **PS-1** (6.2 mg, 4.2x10^{-3} mmol, 2 mol %) and 1,4-dioxane (12.2 mg, 0.14 mmol). **Starting material** ^{1}H NMR (500 MHz, acetone-d_6): δ 5.78 (dddd, J = 6.0, 7.5, 10.0, 18.0, 1H), 5.00 (tdd, J = 2.0, 2.5, 17.5, 1H), 4.95 (tdd, J = 1.0, 1.0, 10, 1H), 2.44-2.50 (m, 1H), 2.33-2.43 (m, 2H), 2.28 (tddd, J = 1.5, 1.5, 1.5, 13, 1H), 2.08-2.14 (m, 1H), 2.00-2.04 (m, 1H), 1.90-1.97 (m, 1H), 1.81-1.87 (m, 1H), 1.57-1.76 (m, 2H), 1.32 ppm (dtd, J = 3.5, 12.5, 13.0, 1H). **2-(prop-2-en-1-yl)cyclohexan-1-one** in the mixture: ^{1}H NMR (500 MHz, acetone-d_6) δ 5.63 (qdd, J = 1.5, 7.0, 15.5,1H), 5.42 (dqd, J = 1.5, 6.5, 19.5, 1H), 2.99-3.03 (m, 1H), 2.24-2.36 (m, 2H), 1.95-2.06 (m, 2H), 1.82-1.88 (m, 1H), 1.66-1.78 (m, H), 1.65 (qd, J = 1.0, 6.5, 3H), 1.54-1.62 ppm (m, 1H).

Table 3.23. Isomerization of 2-allylcyclohexanone with PS-1

Time (h)	Starting material (%)	Isomerized product (%)
1	7.5	78.1
2	7.2	75.9[a]
23	5.3	60.8[a]
48	5.0	52.9[a]

[a] Further isomerization to α-β unsaturated ketone, 2-propylidenecyclohexanone is observed.

Isomerization of 2-allylcyclohexanone with PSL-1. General procedure D was followed using 2-allylcyclohexanone (29.4 mg, 0.21 mmol), **PSL-1** (6.8 mg, 4.4 x 10^{-3} mmol, 2 mol %) and tetrakis(trimethylsilyl)methane (11.4 mg, 0.13 mmol).

Table 3.24. Isomerization of 2-allylcyclohexanone with PSL-1

Time (h)	Starting material (%)	Isomerized product (%)
1	40.1	51.3
2	27.0	64.2
23	7.1	81.8
48	6.1	76.8[a]

[a] Further isomerization to α-β unsaturated ketone, 2-propylidenecyclohexanone is observed.

Isomerization of 2-allylcyclohexanone with 2.10. A J. Young NMR tube was charged with tetrakis(trimethylsilyl)methane (1.3 mg, 4.26 x 10^{-3} mmol), 2-allylcyclohexanone (28.2 mg, 0.20 mmol) in acetone-d_6 (about 1 mL). After acquisition of an initial spectrum to set the integral values, **2.10** (2.4 mg, 4.0 x 10^{-3} mmol, 2 mol %) was transferred quantitatively from a vial using acetone-d_6 in several portions into the J. Young NMR tube. Total reaction volume was adjusted to 1.2 mL by addition of acetone-d_6.

Table 3.25. Isomerization of 2-allylcyclohexanone with 2.10

Time (min)	Starting material (%)	Isomerized product (%)
8	38.7	60.6
20	13.8	84.3
30	7.1	90.0
45	5.8	91.6

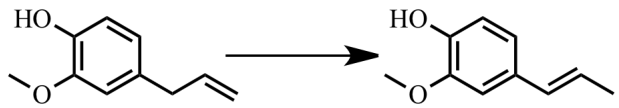

Figure 3.34. Isomerization of eugenol

Isomerization of eugenol with PS-1. General procedure B was followed using eugenol (24.8 mg, 0.15 mmol), 1,4-dioxane (5.1 mg, 0.058 mmol) and **PS-1** (2.0 mg, 1.4 x 10^{-3} mmol, 1 mol %). **Starting material eugenol** ^{1}H NMR (500 MHz, acetone-d_6) δ 7.26 (s, 1H), 6.78 (d, J = 2, 2H), 6.77 (d, *J* = 8, 1H), 6.64 (dd, *J* = 1.0, 8.0, 1H), 5.95 (tdd, *J* = 6.5, 10.5, 17.0, 1H), 5.06 (dtd, J = 1.5, 1.5, 17.0, 1H), 4.99 (tdd, J = 1.0, 2.5, 10.0, 1H), 3.81 (s, 3H), 3.29 ppm (d, *J* = 7, 2H). **(*E*)-isoeugenol** in the mixture: ^{1}H NMR (500 MHz, acetone-d_6) δ 7.43 (s, 1H), 6.99 (d, *J* = 2.0, 1H), 6.80 (dd, *J* = 2, 8, 1H), 6.74 (d, *J* = 8, 1H), 6.32 (dd, *J* = 1.5, 15.5, 1H), 6.11 (qd, *J* = 6.5, 15.5, 1H), 3.85 (s, 3H), 1.81 ppm (dd, *J* = 2, 7, 3H).

Table 3.26. Isomerization of eugenol with PS-1

Time (min)	Starting material (%)	Product (%)
5	57.0	40.2
10	37.7	62.1
20	12.1	88.7
30	4.3	93.2
45	<1.0	98.5

Isomerization of eugenol with PSL-1. General procedure B was followed using eugenol (25.1 mg, 0.15 mmol), 1,4-dioxane (5.2 mg, 0.059 mmol) and **PSL-1** (2.3 mg, 1.5 x 10^{-3} mmol, 1 mol %).

Table 3.27. Isomerization of eugenol with PSL-1

Time (min)	Starting material (%)	Product (%)
5	69.6	23.4
10	55.7	34.7
20	32.5	62.9
30	17.8	76.5
40	8.9	87.1
52	3.2	94.4

Isomerization of eugenol with 2.10. A J. Young NMR tube was charged with tetrakis(trimethylsilyl)methane (1.4 mg, 4.59 x 10^{-3} mmol), eugenol (25.7 mg, 0.16 mmol) in acetone-d_6 (about 1 mL). After acquisition of an initial spectrum to set the integral values, **2.10** (1.0 mg, 1.65 x 10^{-3} mmol, 1 mol %) was transferred quantitatively from a vial using acetone-d_6 in several portions into the J. Young NMR tube. Total reaction volume was adjusted to 1.0 mL by addition of acetone-d_6.

Table 3.28. Isomerization of eugenol with 2.10

Time (min)	Starting material	Isomer
4	-	98.8

Isomerization with PS-1 and PSL-1 under neat conditions

Neat isomerization of 4-penten-2-ol with PS-1. Using a 2 dram vial with Teflon-lined cap and 4-penten-2-ol (125.8 mg, 1.46 mmol) was mixed with few drops of 1,4-dioxane. A small sample (<3 μL) was removed by capillary action into the tip of a Pasteur pipette and the sample was analyzed in acetone-d_6 to get an initial ^{1}H NMR spectrum to set the integral values. **PS-1** (44.6 mg, 0.020 mmol, 2 mol %) was added and vial was sealed and immersed in an oil bath at 70°C. The progress of the reaction was monitored by taking the vial inside the glovebox and removing a sample by a Pasteur pipette tip from the reaction mixture. Then the conical vial was returned to oil bath. Samples were analyzed in acetone-d_6 by ^{1}H NMR, see Table 3.29.

Table 3.29. Neat isomerization of 4-penten-2-ol with PS-1

Time (h)	Starting material (%)	2- and 3-alkenes (%)	Product (%)
1	79.0	35.7	2.2
2	27.6	63.8	19.9
3	6.1	30.6	63.4
5	2.3	3.9	90.8
18	1.8	3.0	92.5

Neat isomerization of 4-penten-2-ol with PSL-1. The procedure described above was carried out with 4-penten-2-ol (124.9 mg, 1.45 mmol), a few drops of 1,4-dioxane and **PSL-1** (46.6 mg, 0.020 mmol, 2 mol %).

Table 3.30. Neat isomerization of 4-penten-2-ol with PSL-1

Time (h)	Starting material (%)	2- and 3-alkenes (%)	Product (%)
1	8.8	13.3	77.5
2	4.8	1.0	90.7

Neat isomerization of eugenol with PS-1. Using a 2 dram vial with Teflon-lined cap, eugenol (167.1 mg, 1.0 mmol) was mixed with 1,4-dioxane (21.0 mg, 0.24 mmol). A small sample (<3 μL) was removed by capillary action into the tip of a Pasteur pipette and the sample was analyzed in acetone-d_6 to get an initial ^{1}H NMR spectrum to set the integral values. **PS-1** (14.5 mg, 0.010 mmol, 1 mol %) was added and vial was sealed and placed on a nutator. Progress of the reaction was monitored by stopping the nutator briefly and removing a sample by a Pasteur pipette tip from the reaction mixture. Samples are analyzed in acetone-d_6 by ^{1}H NMR and progress of isomerization specified is tabulated**.**

Table 3.31. Neat isomerization of eugenol with PS-1

Time (min)	Starting material (%)	Product (%)
2	96.6	1.9
5	75.1	20.4
24	-	>99.9

Neat isomerization of eugenol with PSL-1. The procedure described above was carried out with eugenol (165.5 mg, 1.0 mmol), 1,4-dioxane (26.3 mg, 0.3 mmol), and **PSL-1** (16.1 mg, 0.010 mmol, 1 mol %).

Table 3.32. Neat isomerization of eugenol with PSL-1

Time (min)	Starting material (%)	Product (%)
2	95.3	8.4
5	20.2	80.8
24	-	>99.9

Neat isomerization of 2-allylcyclohexanone with PS-1. Using a 2 dram vial with Teflon-lined cap, 2-allylcyclohexanone (140.4 mg, 1.0 mmol) was mixed with 1,4-dioxane (12.6 mg, 0.14 mmol). A small sample (<3 μL) was removed by capillary action into the tip of a Pasteur pipette and the sample was analyzed in acetone-d_6 to get an initial ^{1}H NMR spectrum to set the integral values. **PS-1** (16.5 mg, 0.010 mmol, 1 mol %) was added and vial was sealed and immersed in an oil bath at 70°C. Progress of the reaction was monitored by taking the vial inside the glovebox and removing a sample by a Pasteur pipette tip from the reaction mixture. Then conical vial is returned to oil bath. Samples are analyzed in acetone-d_6 by ^{1}H NMR and progress of isomerization specified is tabulated.

Table 3.33. Neat isomerization of 2-allylcyclohexanone with PS-1

Time (min)	Starting material (%)	Product (%)
1	13.8	82.3
2	9.3	86.0
5	9.1	90.3
24	6.7	70.4[a]

[a] Further isomerization to α, β unsaturated ketone, 2-propylidenecyclohexanone is observed.

Neat isomerization of 2-allylcyclohexanone with PSL-1. The procedure described above was carried out with 2-allylcyclohexanone (141.4 mg, 1.0 mmol) mixed with 1,4-dioxane (12.4 mg, 0.14 mmol), and **PS-1** (16.7 mg, 0.010 mmol, 1 mol %).

Table 3.34. Neat isomerization of 2-allylcyclohexanone with PSL-1

Time (min)	Starting material (%)	Product (%)
1	12.6	82.6
2	9.4	91.8
5	8.7	99.0
24	7.6	66.0[a]

[a] Further isomerization to α, β unsaturated ketone, 2-propylidenecyclohexanone is observed.

Sequential isomerization and metathesis reactions

Silica-supported 2nd generation Grubbs-Hoveyda catalyst[41] was prepared according to literature in gram scale.

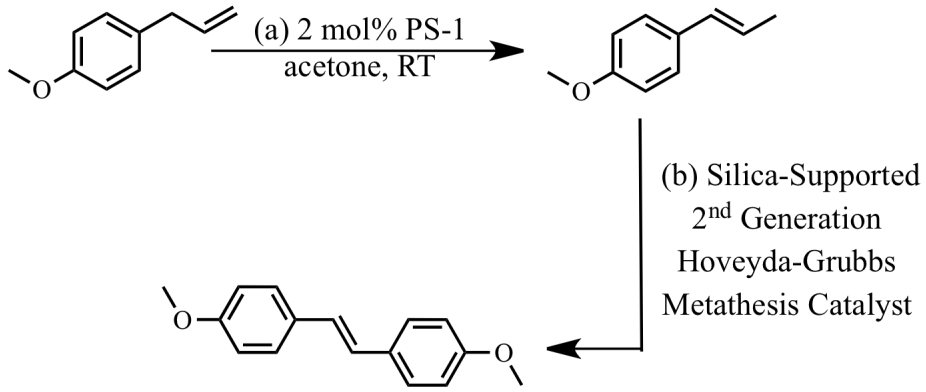

Figure 3.35. Sequential isomerization and metathesis of 4-allylanisole

Conversion of 4-allylanisole (run 1): In the glovebox, a J-Young NMR tube was charged with **PS-1** (8.9 mg, 6.0×10^{-3} mmol, 2 mol%) and acetone-d_6 was added to swell the polymer supported catalyst. In a separate vial, 4-allylanisole (45.3 mg, 0.31 mmol) and tetrakis(trimethylsilyl)methane (1.0 mg, 3.28×10^{-3} mmol) were dissolved in acetone-d_6. A small sample (<3 μL) was removed by capillary action into the tip of a Pasteur pipette and the sample was analyzed in acetone-d_6 to get an initial ^{1}H NMR spectrum to set the integral values using tetrakis(trimethylsilyl)methane as internal standard. The solution of substrate and internal standard was quantitatively transferred to the J. Young NMR tube using portions of acetone-d_6. The reaction was mixed by a nutator at room temperature. Analysis of an aliquot by ^{1}H NMR spectroscopy confirmed completion of the reaction.

After complete isomerization to (*E*)-anethole, in the glovebox, the reaction solution was decanted through a Pasteur pipette containing a cotton and silica plug into a

pre-weighed scintillation vial. The J. Young NMR tube was washed with additional acetone (1 mL x 3) and washings were run through the plug. The plug was washed with acetone and hexanes (1 mL each). Solvents were reduced under vacuum (45.1 mg recovered). Additional tetrakis(trimethylsilyl)methane (1.6 mg, 5.25 x 10^{-3} mmol) was weighed in the scintillation vial as internal standard and all material dissolved in hexanes (0.4 mL). A small sample (<3 μL) was removed by capillary action into the tip of a Pasteur pipette and the sample was analyzed in acetone-d_6 to get an initial ^{1}H NMR spectrum to set the integral values using tetrakis(trimethylsilyl)methane as internal standard. Another scintillation vial was charged with silica-supported 2nd generation Grubbs-Hoveyda catalyst[6] (201.9 mg, 0.65 mol % Ru), hexanes (0.6 mL) and equipped with magnetic stir bar. The solution of (*E*)-anethole with tetrakis(trimethylsilyl)methane was quantitatively transferred with portions of hexanes to the scintillation vial, giving a total reaction volume of 5 mL. The scintillation vial was sealed and immersed in oil bath at 70 °C outside the glovebox overnight (14h). After the scintillation vial was cooled to room temperature, 0.1 mL was removed from the reaction solution inside the glovebox. After reducing the solvents under vacuum, acetone-d_6 was added as NMR solvent. ^{1}H NMR analysis showed 91.0 % metathesis product along with observation of 9.0% (*E*)-anethole.

Conversion of 4-allylanisole (run 2, isolated): A second experiment was performed in the same way as the first, alkene isomerization conditions are kept the same but higher catalytic loading and shorter time was used to achieve metathesis reaction. **PS-1** (8.7 mg, 6.0 x 10^{-3} mmol, 2 mol%), 4-allylanisole (47.1 mg, 0.32 mmol), and tetrakis(trimethylsilyl)methane (2.1 mg, 6.89 x 10^{-3} mmol).

(*E*)-anethole was obtained (40.5 mg, 86.0 %), which was then treated with silica-supported 2nd generation Grubbs-Hoveyda catalyst (1006.8 mg, 9.96 x 10^{-3} mmol, 3.1 mol% Ru). After 2 h at 70 °C, analysis of an aliquot by ^{1}H NMR spectroscopy revealed 87.8 % metathesis (and 12.2 % starting material left).

The metathesis product was isolated as a white solid (24.1 mg, 73.5 % yield by mass). ^{1}H NMR (400 MHz, chloroform-*d*) δ 7.44 (d, *J* = 8.8, 4H), 6.94 (s, 2H), 6.90 (d, *J* = 8.8, 4H), 3.84 (s, 6H). Data were similar to the reported ^{1}H NMR spectrum of (*E*)-4,4'-dimethoxystilbene.[55-57]

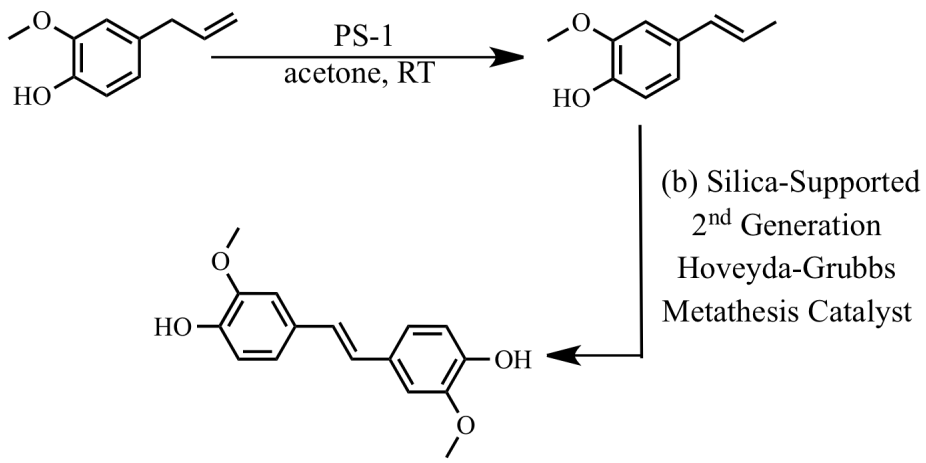

Figure 3.36. Sequential isomerization and metathesis of eugenol

Conversion of eugenol: In the glovebox, a J. Young NMR tube was charged with **PS-1** (10.3 mg, 7.0x10^{-3} mmol, 2 mol%) and acetone-d_6 was added to swell the polymer supported catalyst. In a separate vial, eugenol (48.8 mg, 0.30 mmol) and tetrakis(trimethylsilyl)methane (1.2 mg, 3.94 x 10^{-3} mmol) were dissolved in acetone-d_6. A small sample (<3 μL) was removed by capillary action into the tip of a Pasteur pipette and the sample was analyzed in acetone-d_6 to get an initial ^{1}H NMR spectrum to set the integral values using tetrakis(trimethylsilyl)methane as internal standard. The solution of

substrate and internal standard is quantitatively transferred to the J. Young NMR tube using portions of acetone-d_6. The reaction is mixed by a nutator at room temperature. Analysis of an aliquot by ^{1}H NMR spectroscopy confirmed completion of the reaction. After complete isomerization to (*E*)-isoeugenol, in the glovebox, the reaction solution was decanted through a Pasteur pipette containing a cotton and silica plug into a pre-weighed scintillation vial. The J. Young NMR tube was washed with additional acetone (3 x 1 mL) and washings were run through the plug. The plug was washed with acetone and hexanes (1 mL each). Solvents were reduced under vacuum (51.6 mg recovered, solvent present by ^{1}H NMR analysis).

After addition of hexanes (0.4 mL), a small sample (<3 μL) was removed by capillary action into the tip of a Pasteur pipette and the sample was analyzed in acetone-d_6 to get an initial ^{1}H NMR spectrum to set the integral values using tetrakis(trimethylsilyl)methane as internal standard. Another scintillation vial was charged with silica-supported 2nd generation Grubbs-Hoveyda catalyst (298.4 mg, 2.95 x 10^{-3} mmol Ru, 1.0 mol % Ru), hexanes (0.6 mL) and equipped with magnetic stir bar. The solution of (*E*)-isoeugenol with tetrakis(trimethylsilyl)methane was quantitatively transferred with portions of hexanes to the scintillation vial. Total reaction volume is 5 mL. The scintillation vial was sealed and immersed in oil bath at 70 °C outside the glovebox overnight. After the scintillation vial was cooled to room temperature, 0.1 mL was removed from the reaction solution inside the glovebox. After reducing the solvents under vacuum, acetone-d_6 was added as NMR solvent. ^{1}H NMR spectroscopic analysis showed 95.9 % metathesis product along with observation of 4.1 % (*E*)-isoeugenol. ^{1}H NMR (500 MHz, benzene-d_6) δ 7.03 (d, J = 7.5, 2H), 7.00 (dd, J = 8.0, 1.5, 2H), 6.94 (s,

2H), 6.83 (d, J = 2.0, 2H), 5.48 (s, 2H), 3.21 (s, 6H). Data were in accordance with those previously reported.[43,55-58] ^{1}H NMR (400 MHz, chloroform-*d*) 7.02 (d, J = 8.8, 4H), 7.19 (s, 2H), 7.07 (d, J = 8.8, 4H), 3.95 (s, 6H).

Isolation of the eugenol possibly resulted in oxidation of the OH moiety suggested by color change of the silica from green to deep red-brown and observance of additional olefinic peaks around 5.8 and 4.9 ppm along with several new aromatic peaks and OCH_3 peaks in ^{1}H NMR spectrum.

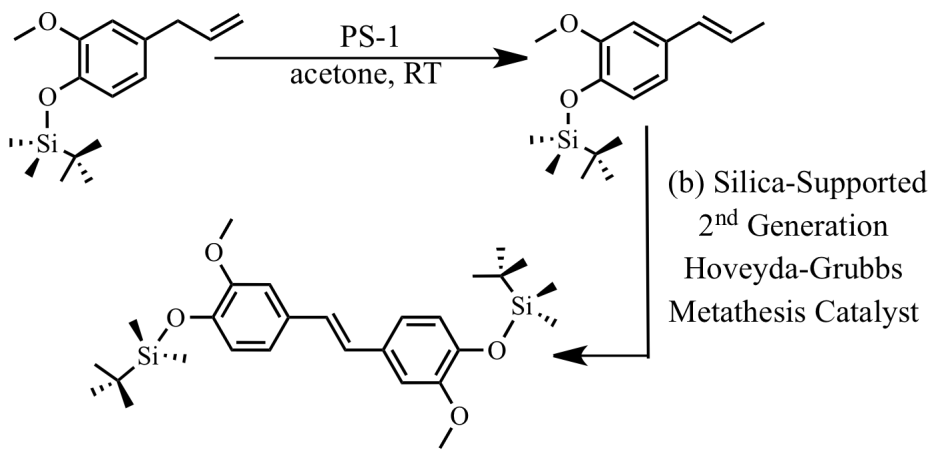

Figure 3.37. Sequential isomerization and metathesis of protected eugenol, (4-allyl-2-methylphenoxy)(*tert*-butyl)dimethylsilane

Conversion of protected eugenol, (4-allyl-2-methoxyphenoxy)(*tert*-butyl)dimethylsilane: In the glovebox, a J. Young NMR tube is charged with **PS-1** (6.4 mg, 4.4 x 10^{-3} mmol, 2.2 mol%) and acetone-d_6 were added to swell the polymer supported catalyst. In a separate J. Young tube (4-allyl-2-methoxyphenoxy)(*tert*-butyl)dimethylsilane (56.3 mg, 0.20 mmol) and tetrakis(trimethylsilyl)methane (2.1 mg, 6.89 x 10^{-3} mmol) were dissolved in about 1.0 mL acetone-d_6**.** This sample was analyzed in acetone-d_6 to get an initial ^{1}H NMR spectrum to set the integral values using tetrakis(trimethylsilyl)methane as internal standard. The solution of substrate and internal

standard was quantitatively transferred to the J. Young NMR tube using portions of acetone-d_6. The reaction was mixed by a nutator at room temperature. Analysis of an aliquot by ^{1}H NMR spectroscopy confirmed completion of the reaction.

After complete isomerization to protected (*E*)-isoeugenol, in the glovebox, the reaction solution was decanted through a Pasteur pipette containing a cotton and silica plug into a pre-weighed scintillation vial. The J. Young NMR tube was washed with additional acetone (3 x 1 mL) and washings were run through the plug. The plug was washed with acetone and hexanes (1 mL each). Solvents were reduced under vacuum (54.3 mg, 96.5% yield recovered).

After addition of hexanes (0.4 mL), a small sample (<3 μL) was removed by capillary action into the tip of a Pasteur pipette and the sample was analyzed in acetone-d_6 to get an initial ^{1}H NMR spectrum to set the integral values using tetrakis(trimethylsilyl)methane as internal standard. Another scintillation vial was charged with silica-supported 2nd generation Grubbs-Hoveyda catalyst (968.3 mg, 9.6 x 10^{-3} mmol Ru, 4.8 mol % Ru), hexanes (3 mL) and equipped with magnetic stir bar. The solution of protected (*E*)-isoeugenol with tetrakis(trimethylsilyl)methane was quantitatively transferred with portions of hexanes to the scintillation vial, giving a total reaction volume is 10 mL. The scintillation vial was sealed and immersed in oil bath at 60 °C outside the glovebox overnight. After the scintillation vial was cooled to room temperature, the reaction solution was decanted through a Pasteur pipette containing a cotton and silica plug into a pre-weighed vial. The reaction vial and silica-supported 2nd generation Grubbs-Hoveyda catalyst were washed with warm toluene (3 x 5 mL) and washings were run through the plug. Solvents were reduced under vacuum to give final

product as yellow liquid. (43.6 mg, 87.0 % yield).

^{1}H NMR (500 MHz, chloroform-*d*) δ 7.01 (d, *J* = 2.0, 2H), 6.96 (dd, *J* = 2.0, 8.0, 2H), 6.91 (s, 2H), 6.83 (d, *J* = 8.0, 2H), 3.87 (s, 6H), 1.01 (s, 18H).

Data were similar to the reported ^{1}H NMR spectrum of (*E*)-4,4'-dihydroxy-3,3'-dimethoxystilbene. [43,55-58]

Catalyst recycling and ruthenium leaching experiments performed with eugenol

The experiment is designed on the basis that Ru concentration is reliably detected in the range of 1-10 ppm after the ICP-OES is calibrated with Ru standards (10, 1, and 0.1 ppm Ru) prepared from $RuCl_3.xH_2O$ (42.43% Ru) with aqueous 2% HCl solution. ICP-OES measurements were obtained on Perkin Elmer DV-4300 ICP-OES with Meinhardt C nebulizer with a cyclonic spray chamber. The method used was power 1500 W, axial view, plasma flow 15 L/min, auxiliary flow 0.2 min/L, nebulizer flow 0.8 L/min and sample flow 1.50 mL/min. Readings were taken at 240.272, 349.894 and 279.535 nm.

The ruthenium content of the combined filtrates and washes (5) was determined by inductively coupled plasma optical emission spectroscopy (ICP-OES) analysis.

Table 3.35. Amount of starting material and internal standard used for recycling experiments

	PS-1		PSL-1	
Cycle #	**Eugenol (mg)**	**1,4-Dioxane (mg)**	**Eugenol (mg)**	**1,4-Dioxane (mg)**
I	123.3	19.1	123.4	29.5
II	123.2	20.5	123.5	27.1
III	123.2	22.1	123.3	28.2
IV	123.4	23.4	123.2	26.2
V	123.3	22.8	123.4	26.2

In the glovebox, immobilized catalyst (**PS-1** 11.1 mg, **PSL-1** 11.5 mg, 7.5×10^{-3} mmol, 1 mol%) was weighed in a conical vial and acetone was added to swell the polymer-supported catalyst. In separate vials, eugenol and 1,4-dioxane (Table 3.35) was added as internal standard. Acetone (0.5 mL) was added to ensure complete dissolution of all material. A small sample (<3 μL) was removed by capillary action into the tip of a Pasteur pipette and the sample was analyzed in acetone-d_6 to get initial ^{1}H NMR spectra to set the integral values. The solution of substrate and internal standard for *cycle I* was added to the conical vial. The substrate vial was washed with additional acetone and washings were added to conical vial. The reaction volume was adjusted to 5 mL. The reaction was mixed by a nutator at room temperature. After the isomerization reaction (1 h for **PS-1**, 1.5 h for **PSL-1**) the solution was moved from the conical vial to a scintillation vial. A sample (0.1 mL) was placed in an NMR tube and acetone-d_6 was added as NMR solvent, and the resulting sample was analyzed by ^{1}H NMR spectroscopy to give the values in Table 3.36. **PS-1** was washed in the conical vial with additional

acetone and the washings were added to the scintillation vial for the same cycle. The residual **PS-1** was dried in a conical vial under reduced pressure with oil-pump vacuum for about 45 min. The solution of substrate and internal standard for *cycle II* was added to the conical vial and the consecutive cycles were performed as just described.

The ruthenium leaching into the organic phase was determined by ICP. Acetone solutions from the scintillation vials were reduced under vacuum to a volume of approximately 0.2 mL and transferred to thick-walled and flame cut glass tubes. The solutions were further concentrated under oil-pump vacuum to dryness. To the residue was added 20 drops of concentrated HCl while cooling in an ice-water bath. Each tube was placed under vacuum in liquid nitrogen and after the contents were frozen, the tube was flame-sealed. After reaching room temperature, the flame-sealed tubes were immersed in an oil bath at 80 °C overnight. After cooling to room temperature, the glass tubes were scored with a glasscutter and snapped in two, and the contents were filtered through a cotton plug into a 5 mL volumetric flask. The glass tubes were washed with DI H_2O in portions and the washings are added to the respective volumetric flasks. Aqueous samples from each cycle were analyzed by ICP-OES.

Table 3.36. Isomerization activity from recycling experiments with PS-1 and PSL-1

	PS-1		**PSL-1**	
Cycle #	**% Eugenol**	**% *E*-Isoeugenol**[a]	**% Eugenol**	**% *E*-Isoeugenol**[a]
I	0.6	98.1	6.1	97.5
II	0.9	99.4	2.1	95.8
III	0.3	99.9	4.6	97.7
IV	0.2	98.4	2.9	97.8
V	0.2	97.1	9.5	94.9

[a] Percent yield calculated from ^{1}H NMR

Results of these analyses show that 1.04 % of the initial 1% rutheunium loading was lost after 5 cycles without any significant reduction in activity when **PS-1** is used as the catalyst. In other words, because 11.1 mg **PS-1** contains 7.57 x 10^{-3} mmol Ru, and 7.86 x 10^{-5} mmol Ru was leached to the organic phase, therefore 1.04 % Ru was lost over 5 cycles. Extrapolating these results, if 1 g eugenol were used for isomerization, in the first cycle, 43.8 µg Ru would be present in 1 g (*E*)-isoeugenol.

Table 3.37. Ruthenium leaching from recycling experiments performed with PS-1 and PSL-1

	PS-1	**PSL-1**
Cycle #	**[Ru] (ppm)** [b]	**[Ru] (ppm)** [b]
I	1.08	0.41
II	0.51	0.33
III	0.17	0.06
IV	0.11	0.12
V	0.07	0.61

[b] Ru concentration from ICP-OES

Table 3.38. Leaching in mass ruthenium per cycle with PS-1

PS-1				
Cycle #	**Eugenol (mg)**	**[Ru] (ppm)**	**Ru in 5 mL sample**	**Ru in 5 mL sample**
I	123.3	1.08	5.40 µg	5.34 x 10^{-5} mmol
II	123.2	0.51	2.55 µg	2.52 x 10^{-5} mmol
III	123.2	0.17	0.85 µg	8.41 x 10^{-6} mmol
IV	123.4	0.11	0.55 µg	5.44 x 10^{-6} mmol
V	123.3	0.07	0.34 µg	3.36 x 10^{-6} mmol
Total	616.4		9.69 µg	7.86 x 10^{-5} mmol

- ppm = mg/L

REFERENCES

(1) Hartley, F. R. *Supported metal complexes : a new generation of catalysts*; D. Reidel ; Sold and distributed in the U.S.A. and Canada by Kluwer Academic Publishers: Dordrecht ; Boston Hingham, MA, U.S.A., 1985.

(2) Sheldon, R. A. *Chemtech* **1994**, *24*, 38.

(3) Iwasawa, Y. *Tailored metal catalysts*; D. Reidel Pub. Co. ; Sold and distributed in the U.S.A. and Canada by Kluwer Academic Publishers: Dordrecht ; Boston Hingham, MA, U.S.A., 1986.

(4) Ermakov, I. U. I.; Kuznet´s˘ov, B. N.; Zakharov, V. A. *Catalysis by supported complexes*; Elsevier Scientific Pub. Co. ; Distributors for the United States and Canada, Elsevier North-Holland: Amsterdam ; New York New York, 1981.

(5) Whitehurst, D. D. *Chemtech* **1980**, *10*, 44.

(6) Merrifield, R. B. *J Am Chem Soc* **1963**, *85*, 2149.

(7) McNamara, C. A.; Dixon, M. J.; Bradley, M. *Chemical Reviews* **2002**, *102*, 3275.

(8) Cole-Hamilton, D. J. *Science* **2003**, *299*, 1702.

(9) Font, D.; Jimeno, C.; Pericas, M. A. *Org Lett* **2006**, *8*, 4653.

(10) Font, D.; Bastero, A.; Sayalero, S.; Jimeno, C.; Pericas, M. A. *Org Lett* **2007**, *9*, 1943.

(11) Alza, E.; Rodriguez-Escrich, C.; Sayalero, S.; Bastero, A.; Pericas, M. A. *Chem-Eur J* **2009**, *15*, 10167.

(12) Hu, Y. H.; Porco, J. A.; Labadie, J. W.; Gooding, O. W.; Trost, B. M. *J Org Chem* **1998**, *63*, 4518.

(13) Grela, K.; Tryznowski, M.; Bieniek, M. *Tetrahedron Lett* **2002**, *43*, 9055.

(14) Tooley, P. A.; Arndt, L. W.; Darensbourg, M. Y. *J Am Chem Soc* **1985**, *107*, 2422.

(15) Markovic, D.; Varela-Alvarez, A.; Sordo, J. A.; Vogel, P. *J Am Chem Soc* **2006**, *128*, 7782.

(16) Kaskel, S.; Schlichte, K. *J Catal* **2001**, *201*, 270.

(17) Ono, Y.; Baba, T. *Catal Today* **1997**, *38*, 321.

(18) Harmer, M. A.; Sun, Q.; Vega, A. J.; Farneth, W. E.; Heidekum, A.; Hoelderich, W. F. *Green Chem* **2000**, *2*, 7.

(19) Coleto, I.; Roldan, R.; Jimenez-Sanchidrian, C.; Gomez, J. P.; Romero-Salguero, F. J. *Catal Today* **2010**, *149*, 275.

(20) Gee, J. C.; Chevron Phillips Chemical Company LP, USA . 2009, p 10 pp.

(21) Cano, M. L.; Doll, M. J.; Garza, H.; Springer, R. B.; Worstell, J. H.; Shell Oil Company, USA; Shell International Research Maatschappij B.V. . 2008, p 22pp.

(22) Koenigsmann, L.; Schwab, E.; Hahn, T.; Kons, G.; BASF SE, Germany . 2011, p 15pp.

(23) Iselborn, S.; Heidemann, T.; Basf Se, Germany . 2009, p 34pp.

(24) Tang, H. G.; Sherrington, D. C. *J Mol Catal* **1994**, *94*, 7.

(25) Freeman, M. B.; Patrick, M. A.; Gates, B. C. *J Catal* **1982**, *73*, 82.

(26) Motoyama, Y.; Abe, M.; Kamo, K.; Kosako, Y.; Nagashima, H. *Chem Commun* **2008**, 5321.

(27) Augustine, R. L.; Jiwan, L. *J Mol Catal* **1986**, *37*, 189.

(28) Lau, C. P.; Chang, B. H.; Grubbs, R. H.; Brubaker, C. H. *J Organomet Chem* **1981**, *214*, 325.

(29) Bergbreiter, D. E.; Parsons, G. L. *J Organomet Chem* **1981**, *208*, 47.

(30) Baxendale, I. R.; Lee, A. L.; Ley, S. V. *Synlett* **2001**, 1482.

(31) Baxendale, I. R.; Lee, A. L.; Ley, S. V. *J Chem Soc Perk T 1* **2002**, 1850.

(32) Baxendale, I. R.; Lee, A. L.; Ley, S. V. *Synlett* **2002**, 516.

(33) Grotjahn, D. B.; Larsen, C. R.; Gustafson, J. L.; Nair, R.; Sharma, A. *J Am Chem Soc* **2007**, *129*, 9592.

(34) Larsen, C. R. M., C. E.; Grotjahn, D. B.; Rheingold, A. L. in progress.

(35) Annis, D. A.; Jacobsen, E. N. *J Am Chem Soc* **1999**, *121*, 4147.

(36) Baleizao, C.; Gigante, B.; Garcia, H.; Corma, A. *J Catal* **2003**, *215*, 199.

(37) Clark, J. H.; Macquarrie, D. J. *Handbook of green chemistry and technology*; Blackwell Science: Oxford ; Malden, MA, 2002.

(38) Ferre-Filmon, K.; Delaude, L.; Demonceau, A.; Noels, A. F. *Eur J Org Chem* **2005**, 3319.

(39) Jang, M.; Cai, L.; Udeani, G. O.; Slowing, K. V.; Thomas, C. F.; Beecher, C. W.; Fong, H. H.; Farnsworth, N. R.; Kinghorn, A. D.; Mehta, R. G.; Moon, R. C.; Pezzuto, J. M. *Science* **1997**, *275*, 218.

(40) Rayne, S.; Goss, C. D.; Forest, K.; Friesen, K. J. *Med Chem Res* **2010**, *19*, 864.

(41) Van Berlo, B.; Houthoofd, K.; Sels, B. F.; Jacobs, P. A. *Adv Synth Catal* **2008**, *350*, 1949.

(42) Jinesh, C. M.; Rives, V.; Carriazo, D.; Antonyraj, C. A.; Kannan, S. *Catal Lett* **2010**, *134*, 337.

(43) Yang, L. R.; Mayr, M.; Wurst, K.; Buchmeiser, M. R. *Chem-Eur J* **2004**, *10*, 5761.

(44) Keraani, A.; Fischmeister, C.; Renouard, T.; Le Floch, M.; Baudry, A.; Bruneau, C.; Rabiller-Baudry, M. *Journal of Molecular Catalysis A: Chemical* **2012**, *357*, 73.

(45) Brennan, M. *A practical approach to quantitative metal analysis of organic matrices*; Wiley: Chichester, U.K., 2008.

(46) Hodge, P.; Sherrington, D. C. *Polymer-supported reactions in organic synthesis*; J. Wiley: Chichester ; New York, 1980.

(47) Haag, R.; Roller, S. *Top Curr Chem* **2004**, *242*, 1.

(48) Datta, A.; Ebert, K.; Plenio, H. *Organometallics* **2003**, *22*, 4685.

(49) Malanga, M. *Adv Mater* **2000**, *12*, 1869.

(50) Shin, J.; Jensen, S. M.; Ju, J.; Lee, S.; Xue, Z.; Noh, S. K.; Bae, C. *Macromolecules* **2007**, *40*, 8600.

(51) Shin, J.; Bertoia, J.; Czerwinski, K. R.; Bae, C. *Green Chem* **2009**, *11*, 1576.

(52) Desrochers, P. J.; Duong, D. S.; Marshall, A. S.; Lelievre, S. A.; Hong, B.; Brown, J. R.; Tarkka, R. M.; Manion, J. M.; Holman, G.; Merkert, J. W.; Vicic, D. A. *Inorg Chem* **2007**, *46*, 9221.

(53) Pinchuk, A. N.; Rampy, M. A.; Longino, M. A.; Skinner, R. W. S.; Gross, M. D.; Weichert, J. P.; Counsell, R. E. *J Med Chem* **2006**, *49*, 2155.

(54) De Feyter, S.; Abdel-Mottaleb, M. M. S.; Schuurmans, N.; Verkuijl, B. J. V.; van Esch, J. H.; Feringa, B. L.; De Schryver, F. C. *Chem-Eur J* **2004**, *10*, 1124.

(55) Mali, R. S.; Jagtap, P. G. *Synthetic Commun* **1991**, *21*, 841.

(56) Andrus, M. B.; Mendenhall, K. G.; Meredith, E. L.; Sekhar, B. B. V. S. *Tetrahedron Lett* **2002**, *43*, 1789.

(57) Andrus, M. B.; Song, C.; Zhang, J. Q. *Org Lett* **2002**, *4*, 2079.

(58) Warner, P.; Sutherland, R. *J Org Chem* **1992**, *57*, 6294.

CHAPTER 4

MILD AND SELECTIVE HYDROGEN / DEUTERIUM EXCHANGE AT ALLYLIC POSITIONS OF OLEFINS

INTRODUCTION

Deuterium- and tritium-labeled compounds are widely used as research tools in studies of drug metabolism, reaction mechanisms and kinetics, and structural elucidation of biological macromolecules, among other purposes.[1] The heavy isotopes of hydrogen can be introduced either using multistep syntheses or by catalyzed exchange. The former strategy involves several synthetic operations with labeled material. In contrast, catalyzed exchange of hydrogen for deuterium or tritium is very attractive because it can be done in one step, with existing unlabeled material, therefore, selective C-H bond activation by metal complexes under mild conditions is a major area of research.[2,3] Most of the methods investigated require drastic conditions like high temperature and/or high pressure (in conditions where D_2 is the source of deuterium), acidic or basic additives.

The great challenge for catalyzed exchange is regio- and chemoselectivity and functional group tolerance. Methods that label regioselectively with high efficiency using either deuterium or tritium oxide are especially attractive because of the low cost and toxicity of the labeling reagent.[3] The H/D exchange of aromatic and aliphatic C-H bonds have been investigated with various methods including acid, base and metal catalysis. Garnett and co-workers reported one of the first examples in this area and demonstrated exchange of aromatic hydrogens with deuterium using K_2PtCl_4 in presence of deuterium oxide and acetic acid and deuteriochloric acid.[4] Since then, regioselective and efficient incorporation of deuterium into C-H bonds has become an important tool for preparation of deuterium-labeled organic molecules. General procedures for the incorporation of deuterium into the C-H bonds are often limited to aromatic and aliphatic C-H bonds of

organic compounds. Cp*Ir complexes with phosphine ligands[5-9] or N-heterocyclic carbene ligands[10-12] have been shown to catalyze H/D exchange. These complexes can use methanol-d_4,[10] deuterium oxide,[5,8] or a methanol-*d*/deuterium oxide system[12] as the deuterium source. Among Cp*Ir-based catalysts, Cp*Ir(PMe_3)Cl_2, **4.1** reported by Bergman[5] et al. reaches high to moderate deuterium incorporation (Figure 4.1).

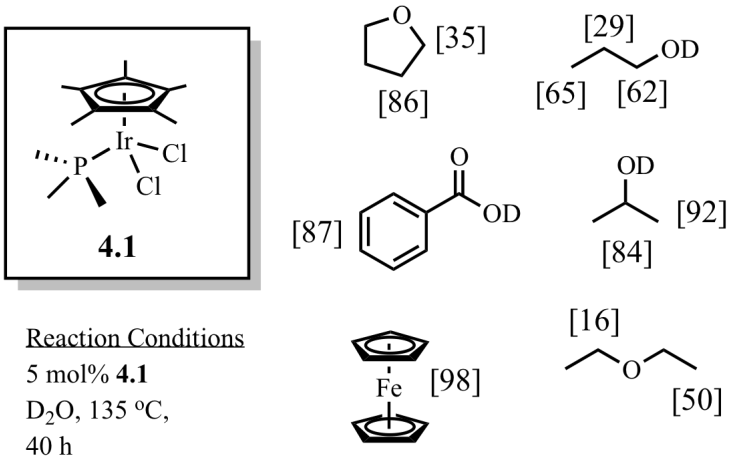

Figure 4.1. H/D exchange of aromatic and aliphatic C-H bonds reported by Bergman and coworkers

In 2003, Lin and Lau et al. reported H/D exchange between methane and deuterated solvents such as benzene-d_6, tetrahydrofuran-d_8, diethylether-d_{10}, 1,4-dioxane-d_8 using the ruthenium complex TpRu(PPh_3)(CH_3CN)H (Tp = hydro(trispyrazolyl)borate).[13] Later in 2007, they reported catalytic H/D exchange between organic molecules and deuterium oxide at a reaction temperature of 110 ^oC. Argon pressure (10 atm) was applied to ensure that reactants and reagents did not boil. At 0.4 mol% loading, TpRu(PPh_3)(CH_3CN)H is capable of incorporating 24 and 13 percent deuterium into diethyl ether and tetrahydrofuran, respectively.[14]

Although there are many reports of H/D exchange at aromatic and aliphatic C-H

bonds[15-26] there are fewer such reports for alkenes and much less work has been carried out on direct catalytic H/D exchange between olefins and deuterium oxide. The high temperature-dilute acid method has been explored in the 1980s for the H/D exchange between deuterium oxide and olefins,[27,28] however; the method suffers from side reactions of skeletal rearrangements, acid catalyzed hydration of the alkene, or polymerization and oligomerization of olefins.

H/D exchange catalyzed by Pd/C of cyclooctene and cyclohexene with deuterium oxide (Figure 4.2) has been reported by Anet et al. at tempreratures of >140 ^{o}C and by Matsubara[29] et al. under hydrothermal conditions (250 ^{o}C, 5 MPa).

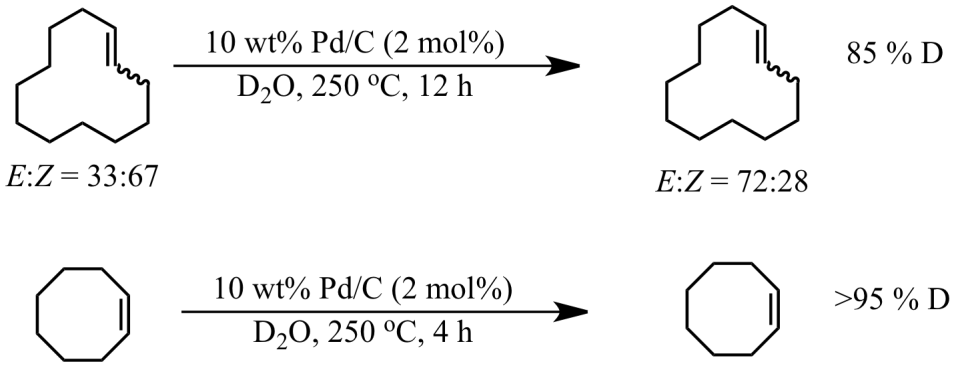

Figure 4.2. Deuteration of cyclooctene under hydrothermal conditions by Matsubara and coworkers

Later in 2007, Matsubara et al. demonstrated that cyclic olefins such as cyclohexene and cyclodecene (Figure 4.3) can undergo H/D exchange with deuterium oxide under microwave irradiation in the presence of homogenous catalyst $RuCl_2(PPh_3)_3$ (5 mol%, 140 ^{o}C, 0.34 MPa) and sodium dodecylsulfate (SDS) as an additive. SDS partially hydrolyzes to give dodecanol, which provides hydride and stabilizes the ruthenium species by micelle formation.[30]

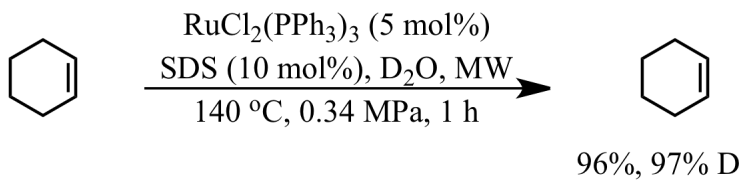

Figure 4.3. Deuteration of cyclohexene using microwave irradiation

Brookhart et al. illustrated catalytic H/D exchange reactions (Figure 4.4) in which deuterium can be transferred from deuterated solvents (benzene-d_6, toluene-d_8, chlorobenzene-d_5, or acetone-d_6), to the CH bonds of alkenes bound on complex **4.2** at 50 °C. Thermolysis at higher temperatures results in further H/D exchange and deuteration of both the $SiMe_3$ and C_5Me_5 groups. Heating **4.2** in benzene-d_6 with cyclopentene resulted in moderate (49%) deuteration of vinylic, allylic and homoallylic sites. Higher degrees of deuteration are observed with aniline, Cp_2Fe, and EtOAc.[17]

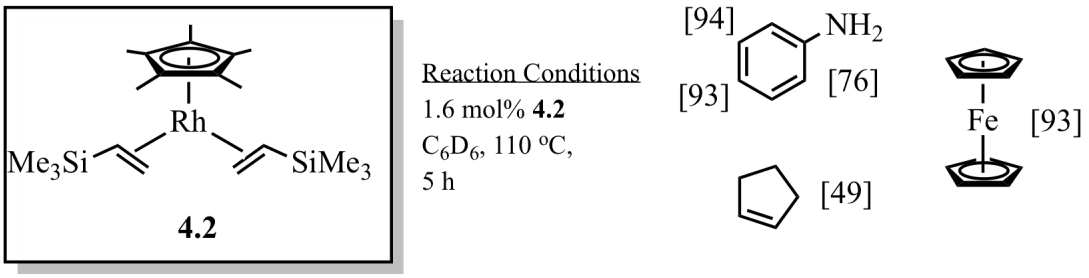

Figure 4.4. H/D exchange reported by Brookhart and coworkers

When $[Cp^*Ir(PMe_3)H_3]OTf$, a hydride analogue of **4.1**, also reported by Bergman et al. is used, deuterium incorporation into olefinic sites can be achieved. Reactions with cyclohexene at 75 °C resulted in 95%, 83%, and 88% deuterium in vinylic, allylic, and homoallylic positions, respectively, and for analogous positions on cyclopentene results were 95%, 96%, and 90%, respectively. When 1-hexene was subjected to same reaction conditions internal alkene isomers were observed. Overall, 26% of the vinylic positions

of 1-hexene were deuterated as were 23% of internal methylene positions, although the terminal methyl group was not deuterated.[8]

Morrill et al. observed that partial deuteration of octene, cyclohexene, and styrene during labeling studies of alkene isomerization using $RhCl_3/BH_3$ in the presence of D_2O. In the case of styrene, where no isomerization is possible the fact that deuterium incorporation took place suggests that alkene insertion is responsible for H/D exchange.[31]

Amidoiridium hydride complex [(dtbpp)Ir(H)(NH_2)] **4.3** (Figure 4.5, dtbpp = 1,5-bis(di-*tert*-butylphosphino)pentan-3-yl), reported by Zhou et al.[32] activates vinylic C-H bonds and performs H/D exchange reactions with control of carbon-carbon double bond isomerization and tolerance to different functional groups. The functional group selectivity and tolerance is demonstrated by subjecting natural products, such as forskolin, altrenogest, (Figure 4.5) and tiamulin to **4.3** to H/D exchange in benzene-d_6 at room temperature. Complex **4.3** also catalyzed H/D exchange of substituted aromatic and heteroaromatic compounds, even pyridine, which can deactivate catalytic activity of several other iridium complexes, presumably through competitive binding at nitrogen.[8,33]

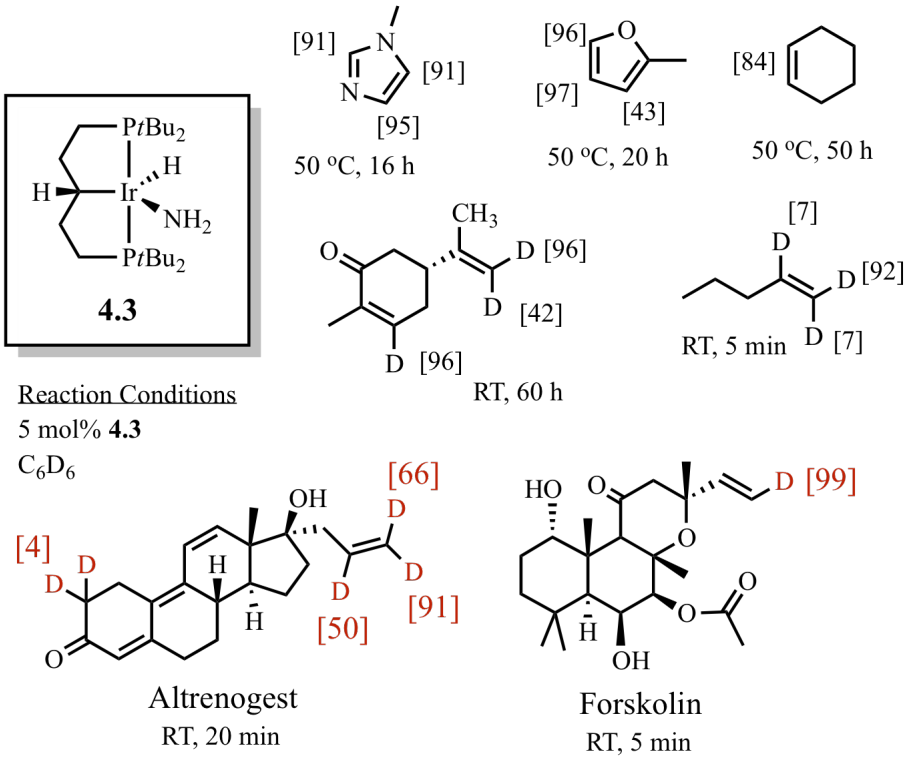

Figure 4.5. Scope of H/D exchange with [(dtbpp)Ir(H)(NH_2)]

Although the study of H/D exchange reactions has tended to concentrate on aromatic or aliphatic compounds, there is an increasing interest in the deuteration of vinylic derivatives. Since 2009, several reports of H/D exchange have emerged. Li and Jia, et al. investigated H/D exchange reactions using six-coordinate 18-electron complexes $MHCl(CO)(PPh_3)_3$ (M = Ru, Os) and found that the readily available hydride complex $RuHCl(CO)(PPh_3)_3$ can effectively catalyze H/D exchange reactions of deuterium oxide with both terminal and internal alkenes. Through H/D exchange between metal hydride and deuterium oxide, and reversible olefin insertion into a Ru-D(H) bond, protons attached to alkene carbons and the alkyl chains of alkenes can all undergo H/D exchange with deuterium oxide. Both terminal and internal alkenes, for example, styrene, stilbene and cyclooctene can be deuterated.[34]

Moreover, selectivity towards olefinic versus aromatic protons is an important challenge. For example, Milstein's pincer-type ruthenium hydride complex[20,24] [Ru-(2,6-bis((di-*tert*-butylphosphino)methyl)pyridine)(η^2-H_2)H_2] can incorporate deuterium into aromatic positions as well as olefinic positions. Oro et al. reported highly active and selective H/D exchange at the β position of aromatic α-olefins by a rhodium(III)–N-heterocyclic carbene–hydride catalyst that contains a bulky carbene, 3-bis-(2,6-diisopropylphenyl)imidazol-2-carbene (IPr), and a chelating quinolinate ligand. [RhClH(κ^2O,N-(C_9H_6NO)(IPr)] exchanges β-H of olefinic sites and α-H exhange can be controlled by the bulky IPr groups on the carbene.[35]

The overall challenge for catalyzed H/D exchange is regio-selectivity, and chemoselectivity in presence of different functional groups. The review of literature shows that research in H/D exchange has been heavily concentrated on aromatic, aliphatic and vinylic sites of olefinic sites and many of the systems execute H/D exchange of more than one type of C-H bond.

USE OF ALKENE ISOMERIZATION CATALYST 2.10 IN H/D EXCHANGE

In 2009, we reported H/D exchange at *allylic* positions of alkenes catalyzed by recently reported alkene zipper catalyst **2.10** (see chapter 2) in homogeneous and biphasic reactions using inexpensive deuterium oxide as the isotope source.[36,37] Study of the complex **2.10** has revealed that it is a versatile bifunctional catalyst suitable for the study of catalytic isomerization of alkenes and H/D exchange of accessible allylic alkene

protons. Bifunctional catalyst **2.10** has been reported to isomerize various other functionalized olefins including, but not limited to, alkenols, silyl ethers, amines, and esters. As mentioned in chapter 3, distinguishing characteristics of **2.10** include formation of *(E)*-isomer products with low catalyst loadings (2-5 mol%) at moderate temperatures (25-70°C).[38]

The imidazole group on the phosphine ligand is proposed to act as an internal base facilitating the isomerization by deprotonating accessible allylic position(s) of a coordinated alkene. The protonated nitrogen could be expected to undergo H/D exchange in the presence of deuterium oxide. In order to investigate the mechanism proposed in Figure 5.6 and explore possible application of **2.10**, deuterium oxide was added to the isomerization reactions.

In our experiments, substrate was dissolved in acetone-d_6 and deuterium oxide was added to provide 20 D for each exchangeable H present in the substrate. For example, 1-butene has eight exchangeable protons, therefore, 80 equivalents of deuterium oxide was added to the reaction. Assuming equal distribution of D among all exchangeable positions, each such position should be 95% deuterated, judged to be a synthetically useful goal. The effects of isotope fractionation have also been considered. Experimental data summarized in Table 9 of reference 39 for ethylene and methane suggests that insignificant fractionation between vinylic and alkyl C-H bonds should occur, and the effect of fractionation between these hydrocarbon C-H bonds and the O-H bonds should have less than 1-2% effect on the degree of substrate deuteration under our conditions.[39]

Progress of the reaction was monitored by ^{1}H NMR spectroscopy; deuteration is calculated from integration and corrections are done according to theoretical deuteration. For a reaction at elevated temperatures, the reaction was set up in the same manner described above and the J. Young NMR tube was immersed in an oil bath at 70 °C.

When 1-propene is exposed to **2.10** and deuterium oxide, deuterium incorporation is observed only at *C*1 and *C*3, reaching 97.5-98.5% of theoretical deuteration within 24 h (Figure 4.7). In stark contrast, the single proton at *C*2 remained intact (as observed up to 60 d). Similar deuteration at only *C*1 and *C*3 was seen when 4-allylanisole was heated with **2.10** and deuterium oxide at 70 °C. Isomerization of diallyl ether gave (*E, E*)-dipropenyl ether without any detectable (*E, Z*)- or (*Z, Z*)-isomer.[7] In presence of deuterium oxide, H/D exchange is seen only at positions *C*1 and *C*3,[7] consistent with the other two examples.

The observed selectivity, retention of H at *C*2, renders the alternative mechanism, metal hydride formation, alkene insertion, and β-hydride elimination, seen for many other alkene isomerization catalysts[40-43] highly unlikely (Chapter 2).

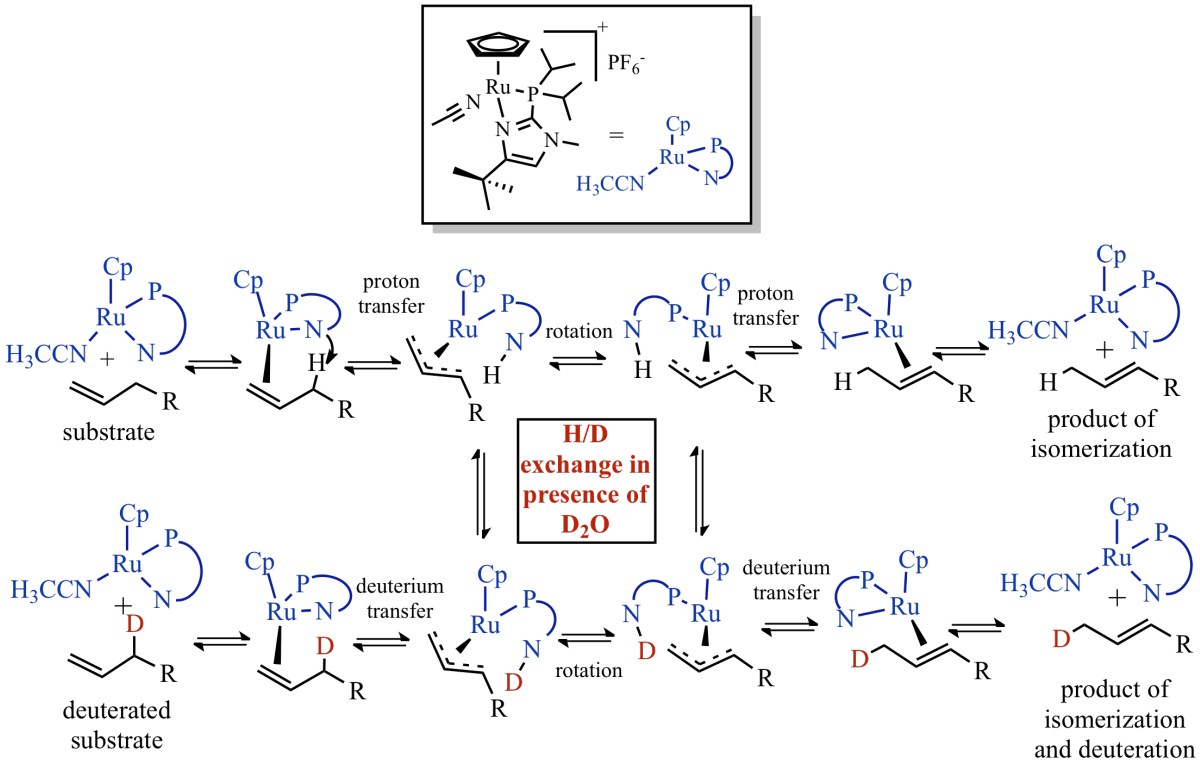

Figure 4.6. Proposed mechanism of isomerization and deuteration by 2.10

The case of 4-allylanisole deserves additional comment. Isomerization of the double bond is complete within 5 min at room temperature, yet full deuteration requires days at 70 ^{o}C. This is consistent with the high selectivity, dictated by sterics, of **2.10** (Figure 4.6; see also Figures 2.10 and 2.11 in Chapter 2 and discussion).

In contrast to the case of substrates with isolated allyl groups, where the alkene can migrate over two bonds or more, (*E*)-2-butene and 1-pentene were exposed to deuterium oxide and **2.10**; H/D exchange occurred at previously unreactive vinylic positions and total deuteration was observed (Figure 4.7). Presumably η^3-allyl intermediates (Figure 4.6) formed along the chain, allowing all positions to become allylic through isomerization. Thus, full deuteration of these substrates can be achieved with 2 to 5 mol % catalyst loading and reasonable reaction times.

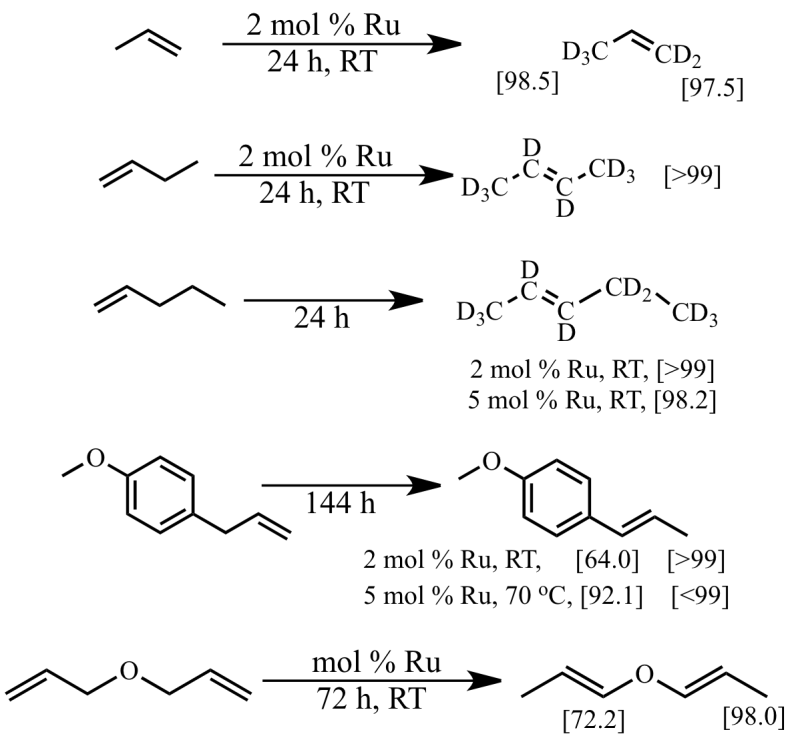

Figure 4.7. Isomerization of linear olefins

The very high kinetic selectivity of the catalyst for making or acting on (*E*)-alkenes without isomerization to (*Z*)-alkenes is highlighted by the following experiments with isomers of butene with either D_2O or H_2O as a control. Starting with either (*E*)- or (*Z*)-2-butene and 2 mol % **2.10**, the half-life for equilibration of the two isomers was measured to be about 10 days, a result unchanged by addition of H_2O (Figure 4.8). In comparison, exposure of (*E*)-2-butene to **2.10** and deuterium oxide led to complete deuteration within 24 h, without formation of detectable formation of the (*Z*)-isomer. Thus, **2.10** deuterates (*E*)-2-butene quickly ($t_{1/2}$ = ca. 1.2 h), but only slowly ($t_{1/2}$ > ca. 240 h) isomerizes it to the (*Z*)-isomer, a rate difference of ca. 200-fold! Exposure of (*Z*)-2-butene to **2.10** and deuterium oxide showed lack of deuterium incorporation to (*Z*)-2-butene unless it isomerized to (*E*)-2-butene. These experiments shed valuable

mechanistic insight on the action of **2.10**. The isomerization of (*E*)-alkenes to terminal alkenes is shown by perdeuteration of 1-pentene (vide supra).

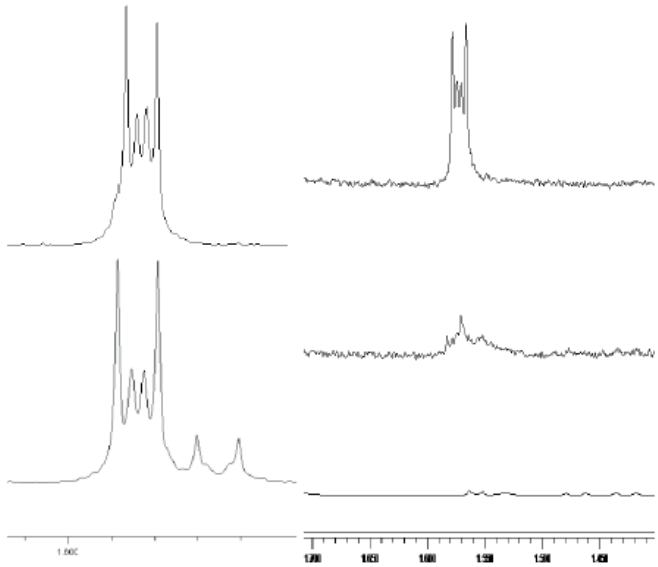

Figure 4.8. (left) ^{1}H NMR spectrum of 2-butene in presence of water. Geometrical isomerization to a mixture of (*E*)- (major) and (*Z*)- (minor) 2-butenes in acetone-d_6; (right) ^{1}H NMR spectrum of 2-butene in presence of deuterium oxide. Conclusion: Deuteration is much more rapid than geometrical isomerization.

Branched substrates (Figure 4.9) provide additional examples of highly selective deuteration. For example, 4-methyl-1-pentene isomerized to *(E)*-4-methyl-2-pentene and deuteration was observed only at *C*1 and *C*3, leaving the *C*2 proton intact.[9] Further isomerization was not observed even at elevated temperatures over time. Selective deuteration is observed with branched substrates. The natural product (+)-limonene underwent H/D exchange mainly at the exocyclic isopropenyl group. Deuterium incorporation is observed at the endocyclic double bond but is far from complete, which can be attributed to steric hindrance to **1** forming an η^3-allyl complex at this position. Deuteration of (+)-valencene was even more selective. Exocyclic isopropenyl groups are

found in many terpenoid natural products, hence facile pentadeuteration at such sites is of particular interest.

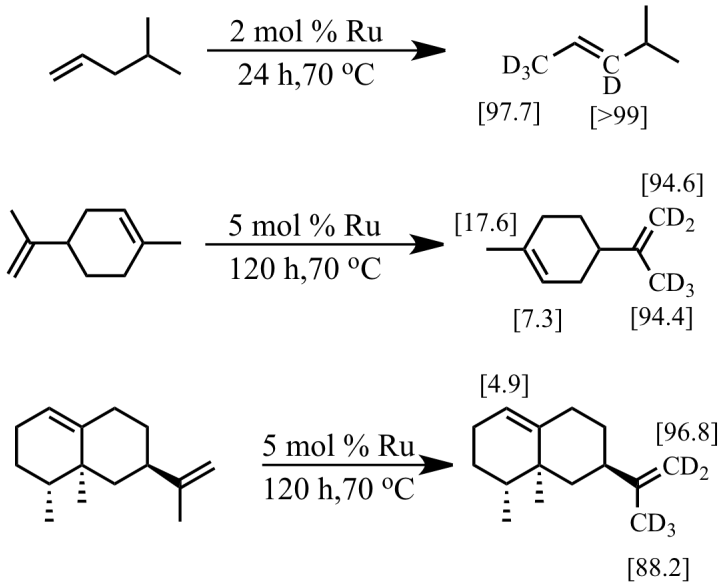

Figure 4.9. Isomerization and selective deuteration of branched olefins

Biphasic reactions were performed on liquid substrate 4-allylanisole by stirring it with only catalyst and deuterium oxide. Higher deuterium content was reached in shorter time compared to homogeneous reactions (Figure 4.10). In a biphasic experiment setting where deuterium oxide was added in portions, phase separation allows for extraction of the aqueous phase. Removal of the aqueous phase after equilibration to ca. 80% deuteration and recharging the reaction system with fresh deuterium oxide allows for further exchange. Loss of catalyst during extraction is negligible since the catalyst **2.10** is dissolved in the organic phase and coloration of aqueous phase is minimal. Remarkably, in these experiments there was no need to add surfactants or other ionic materials to achieve the proper distribution of catalyst between the two phases.

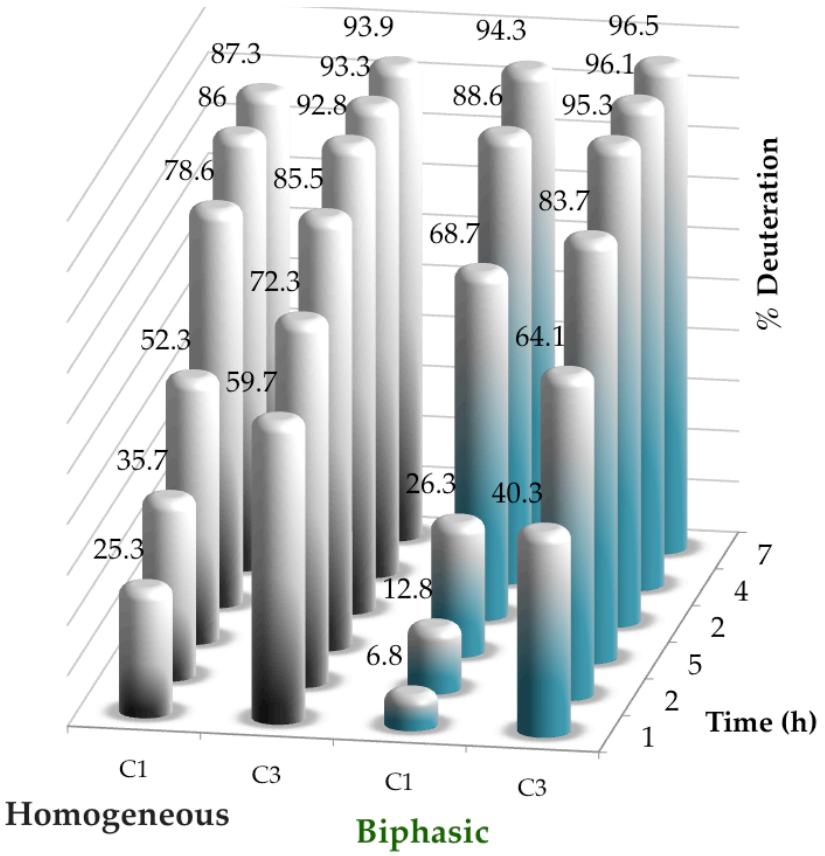

Figure 4.10. Comparison progression of isomerization and H/D exchange of 4-allylanisole in homogeneous and biphasic settings over time

Attempts to exchange hydrogens for deuterium failed with cyclohexene and cyclooctene. In cases with primary or secondary alcohols like 4-penten-1-ol or 4-penten-2-ol, although deuterium incorporation was achieved, high isotope content was not achieved possibly due to aldehyde or ketone formation providing a stable product rendering the reaction irreversible.

In conclusion, unlike previous catalysts, **2.10** exchanges allylic protons of olefins with deuterium from deuterium oxide with outstanding control of isomerization when it occurs. Deuterium oxide is an attractive isotope source because of its low cost, safety, and low toxicity and ease of handling. An exceptional degree of deuteration is achieved

at positions accessible by isomerization in homogeneous and biphasic reaction settings. The high steric selectivity of **2.10** for (*E*)-alkenes gives the catalyst a distinctive reactivity and selectivity profile, which is especially useful in labeling complex substrates either at a late stage of a synthesis, or using material directly from natural sources, as illustrated by the cases of (+)-limonene and (+)-valencene.

EXPERIMENTAL SECTION

All manipulations were carried out in a nitrogen filled glovebox or using Schlenk techniques. D_2O, acetone-d_6 and THF-d_8 were received from Cambridge Isotope Laboratories, Inc., and further deoxygenated by bubbling N_2 gas through the liquid prior to use. D_2O had a deuterium content of 99.9% and was stored and used in the glovebox to avoid dilution with atmospheric moisture. NMR spectra were obtained at 30 °C on either a 500-MHz INOVA (500 MHz listed below for ^1H = 499.940 MHz and 125.7 MHz for ^{13}C = 125.718 MHz), a 400-MHz Varian NMR-S (400 MHz listed below for ^1H = 399.763 MHz and 100 MHz for ^{13}C = 100.525 MHz), or a 200 MHz Gemini (^{31}P data at 80.95 MHz) spectrometer. ^1H NMR chemical shifts were reported as mentioned in chapter 2.

Calculation of Deuterium Content

Degree of deuteration can be expressed in a wide variety of ways. In this work, our major goal was to perform experiments with sufficient deuterium source that a synthetically appealing and useful degree of deuteration (greater or equal to 95%) could be obtained. Here in this section using one example (for Table 4.3) we calculate observed deuteration as a per cent of the theoretical maximum, taking into account not only the ratio of available deuterium (from deuterium oxide, D_2O), to the number of exchangeable H on the substrate (for example 4-allylanisole has 5 exchangeable protons), but also taking into account the measured amount of protium in the D_2O used (called HDO below). The D_2O

employed in this work had a nominal deuterium content of 99.9%, and was stored and used in the glovebox to avoid any dilution by atmospheric water.

Amount of 4-allylanisole weighed 29.9 mg

$$29.9mg \times \frac{1g}{10^3 mg} \times \frac{1mol}{148.20g} \times \frac{10^3 mmol}{1mol} = 0.202mmol$$

Total number of moles of hydrogen in 4-allylanisole (including non-exchangeable ones)

$$0.202mmol \times \frac{12molH}{1mol\ 4-allylanisole} = 2.42mmolH$$

From ^{1}H-NMR Spectrum $2.42mmolH = 335.78units$

Integration of HDO peak is 8.81 units, giving

$$8.81units \times \frac{2.42mmol}{335.78units} = 0.0635mmolH$$

$$0.0635mmolH = 0.0635mmolHDO$$

$$Mass_{HDO} = mol_{HDO} \times MW_{HDO}$$

$$M_{HDO} = 0.0635mmol \times \frac{19.01mgHDO}{1mmol} = 1.21mgHDO$$

$$Mass_{addedD_2O} = 160.4mg$$

$$Mass_{addedD_2O} = Mass_{D_2O} + Mass_{HDO},\ where\ Mass_{D_2O}\ is\ the\ mass\ of\ D_2O\ actually\ present$$

$$160.4mg = M_{D_2O} + 1.21mg$$

$$M_{D_2O} = 159.19mg$$

$$mol_{D_2O} = 159.19mg \times \frac{1mmolD_2O}{20.03mgD_2O} = 7.9485mmol$$

$$mol_D = mol_{Df\,romD_2O} + mol_{HDO}$$

$$mol_{Df\,romD_2O} = 2 \times mol_{D_2O}$$

$$mol_D = (2 \times 7.9485mmol) + 0.0635mmol = 15.960mmol$$

Now to calculate the total mmol of exchangeable H (from both HDO and substrate) and D (from the D_2O and its HDO impurity):

$$\sum n_H + n_D = n_D + n_{Hf\,romHDO} + n_{Hexchangeablef\,rom4-allylanisole}$$

$$\sum n_H + n_D = 15.960 + 0.0635mmol + (0.202mmol \times 4) = 16.830mmol$$

Theoretically maximum deuteration (assumed for simplicity to be same at all exchangeable positions) is:

93.9 x (100 ÷ 94.8) = 99.1 % of the theoretical maximum deuteration.

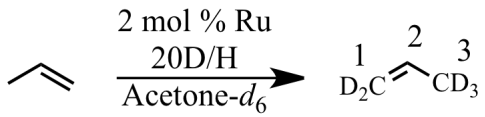

Figure 4.11. Deuteration of propene

Deuteration of propene. Propene was bubbled through a J. Young NMR tube containing 1,4-dioxane (1.6 mg, 0.018 mmol) in acetone-d_6 (about 1 mL). After determination of the number of moles of propene (0.21 mmol) present, deuterium oxide (206.8 g, 10.3 mmol) was added to the tube followed by **2.10** (2.5 mg, 0.0042 mmol, 2 mol %), transferred quantitatively from a vial using acetone-d_6 in several portions. Total reaction volume was adjusted to 2.0 mL by addition of acetone-d_6. Hydrogen-deuterium exchange was observed via ^{1}H NMR at several time intervals (Table 4.1). Starting material ^{1}H NMR (500 MHz, acetone-d_6) δ 5.76 (qdd, J = 6.4, 10.2, 16.8 Hz, 1H), 4.95 (qdd, J = 1.8, 2.2, 16.8 Hz, 1H), 4.85 (qdd, J = 1.6, 2.4, 10.1 Hz, 1H), 1.62 (ddd, J = 1.4, 1.8, 6.4 Hz, 3H). Product ^{1}H NMR at 24 h (500 MHz, acetone-d_6) δ 5.76 (bs, 1H), 4.96 (d, J = 17 Hz, 0.085H), 4.86 (d, J = 10 Hz, 0.085H), 1.64-1.59 (m, 0.20H).

Table 4.1. % Hydrogen left at indicated positions of propene after specified time

Time (min)	1	2	3
0	106.7	93.8	101.6
1	50.9	109.2	38.9
2	24.9	101.2	17.9
5	9.8	99.3	7.9
24	7.5	96.7	6.5

Note on 2-butene NMR spectra. Both 2-butene isomers are examples of $A_3A'_3XX'$ proton spin systems, and their ^{1}H NMR spectra (Fig. 4.12) are non-first-order. Here we report methyl and methine proton signals as "m," meaning $A_3A'_3$ of $A_3A'_3XX'$ for methyl protons and XX' of $A_3A'_3XX'$ for methine protons. In the literature[44,45] these peaks are reported variously as either d or dd when in fact they are not first order. Rummens and Kaslander reported observed coupling constants for (*Z*)- and (*E*)-2-butene in *Canadian Journal of Spectroscopy*, **1972**, *17*, 99-102.[46]

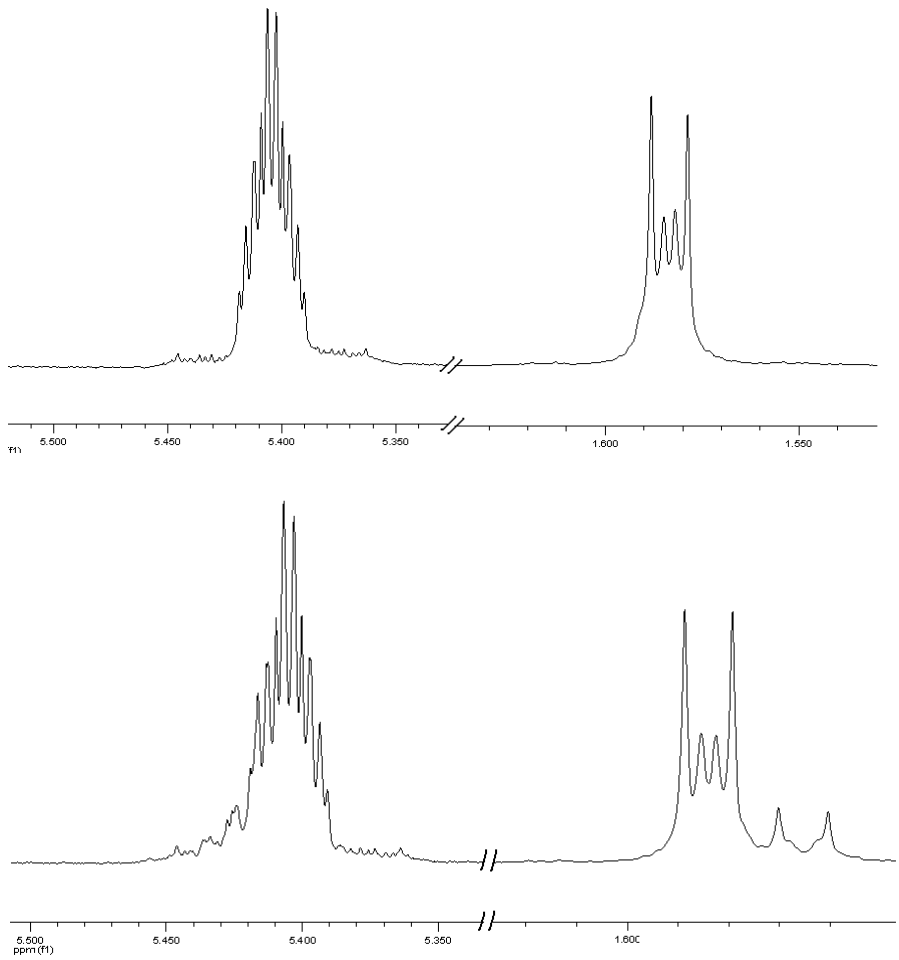

Figure 4.12. ^{1}H NMR Spectrum of (*E*)-2-butene in acetone-d_6 (upper); (*E*)- (major) and (*Z*)- (minor) 2-butenes in acetone-d_6

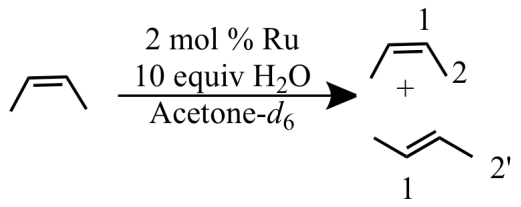

Figure 4.13. Control experiment with (*Z*)-2-butene in presence of water

Isomerization of (*Z*)-2-butene in presence of H_2O. (*Z*)-2-butene was bubbled through a J. Young NMR tube containing 1,4-dioxane (4.3 mg, 0.049 mmol) and acetone-d_6 (about 1 mL). After determination of the number of moles of (*Z*)-2-butene (0.158 mmol) present, water (28.5 g, 1.58 mmol, 10 equiv) was added followed by **2.10** (1.9 mg, 0.0032 mmol, 2 mol %), transferred quantitatively from a vial using acetone-d_6 in several portions into the J. Young tube. Total reaction volume was adjusted to 2.0 mL by addition of acetone-d_6. Reaction observed via ^{1}H NMR in several time intervals (Table 5.2). Starting material ^{1}H NMR (500 MHz, acetone-d_6) δ 5.44-5.37 (m, 2H), 1.59-1.52 (m, 6H). ^{1}H NMR at 840 h (500 MHz, acetone-d_6) δ 5.464-5.35 (m, 2H), 1.58-1.57 (m, 3.03H), 1.56-1.55 (m, 2.86H).

Table 4.2. % Hydrogen atoms present at specified positions in reaction of (*Z*)-2-butene in presence of water

Time (min)	1	2	2'	(*Z*):(*E*) ratio[a]
0	1.99	6.01	-	1:0
5	2.01	6.07	-	1:0
48	1.99	5.42	0.60	1:0.1
240	2.02	4.43	1.58	1:0.4
480	1.98	3.79	2.28	1:0.6
840	1.93	2.86	3.03	1:1.1

[a] Ratio of (*Z*)- and (*E*)-isomers are calculated from integration of assigned methylene peaks.

In a control experiment to show that catalyst was still active, 50 d after addition of **2.10**, 1-pentene (2.1 mg, 0.030 mmol) was added to the J. Young NMR tube. In 1 h, 51.9% 1-pentene had isomerized to 2-pentene, and in 22 h 1-pentene was completely isomerized.

Note on geometrical isomerization of 2-butenes: Isomerization of (*Z*)-2-butene to (*E*)-2-butene has been observed previously[47,48] as well. Considering the equilibrium constants reported in these reports, (*Z*)-(*E*) isomerization has not yet reached equilibrium in our experiments.

Note: Isotope exchange between the solvent (acetone-d_6) and H_2O can take place over prolonged periods. If this is the case, (*E*)-2-butene will undergo hydrogen-deuterium exchange and in turn, (*E*)-2-butene-d_8 can undergo geometric isomerization to give (*Z*)-2-butene-d_8. The NMR measurements used cannot determine the amount (*Z*)-2-butene-d_8 that may be present in the reaction mixture.

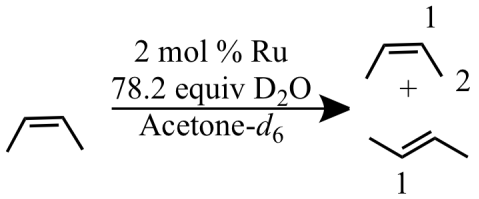

Figure 4.14. Control experiment with (*Z*)-2-butene in presence of deuterium oxide

Isomerization of (*Z*)-2-butene in presence of deuterium oxide. (*Z*)-2-butene was bubbled through a J. Young NMR tube containing 1,4-dioxane (3.6 mg, 0.041 mmol) and acetone-d_6 (about 1 mL). After determination of the number of moles of (*Z*)-2-butene (0.199 mmol) present, deuterium oxide (311.6 mg, 15.6 mmol, 78.2 equiv) was added followed by **2.10** (2.4 mg, 0.0040 mmol, 2 mol %), transferred quantitatively from a vial using acetone-d_6 in several portions into the J. Young tube. The vial containing **2.10** was

washed with additional acetone-d_6 and washings were added to the tube. Total reaction volume was adjusted to 2.0 mL by addition of acetone-d_6. Reaction was observed via ^{1}H NMR at several time intervals (Table 4.3). Starting material ^{1}H NMR (500 MHz, acetone-d_6) δ 5.44-5.37 (m, 2H), 1.50-1.47 (m, 6H). ^{1}H NMR at 840 h (500 MHz, acetone-d_6) δ 5.44-5.34 (m, 0.54H), 1.52-1.49 (m, 1.59H); ^{2}D NMR at 822 h (400 MHz, acetone-d_6) δ 5.36, 1.47.

Table 4.3. % Hydrogen atoms present at specified positions in reaction of (*Z*)-2-butene in presence of deuterium oxide

Time (min)	1	2
0	100.5	100.5
5	98.5	100.5
48	94.0	96.3
240	69.0	68.2
480	45.5	46.2
840	27.0	26.5

In a control experiment to show that catalyst was still active, 50 d after addition of **2.10**, 1-pentene (2.3 mg, 0.033 mmol) was added to the J. Young NMR tube. In 1 h, 68.3% 1-pentene had isomerized to 2-pentene, and in 22 h 1-pentene was completely isomerized.

Note: Apparent reduction of the amount of (*Z*)-2-butene is due to its geometrical isomerization into (*E*)-2-butene (vide supra), which undergoes hydrogen-deuterium exchange in presence of deuterium oxide.

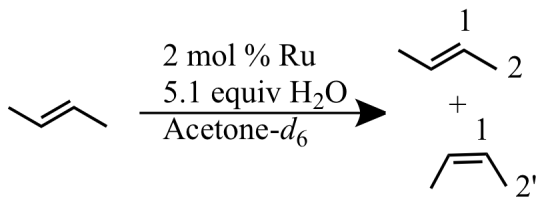

Figure 4.15. Control experiment with (*E*)-2-butene in presence of water

Isomerization of (*E*)-2-butene in presence of H_2O. (*E*)-2-butene (2.0 mL, 0.082 mmol) was bubbled through a J. Young tube containing 1,4-dioxane (10.8 mg, 0.123 mmol) and H_2O (7.8 mg, 0.43 mmol) in acetone-d_6 (about 0.8 mL). After acquisition of an initial spectrum to set the integral values, **2.10** (1.1 mg, 0.0018 mmol, 2 mol %) was transferred quantitatively from a vial using acetone-d_6 in several portions to the J. Young NMR tube. The vial containing **2.10** was washed with additional acetone-d_6 and washings were added to the tube. Reaction was observed via ^{1}H NMR in several time intervals (Table 5.4). Starting material (400 MHz, acetone-d_6) δ 5.43-5.40 (m, 2H), 1.60-1.59 (m, 6H). ^{1}H NMR at 216 h (400 MHz, acetone-d_6) δ 5.46-5.40 (m, 1.88H), 1.60-1.57 (m, 5.53H).

Table 4.4. % Hydrogen atoms present at specified positions in reaction of (*E*)-2-butene in presence of water

Time (min)	1	2	2'	(*Z*):(*E*) ratio[a]
0	103.5	98.8	-	-
24	94.5	91.7	8.0	11.5:1
48	94.5	91.2	9.2	9.9:1
96	94.5	84.3	12.0	7.0:1
144	94.0	80.2	16.2	5.0:1
216	94.0	71.5	20.7	3.5:1

[a] Ratio of (*Z*)- and (*E*)-isomers are calculated from integration of assigned methylene peaks.

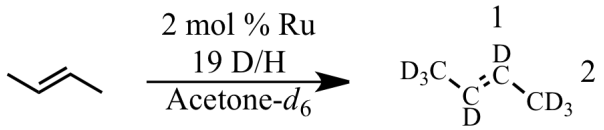

Figure 4.16. Deuteration of (*E*)-2-butene

Deuteration of (*E*)-2-butene. (*E*)-2-butene was bubbled through a J. Young NMR tube containing 1,4-dioxane (3.7 mg, 0.042 mmol) in acetone-d_6 (about 1 mL). After determination of the number of moles of (*E*)-2-butene (0.19 mmol) present, deuterium oxide (206.6 g, 15.3 mmol) was added followed by addition of **2.10** (2.4 mg, 0.0039 mmol, 2 mol %), transferred quantitatively from a vial using acetone-d_6 in several portions into the J. Young tube. Total reaction volume was adjusted to 2.0 mL by addition of acetone-d_6. Reaction was observed via ^{1}H NMR at several time intervals (Table 5.5). After 24 h, **2.10** was inactivated by briefly bubbling carbon monoxide gas through the tube. Starting material ^{1}H NMR (400 MHz, acetone-d_6) δ 5.39-5.29 (m, 2H), 1.52-1.51 (m, 6H). Product at 24 h ^{1}H NMR (400 MHz, acetone-d_6) δ 5.38-5.42 (m, 0.09H), 1.52-1.48 (m, 0.10H). ^{2}D NMR (61.366 MHz, acetone-d_6) δ 5.353, 1.514, 1.477. ^{13}C NMR (150.823 MHz, acetone-d_6) 126.18-125.71 (m), 17.44-16.64 (m).

Note: In the ^{13}C NMR spectrum of an authentic (*Z*)- and (*E*)-2-butene mixture in acetone-d_6 peaks at 124.5, 124.2, 17.0, 11.4 ppm are observed. Peaks at 124.2 and 11.4 ppm are assigned to the (*Z*) isomer and peaks at 124.5 and 17.0 ppm are assigned to the (*E*) isomer according to literature. (Silverstein, R. M.; Bassler, G. C.; Morrill, T. C. *Spectrometric Identification of Organic Compounds*; 1981; p 263; Wang, R.; Groux, L. F.; Zargarian, D. *Organometallics* **2002**, *21*, 5531-5537) Looking at the methyl region of the spectrum, one will be able to observe presence of *cis* isomer clearly. In our experiment (*Z*) isomer was not detected; the estimated detection limit is as high as 10%, because the ^{13}C NMR

peaks for fully deuterated material are split by the D nuclei, hence achieving reasonable signal-to-noise on the sample above required nearly 2 days).

Table 4.5. % Hydrogen atoms present at specified positions in reaction of (*E*)-2-butene in presence of deuterium oxide

Time (min)	1	2
0	97.9	100.7
1	56.6	59.7
5	18.7	13.1
24	4.6	5.0

In a control experiment to show that catalyst was still active, 40 d after addition of **2.10**, 1-pentene (7.2 mg, 0.10 mmol) was added to to the J. Young NMR tube. In 20 h, 1-pentene had completely isomerized to 2-pentene.

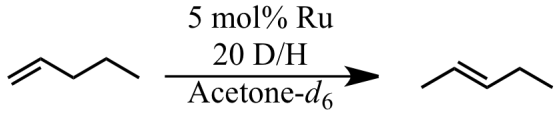

Figure. 4.17. Isomerization and deuteration of 1-pentene

Isomerization and deuteration of 1-pentene. A J. Young NMR tube was charged with tetrakis(trimethylsilyl)methane (a few small crystals), 1-pentene (7.1 mg, 0.10 mmol) and deuterium oxide (201.3 mg, 10.0 mmol) in acetone-d_6 (1.0 mL). After acquisition of an initial spectrum to set the integral values, **2.10** (3.0 mg, 0.0049 mmol, 5 mol %) was transferred quantitatively from a vial using acetone-d_6 in several portions into the J. Young NMR tube. Progress of the reaction was monitored via ^{1}H NMR (refer to table 5.6). Starting material ^{1}H NMR (500 MHz, acetone-d_6) δ 5.75 (ddt, J = 6.5, 10.5, 15.5 Hz, 1H), 4.93 (ddt, J = 1.5, 2.0, 17.0 Hz, 1H), 4.87 (ddt, J = 1.5, 2.0, 10.0 Hz, 1H), 1.95

(~tdd, $^4J_{H1\text{-}H3}$ = 2.0 Hz, $^3J_{H2\text{-}H3}$ = $^3J_{H3\text{-}H4}$ = 7.4 Hz, 2H), 1.33 (tq, $^3J_{H4\text{-}H5}$ = $^3J_{H3\text{-}H4}$ = 7.5 Hz, 2H), 0.83 (t, J = 7.2 Hz, 3H). Product ^{1}H NMR at 24 h (500 MHz, acetone-d_6) δ 5.38 (bs, 0.05H), 5.32 (bs, 0.06H), 1.85 (bs, 0.09H), 1.50 (bs, 0.16H), 0.85-0.81 (m, 0.26H).

Table 4.6. % Hydrogen atoms present in 2-pentene with deuterium oxide at room temperature

Time (min)	% H in 2-pentene
1	57.4
2	36.8
24	6.2

Isomerization and deuteration of 1-pentene at 70 ^{o}C. A J. Young NMR tube was charged with tetrakis(trimethylsilyl)methane (a few small crystals), 1-pentene (7.2 mg, 0.10 mmol) and deuterium oxide (200.1 mg, 10.0 mmol) in acetone-d_6 (1.0 mL). After acquisition of an initial spectrum to set the integral values, **2.10** (1.3 mg, 0.0021 mmol, 2 mol %) was transferred quantitatively from a vial using acetone-d_6 in several portions into the J. Young NMR tube. The J. Young NMR tube was placed in an oil bath at 70 ^{o}C. Progress of the reaction was monitored via ^{1}H NMR (Table 5.7). Starting material ^{1}H NMR (500 MHz, acetone-d_6) 5.75 (ddt, J = 6.5, 10.5, 15.5 Hz, 1H), 4.93 (ddt, J = 1.5, 2.0, 17.0 Hz, 1H), 4.87 (ddt, J = 1.5, 2.0, 10.0 Hz, 1H), 1.95 (~tdd, $^4J_{H1\text{-}H3}$ = 2.0 Hz, $^3J_{H2\text{-}H3}$ = $^3J_{H3\text{-}H4}$ = 7.4 Hz, 2H), 1.33 (tq, $^3J_{H4\text{-}H5}$ = $^3J_{H3\text{-}H4}$ = 7.5 Hz, 2H), 0.83 (t, J = 7.2 Hz, 3H). Product ^{1}H NMR at 24 h (500 MHz, acetone-d_6) δ 5.38 (bs, 0.05H), 5.32 (bs, 0.08H), 1.86 (bs, 0.10H), 1.51 (bs, 0.20H), 0.86-0.79 (m, 0.28H).

Table 4.7. % Hydrogen atoms present in 2-pentene with deuterium oxide at 70 °C

Time (min)	% H in 2-pentene
1	32.8
2	18.7
5	8.2
24	6.9

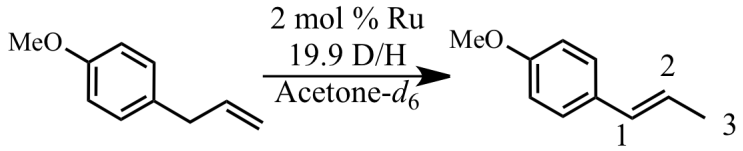

Figure 4.18. Isomerization and deuteration of 4-allylanisole

Isomerization and deuteration of 4-allyl anisole. A J. Young NMR tube was charged with tetrakis(trimethylsilyl)methane (a few small crystals), 4-allyl anisole (29.8 mg, 0.20 mmol), deuterium oxide (160.3 mg, 8.0 mmol) in acetone-d_6 (about 1 mL). After acquisition of an initial spectrum to set the integral values, **2.10** (2.6 mg, 0.0043 mmol, 2 mol %) was transferred quantitatively from a vial using acetone-d_6 in several portions into the J. Young NMR tube. Total reaction volume was adjusted to 2.0 mL by addition of acetone-d_6. 4-allyl anisole isomerized and deuterated to *trans*-anethole-d_4, as specified in Table 4.8. The data in Table 4.9 are for a reaction at elevated temperatures, where the reaction was set up in the same manner described above and the J. Young NMR tube was immersed in an oil bath at 70 °C. Starting material ^{1}H NMR (500 MHz, acetone-d_6) δ 7.07 (~d, AA' of AA'BB', J = 8.8 Hz, 2H), 6.73 (~d, BB' of AA'BB', J = 8.8 Hz, 2H), 5.91 (tdd, J = 6.8, 10.0, 16.8 Hz, 1H), 5.01 (tdd, J = 1.6, 2.0, 17.2 Hz, 1H), 4.96 (tdd, J =

1.2, 2.0, 10.0 Hz, 1H), 3.73 (s, 3H), 3.27 (d, J = 6.8 Hz, 2H). Product ^{1}H NMR after 144 h at RT (500 MHz, acetone-d_6) δ 7.26 (~d, AA' of AA'BB', J = 9.2 Hz, 2H), 6.83 (~d, BB' of AA'BB', J = 8.8 Hz, 2H), 6.34-6.30 (m, 0.39H), 6.13-6.05 (bs, 0.97H), 3.74 (s, 2.92H), 1.80-1.73 (m, 0.18H); ^{2}D NMR at 144 h (400 MHz, acetone-d_6) δ 6.37-6.33 (m), 1.75-1.73 (m). In the case of the RT reaction, ^{31}P NMR taken at 65 d showed a peak for **2.10** along with peaks for three other species.

Table 4.8. % Hydrogen left at indicated positions of (*E*)-anethole after specified time at room temperature

Time (min)	1	2	3
1	90.7	100.1	50.7
2	85.1	98.2	41.3
5	80.7	98.7	28.0
24	67.4	99.8	8.8
48	58.5	98.7	6.4
144	39.2	97.0	6.0

Table 4.9. % Hydrogen left at indicated positions of (*E*)-anethole after specified time at 70 ^{o}C

Time (min)	1	2	3
1	74.7	99.5	40.3
2	64.3	97.2	27.7
5	47.7	97.2	14.5
24	21.4	96.7	7.2
48	14.0	95.8	6.7
144	12.7	97.7	6.1

Isomerization and deuteration of 4-allyl anisole in a biphasic reaction setting. A conical vial was charged with tetrakis(trimethylsilyl)methane (a few small crystals), 4-allyl anisole (148.6 mg, 1.00 mmol), deuterium oxide (1.0042 g, 50.1 mmol) is added to the conical vial and charged with a magnetic stir bar. A small sample (<3 μL) was removed by capillary action into the tip of a Pasteur pipette and the sample was analyzed in acetone-d_6 to get an initial spectrum to set the integral values. In the glovebox, **2.10** (12.2 mg, 0.020 mmol, 2 mol %) was transferred quantitatively from a vial using acetone-d_6 in several portions to the reaction mixture. Progress of the reaction was monitored by stopping the stirring briefly to allow phase separation, and removing a sample by a Pasteur pipette tip from the top organic layer. The observed degree of deuteration is specified in Table 5.10. Starting material ^{1}H NMR (500 MHz, acetone-d_6) δ 7.10 (~d, AA' of AA'BB', J = 8.8 Hz, 2H), 6.85 (~d, BB' of AA'BB', J = 8.8 Hz, 2H), 5.94 (tdd, J = 6.8, 10.0, 16.8 Hz, 1H), 5.05 (tdd, J = 1.6, 2.0, 17.2 Hz, 1H), 5.00 (tdd, J = 1.2, 2.0, 10.0 Hz, 1H), 3.76 (s, 3H), 3.31 (d, J = 6.8 Hz, 2H). Product ^{1}H NMR at 96 h (500 MHz, acetone-d_6) δ 7.29 (~d, AA' of AA'BB', J = 9.2 Hz, 2H), 6.85 (~d, BB' of AA'BB', J = 8.8 Hz, 2H), 6.37-6.34 (m, 0.02H), 6.10 (bs, 0.98H), 3.77 (s, 2.92H), 1.80-1.75 (m, 0.18H).

Table 4.10. % Hydrogen left at indicated positions of (*E*)-anethole after specified time at room temperature under biphasic setting

Time (min)	1	2	3
1	93.2	99.6	59.7
2	87.2	98.6	35.9
5	73.7	99.2	16.3
24	31.3	99.1	4.7
48	11.4	98.5	3.9
72	5.7	98.6	3.5

Demonstration of the ability to wash out H using two successive "extractions" with D_2O: Isomerization and deuteration of 4-allyl anisole in a biphasic reaction setting. A conical vial was charged with tetrakis(trimethylsilyl)methane (3.2 mg), 4-allyl anisole (297.1 mg, 2.00 mmol), deuterium oxide (402.9 mg, 20.1 mmol) is added to the conical vial and charged with a magnetic stir bar. A small sample (<3 μL) was removed by capillary action into the tip of a Pasteur pipette and the sample was analyzed in acetone-d_6 to get an initial spectrum to set the integral values. In the glovebox, **2.10** (24.3 mg, 0.040 mmol, 2 mol %) was transferred to the reaction mixture. The sealed conical vial was immersed in an oil bath at 70 ^{o}C. Progress of the reaction was monitored by stopping the stirring briefly to allow phase separation, and removing a sample by a Pasteur pipette tip from the top organic layer. At 24 h, when maximum theoretical deuteration is reached, as much of the aqueous layer as possible (312.1 mg) was removed with a micro-syringe and a fresh batch of deuterium oxide (418.1 mg, 20.9 mmol) was added. Further deuteration was observed after 24 h of heating (total 48 h). The observed degree of

deuteration is specified in Table 4.11. Starting material ^{1}H NMR (500 MHz, acetone-d_6) δ 7.10 (~d, AA' of AA'BB', J = 8.8 Hz, 2H), 6.85 (~d, BB' of AA'BB', J = 8.8 Hz, 2H), 5.94 (tdd, J = 6.8, 10.0, 16.8 Hz, 1H), 5.05 (tdd, J = 1.6, 2.0, 17.2 Hz, 1H), 5.00 (tdd, J = 1.2, 2.0, 10.0 Hz, 1H), 3.76 (s, 3H), 3.31 (d, J = 6.8 Hz, 2H). Product ^{1}H NMR at 48 h (500 MHz, acetone-d_6) δ 7.29 (~d, AA' of AA'BB', J = 9.2 Hz, 2H), 6.85 (~d, BB' of AA'BB', J = 8.8 Hz, 2H), 6.37-6.34 (m, 0.09H), 6.10 (bs, 0.96H), 3.77 (s, 3H), 1.80-1.75 (m, 0.16H).

Table 4.11. % Hydrogen left at indicated positions of (*E*)-anethole after specified time at 70 °C under biphasic setting

Time (min)	1	2	3
1	92.1	98.7	81.7
5	56.0	100.0	39.9
24	21.3	99.6	18.4
48[a]	9.9	96.1	5.3

[a] Twenty-four hours after removal of first portion of D_2O and addition of the second, fresh portion.

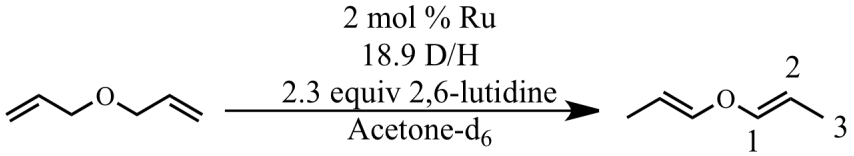

Figure 4.19. Isomerization and deuteration of allyl ether

Isomerization and deuteration of allyl ether. A J. Young NMR tube was charged with tetrakis(trimethylsilyl)methane (a few small crystals), diallyl ether (15.3 mg, 0.16 mmol), 2,6-lutidine (4.0 mg, 0.37 mmol) and deuterium oxide (242.9 mg, 12.1 mmol) in acetone-d_6 (about 1.2 mL). After acquisition of an initial spectrum to set the integral values, **2.10**

(4.6 mg, 0.0076 mmol, 5 mol %) was transferred quantitatively from a vial using acetone-d_6 in several portions in the J. Young NMR tube. The vial containing **2.10** was washed with additional acetone-d_6 and washings were added to the tube. Total reaction volume was adjusted to 1.6 mL by addition of acetone-d_6. Isomerization and deuteration of the substrate was monitored at several time intervals with ^{1}H NMR (Table 4.12). Starting material ^{1}H NMR (500 MHz, acetone-d_6) δ 5.84 (tdd, J = 3.2, 12.8, 17.6 Hz, 2H), 5.20 (qd, J = 1.8, 17.2 Hz, 2H), 5.06 (qd, J = 1.4, 10.4 Hz, 2H), 3.90 (td, J = 1.6, 6.2 Hz, 4H). Product ^{1}H NMR at 48 h (500 MHz, acetone-d_6) δ 6.28-6.22 (m, 0.75H), 5.06-4.90 (m, 2H), 1.45-1.52 (m, 0.53H).

Table 4.12. % Hydrogen left at the specified positions of (*E*)-propenyl ether with deuterium oxide at room temperature

Time (min)	1	2	3
1	76.6	103.1	63.1
2	72.9	102.5	58.1
5	65.7	102.3	46.6
24	47.1	100.7	17.5
48	37.3	100.7	8.9
72	31.4	99.0	7.0

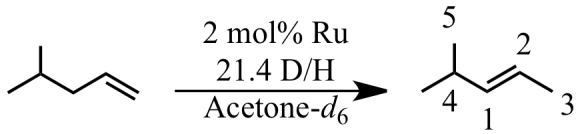

Figure 4.20. Isomerization and deuteration of 4-methyl-1-pentene

Isomerization and deuteration of 4-methyl-1-pentene. A J. Young NMR tube was charged with tetrakis(trimethylsilyl)methane (a few small crystals), 4-methyl-1-pentene

(13.9 mg, 0.165 mmol) and deuterium oxide (142.1 mg, 7.09 mmol) in acetone-d_6 (1.0 mL). After acquisition of an initial spectrum to set the integral values, **2.10** (3.7 mg, 0.0061 mmol, 2 mol %) was transferred quantitatively from a vial using acetone-d_6 in several portions into the J. Young NMR tube. Progress of the reaction was monitored via ^{1}H NMR (refer to Table 4.13). Starting material ^{1}H NMR (400 MHz, acetone-d_6) δ 5.73 (tdd, J = 7.2, 10.0, 16.8 Hz, 1H), 4.92 (ddt, J = 1.6, 2.0, 14.8 Hz, 1H), 4.87 (ddt, J = 1.2, 2.4, 7.2 Hz, 1H) 1.87 (tt, J = 2.4, 7.2 Hz, 2H), 1.56 (n, J = 6.8 Hz, 1H), 0.82 (d, J = 6.8 Hz, 6H). Product ^{1}H NMR at 24 h (400 MHz, acetone-d_6) δ 5.34-5.30 (m, 1.0H), 2.19-2.1 (m, 0.99H), 1.59-1.51 (m, 0.25H), 0.89 (d, J = 6.8 Hz, 6H). ^{2}D NMR at 322 h (400 MHz, acetone-d_6) δ 5.38 (dd, J = 1.0, 2.4 Hz, 1H), 1.52 (d, J = 1.0 Hz, 3H). ^{13}C NMR (400 MHz, acetone-d_6) δ 139.5, 139.2, 139.1, 138.9, 121.9, 31.5, 22.8 (m).

Table 4.13. % Hydrogen left at the specified positions of 4-methyl-2-pentene with deuterium oxide at room temperature

Time (min)	1+2	3	4	5
1	73.6	40.0	98.1	101.7
2	68.3	29.0	97.9	100.0
5	61.1	13.9	89.6	97.1
24	50.1	8.6	99.2	102.0

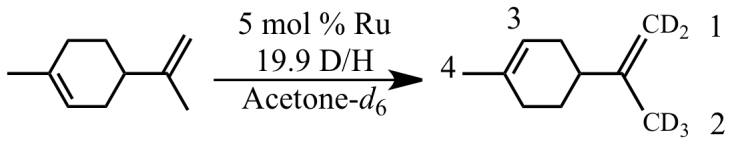

Figure 4.20. Selective deuteration of (+)-limonene

Deuteration of (+)-limonene A J. Young NMR tube was charged with tetrakis(trimethylsilyl)methane (a few small crystals), (+)-limonene (13.7 mg, 0.10

mmol) and deuterium oxide (100.2 mg, 5.0 mmol) in acetone-d_6 (about 0.8 mL). After acquisition of an initial spectrum to set the integral values, **2.10** (3.0 mg, 0.0049 mmol, 5 mol %) was transferred quantitatively from a vial using acetone-d_6 in several portions into the J. Young NMR tube was placed in an oil bath at 70 ^{o}C. Progress of the reaction was monitored via ^{1}H NMR (Table 5.14). No isomerization of the double bonds over 144 h at 70 ^{o}C was apparent in either this experiment, or a separate control experiment conducted in the absence of D_2O. Starting material ^{1}H NMR (500 MHz, acetone-d_6) δ 5.35-5.33 (m, 1H), 4.65-4.64 (m, 2H), 2.03-1.79 (m, 5H), 1.75-1.70 (m, 1H), 1.67 (t, J = 1 Hz, 3H), 1.57 (bs, 3H), 1.44-1.36 (m, 1H). Product ^{1}H NMR at 48 h (500 MHz, acetone-d_6) δ 5.37-5.35 (m, 0.97H), 4.67-4.65 (m, 0.87H), 2.09-1.81 (m, 5H), 1.77-1.72 (m, 1H), 1.69-1.64 (m, 1.30H), 1.59 (bs, 2.83H), 1.46-1.38 (m, 1H).

Table 4.14. % Hydrogen left at the specified positions of (+)-limonene with deuterium oxide at 70 ^{o}C

Time (min)	1	2	3	4
0	100.6	98.5	99.1	98.4
1	97.9	97.8	99.6	98.6
2	95.8	94.4	99.1	97.9
5	90.7	90.4	98.4	96.7
24	66.8	66.2	99.4	97.3
48	43.7	43.4	97.1	94.4
120	13.6	13.8	93.3	83.9

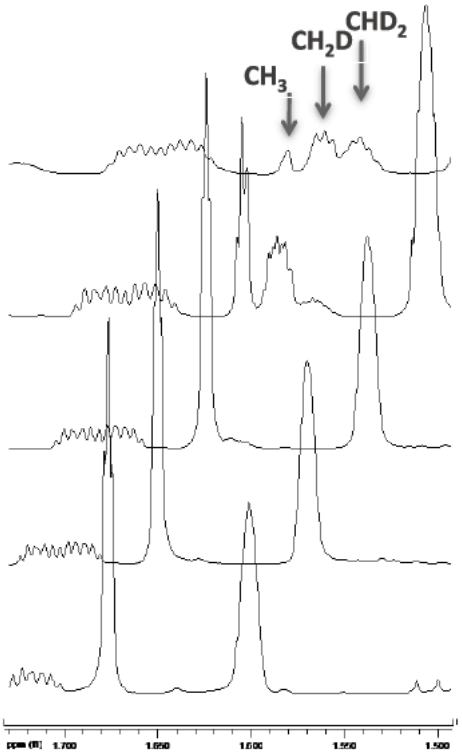

Figure 4.21. ^{1}H NMR Spectrum of (+)-limonene methyl peak 2

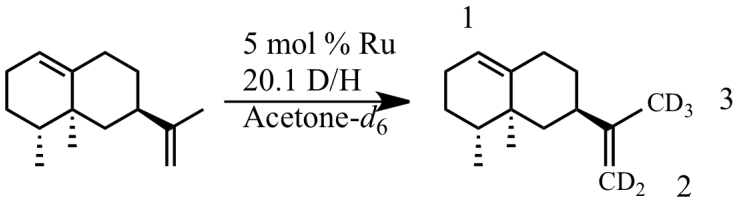

Figure 4.22. Selective deuteration of (+)-valencene

Deuteration of (+)-valencene A J. Young NMR tube was charged with tetrakis(trimethylsilyl)methane (1.6 mg), (+)-valencene (20.5 mg, 0.10 mmol; sample was assayed as 88.3% pure by Aldrich) and deuterium oxide (100.6 mg, 5.02 mmol) in acetone-d_6 (about 0.8 mL). After acquisition of an initial spectrum to set the integral values, **2.10** (3.0 mg, 0.005 mmol, 5 mol %) was transferred quantitatively from a vial using acetone-d_6 in several portions into the J. Young NMR tube. The J. Young NMR

tube was placed in an oil bath at 70□C. Progress of the reaction was monitored via ^{1}H NMR (Table S15). No isomerization of the double bonds over 500 h at 70 ^{o}C was apparent in this experiment. Starting material ^{1}H NMR (400 MHz, acetone-d_6) δ 5.27-5.25 (m, 1H), 4.68-4.62 (m, 2H), 2.31-1.68 (m, 7H), 1.65 (s, 3H), 1.61-1.31 (m, 4H), 1.15-1.02 (m, 1H), 0.90-0.82 (m, 6H). Product ^{1}H NMR at 144 h (400 MHz, acetone-d_6) δ 5.36-5.34 (m, 0.95H), 4.70-4.63 (m, 0.14H), 2.38-1.78 (m, 7.05H), 1.70-1.63 (m, 0.45H), 1.64-1.13 (m, 5.04H), 0.99-0.91 (m, 6.24H). Underlined resonances are those assigned to exocyclic isopropenyl group.

Table 4.15. % Hydrogen left at the specified positions of (+)-valencene with deuterium oxide at 70 ^{o}C

Time (min)	1	2	3
1	101.1	94.5	93.5
24	104.5	49.1	44.1
100	103.3	11.8	19.5
144	95.3	6.9	15.2

Chapter 4 contains material are similar to the material published in the following papers: Erdogan, Gulin; Grotjahn, Douglas B. "Catalysis of Selective Hydrogen/Deuterium Exchange at Allylic Positions Using Deuterium Oxide" *Topics in Catalysis* **2010**, 53, 1055, Erdogan, Gulin; Grotjahn, Douglas B. "Mild and Selective Deuteration and Isomerization of Alkenes by a Bifunctional Catalyst and Deuterium Oxide" *J. Am. Chem. Soc.*, **2009**, 131, 30, 10354, and Grotjahn, Douglas B; Larsen, Casey R.; Erdogan, Gulin; Gustafson, Jeffery L.; Nair, Reji; Sharma, Abhinandini "Bifunctional Catalysis of Alkene Isomerization and Its Applications", *Catalysis of*

Organic Reactions **2009**, 123, 379. The dissertation author was the primary researcher for the data presented.

REFERENCES

(1) Thomas, A. F. *Deuterium Labbeling in Organic Chemistry*; Appleton-Century-Crofts: New York, New York, 1971.

(2) Junk, T.; Catallo, W. J. *Chem Soc Rev* **1997**, *26*, 401.

(3) Atzrodt, J.; Derdau, V.; Fey, T.; Zimmermann, J. *Angew Chem Int Ed Engl* **2007**, *46*, 7744.

(4) Garnett, J. L.; Hodges, R. J. *J Am Chem Soc* **1967**, *89*, 4546.

(5) Klei, S. R.; Golden, J. T.; Tilley, T. D.; Bergman, R. G. *J Am Chem Soc* **2002**, *124*, 2092.

(6) Golden, J. T.; Andersen, R. A.; Bergman, R. G. *J Am Chem Soc* **2001**, *123*, 5837.

(7) Klei, S. R.; Tilley, T. D.; Bergman, R. G. *Organometallics* **2002**, *21*, 4905.

(8) Yung, C. M.; Skaddan, M. B.; Bergman, R. G. *J Am Chem Soc* **2004**, *126*, 13033.

(9) Skaddan, M. B.; Yung, C. M.; Bergman, R. G. *Org Lett* **2004**, *6*, 11.

(10) Corberan, R.; Sanau, M.; Peris, E. *J Am Chem Soc* **2006**, *128*, 3974.

(11) Corberan, R.; Sanau, M.; Peris, E. *Organometallics* **2006**, *25*, 4002.

(12) Feng, Y.; Jiang, B.; Boyle, P. A.; Ison, E. A. *Organometallics* **2010**, *29*, 2857.

(13) Ng, S. M.; Lam, W. H.; Mak, C. C.; Tsang, C. W.; Jia, G. C.; Lin, Z. Y.; Lau, C. P. *Organometallics* **2003**, *22*, 641.

(14) Leung, C. W.; Zheng, W. X.; Wang, D. X.; Ng, S. M.; Yeung, C. H.; Zhou, Z. Y.; Lin, Z. Y.; Lau, C. P. *Organometallics* **2007**, *26*, 1924.

(15) Lenges, C. P.; Brookhart, M.; Grant, B. E. *J Organomet Chem* **1997**, *528*, 199.

(16) Barthez, J. M.; Filikov, A. V.; Frederiksen, L. B.; Huguet, M. L.; Jones, J. R.; Lu, S. Y. *Can J Chem* **1998**, *76*, 726.

(17) Lenges, C. P.; White, P. S.; Brookhart, M. *J Am Chem Soc* **1999**, *121*, 4385.

(18) Rybtchinski, B.; Cohen, R.; Ben-David, Y.; Martin, J. M. L.; Milstein, D. *J Am Chem Soc* **2003**, *125*, 11041.

(19) Yamamoto, M.; Oshima, K.; Matsubara, S. *Heterocycles* **2006**, *67*, 353.

(20) Prechtl, M. H. G.; Holscher, M.; Ben-David, Y.; Theyssen, N.; Milstein, D.; Leitner, W. *Eur J Inorg Chem* **2008**, 3493.

(21) Meier, S. K.; Young, K. J. H.; Ess, D. H.; Tenn, W. J.; Oxgaard, J.; Goddard, W. A.; Periana, R. A. *Organometallics* **2009**, *28*, 5293.

(22) Iluc, V. M.; Fedorov, A.; Grubbs, R. H. *Organometallics* **2011**, *31*, 39.

(23) Rhinehart, J. L.; Manbeck, K. A.; Buzak, S. K.; Lippa, G. M.; Brennessel, W. W.; Goldberg, K. I.; Jones, W. D. *Organometallics* **2012**, *31*, 1943.

(24) Prechtl, M. H. G.; Holscher, M.; Ben-David, Y.; Theyssen, N.; Loschen, R.; Milstein, D.; Leitner, W. *Angew Chem Int Edit* **2007**, *46*, 2269.

(25) Werstiuk, N. H.; Chen, J. *Can J Chem* **1989**, *67*, 5.

(26) Werstiuk, N. H.; Chen, J. *Can J Chem* **1989**, *67*, 812.

(27) Werstiuk, N. H.; Timmins, G. *Can J Chem* **1985**, *63*, 530.

(28) Werstiuk, N. H.; Timmins, G. *Can J Chem* **1988**, *66*, 2309.

(29) Matsubara, S.; Yokota, Y.; Oshima, K. *Chem Lett* **2004**, *33*, 294.

(30) Ishibashi, K.; Matsubara, S. *Chem Lett* **2007**, *36*, 724.

(31) Morrill, T. C.; D'Souza, C. A. *Organometallics* **2003**, *22*, 1626.

(32) Zhou, J. R.; Hartwig, J. F. *Angew Chem Int Edit* **2008**, *47*, 5783.

(33) Santos, L. L.; Mereiter, K.; Paneque, M.; Slugovc, C.; Carmona, E. *New J Chem* **2003**, *27*, 107.

(34) Tse, S. K. S.; Xue, P.; Lin, Z.; Jia, G. *Adv Synth Catal* **2010**, *352*, 1512.

(35) Di Giuseppe, A.; Castarlenas, R.; Pérez-Torrente, J. J.; Lahoz, F. J.; Polo, V.; Oro, L. A. *Angewandte Chemie International Edition* **2011**, *50*, 3938.

(36) Erdogan, G.; Grotjahn, D. B. *J Am Chem Soc* **2009**, *131*, 10354.

(37) Erdogan, G.; Grotjahn, D. B. *Top Catal* **2010**, *53*, 1055.

(38) Grotjahn, D. B.; Larsen, C. R.; Gustafson, J. L.; Nair, R.; Sharma, A. *J Am Chem Soc* **2007**, *129*, 9592.

(39) Harris, N. J. *J Phys Chem-Us* **1995**, *99*, 14689.

(40) Courchay, F. C.; Sworen, J. C.; Ghiviriga, I.; Abboud, K. A.; Wagener, K. B. *Organometallics* **2006**, *25*, 6074.

(41) Mcgrath, D. V.; Grubbs, R. H. *Organometallics* **1994**, *13*, 224.

(42) Bergens, S. H.; Bosnich, B. *J Am Chem Soc* **1991**, *113*, 958.

(43) Hendrix, W. T.; Vonrosenberg, J. L. *J Am Chem Soc* **1976**, *98*, 4850.

(44) Wang, R.; Groux, L. F.; Zargarian, D. *Organometallics* **2002**, *21*, 5531.

(45) Sui-Seng, C.; Groux, L. F.; Zargarian, D. *Organometallics* **2005**, *25*, 571.

(46) Rummens, F. H. A.; Kaslande.L *Can J Spectrosc* **1972**, *17*, 99.

(47) Voge, H. H.; May, N. C. *J Am Chem Soc* **1946**, *68*, 550.

(48) Kapteijn, F.; Steen, A. J. v. d.; Mol, J. C. *The Journal of Chemical Thermodynamics* **1983**, *15*, 137.

CHAPTER 5

CONCLUSIONS AND FUTURE DIRECTIONS

Applications of imidazolyl phosphines in homogenous and polymer-supported alkene isomerization and hydrogen-deuterium exchange have been established. Positional migration of carbon-carbon double bonds can efficiently be achieved with alkene isomerization catalyst **2.10** with exceptional selectivity for (*E*)-internal alkenes with excellent functional group tolerance. Upon immobilization on an insoluble polymer resin, the selectivity was completely retained with very low metal leaching from the support. Moreover, **2.10** also proved to be a very efficient catalyst for exchange of allylic protons of olefins in presence of deuterium oxide. An exceptional degree of deuterium incorporation was achieved in positions accessible by isomerization in homogenous and biphasic reaction settings. Further development of **2.10** led to discovery of complexes that could be capable of controlled mono-isomerization of linear alkenes. Using different combinations of more hindered phosphines and imidazoles, one can achieve diverse mixtures of alkenes including polyfunctional examples.

With a bifunctional phosphine library available, one can imagine improving other organic transformations during which proton transfer or hydrogen bonding could be important. One of these reactions relevant is palladium-catalyzed coupling reactions that provide easy access to pharmaceutical ingredients, natural products and many other fine chemicals. Development and application of highly practical new systems for construction of C-C and C-X (X = N, O, S) in cross-coupling chemistry have revolutionized the methods of organic synthesis.[1,2] Recently Heck, Negishi and Suzuki have been awarded the Nobel Prize for their contributions and since the introduction of coupling chemistry in the early 1970s various industrial processes have been based on this chemistry. For example, (1) Buchwald-Hartwig amination is used in the Novartis route for synthesis of

Gleevec[3] (Imatinib), (2) Heck coupling is employed in a process for Singulair[4-6] developed by Merck and Pfizer's process for hepatitis C polymerase inhibitor,[7] and (3) Suzuki coupling is employed in synthesis of Losartan[8,9] (originally by Merck-Dupont, now Bristol-Myers Squibb).

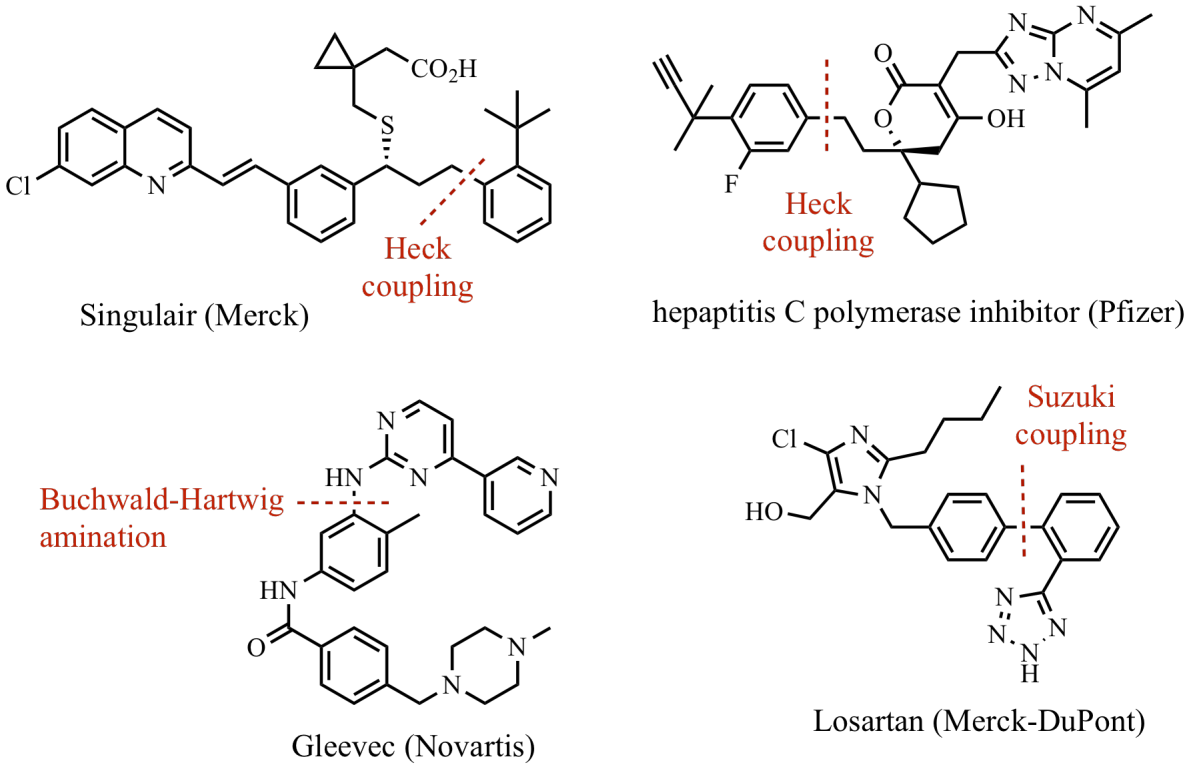

Figure 5.1. Pharmaceutical applications of cross-coupling reactions.

The importance of ligand effects on reactivity suggests that ligand electronics and sterics have profound influence on the oxidative and reductive elimination steps thought to take place during the catalysis. Palladium coupling reactions of aryl bromides, iodides and triflates takes place smoothly with widely used triphenyl phosphine, PPh_3. Fu et al.[10] introduced the use of sterically hindered, electron rich trialkylphosphine ligands (t-Bu_3P and Cy_3P) for reactions of aryl chlorides that are more sluggish due to the high bond dissociation energy of the C-Cl bond, which may be what makes oxidative addition to

Pd(0) slower.[11] Milstein et al. introduced a chelating bisphosphine ligand, 1,3-bis[di-isopropylphosphino)propane], (dippp), for the carbonylation, formylation, and Heck reactions of aryl chlorides.[12-15] Wide use of several families of ligands has been implemented: biarylphosphines (Buchwald),[16,17] ferrocenylphosphine (e.g. Q-Phos, Hartwig),[18,19] adamantyl phosphines (Beller),[20] N-heterocyclic carbenes (Nolan, Herrmann).[21] The importance of bidentate ligands has been long recognized; they can accelerate the reductive elimination step in the catalytic cycle and reduce the competition from the beta-hydride elimination side-product formation.[22-24] Use of P,N ligands have recently been employed by Nishikawa,[25-27] Andersson,[28] and Beller.[20,29,30] The family of P,N bifunctional ligands has great versatility, including possibilities for catalyst tuning as discussed in Chapter 2.

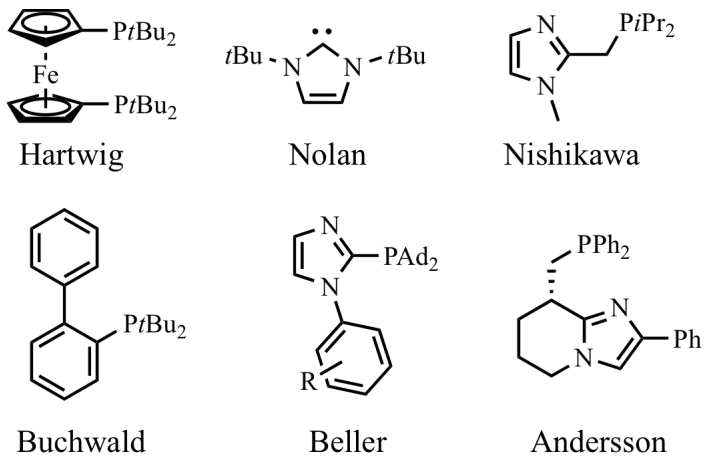

Figure 5.2. Representative ligands used for cross-coupling reactions

Spectacular successes in improving palladium-catalyzed coupling reactions have occurred through extensive ligand development. We are investigating the use of heteroaryl phosphines, which might facilitate stabilization of low coordinate species by binding to the metal momentarily. Using the imidazolyl ligand library at hand, former

group member, Reji Nair, synthesized the following (η^3-allyl)palladium chloride complexes.

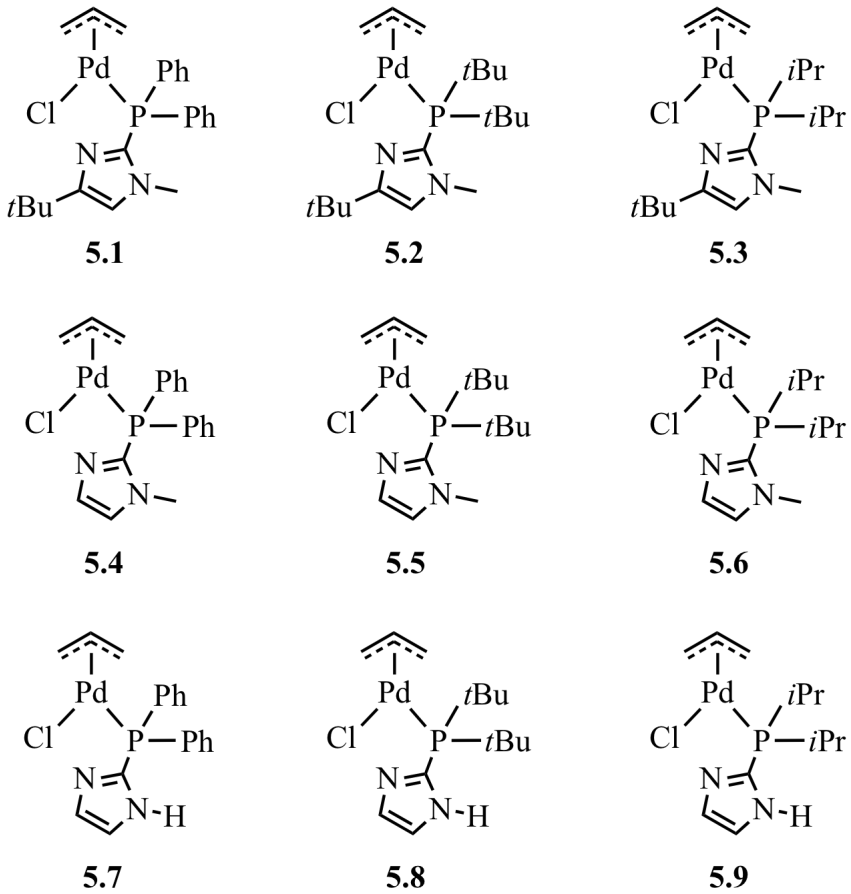

Figure 5.3. (η^3-Allyl)palladium chloride complexes prepared by Reji Nair

In order to investigate the possible application of these complexes in palladium catalyzed arylamination reactions, coupling between aryl halide and morpholine (1.5 equivalent) with sodium *tert*-butoxide (2 equiv) in dimethoxyethane (DME) as solvent with 5 mol % catalyst **5.1**-**5.9** was investigated. The reactions were carried out initially at room temperature, and then heated at 65 ^{o}C if no significant progress was observed. The initial goal was not necessarily to make the best known catalyst for aryl amination, but to

begin to see what combination of R groups on phosphorus and heterocycle were optimal, and also see if we could gather evidence for rate acceleration by the heteroaryl group.

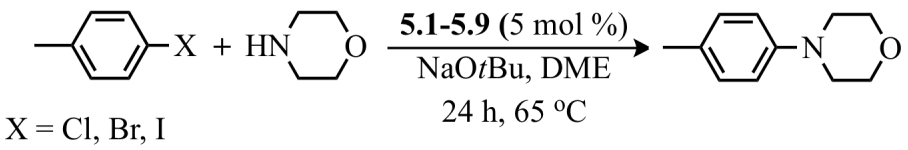

Figure 5. 4. Screening reaction and conditions for arylamination

Table 5.1. Results of initial arylamination screening with pre-formed complexes

Pd-complex	Yield (%) of 4-(p-tolyl)morpholine		
	Chlorotoluene	**Bromotoluene**	**Iodotoluene**
5.1	0	15.9	7.7
5.2	0.5	40.2	27.1
5.3	0.4	27.0	19.8
5.4	0	11.7	3.9
5.5	0.2	62.7	39.1
5.6	0.5	18.3	18.5
5.7	0	2.6	1.9
5.8	0.5	9.2	NA
5.9	1.0	17.3	8.3

Screening with these pre-formed complexes showed that several complexes are capable of product formation with 4-iodo- and 4-bromotoluene under the conditions tested. With results from these initial screenings, testing of catalysts generated more conveniently *in situ* is being investigated to determine the practicality of these ligands along with control ligands to determine the effect of imidazolyl phosphines. Another study is to be conducted on the effect of palladium source used; a recent review[31] suggests that the crotylpalldium complexes are superior to allylpalldium complexes in

amination of 4-bromoanisole with N-methylaniline[32] and Suzuki coupling of 4-bromoanisole with p-(*tert*-butyl)phenyl)boronic acid.[31]

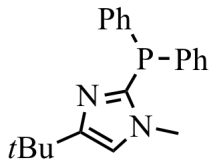

5.13

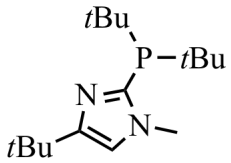

5.14

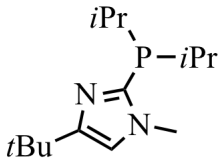

5.15

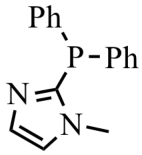

5.16

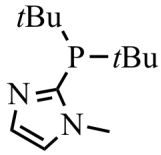

5.17

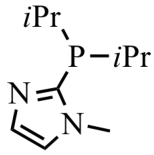

5.18

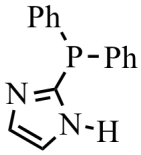

5.19

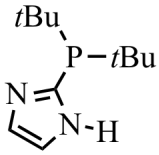

5.20

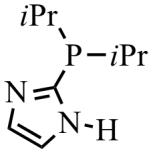

5.21

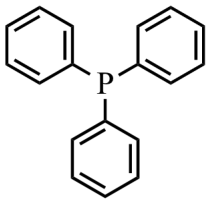

5.22

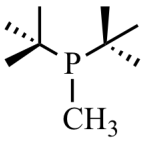

5.23

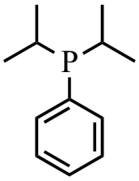

5.24

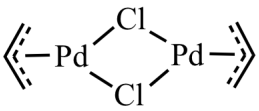

Allylpalladium(II) chloride dimer

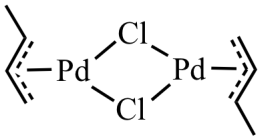

Crotylpalladium(II) chloride dimer

Figure 5.5. *In situ* arylamination screening ligands and palladium precursors

These studies in part are being currently investigated and prepared for future submission for publication by Reji Nair, Gulin Erdogan, Christoffel van Niekerk, Alice Lu, James Golen, Antonio DiPasquale, Arnold Rheingold, and Douglas Grotjahn.

In summary, use of P, N ligands that have a pendant nitrogen (imidazole, pyridine) which can act as proton or hydrogen bond acceptor has led to dramatic improvement in a variety of reactions. In the case of *anti*-Markovnikov alkyne hydration, the change in rate introduced by **1.6** (Chapter 1) was greater than 2.4 x 10^{11} and the change in selectivity was 300,000 that can be compared to enzyme-like enhancements. Here in this thesis, alkene isomerization catalyst **2.10** (Chapter 2), improves TOF as much as 10,000 times compared to a system that lacks the nitrogen bifunctionality. Now, the two bifunctional catalysts mentioned are both sold commercially, showing broad impact of the research.

All of these observations suggest that use of P, N ligands with pendant bases can be useful tools in reactions that involve proton movements, other than the reactions discussed here, such as alkene or diene functionalization with protic reactants like alcohols or amines, and C-H activations or functionalizations, all possibilities for future investigation.

Chapter 5, in part is currently being prepared for submission for publication of the material. Nair, Reji; Erdogan, Gulin; van Niekerk, Christoffel, Golen, James; Rheingold, Arnold; Grotjahn, Douglas. The dissertation author was the primary researcher for the data presented.

REFERENCES

(1) Cornils, B.; Herrmann, W. A. *Applied homogeneous catalysis with organometallic compounds : a comprehensive handbook in three volumes*; 2nd, completely rev. and enlarged ed.; Wiley-VCH: Weinheim, 2002.

(2) Meijere, A. d.; Diederich, F. *Metal-catalyzed cross-coupling reactions*; 2nd, completely rev. and enl. ed.; Wiley-VCH: Weinheim, 2004.

(3) Loiseleur, O.; Kaufmann, D.; Abel, S.; Buerger, H. M.; Meisenbach, M.; Schmitz, B.; Sedelmeier, G.; Novartis A.-G., Switz.; Novartis Pharma G.m.b.H. . 2003, p 38 pp.

(4) King, A. O.; Corley, E. G.; Anderson, R. K.; Larsen, R. D.; Verhoeven, T. R.; Reider, P. J.; Xiang, Y. B.; Belley, M.; Leblanc, Y. *The Journal of Organic Chemistry* **1993**, *58*, 3731.

(5) Shinkai, I.; King, A. O.; Larsen, R. D. *Pure Appl Chem* **1994**, *66*, 1551.

(6) Higgs, G. *Chem Ind-London* **1997**, 827.

(7) Camp, D.; Matthews, C. F.; Neville, S. T.; Rouns, M.; Scott, R. W.; Truong, Y. *Org Process Res Dev* **2006**, *10*, 814.

(8) Smith, G. B.; Dezeny, G. C.; Hughes, D. L.; King, A. O.; Verhoeven, T. R. *The Journal of Organic Chemistry* **1994**, *59*, 8151.

(9) Larsen, R. D.; King, A. O.; Chen, C. Y.; Corley, E. G.; Foster, B. S.; Roberts, F. E.; Yang, C.; Lieberman, D. R.; Reamer, R. A. *The Journal of Organic Chemistry* **1994**, *59*, 6391.

(10) Littke, A. F.; Dai, C. Y.; Fu, G. C. *J Am Chem Soc* **2000**, *122*, 4020.

(11) Grushin, V. V.; Alper, H. *Chemical Reviews* **1994**, *94*, 1047.

(12) Bendavid, Y.; Portnoy, M.; Milstein, D. *J Am Chem Soc* **1989**, *111*, 8742.

(13) Portnoy, M.; Milstein, D. *Organometallics* **1993**, *12*, 1665.

(14) Portnoy, M.; Milstein, D. *Organometallics* **1993**, *12*, 1655.

(15) Portnoy, M.; Bendavid, Y.; Milstein, D. *Organometallics* **1993**, *12*, 4734.

(16) Wolfe, J. P.; Singer, R. A.; Yang, B. H.; Buchwald, S. L. *J Am Chem Soc* **1999**, *121*, 9550.

(17) Aranyos, A.; Old, D. W.; Kiyomori, A.; Wolfe, J. P.; Sadighi, J. P.; Buchwald, S. L. *J Am Chem Soc* **1999**, *121*, 4369.

(18) Shelby, Q.; Kataoka, N.; Mann, G.; Hartwig, J. *J Am Chem Soc* **2000**, *122*, 10718.

(19) Hartwig, J. F. *Accounts Chem Res* **2008**, *41*, 1534.

(20) Zapf, A.; Ehrentraut, A.; Beller, M. *Angew Chem Int Edit* **2000**, *39*, 4153.

(21) Marion, N.; Diez-Gonzalez, S.; Nolan, I. P. *Angew Chem Int Edit* **2007**, *46*, 2988.

(22) Dreher, S. D.; Dormer, P. G.; Sandrock, D. L.; Molander, G. A. *J Am Chem Soc* **2008**, *130*, 9257.

(23) Melzig, L.; Gavryushin, A.; Knochel, P. *Org Lett* **2007**, *9*, 5529.

(24) Chemler, S. R.; Trauner, D.; Danishefsky, S. J. *Angewandte Chemie International Edition* **2001**, *40*, 4544.

(25) Jalil, M. A.; Yamada, T.; Fujinami, S.; Honjo, T.; Nishikawa, H. *Polyhedron* **2001**, *20*, 627.

(26) Jalil, M. A.; Fujinami, S.; Nishikawa, H. *J Chem Soc Dalton* **2001**, 1091.

(27) Jalil, M. A.; Fujinami, S.; Senda, H.; Nishikawa, H. *J Chem Soc Dalton* **1999**, 1655.

(28) Henriksen, S. T.; Norrby, P. O.; Kaukoranta, P.; Andersson, P. G. *J Am Chem Soc* **2008**, *130*, 10414.

(29) Schulz, T.; Torborg, C.; Schaffner, B.; Huang, J.; Zapf, A.; Kadyrov, R.; Borner, A.; Beller, M. *Angew Chem Int Edit* **2009**, *48*, 918.

(30) Milde, B.; Schaarschmidt, D.; Ruffer, T.; Lang, H. *Dalton T* **2012**, *41*, 5377.

(31) Li, H.; Seechurn, C.; Colacot, T. J. *ACS Catalysis* **2012**.

(32) Seechurn, C. C. C. J.; Parisel, S. L.; Colacot, T. J. *J Org Chem* **2011**, *76*, 7918.